



HAL
open science

Maladie parodontale, microbiote et fer

Emile Boyer

► **To cite this version:**

Emile Boyer. Maladie parodontale, microbiote et fer. Médecine humaine et pathologie. Université de Rennes, 2019. Français. NNT : 2019REN1B054 . tel-02893545

HAL Id: tel-02893545

<https://theses.hal.science/tel-02893545>

Submitted on 8 Jul 2020

HAL is a multi-disciplinary open access archive for the deposit and dissemination of scientific research documents, whether they are published or not. The documents may come from teaching and research institutions in France or abroad, or from public or private research centers.

L'archive ouverte pluridisciplinaire **HAL**, est destinée au dépôt et à la diffusion de documents scientifiques de niveau recherche, publiés ou non, émanant des établissements d'enseignement et de recherche français ou étrangers, des laboratoires publics ou privés.

THESE DE DOCTORAT DE

L'UNIVERSITE DE RENNES 1
COMUE UNIVERSITE BRETAGNE LOIRE

ECOLE DOCTORALE N° 605
Biologie Santé
Spécialité : *Sciences Odontologiques*

Par

Émile BOYER

Maladie parodontale, microbiote et fer

Thèse présentée et soutenue à Rennes, le 9 décembre 2019
Unité de recherche : U-1241 Nutrition Metabolisms and Cancer
U.F.R. d'Odontologie, Université de Rennes 1
2, avenue du Pr. Léon Bernard, 35043 RENNES

Rapporteurs avant soutenance :

Frédéric CUISINIER
Patricia LEPAGE

Professeur d'université – Praticien hospitalier, Université de Montpellier
Chargée de recherche, Université de Paris-Saclay

Composition du Jury :

Président : Marie-Laure COLOMBIER

Professeur d'université – Praticien hospitalier, Université de Paris Descartes

Examineurs : Frédéric CUISINIER
Patricia LEPAGE
Guy CATHELINÉAU

Professeur d'université – Praticien hospitalier, Université de Montpellier
Chargée de recherche, Université de Paris-Saclay
Professeur d'université – Praticien hospitalier, Université de Rennes 1

Dir. de thèse : Martine BONNAURE-MALLET
Co-dir. de thèse : Vincent MEURIC

Professeur d'université – Praticien hospitalier, Université de Rennes 1
Maître de conférences – Praticien hospitalier, Université de Rennes 1

Production scientifique

Publications internationales

- Signature of Microbial Dysbiosis in Periodontitis. *Applied and Environmental Microbiology* **83**, e00462-17 (2017).
Troisième auteur.
Impact Factor : **3,633**
[PMID : 28476771](#)
Voir page 7.
- Periodontal status and serum biomarkers levels in *HFE* hemochromatosis patients. A case-series study. *Journal of Clinical Periodontology* **44**, 892-897 (2017).
Troisième auteur.
Impact Factor : **4,046**
[PMID : 28586532](#)
Voir page 19.
- Increased transferrin saturation is associated to subgingival microbiota dysbiosis and severe periodontitis in genetic haemochromatosis. *Scientific Reports* **8**, 15532 (2018).
Premier auteur.
Impact Factor : **4,011**
[PMID : 30341355](#)
Voir page 34.
- Lithium and boron in calcified tissues of vicuna and its relation to the chronic exposure by water ingestion in the andean lithium triangle. *Environmental Toxicology and Chemistry* ahead of print (2019).
Troisième auteur.
Impact Factor ¹ : **3,421**
[PMID : 31614392](#)
- Periodontal Pathogens and Clinical Parameters in Chronic Periodontitis. *Molecular Oral Microbiology* ahead of print (2019).

1. L'Impact Factor présenté correspond à celui calculé pour l'année 2018.

Premier auteur.

Impact Factor² : 2,925.

[PMID : 31782910](#)

Voir page 37.

- Alteration and loss of mandibular alveolar bone in *Hfe* knocked-out mice. A pilot study. *Journal of Clinical Periodontology*.

Premier auteur.

En révision.

Voir page 42.

- Oral dysbiosis model with *Porphyromonas gingivalis* is strain-dependant.

Premier auteur.

En préparation.

Voir page 45.

Publications nationales

- Prise en charge orthodontique en oncologie pédiatrique. *La Revue d'Orthopédie Dento-Faciale* **50**, 385-394 (2016).

Premier auteur.

[doi: 10.1051/odf/2016035](https://doi.org/10.1051/odf/2016035).

- Orthodontic strategies in pediatric oncology. *Journal of Dentofacial Anomalies and Orthodontics* **20**, 104 (2017).

Premier auteur.

[doi: 10.1051/odfen/2016035](https://doi.org/10.1051/odfen/2016035)

- Bactériologie parodontale versus bactériologie implantaire. *Journal de Parodontologie et d'Implantologie Orale* **37**, 275-283 (2018).

Premier auteur.

<http://preprod.editionsmdp.fr/revues/jpio/article/n-3704>

Ouvrages

- Le microbiote buccal : bases fondamentales et applications en physiopathologie. Dans : *Encyclopédie Médico-Chirurgicale, traité de Médecine Buccale*. Elsevier Masson.

Premier auteur.

Sous presse.

Voir page 4.

2. L'Impact Factor présenté correspond à celui calculé pour l'année 2018.

- La mise en place du microbiote buccal depuis la naissance. Dans : *La bouche de l'enfant et de l'adolescent*, 1^{re} édition, coordonné par Béatrice THIVICHON-PRINCE et Brigitte ALLIOT-LICHT. Elsevier Masson.

Dernier auteur.

<https://www.sciencedirect.com/book/la-bouche-de-lenfant-et-de-ladolescent>

Communications internationales

- Periodontal microbiota in patients with hemochromatosis, an iron overload disease. *Oral Health Research Congress – Continental European & Scandinavian divisions (CED-IADR/NOF) of the International Association for Dental Research (IADR)*.

Communication affichée.

Vienne, septembre 2017.

Voir en annexe A, page 62.

- Systemic Condition, Local Disorder : a Periodontitis-Haemochromatosis Relationship Through Iron Homeostasis. *IADR/AADR/CADR General Session & Exhibition*.

Communication orale et président de séance.

Seq. #334 : Microbiology/Immunology – Oral Microbes and Systemic Disease.

Vancouver, juin 2019.

Voir en annexe B, page 64.

Communications nationales

- Microbiote sous-gingival et surcharge en fer chez des patients hémochromatosisques. *3^e Journée Scientifique des Hôpitaux Universitaires du Grand Ouest (HUGO)*.

Communication affichée.

Rennes, novembre 2017.

Voir en annexe C, page 66.

- Periopathogens and clinical parameters in chronic periodontitis – An exploration of complexity. *Journées du Collège National des Enseignants en Sciences Biologiques Odontologiques*.

Communication affichée.

Rennes, octobre 2018.

- Periodontitis and haemochromatosis – a potential link through iron homeostasis. *Congrès de l'Association Dentaire Française*.

Communication orale.

Paris, novembre 2018.

- Alveolar bone status in knocked-out mice with iron overload. *Forum des Jeunes Chercheurs en Odontologie*.
Communication affichée.
Marseille, octobre 2019.
Voir en annexe [D](#), page [68](#).

Bourses et appels à projet

En tant que porteur de projet :

- Appel d'offres du Comité de la recherche clinique et translationnelle du CHU de Rennes
 - Projet MicrObes : microbiome buccal chez l'enfant de 12 ans, en association avec le surpoids et l'obésité
 - Porteur du projet
 - Bourse de 39 000 euros
 - Année d'obtention : 2018

En tant que partenaire du projet :

- Appel à projets de l'Institut Français pour la Recherche en Odontologie
 - Caractérisation des mécanismes impliqués dans la survenue et la sévérité des parodontites dans des souris *Hfe^{-/-}*
 - Porteur du projet : Sandrine DAVID-LE GALL
 - Bourse de 15 000 euros
 - Année d'obtention : 2016
- Appel à projets Sciences Humaines et Sociales 2018 France Parkinson
 - Projet Bucco-Park : Impact de l'éducation thérapeutique buccodentaire sur l'évolution clinique et le devenir du microbiote de patients parkinsoniens stimulés
 - Porteur du projet : Manon AUFFRET
 - Bourse de 44 800 euros
 - Année d'obtention : 2018
- Recherche Hospitalo-Universitaire en Santé – ANR
 - Consortium iVasc : Innovations in Atherothrombosis Science
 - WorkPackage 4 : Athérombose et santé orale
 - Porteur : Assistance Publique Hôpitaux de Paris
 - Bourse de 100 000 euros
 - Année d'obtention : 2016

Table des matières

Production scientifique	i
Table des matières	v
Table des figures	vii
1 Introduction et problématique	1
1.1 Le microbiote buccal	2
1.2 La maladie parodontale	6
1.3 Fer, bactéries et cavité buccale	10
1.4 Hémochromatose héréditaire et maladie parodontale	17
1.5 Problématique et objectifs	21
1.6 Références	22
2 Observations chez l'Homme	33
2.1 Increased transferrin saturation is associated with subgingival microbiota dysbiosis and severe periodontitis in genetic haemochromatosis, <i>Scientific Reports</i> 2018	34
2.2 Periodontal pathogens and clinical parameters in periodontitis, <i>Molecular Oral Microbiology</i> 2019	37
2.3 Références	40
3 Modèles expérimentaux chez la souris	41
3.1 Alteration and loss of mandibular alveolar bone in <i>Hfe</i> knocked-out mice. A pilot study. Soumis dans <i>Journal of Clinical Periodontology</i>	42
3.2 Oral dysbiosis model with <i>Porphyromonas gingivalis</i> is strain-dependent, soumis dans <i>Journal of Dental Research</i>	45
3.3 Références	47

4 Perspectives	49
4.1 Croisement des modèles animaux	50
4.2 Lien entre microbiotes oral et digestif	52
4.3 Dysbioses induites par <i>Porphyromonas gingivalis</i> et altérations de l'état général	53
4.4 Études à long terme et prospectives	54
4.5 Références	56
Conclusion	60
Appendices	62
A Communication affichée au <i>Oral Health Research Congress</i> de Vienne	62
B Communication orale à la 97^e session générale de l'<i>IADR</i> à Vancouver	64
C Communication affichée à la Journée Scientifique des Hôpitaux Universitaires du Grand Ouest	66
D Communication affichée au Forum des Jeunes Chercheurs en Odontologie	68
E Première version du manuscrit adressé au <i>Journal of Clinical Periodontology</i>	70
F Commentaires des relecteurs du <i>Journal of Clinical Periodontology</i>	101
G Accusé de réception du manuscrit révisé soumis à <i>Journal of Clinical Periodontology</i>	104
H Accusé de réception du manuscrit soumis à <i>Journal of Dental Research</i>	106

Table des figures

1.1 Publications sur le microbiote oral	3
1.2 La maladie parodontale	6
1.3 Régulation du taux de fer plasmatique par l'hepcidine	11
4.1 Méthodologie de l'expérimentation de croisement des modèles <i>Hfe</i> ^(-/-) et parodontite induite.	51

Chapitre 1

Introduction et problématique

Sommaire

1.1	Le microbiote buccal	2
1.1.1	Le microbiote buccal : bases fondamentales et applications en physiopathologie, <i>EMC Traité de Médecine Buccale</i> 2019	4
1.2	La maladie parodontale	6
1.2.1	Signature of Microbial Dysbiosis in Periodontitis, <i>Applied and Environmental Microbiology</i> 2017	7
1.3	Fer, bactéries et cavité buccale	10
1.3.1	Un enjeu nutritionnel pour les bactéries et leur hôte	10
1.3.2	Séquestration immunitaire du fer	12
1.3.3	Stratégies bactériennes d'acquisition	13
1.3.4	Le fer dans la cavité buccale	14
1.3.5	Pathogènes parodontaux et fer	15
1.4	Hémochromatose héréditaire et maladie parodontale	17
1.4.1	Periodontal status and serum biomarkers levels in <i>HFE</i> hemochromatosis patients. A case-series study, <i>Journal of Clinical Periodontology</i> 2017	19
1.5	Problématique et objectifs	21
1.6	Références	22

1.1 Le microbiote buccal

Le microbiote désigne l'ensemble des micro-organismes vivants qui composent un environnement. Sa définition est assez large, puisqu'elle englobe, en principe, les bactéries, les archées, les virus, les levures et les autres eucaryotes unicellulaires. Il est souvent confondu avec le terme microbiome, qui représente l'ensemble de l'information génétique contenue dans les micro-organismes. Au sein du microbiote, les procaryotes, et plus particulièrement les bactéries, sont majoritairement étudiés. De ce fait, le terme bactériome serait plus approprié, et à mettre en parallèle de l'archéome, du virome, du mycobiome, etc.

La sur-représentation des bactéries dans l'étude du microbiote n'est pas un hasard. Elle tient compte du poids historique que représente la bactériologie dans la santé humaine : dans la recherche sur les agents infectieux, bien sûr, mais également sur les micro-organismes résidents. Le site de colonisation que représente le tube digestif a toujours concentré les efforts de recherche à propos de la communauté bactérienne qui y est naturellement présente. Celle-ci a longtemps été nommée flore, ou microflore, intestinale. Elle deviendra progressivement le microbiote intestinal, au fur et à mesure du délaissement des méthodes d'analyse par culture, pour la biologie moléculaire [1].

La prédominance des bactéries dans l'étude du microbiote découle aussi de la méthodologie employée : sélection d'une portion de génome des micro-organismes, clonage, séquençage, puis identification par comparaison avec des bases de données. Chez les bactéries — et les archées —, le gène codant pour l'ARNr 16S est un candidat parfait. Il est à la fois universel, car composant essentiel du ribosome, et spécifique à chaque espèce, grâce aux régions variables présentes dans sa séquence. Quant aux bases de données recensant les séquences génétiques déjà connues, elles n'ont cessé de croître au fur et à mesure des publications. Profitant des débuts de l'internet, le « *Ribosomal Database Project* » (RDP, <https://rdp.cme.msu.edu>) a été initié en 1993 [2]. Il comptait déjà les séquences codantes pour la sous-unité du ribosome d'environ 1 400 bactéries et 100 archées, mais aussi de 350 eucaryotes, toutes mises à la disposition des chercheurs, sous réserve d'une connexion FTP et de la possession d'une adresse mail. Celle-ci servait alors de mot de passe. Sa plus récente version (version 11.5, <https://rdp.cme.msu.edu/index.jsp>) recense 3 358 809 séquences, correspondant à 12 681 espèces bactériennes et 531 archées.

Initialement, le champ d'application de ces méthodes de biologie moléculaire, et notamment l'utilisation du gène de l'ARNr 16S, a été l'écologie environnementale, avec l'exploration des écosystèmes marins ou du sol [3, 4]. Quel que soit le site de prélèvement, les conclusions étaient unanimes : les méthodes traditionnelles, par culture, avaient sous-estimé la biodiversité des milieux. De fait, que ce soit par manque de nutriments, de partenaires ou par antagonisme, l'identification après culture omettait les micro-organismes n'ayant pas réussi à se développer. C'est ainsi que nombre d'espèces bactériennes, non encore cultivables (ou en passe de l'être [5]), ont été découvertes. Rapidement, la même méthodologie a été employée avec des échantillons

humains. Toujours en utilisant le 16S, en séquence partielle, puis complète, les conclusions précédentes ont pu être élargies : la diversité bactérienne de la flore intestinale avait aussi été jusque là sous-estimée [6, 7].

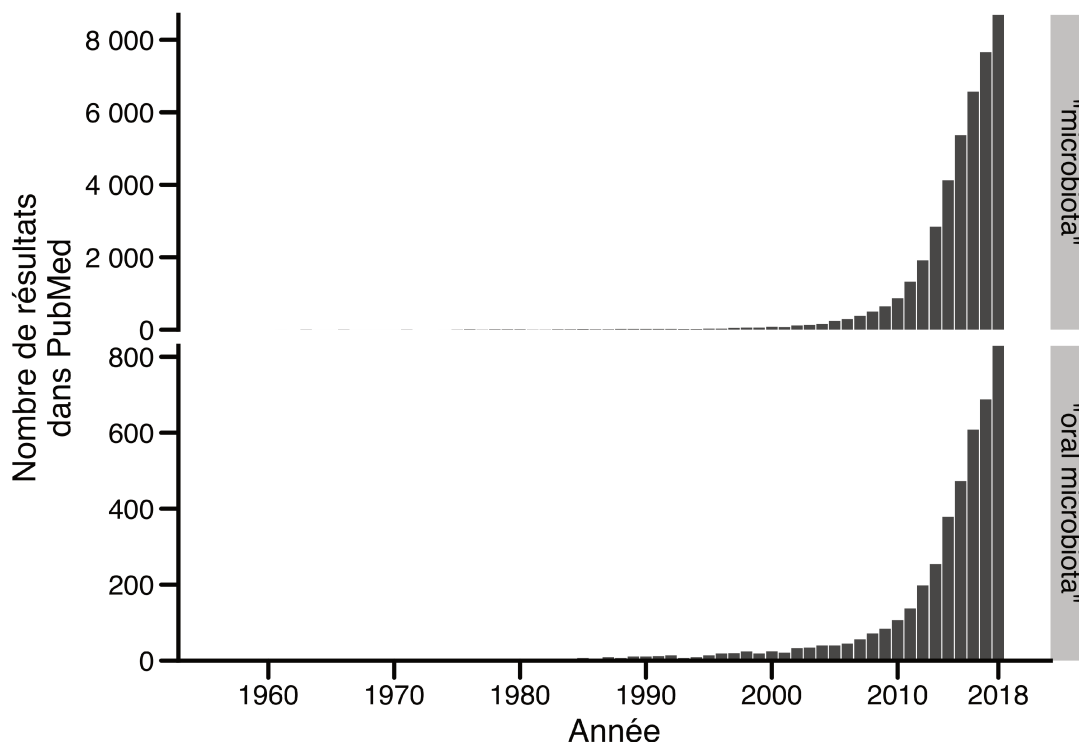


FIGURE 1.1 – Répartition par année du nombre de résultats renvoyés par PubMed (<https://www.ncbi.nlm.nih.gov/pubmed/>), avec les termes de recherche « *microbiota* » et « *oral microbiota* ».

Le sujet du microbiote a néanmoins pris son essor à partir de 2010 avec l'arrivée du séquençage de masse, permis par la seconde génération de séquenceurs. En remplaçant la méthode de Sanger, ces machines ont simplifié l'analyse en réduisant les coûts, les délais, et en augmentant la quantité d'ADN séquencé. Champ disciplinaire à part entière, des équipes sont maintenant spécialisées en microbiote digestif, cutané, nasal, vaginal, etc. L'étude de la flore buccale n'a pas échappé à cette révolution, et elle a même pris le train en marche. En témoigne l'accroissement du nombre de publications relatives au microbiote buccal, dont la courbe se superpose avec celle du microbiote humain en général (voir la Figure 1.1).

La recherche en Odontologie à Rennes a depuis longtemps une expertise sur la bactériologie buccale, et plus particulièrement la culture en anaérobie de pathogènes parodontaux comme *Porphyromonas gingivalis* et *Treponema denticola*. Le laboratoire a suivi l'évolution des techniques. Des prélèvements sous-gingivaux en vue d'analy-

ser la composition du microbiote sous-gingival ont ainsi été réalisés dès 2010-2011¹. Plus récemment, la méthodologie d'analyse du microbiote (biologie moléculaire et bioinformatique) a également été mise en place. Dans ce cadre, l'intégration des outils de bioinformatique dans notre environnement de travail a permis de créer une plateforme d'analyse apte à recevoir des échantillons externes. Parmi ces outils, citons : « *Quantitative Insights Into Microbial Ecology* » (QIIME1 puis QIIME2, <https://qiime2.org/>), *mothur* (<https://mothur.org/>) et *Cytoscape* (<https://cytoscape.org/>).

Aujourd'hui, après presque dix ans d'analyse par les nouvelles générations de séquençage (NGS), l'apport de ces outils est indéniable. Les variations de composition du microbiote buccal au cours de la vie et dans les différents sites de la cavité buccale, ainsi que sa relation avec l'hôte et son implication dans des maladies, locales (carie et parodontite) et à distance (liens microbiote buccal et maladies systémiques), sont autant d'éléments nouveaux. Récemment, nous avons réalisé un état des lieux des connaissances acquises et de notre expérience personnelle. Le résultat de ce travail est présenté dans la section suivante.

1.1.1 Le microbiote buccal : bases fondamentales et applications en physiopathologie, *EMC Traité de Médecine Buccale 2019*

Cette revue de littérature a été publiée le 20 décembre 2019 dans le *Traité de Médecine Buccale* de l'*Encyclopédie Médico Chirurgicale* (<https://www.em-consulte.com/article/1340101/>).

L'approfondissement des connaissances sur le microbiote, bien que le sujet soit finalement encore jeune, aura probablement un impact sur notre pratique clinique. Comme le mentionne la conclusion de cette revue de littérature, les progrès couplés de la bioinformatique et des intelligences artificielles auront une application pratique dans nos cabinets dentaires, comme elles en ont déjà dans d'autres domaines médicaux [8]. L'incidence des NGS sur notre travail de microbiologiste est déjà évident : devenus également bioinformaticiens, nous passons souvent plus de temps devant un écran d'ordinateur que devant une paillasse. Mais, il est nécessaire de rester critique vis-à-vis de certaines conclusions obtenues par des algorithmes, qui nous fournissent cependant des hypothèses de travail. Il est alors important de revenir à la culture *in vitro* et à des modèles *in vivo* pour pouvoir les évaluer.

Dans un article paru dans *Periodontology 2000* et qui faisait l'introduction du numéro de juin 2000, les auteurs s'enthousiasmaient de voir réemerger la « *médecine parodontale* » [9]. Un concept simple, et ancien, reconnaissant l'apport de la maladie parodontale, ou de la cavité buccale, dans l'état de santé générale de l'individu. Le lien entre santé parodontale et santé générale était pourtant devenu anecdotique lors du dernier siècle. Mais, à l'occasion de nouvelles recherches, il est redevenu une théorie

1. Voir à ce sujet l'analyse de ces échantillons dans le travail présenté dans la section 2.1 [Increased transferrin saturation is associated with subgingival microbiota dysbiosis and severe periodontitis in genetic haemochromatosis, *Scientific Reports* 2018](#) en page 34.

acceptable. Les auteurs relevaient l'importance de cette nouvelle, en faisant référence aux associations entre parodontite et maladies cardiovasculaires, diabète ou naissance prématurée qui avaient été publiés peu de temps auparavant [10–12]. Et ces mêmes auteurs de plaider pour de nouvelles stratégies de diagnostic et de traitement, reconnaissant le lien entre maladie parodontale et maladies systémiques. Ce constat est toujours d'actualité, et s'il est un élément qui participe significativement à la compréhension de ce concept, c'est bien l'étude du microbiote buccal.

Le microbiote buccal : bases fondamentales et applications en physiopathologie

Émile BOYER, Martine BONNAURE-MALLET et Vincent MEURIC

6 954 mots

48 494 caractères (espaces compris)

24 pages

10 figures

INTRODUCTION

La cavité buccale est la deuxième communauté bactérienne la plus diversifiée du corps humain, abritant plus de 700 espèces de bactéries qui colonisent les surfaces dentaires dures des dents et les tissus mous de la muqueuse (1). Ce sont plus de 10^8 bactéries qui sont retrouvées dans un millilitre de salive. Ces bactéries de la cavité buccale ont initialement été visualisées, il y a maintenant plus de trois siècles, par Van Leeuwenhoek qui décrivait alors des « animalcules ». Elles sont bien connues des chirurgiens-dentistes dans la plaque dentaire qui recouvre les dents, et sont considérées comme responsables des pathologies buccales telles que caries, gingivite et parodontite. Cette plaque dentaire est aussi appelée biofilm dentaire ; ce dernier comprenant les bactéries et la matrice extracellulaire dans laquelle les bactéries sont engluées. Aujourd'hui, le terme le plus approprié pour parler de l'ensemble des micro-organismes de la cavité buccale est le « microbiote buccal ». Le microbiote buccal comprend l'ensemble des micro-organismes vivants (bactéries, virus, archées, protozoaires). Le microbiome est la somme des micro-organismes, de leur information génétique et de l'environnement dans lequel ils interagissent. C'est donc l'ensemble de la communauté écologique de micro-organismes commensaux, symbiotiques et pathogènes, qui partage l'espace corporel (2).

L'étude des bactéries buccales a commencé par la culture et l'identification (méthodes pasteurienne). Les techniques de biologie moléculaire ont permis de gagner en rapidité avec le développement de la Polymerase Chain Reaction (PCR – 1985) ou encore de l'hybridation de sondes ADN spécifiques pour identifier des bactéries déjà connues (3). Puis, le clonage et séquençage de l'ADN ont permis la découverte de nouvelles espèces. L'émergence de nouvelles technologies de séquençage à très haut débit (NGS) dans les années 2000, et largement utilisées à partir de 2010, associée à la bioinformatique, permet aujourd'hui de visualiser rapidement et à moindre coût l'ensemble des microbiotes (**Figure 1**). Ce développement d'expertise et de la compréhension des microbiotes humains a été réalisé grâce au Human Microbiome Project (HMP) aux USA (4) et au projet MetaHIT (Metagenomics of the Human Intestinal Tract) en Europe (MetaHIT Consortium – <http://www.metahit.eu>). Les travaux réalisés avec les NGS utilisent soit le pyroséquençage (454, Roche), soit le séquenceur par terminateur réversible (MiSeq, Illumina). Ils permettent la lecture de plusieurs millions de séquences en parallèle et sans *a priori*. C'est le gène de l'ARN ribosomal 16S (ARNr 16S) qui est utilisé comme un « code barre », chaque espèce bactérienne possédant sa propre variation de l'ARNr 16S. Son séquençage sans distinction permet de détecter et classer l'ensemble des bactéries sous forme de « variants », y compris des espèces non cultivables (qui représentent plus du tiers des bactéries buccales) voire inconnues jusqu'alors ; citons par exemple les membres du phylum TM7 qui auraient un rôle dans la maladie parodontale (5). Aujourd'hui, ce sont plus de 1 500 taxons (Table 1) qui sont distingués dans la base de données de l'HOMD (Human Oral Microbiome Database).

Règne	Phylum	Classe	Ordre	Famille	Genre	Espèce	Souche
Bacteria	Bacteroidetes	Bacteroidetes	Bacteroidales	Porphyromonadaceae	Porphyromonas	gingivalis	ATCC308
Bacteria	Firmicutes	Bacilli	Lactobacillales	Streptococcaceae	Streptococcus	mutans	ATCC25175

Table 1 : Classification taxonomique. L'utilisation des NGS ne permet pas à chaque fois d'identifier avec certitude la bactérie précise. Le rang taxonomique supérieure lui est alors attribué afin d'éviter tout erreur d'interprétation. Ici, deux exemples de taxonomie pour des bactéries souvent citées dans la littérature : *Porphyromonas gingivalis* et *Streptococcus mutans*.

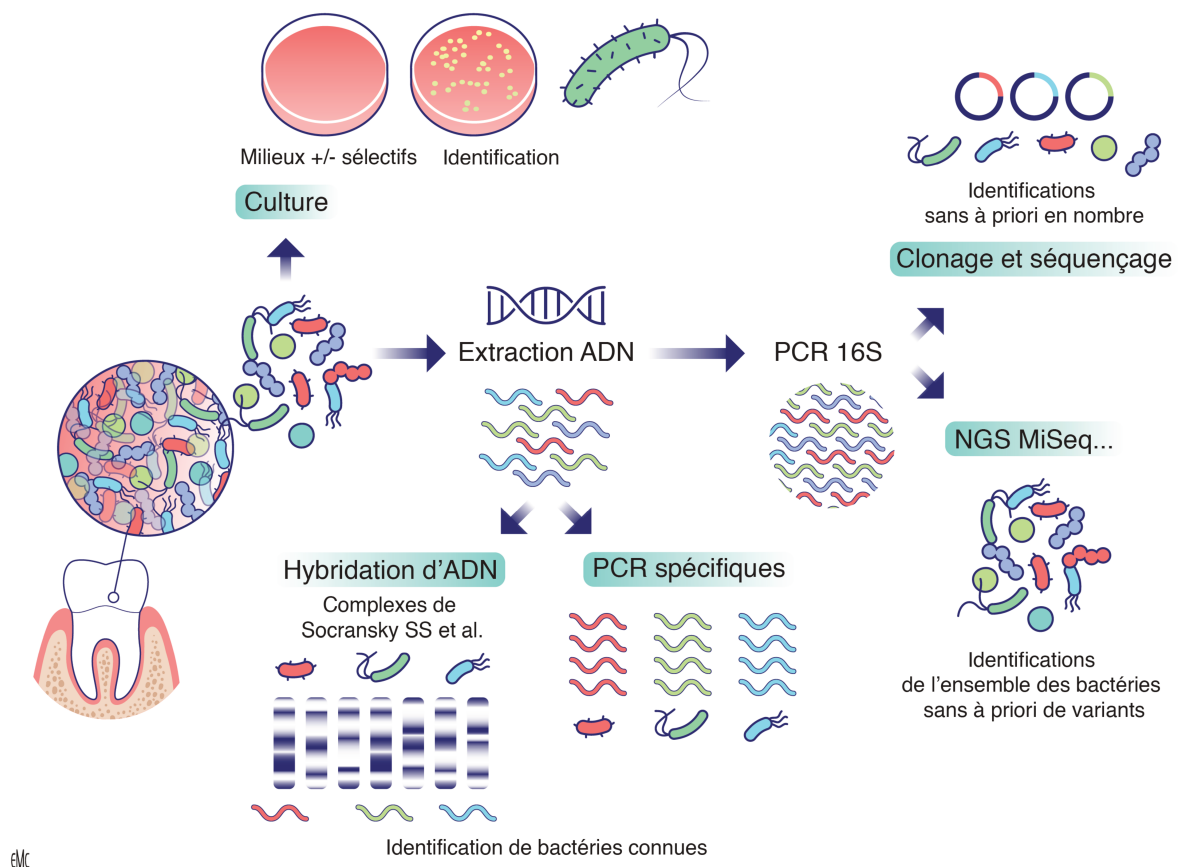


Figure 1 : Méthodologies d'étude du microbiote. ADN : acide désoxyribonucléique ; PCR : Polymerase Chain Reaction ; NGS : nouvelles générations de séquençage.

La méthode d'étude du microbiote par séquençage du gène de l'ARNr 16S permet une analyse extrêmement fine et détaillée de l'ensemble des bactéries présentes. Cependant, elle est sujet à contamination possible à chacune des étapes (prélèvement, extraction de l'ADN bactérien, PCR, séquençage haut débit, traitement bioinformatique) et doit être réalisée avec une grande précaution. En effet, lors du prélèvement de la plaque dentaire sous gingivale, c'est-à-dire du contenu de la poche parodontale, une contamination par la plaque supra-gingivale ou de salive peut fausser les résultats. De plus, l'analyse bioinformatique, qui requiert des compétences en informatique et en biologie, est encore réservée à des spécialistes (laboratoires de recherche et centres hospitalo-universitaires) mais devrait se démocratiser dans les années à venir.

ACQUISITION DU MICROBIOTE BUCCAL

L'acquisition du microbiote buccal primaire est encore à ce jour très controversée. En effet, certaines études ont montré la présence de bactéries d'origine buccale au niveau placentaire, suspectant des bactériémies de bas grade chez la femme enceinte. Ces dernières permettraient ainsi la colonisation placentaire, du liquide amniotique, puis de la cavité buccale de l'enfant à naître. Ces études ont d'abord réalisé une détection *via* l'ADN bactérien, par PCR spécifiques, puis par NGS (6,7). Des observations au microscope réalisées sur des échantillons de placentas par une équipe de l'hôpital de St Louis ont ensuite confirmé la présence de bactéries intracellulaires dans un tiers des échantillons (8). La présence de ces bactéries intracellulaires n'était pas liée à un accouchement prématuré ou à terme. Une étude de 2016 a affiné ces résultats en analysant la composition microbienne du placenta et du liquide amniotique, à la fois par culture conventionnelle et par NGS, provenant de 15 femmes enceintes ayant accouché par césarienne (9). Les critères de sélection excluaient alors toute pathologie ou événement ayant pu aboutir à la contamination des échantillons, comme, par exemple, la rupture de la membrane amniotique. Cependant, de nombreux chercheurs évoquent la possibilité de contamination à d'autres points du processus d'analyse des échantillons, comme lors de l'extraction de l'ADN. Par ailleurs, des résultats contradictoires ont été publiés en 2018, à nouveau à propos d'échantillons de liquide amniotique (10). Tandis que des bactéries étaient détectées dans les échantillons présentant des antécédents de rupture de la membrane amniotique, aucune trace significative de présence bactérienne n'était présente dans les échantillons provenant de cavités amniotiques intactes, ni par détection d'ADN, ni par culture. Ainsi, sans complication pendant la grossesse, la colonisation microbienne commencerait préférablement après la rupture de la membrane amniotique.

Il est cependant admis qu'il n'y a pas une mais plusieurs sources potentielles de microbiotes : maternels (vaginal en cas de naissance par voie basse, cutané en cas de césarienne, mais également par le lait maternel (11)) et environnementaux (accouchement à l'hôpital, à domicile,...). Autant d'éléments qui se combinent pour assurer la colonisation de la cavité buccale de l'enfant. Par la suite, l'environnement buccal précoce est fortement façonné par la mère (jusqu'à 85% de microbiote commun) (12). Avant l'éruption des dents, seules les bactéries majoritairement aérobies et ayant un fort tropisme pour les cellules épithéliales pourront coloniser la cavité buccale, notamment les genres *Streptococcus* (*S. salivarius*, *S. mitis*, *S. epidermidis*) puis *Fusobacterium* (13). Parmi ces colonisateurs précoces, certains streptocoques (en particulier *S. salivarius*) sont favorisés par les premiers sucres ingérés (14). Ils facilitent par la suite l'installation des *Veillonella* et des *Lactobacillus* ; ces derniers pouvant être initialement acquis lors de l'accouchement (14).

TOPOGRAPHIE

À l'âge de 6 mois, l'arrivée des premières dents change drastiquement la morphologie de l'écosystème existant. La création de nouvelles niches – pseudo-poches puis sillons gingivo-dentaires contenant du fluide gingival (potentiellement du

sang), surfaces dures dentaires non desquamantes lisses ou sillons occlusaux – représente autant de nouvelles surfaces aux caractéristiques physico-chimiques nouvelles à coloniser. L'alimentation solide est également introduite à cet âge. Théoriquement associée à l'hygiène bucco-dentaire, elles vont profondément influencer le microbiote (15). Le microbiote buccal est caractérisé par une variabilité élevée et les connaissances actuelles indiquent qu'il atteint vers l'âge de 2 ans une stabilité proche de celle observée chez l'adulte (14). Globalement, la diversité et la richesse bactérienne augmentent et divergent du microbiote maternel lors du développement de la cavité buccale.

Ainsi, la cavité buccale abrite plusieurs micro-niches où le pH, l'oxygène, la température ou le potentiel d'oxydo-réduction peuvent influencer sur l'installation et le développement des micro-organismes et sur le risque de maladie (16). D'une part, les différentes structures que sont la langue, les dents, les muqueuses, le palais et la gencive (supra ou sous gingivale) se sont avérés, tant par la culture que par des approches moléculaires, abriter des microbiotes distincts (17). D'autre part, les facteurs environnementaux peuvent varier au sein d'une même structure, affectant la composition du microbiote. Simón-Soro *et coll.* ont montré en effet que la proportion d'un anaérobie obligatoire comme *Fusobacterium* est plus important dans le sillon gingivo-dentaire lingual, alors que les aérobies et anaérobies facultatifs, tel que *Streptococcus*, sont beaucoup plus communs du côté vestibulaire (18). Ces variations peuvent être expliquées par une plus grande exposition à l'oxygène du versant vestibulaire. Elles sont un exemple, parmi d'autres, des micro-niches présentes dans la cavité buccale et de l'influence du site de prélèvement.

LA SALIVE

Bien que la bouche comporte plusieurs micro-niches distinctes, la salive peut néanmoins être considérée comme une alternative intéressante à la multiplication des sites de prélèvements : elle serait représentative d'une dispersion des bactéries et des métabolites provenant d'autres niches buccales et pourrait donner accès à l'ensemble du microbiote buccal (19). Les genres les plus communs – et généralement les plus abondants – sont *Streptococcus*, suivi des *Prevotella*, *Haemophilus*, *Neisseria* et des *Veillonella* (20). Ces genres représentent ce qu'on appelle le noyau du microbiote (« *core microbiome* ») salivaire, sa portion la plus prévalente. Plusieurs auteurs ont ensuite cherché dans des études à grande échelle, à dresser des profils spécifiques, propres à différents groupes d'individus classés selon leur mode de vie, leur état bucco-dentaire, etc. Dans le cadre d'une étude de cohorte menée depuis 1961 dans la ville d'Hisayama au Japon, l'étude du microbiote salivaire de 2 344 individus (âgés de 40 ans et plus) a montré un enrichissement en genre *Neisseria* dans des conditions de parodonte sain (21). Les genres *Prevotella* et *Veillonella* augmenteraient, à l'inverse, dans les cas de maladies parodontales. Dans une population de 1 500 adolescents espagnols (âgés de 13 à 15 ans), Willis *et coll.* ont identifié deux profils salivaires distincts (22). De la même manière que dans l'étude japonaise, les auteurs ont noté que les genres à l'origine des plus grandes variations étaient les genres *Neisseria* et *Prevotella*, chacun étant marqueur de l'un des deux profils. Les auteurs ne précisent cependant pas l'état bucco-dentaire des participants. Zaura *et coll.* décrivent quant à eux cinq profils distincts à partir des échantillons de 268 néerlandais âgés de 18 à 32 ans et indemnes de pathologie orale (23). Dans cette étude, le niveau

d'analyse taxonomique descend jusqu'à l'espèce. Néanmoins, les espèces représentatives de ces cinq profils appartiennent également aux genres précédemment cités : *Neisseria*, *Prevotella*, *Veillonella*, mais aussi *Streptococcus* et *Haemophilus*.

L'hygiène et les habitudes alimentaires, mais également la qualité de l'eau de boisson (eau du robinet) seraient les principaux facteurs influençant ces microbiotes salivaires dans l'étude de Willis (22). À l'inverse, Zaura *et coll.* ne relevaient pas d'association entre les habitudes alimentaires des participants et le classement de leur microbiote salivaire dans tel ou tel profil (23). L'analyse des paramètres biochimiques de leur salive (flux salivaire, pH, enzymes salivaires) présentée dans la publication illustre, à nouveau, l'adaptation des communautés microbiennes à leur environnement. Une fois entrée dans un modèle statistique, la composition du microbiote permettait aux auteurs de prédire avec une précision correcte le pH et l'activité lysosomale salivaires.

Ces communautés appelées « *stomatotypes* » font référence aux entérotypes qui ont été décrit précédemment au niveau intestinal, mais ne font pas encore consensus (24). D'une part, les compositions de ces microbiotes salivaires sont souvent discutées par les chercheurs, car ils peuvent être considérés comme étant une approximation sommaire des communautés de biofilms issues des différentes niches buccales. D'autre part, le regroupement en différents stomatotypes est soumis à un algorithme statistique. Les résultats (nombre de stomatotypes, constitution des groupes) peuvent donc varier selon l'algorithme utilisé et les paramètres choisis par les chercheurs. Dans une étude allemande de 2017, le nombre optimal de stomatotypes était lui-même estimé par un algorithme statistique (25). Les groupes ainsi définis par leur microbiote séparaient cependant de manière significative les individus souffrant ou non de parodontite.

ORGANISATION DE BIOFILM SAIN

Classiquement, les biofilms buccaux commencent par la mise en place de la Pellicule Acquisée Exogène (PAE) sur laquelle l'attachement de *Streptococcus* et d'*Actinomyces* peut avoir lieu ; ils sont ainsi qualifiés de colonisateurs primaires. Ces micro-organismes servent de substrat pour permettre ensuite l'adhérence de colonisateurs secondaires tels que *Fusobacterium nucleatum*. Ce dernier présente des capacités de liaisons multiples, à la fois avec les colonisateurs précoces et tardifs.

Avec les premières analyses des biofilms par séquençage, le Human Microbiome Project (HMP) a généré des ressources pour faciliter la caractérisation du microbiote humain, et qui sont aujourd'hui presque indispensables. Cet organisme a mis à la disposition de la communauté les résultats de séquençage des microbiotes prélevés sur différents sites du corps (cavité buccale, fosses nasales, peau, etc.) de plus de 300 individus sains. Parmi leurs données, des séquençages d'échantillons de biofilms supra et sous-gingival sont disponibles. La majorité des genres bactériens présents dans ces deux biofilms est représentée sur la **Figure 2** (genres bactériens dont la proportion moyenne dépasse 1% du microbiote total).

l'identité des voisins avec lesquels ils interagissent classiquement et du milieu (sillon gingivo-dentaire, surface occlusale, etc.) qui influencera ces biofilms dans le maintien de la santé ou la progression vers la maladie.

Aujourd'hui, le microbiote supra-gingival est le mieux caractérisé à l'échelle microscopique (de par son accès facile). Welch *et coll.* ont proposé une structure bien déterminée, non liée au hasard, en forme de « hérisson » (29). Le genre *Corynebacterium*, bactérie filamenteuse semble être un élément essentiel à la structure. Les bactéries du genre *Corynebacterium* se lient à un biofilm existant contenant principalement des *Streptococcus* et des *Actinomyces*. En périphérie, des structures en épis de maïs (**Figure 3**) se forment au contact des *Corynebacterium* avec des *Porphyromonas* et des *Streptococcus* eux-mêmes liant des *Haemophilus* et/ou *Aggregatibacter*. Des *Neisseriaceae* sont également présents sous forme de grappes, en périphérie de la structure du biofilm. Les *Streptococcus* vont créer un microenvironnement riche en CO₂, lactate et acétate contenant également du peroxyde mais surtout pauvre en oxygène. Les filaments allongés de *Fusobacterium* et de *Leptotrichia* peuvent alors proliférer dans cet anneau à basse teneur en oxygène et riche en CO₂, dans l'immédiate proximité de la périphérie contenant les épis de maïs. Finalement, au niveau de cette anneau, les conditions physico-chimiques sont favorable aux bactéries capnophiles et les *Capnocytophaga* vont proliférer abondamment. La base de cette structure est dominée par des filaments de *Corynebacterium* et est peuplée par addition de bactéries filamenteuses et de cocci (**Figure 4**).

Les travaux menés sur le biofilm sous-gingival n'ont pu l'être que sur des dents extraites. Dans une étude de 2010, Zijngge *et coll.* ont décrit une architecture en quatre couches (30). Trois d'entre elles se situant entre la dent et la muqueuse gingivale (couches basale, intermédiaire et supérieure), et une couche extérieure. Les auteurs identifient différentes espèces dans chaque couche : *Actinomyces* dans la couche basale, *Fusobacterium nucleatum* et *Tannerella* dans la couche intermédiaire, *Cytophaga*, *Flavobacterium*, *Bacteroides* et *Synergistetes* dans la couche supérieure, *Spirochaetes* dans la couche extérieure. Les bactéries paropathogènes connus ou présumés (*Porphyromonas gingivalis*, *Porphyromonas endodontalis*, *Prevotella nigrescens*, *Prevotella intermedia*, *Parvimonas micra*) sont essentiellement situés dans les couches supérieures, colonisateurs d'un biofilm déjà formé.

Finalement, c'est un nombre modeste de taxons abondants qui constitue la nette majorité des bactéries dans ces structures. Ces taxons sont disposés dans un cadre spatial organisé, dans lequel chaque micro-organisme occupe une position caractéristique permettant aux autres de se développer.

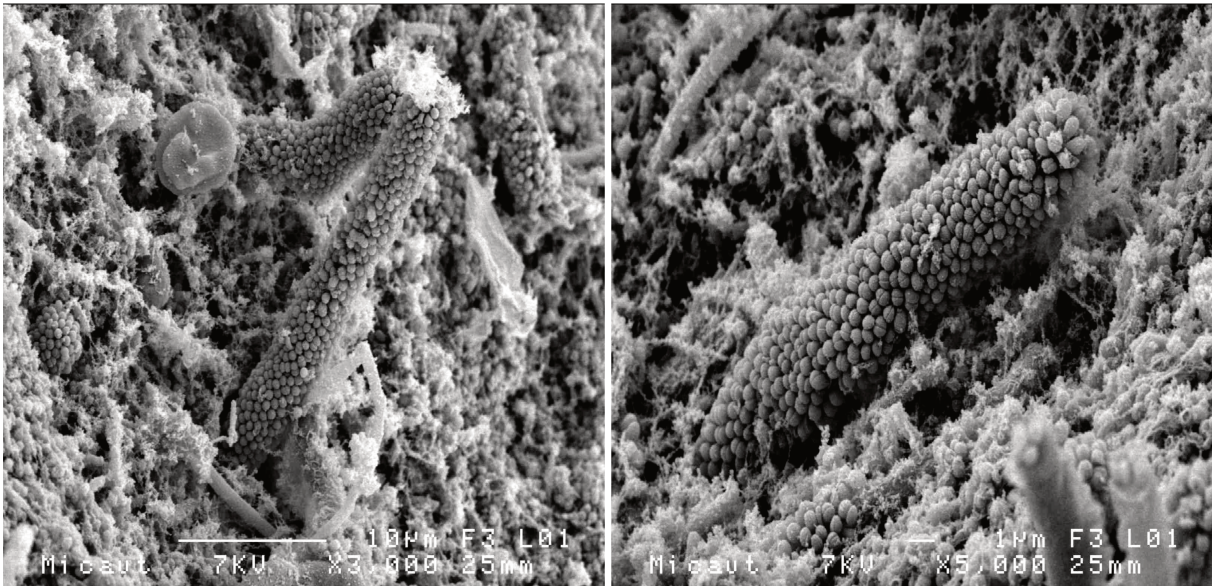


Figure 3 : Structures en épis de maïs (Université de Rennes 1).

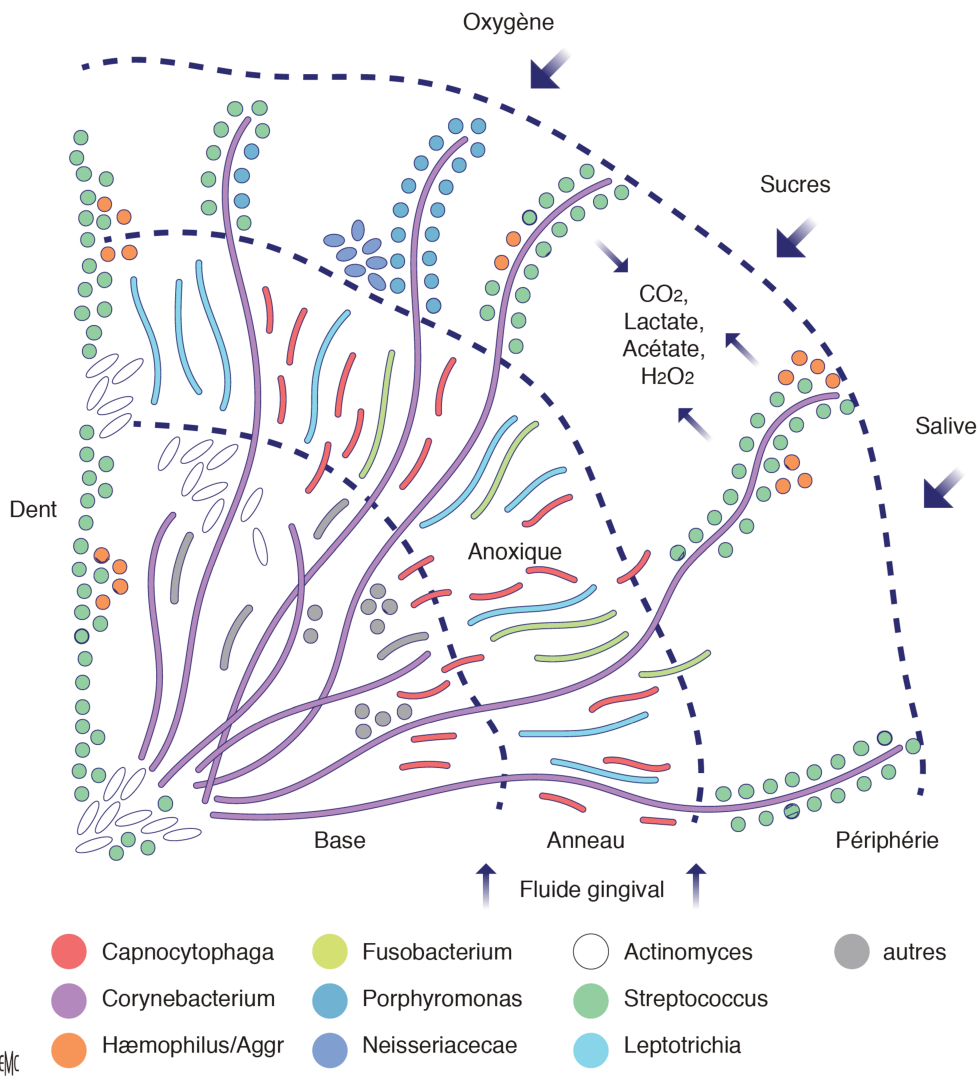


Figure 4 : Organisation spatiale du biofilm / microbiote supra-gingival proposé par Welch *et coll.* (31).

ETATS SAIN ET MALADE DU MICROBIOTE ORAL

Comment définir un état sain et un état malade. Alors que Pasteur et Koch ont identifié des germes spécifiquement responsables de pathologies infectieuses au cours du 19^e siècle, il est beaucoup plus difficile d'en faire autant en ce qui concerne les pathologies buccales telles que les maladies parodontales et les caries dentaires. En effet, comme nous l'avons vu dans les paragraphes précédents, la cavité buccale évolue avec la colonisation de bactéries en fonction de leur capacité à s'installer et se développer dans les différentes niches écologiques présentes. Les bactéries s'installent en symbiose avec l'hôte. Ainsi, les bactéries résidentes ont les deux activités pro et anti-inflammatoires qui sont cruciales pour le maintien de l'homéostasie de sites fortement colonisées telle que la cavité buccale. En raison de l'interaction du système immunitaire de l'hôte avec ses symbiotes microbiens, les infections aiguës de la muqueuse buccale sont plutôt rares, malgré la densité de colonisation microbienne. L'importance de ces interactions hôte-microorganismes est mise en évidence par des observations chez des patients immunodéprimés, qui peuvent faire l'expérience d'infections virales ou fongiques des muqueuses et d'infections buccales par des espèces allogènes (32). La salive et le fluide gingival fournissent des nutriments pour la croissance microbienne, mais contiennent également des composants possédant des activités antimicrobiennes. Cette dichotomie de l'écosystème buccal – tout à la fois nourricier et hostile – est nécessaire pour le développement d'un microbiote équilibré. L'équilibre complexe entre les espèces résidentes de la cavité buccale est responsable du maintien d'un état de santé (en symbiose ou eubiose) ou d'un état associé à une maladie (en dysbiose). Un microbiote dysbiotique est un microbiote dans lequel la diversité et les proportions relatives d'espèces ou de taxons dans le microbiote sont perturbées (33). Des changements biologiques vont affecter l'équilibre des espèces au sein de ces communautés bactériennes. Cela comprend les changements physiologiques – par exemple l'âge, ou les changements hormonaux de la puberté et de la grossesse – auxquels les sujets en bonne santé peuvent souvent s'adapter sans nuisance pour leur santé bucco-dentaire. Des facteurs modifiables peuvent également générer une dysbiose comme un dysfonctionnement des glandes salivaires (modifications du débit ou de la composition salivaire), une mauvaise hygiène buccale, une inflammation gingivale et certains modes de vie (habitudes alimentaires et tabagisme) (**Figure 5**).

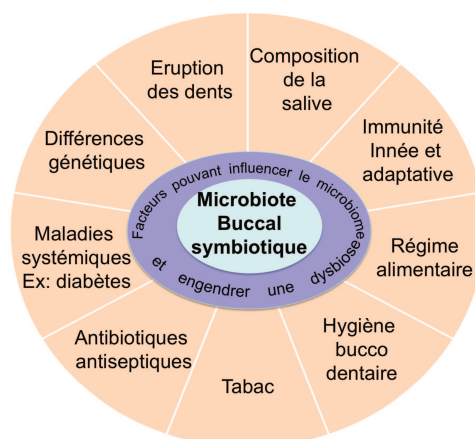


Figure 5 : Facteurs contribuant à la dysbiose (adapté de Marsh (34) et de Kilian *et coll.* (1)).

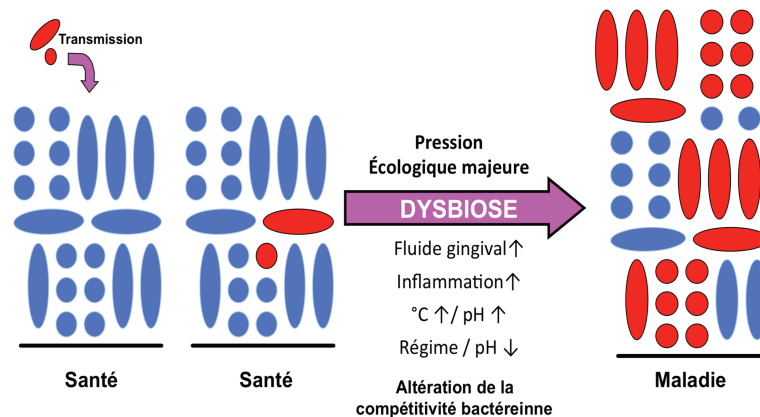


Figure 6 : Modèle de dysbiose (adapté de Marsh (34) et de Kilian *et coll.* (1)).

De nos jours, il est admis que des bactéries considérées historiquement comme pathogènes peuvent coloniser la cavité buccale sans être génératrices de maladie si leur nombre reste restreint et contenu par un microbiote en symbiose avec l'hôte (**Figure 6**). L'augmentation de leur nombre déséquilibrera le microbiote qui deviendra alors dysbiotique.

Exemple des caries dentaires.

Dans les caries, une augmentation de la consommation de sucre ou une réduction du flux salivaire entraîne la formation de biofilms exposés plus fréquemment et pour des durées plus longues à de faibles pH. Ceci sélectionne les organismes qui produisent eux-mêmes des acides ou sont plus tolérants à un environnement acide, aux dépens de bactéries qui se développent dans des conditions neutres ou contribuent à la neutralisation du pH (**Figure 7**).

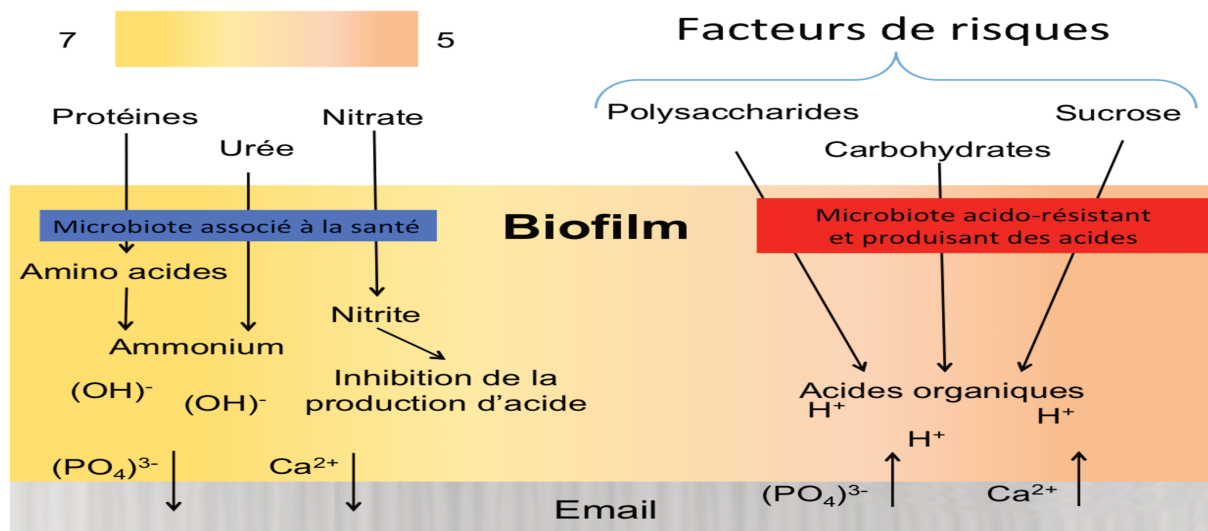


Figure 7 : Modèle d'interactions hôte-microbe dans la pathogenèse des caries.

Ainsi, certains auteurs considèrent les caries comme des troubles métaboliques de la communauté bactérienne (35). Historiquement, *Streptococcus mutans* est considéré comme le principal responsable de la carie dentaire depuis sa découverte en 1924. Cependant, l'abondance relative de *S. mutans* n'est pas toujours associée à la présence de caries dentaires. Ainsi, même si sa présence est un facteur défavorable pour la santé bucco-dentaire, il n'est plus considéré comme le seul agent responsable et de nombreux biofilms oraux cariogènes ont été caractérisés par leur activité métabolique et leur composition taxonomique. Dans une revue de littérature de 2018, Espinoza *et coll.* ont montré que des *Streptococcus*, les *Catonella morbi* et *Granulicatela elegans* étaient augmentés chez des patients présentant des caries dentaires (35). À une plus forte résolution, ce sont 119 espèces de *Streptococcus* qui ont pu être identifiées. Les abondances relatives de *S. parasanguinis*, *S. australis*, *S. salivarius*, *S. intermedius*, *S. constellatus* et *S. vestibularis* sont ainsi augmentées en présence de caries dentaires. Ces derniers ne représentent qu'à peine 5% des *Streptococcus*. Ainsi, l'apparition des caries ne peut pas être expliquée par la présence d'une seule bactérie, mais doit être expliquée comme la perturbation de l'ensemble de l'écosystème.

Exemple des maladies parodontales.

Dans les maladies parodontales, les mécanismes de dysbiose sont multiples et le cycle de ces maladies est présenté **Figure 8**. L'hygiène est un élément essentiel permettant de limiter l'accumulation de biofilm comprenant de nombreuses bactéries non spécifique qui seront à l'origine de la gingivite (36). À ce jour, la suite d'évènements amenant au passage à la parodontite est assez mal comprise.

Concernant les parodontites de haut grade (classification de Chicago 2018 (37), anciennement parodontites agressives), elles sont souvent associées dans les publications à une bactérie particulière : *Aggregatibacter actinomycetemcomitans*, et plus particulièrement au clone JP2 (38). Néanmoins, ces résultats sont contestés par d'autres équipes qui considèrent que la détection des pathogènes parodontaux ne permet pas encore de distinguer les différents grades des parodontites (anciennement, chroniques et agressives) (39).

Les parodontites concernent environ un adulte sur deux dans les pays industrialisés (40,41). Plusieurs pathogènes parodontaux ont été cités par le passé tels que *F. nucleatum*, *P. intermedia*, *Eubacterium nodatum*, *Campylobacter rectus* ou encore *P. gingivalis*, *Treponema denticola*, *Tannerella forsythia* ; les trois derniers appartenant au complexe rouge. Ce dernier, décrit en 1998 dans une étude de Socransky, s'est révélé être fortement associé aux mesures cliniques de la parodontite (3). À une époque où les techniques de détection bactérienne étaient pour la plupart *a priori* (Fig 1), les bactéries du complexe rouge sont longtemps restées les pathogènes clés de la parodontite.

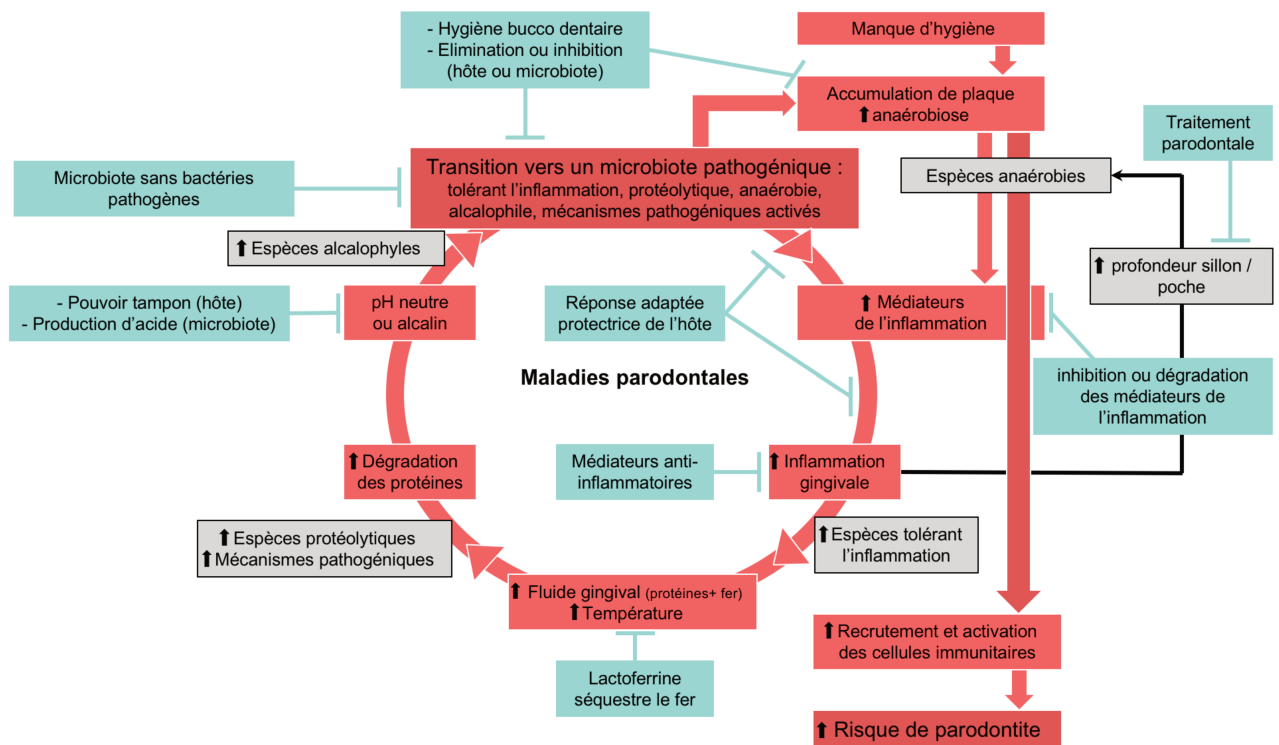


Figure 8 : Cycle des maladies parodontales. En rouge, les éléments en faveur de la maladie, en vert les actions de l'hôte ou du chirurgien-dentiste pour limiter son développement.

L'émergence des NGS a ensuite permis de découvrir l'immense richesse et diversité du microbiote sous-gingival, et ce n'est pas moins de 17 nouvelles espèces qui sont aujourd'hui proposées comme associées aux parodontites, dont les TM7 nouvellement découverts. Une étude de Pérez-Chaparro en a fait une revue systématique en 2014 (42).

Cependant, le fait qu'un microorganisme soit plus susceptible d'être présent de par l'environnement inflammatoire qui lui est favorable lors de la parodontite ne devrait pas lui conférer obligatoirement le terme de « paropathogène ». Ces dernières années, cette discussion autour de la causalité/accident a pris un nouvel élan avec l'introduction de théories sur les événements écologiques associés avec destruction parodontale (**Figure 8**). Ainsi les facteurs environnementaux peuvent conduire à la sélection et prolifération de certains agents pathogènes. Une hypothèse suggère que dans la parodontite, certaines bactéries seraient des « agents pathogènes clé de voûte » avec des capacités d'évitement et de dérégulation de la réponse immunitaire de l'hôte conduisant ainsi la communauté bactérienne à devenir dysbiotique (43). Le pathogène clé de voûte le mieux caractérisé à ce jour est *P. gingivalis* qui peut moduler la réponse immunitaire même en très faible nombre et ainsi favoriser la virulence de la communauté toute entière (44).

Cependant, *P. gingivalis* n'est pas systématiquement retrouvé dans les prélèvements réalisés chez des patients atteints de parodontites. Pour Griffen *et coll.*, chez les sujets sains la prévalence de *P. gingivalis* était de 25 % alors que chez les sujets atteints de parodontite, cette prévalence montait à 79 % (45). Ces résultats confirment l'importance de la symbiose ou de la dysbiose de l'écosystème. En utilisant

une approche plus globale et les nouvelles technologies de séquençage, nous avons défini un microbiote de base sain et impliqué dans les parodontites (46). La **Figure 9** montre les résultats obtenus avec les principaux genres bactériens impliqués. Certains sont communs (*Fusobacterium*, *Streptococcus*) et d'autres sont spécifiques aux parodontites (*Tannerella*). À l'aide d'un ratio de dysbiose sur les abondances relatives des genres présents ($(\% \text{ Porphyromonas} + \% \text{ Treponema} + \% \text{ Tannerella}) / (\% \text{ Rothia} + \% \text{ Corynebacterium})$), la séparation entre patients sains et patients présentant une parodontite a pu être fortement améliorée (46).

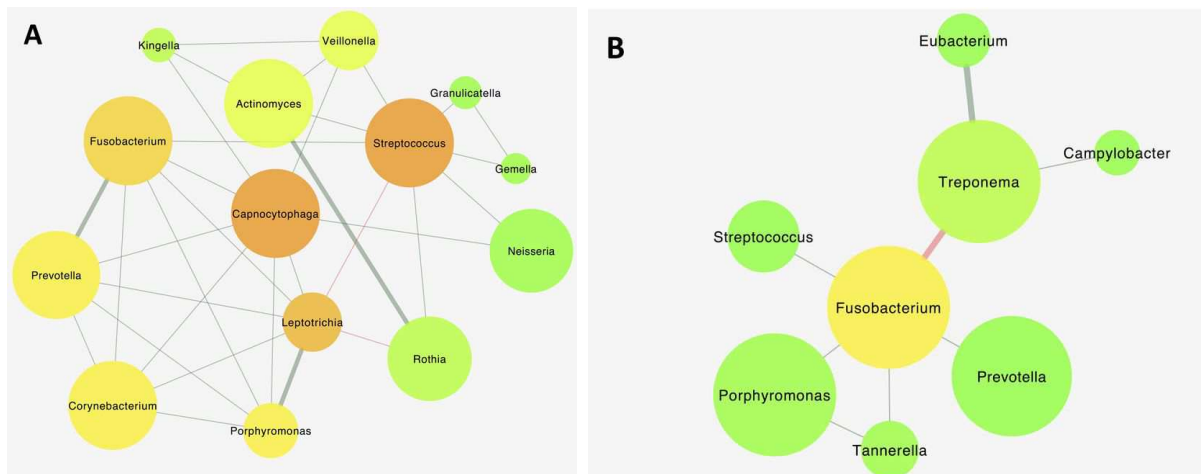


Figure 9 : (a) Réseau des genres principalement retrouvés chez les patients sains. (b) Réseau des genres principalement retrouvés chez les patients atteints de parodontite.

Exemple des mucosites péri-implantaires et les péri-implantites.

Ces pathologies montrent plusieurs similitudes cliniques avec la gingivite pour la mucosite péri-implantaire, et avec la parodontite pour la péri-implantite. Les travaux antérieurs aux NGS ont montré des germes en commun avec les maladies parodontales. Ainsi, le complexe rouge est régulièrement cité comme étant présent en plus grande quantité dans les poches péri-implantaires que dans les sillons ou sites implantaires sains. Il est probable que les espèces présentes dans les poches parodontales puissent coloniser les sites implantaires voisins. Cependant, pour les espèces abondantes, il existe bien deux niches écologiques différentes (47). Concernant la diversité des microbiotes de la péri-implantite, les auteurs se contredisent régulièrement : plus divers pour certains et moins divers pour d'autres lorsqu'on le compare à la parodontite (48,49). Plusieurs espèces, y compris des espèces précédemment insoupçonnées (telles que *Pseudomonas aeruginosa*, *Staphylococcus aureus*, *Staphylococcus warneri* ou encore *Brevundimonas*) ont été uniquement retrouvées dans les sites péri-implantaires. Les maladies péri-implantaires présenteraient des niveaux plus élevés d'*Actinomyces*, *Peptococcus*, *Campylobacter*, *Streptococcus* (non-mutans), *Butyrivibrio* et *Streptococcus mutans* par rapport aux sites implantaires sains (49). Zheng *et coll.*, incriminent également *Eubacterium minutum* dans la péri-implantite (50). Grâce à l'évolution des technologies, les résultats, bien que contradictoires, semblent indiquer que les microbiotes parodontaux et péri-implantaires sont différents.

MICROBIOTE BUCCAL ET MALADIES SYSTÉMIQUES

Si les bactéries sont la principale cause de maladies infectieuses, de nouvelles études indiquent quelles sont aussi indirectement responsables de plusieurs autres maladies, dont plusieurs maladies systémiques. Explorées depuis plusieurs années, les associations entre les bactéries de la cavité buccale et les autres maladies font encore débat. *A priori*, le concept de cavité buccale dysbiotique en tant que source d'infection à distance est aujourd'hui admis. Ainsi, les maladies parodontales, avec leur charge bactérienne importante associée à une défaillance du système immunitaire, sont des facteurs de comorbidité de différentes pathologies d'organes comme les pathologies cardio-vasculaires, pulmonaires, rénales. La masse bactérienne parodontale, ses métabolites et ses facteurs de virulence, entraînent une inflammation ; la chronicité de l'inflammation aboutit à une réponse immunitaire laquelle exacerbe la pathologie d'organe et en retour la maladie parodontale. Inflammation, réponse immunitaire et dysbiose fonctionnent alors dans un cercle vicieux.

À côté des maladies d'organes, les maladies chroniques inflammatoires, métaboliques ou auto-immunes, telles que le diabète, la polyarthrite rhumatoïde (PR) et le lupus érythémateux systémique (LES), augmentent la sensibilité aux maladies parodontales. Des études chez l'homme et l'animal ont montré que ces maladies favorisaient l'inflammation du parodonte et la gravité de la parodontite. L'étude des microbiotes buccaux montre que pour les trois maladies systémiques citées, le nombre de taxons bactériens associés à la santé diminue et le nombre de taxons associés à la maladie augmente. Bien qu'une bactérie buccale spécifique de la maladie parodontale n'ait jamais été mise en évidence, le diabète augmente les niveaux de *Capnocytophaga*, *Porphyromonas* et *Pseudomonas* (51), tandis que *Prevotella* et *Selenomonas* sont augmentés dans les cas de PR (52) et *Selenomonas*, *Leptotrichia* et *Prevotella* dans le LES (53). Dans un modèle animal, le diabète accroît la pathogénicité du microbiote buccal, avec une augmentation de l'inflammation, de l'ostéoclastogénèse et de la perte osseuse (54).

La composition du microbiote, régie par des facteurs locaux, l'est aussi par des facteurs systémiques, lesquels peuvent également avoir un effet significatif. L'un des mécanismes suggérés est que les maladies inflammatoires systémiques augmentent l'inflammation locale. Cela modifie l'expression des médiateurs inflammatoires localement, augmente le recrutement de leucocytes dans le parodonte et modifie la composition du microbiote buccal, ce qui peut engendrer sa dysbiose.

Diabètes et modifications du microbiote buccal

Chez l'enfant et chez l'adulte, les diabètes de type 1 et 2 ont des répercussions sur le parodonte avec une augmentation de la sévérité de l'atteinte parodontale avec la gravité du diabète. L'inflammation du parodonte est identique à celle qui peut être observée dans d'autres tissus affectés par le diabète (55). La destruction parodontale chez les sujets diabétiques est due à une modification de la réponse de l'hôte et à une modification de pathogénicité bactérienne, entraînant une inflammation et des lésions plus importantes. Si plusieurs études montrent que certains genres bactériens augmentent ou diminuent lors de la parodontite chez le sujet diabétique, une étude

longitudinale menée chez la souris montre que le développement de l'hyperglycémie induit un changement dans la composition bactérienne, augmentant les niveaux de Protéobactéries (*Enterobacteriaceae*) et de Firmicutes (*Enterococcus*, *Staphylococcus* et *Aerococcus*) (56). L'installation du diabète a également réduit la diversité du microbiote buccal, comme dans d'autres tissus où le diabète réduit la diversité bactérienne (57). Le vieillissement chez la souris diabétique réduit la diversité bactérienne, laquelle s'accompagne d'une colonisation importante par *P. gingivalis* (58).

À côté des modifications de la composition du microbiote, l'inflammation chronique augmente également la pathogénicité des bactéries avec une augmentation de production d'IL-17 et en réponse une aggravation des signes cliniques de la parodontite (59). Inversement, un traitement intensif de la parodontite pourrait être important pour une gestion efficace du diabète de type 2, montrant ainsi une relation bi-directionnelle entre diabètes et parodontite (60).

Polyarthrite rhumatoïde (PR) et modifications du microbiote buccal

La PR, maladie auto-immune caractérisée par une inflammation chronique partage des signes cliniques communs avec la maladie parodontale : inflammation chronique par poussée, perte osseuse. La prévalence des maladies parodontales est élevée chez les patients atteints de PR (61). La maladie parodontale pourrait favoriser une PR par surproduction ou sur-activité d'enzymes, les peptidylarginines déiminases. Ces enzymes augmentent le taux de citrullination des protéines, au risque de déclencher ou aggraver une auto-antigénicité en favorisant une réponse auto-immune (anticorps anti-protéines citrullinées, ou ACPA). L'utilisation d'antiseptiques réduit la perte osseuse et confirme le rôle du microbiote buccal dans la PR (62). La PR amplifie la réponse inflammatoire dans le parodonte, laquelle en retour modifie le microbiote buccal. L'expression des cytokines telles que le TNF- α , les IL-1, IL-6 et IL-17 est élevée dans le parodonte, tandis que celle des IL-17 et IL-33 est élevée dans la salive de sujets atteints de PR (53). Les mécanismes par lesquels les bactéries et/ou l'inflammation parodontale peuvent intervenir sont présentés **Figure 10**.

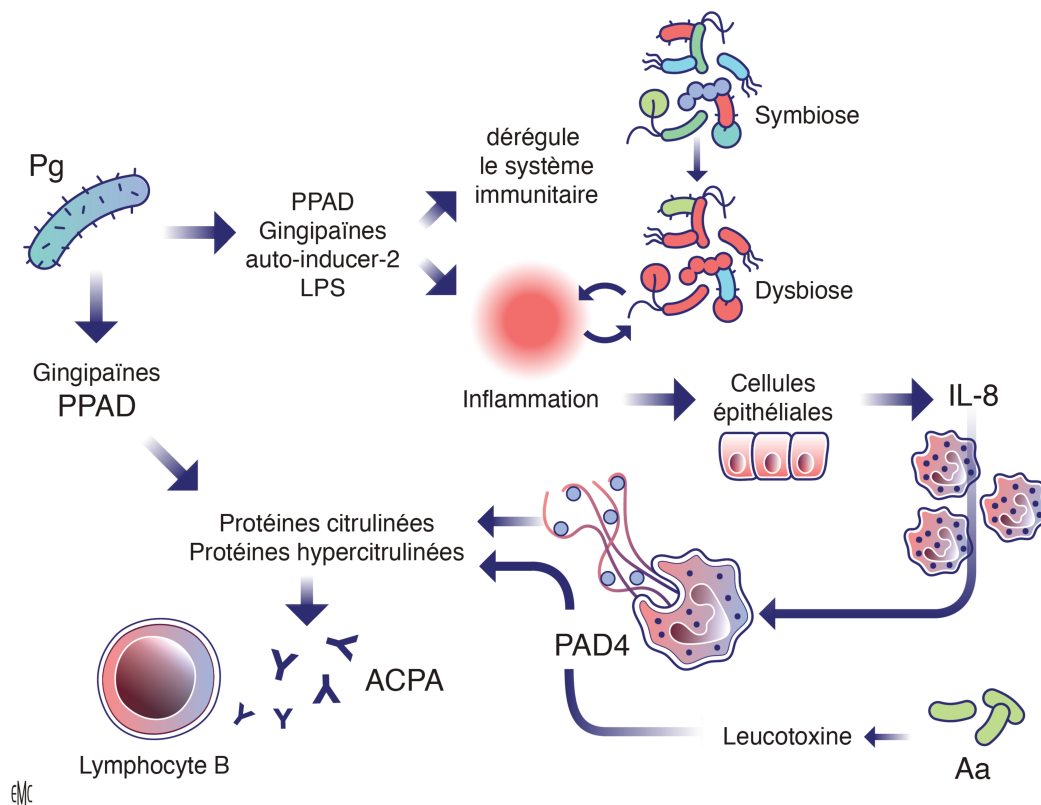


Figure 10 : Mécanismes supposés favorisant la surproduction d'auto-anticorps dirigés contre les protéines citrulinées (ACPA). PPAD : peptidylarginines déiminases de *Porphyromonas* ; PAD4 : peptidylarginine déiminase 4 issue de cellules polynucléaires ; Pg : *P. gingivalis* ; Aa : *A. actinomycetemcomitans* ; LPS : lipopolysaccharides.

Chez l'animal, la PR modifie les microbiotes. Qualitativement chez les souris, dans la salive, *P. micra*, *Selenomonas noxia* et *Veillonella parvula* sont augmentés (63). Chez l'homme, le microbiote associé à la PR est différent de celui du patient sans PR avec une augmentation importante de *Lactobacillus salivarius*, *Atopobium*, *Leptotrichia* et *Prevotella* et une diminution drastique du genre *Streptococcus* (64). Des *Prevotella* et des *Leptotrichia* spécifiques n'ont été observés que chez des patients atteints de PR récente, et *Anaeroglobus geminatus* a été mis en lien avec la présence de peptidylarginine déiminase et de facteurs rhumatoïdes, ainsi qu'avec la parodontite. Plusieurs études confirment que la biomasse microbienne est plus importante dans la cavité buccale du patient atteint de PR par rapport à un sujet sain et ce, quel que soit son statut parodontal (64). Le traitement de la PR a un effet sur la maladie parodontale et en conséquence sur le microbiote buccal avec un retour possible à un microbiote buccal compatible avec la santé parodontale (64). Pour l'ostéo-arthrite, une autre pathologie articulaire, il a été récemment démontré par Chen et coll. que le microbiote salivaire est différent de celui retrouvé chez le sujet atteint de PR et du sujet non atteint de PR (65). À partir d'un modèle prédictif, les auteurs proposent des biomarqueurs diagnostiques spécifiques à partir de prélèvements salivaires.

Lupus érythémateux systémique (LES) et modifications du microbiote buccal

Le LES est une maladie auto-immune caractérisée par une inflammation persistante et qui atteint plusieurs organes comme les reins, les poumons, les articulations, le cœur et le cerveau. L'étiologie est à la fois génétique et environnementale, et est liée à une dysbiose microbienne (53,66). Dans la cavité buccale, le LES peut se manifester par des ulcérations, une xérostomie, une hyposialie et une parodontite. Dans une méta-analyse, un risque multiplié par 1,76 de maladie parodontale chez les sujets atteints de LES a été montré. Ce risque est corrélé à des niveaux élevés de cytokines (IL-6, IL-17 et IL-33) dans la salive de patients atteints de LES. L'inflammation est corrélée à la composition du biofilm sous gingival. Ces observations chez l'homme ne permettent cependant pas de conclure à des liens entre composition du microbiote, grades de la maladie parodontale et marqueurs de l'inflammation.

Néanmoins, chez les patients atteints de LES, le microbiote est altéré avec une forte augmentation de lactobacilles et de *Candida albicans* par rapport à des patients non atteints. Les bactéries associées à la maladie parodontale telles que *Prevotella sp.*, *Leptotrichia*, *S. noxia* et *Lachnospiraceae* sont en nombre élevé chez les patients atteints de LES même dans les sites sains (53). De plus, les bactéries associées à un parodonte sain comme *Capnocytophaga*, *Rothia*, *Streptococcus*, sont diminuées chez les patients atteints de LES et de parodontites. Les marqueurs de l'inflammation sont élevés chez ces mêmes patients (63). Le traitement de la maladie parodontale a des répercussions sur la thérapeutique conventionnelle de LES avec une réduction de l'activité de la maladie (67). Prises ensemble, les données de la littérature mettent en évidence le lien entre le microbiote et le LES et suggèrent qu'une réduction de l'inflammation favoriserait la formation d'un microbiote buccal moins pathogène.

Le syndrome de Sjögren primaire est une autre maladie auto-immune qui a de nombreux signes cliniques communs avec le LES. Les malades atteints de Sjögren ont pourtant un microbiote buccal différent de celui des patients atteints de LES. La diversité bactérienne est très faible chez les patients atteints de Sjögren par rapport aux patients atteints de LES. Cette caractéristique serait liée à la sécheresse buccale chronique chez le patient Sjögren (68).

Hémochromatose et modifications du microbiote buccal

L'hémochromatose liée au gène *HFE* est la forme la plus commune de surcharge en fer d'origine génétique. À l'origine de symptômes hépatiques, cardiaques, articulaires, osseux et buccaux, elle se manifeste biologiquement par une élévation anormale de la saturation de la transferrine (TSAT). À partir de 45% de saturation, une forme particulière du fer – non lié à la transferrine – apparaît dans le plasma. Cette forme toxique est suspectée être à l'origine des symptômes observés lors de l'hémochromatose et peut favoriser la croissance et la virulence bactérienne. Le traitement, par saignées régulières, vise à rétablir un niveau normal de fer dans l'organisme et s'accompagne d'un retour à des valeurs normales de la TSAT. Une association significative a été montrée entre patients hémochromatosiques saturés et parodontite sévère (69). Chez ces patients, les indices d' α et de β diversité du

microbiote ne montraient pas de différence significative selon le niveau de TSAT des patients. Cependant, l'étude des réseaux d'interactions bactériens associés aux tests de corrélation avec les données cliniques et biologiques permet de décrire deux profils microbiologiques distincts. Les patients désaturés (TSAT \leq 45 %) présentaient un microbiote avec deux communautés bactériennes qui s'opposent (saine et pathogénique), suggérant une compétition en cas de faible biodisponibilité du fer. Cette compétition disparaît chez les patients saturés.

Chez les patients désaturés, la TSAT était corrélée positivement avec l'abondance de *Porphyromonas* et de *Treponema*, deux genres impliqués dans les parodontites. Par ailleurs, la TSAT était négativement corrélée avec *Corynebacterium*, genre associé à un parodonte sain. En l'absence d'apparition de fer libre, une TSAT augmentée sélectionne des genres paropathogènes, dont l'affinité pour la transferrine est connue.

Les patients saturés présentaient des indices parodontaux significativement plus élevés, confirmant ainsi l'observation de la précédente étude. Par ailleurs, ces indices étaient positivement corrélés avec les pathogènes classiquement décrits *Porphyromonas*, *Treponema* et *Tannerella*. Ainsi, il semble exister un impact du niveau de saturation de la transferrine sur le microbiote parodontal et l'atteinte parodontale (70). Le niveau de fer dans l'organisme a donc un rôle qui reste à élucider dans l'équilibre des relations entre l'hôte et son microbiote.

Maladies inflammatoires chroniques de l'intestin (MICI) et modifications du microbiote buccal

Les maladies inflammatoires chroniques de l'intestin, maladie de Crohn (CRO) et rectocolite hémorragique (RH), se caractérisent par l'inflammation de la paroi d'une partie du tube digestif, liée à une hyperactivité du système immunitaire digestif. Parmi les étiologies des MICI, le microbiote digestif (depuis la cavité buccale jusqu'au colon) semble jouer un rôle important. Dans la salive, les comparaisons de l'abondance des taxons montrent un enrichissement en *Streptococcaceae* (contenant le genre *Streptococcus*) et *Enterobacteriaceae* chez les patients atteints de RH et *Veillonellaceae* (contenant le genre *Veillonella*) pour les patients atteints de CRO. Ces variations sont accompagnées d'un appauvrissement en *Lachnospiraceae* et *Prevotella* chez les RH et *Neisseriaceae* (contenant le genre *Neisseria*) et *Haemophilus* chez les CRO (71). Des tendances identiques sont retrouvées dans l'intestin des patients atteints de MICI. Au sein des microbiotes buccaux prélevés chez des patients atteints de MICI, il existe des écotypes spécifiques au CRO et à la RH. Ces écotypes ne sont pas spécifiques de la démographie, de la gravité de la maladie et pourraient donc être utilisés comme biomarqueur de la maladie, en particulier pour le diagnostic et le suivi du traitement (72). Ainsi, les maladies systémiques à composante inflammatoire sont fréquemment associées à une augmentation du risque de parodontite (73).

CONCLUSION – PERSPECTIVE

Le microbiote buccal est un domaine de recherche passionnant et en pleine expansion. Organisé en biofilms et formant un écosystème en symbiose avec l'hôte, il est crucial pour la santé. Son déséquilibre peut provoquer des maladies buccales et influencer les maladies systémiques. En effet, la perturbation du microbiote buccal conduit à une dysbiose et à l'émergence d'agents pathogènes. Identifier les microbiotes compatibles avec la santé bucco-dentaire est la première étape de la recherche ainsi que les variations capables de mener aux dysbioses responsables des différentes pathologies.

La recherche sur le microbiote est actuellement à un stade très naissant. De nombreuses recherches sont en cours et des données sont ajoutées en permanence. Les avancées technologiques, la baisse des coûts de séquençage permettront d'obtenir des connaissances à l'échelle de populations entières ce qui est nécessaire pour lisser les biais relatifs à la méthode d'échantillonnage, d'analyse et aux variations individuelles.

Ces travaux d'analyse ont montré qu'il existait potentiellement plusieurs stromatotypes et en conséquence des dysbioses variables. De nouvelles espèces sont décrites tous les jours, dont certaines potentiellement impliquées dans les pathologies bucco-dentaires. Il semble aujourd'hui obsolète d'envisager la classification des espèces bactériennes de façon binaire : commensale ou pathogène. En effet, le comportement des bactéries dépend de la dynamique au sein du microbiote et de leur relation à l'hôte. *S. mutans* et *P. gingivalis* sont retrouvés chez des patients sains. Ainsi, les tests existant sur le marché en cariology et parodontologie ne sont pas encore à même de refléter le niveau de complexité d'un biofilm à plusieurs centaines d'espèces en communication permanente avec leur hôte. De la même manière, le choix de bactéries qui pourrait influencer le microbiote pour rétablir ou maintenir la symbiose avec l'hôte c'est à dire des probiotiques, reste aujourd'hui à bien définir.

Cependant l'étude de ces microbiotes et de leurs variations est prometteuse pour l'avenir. En effet, qu'il s'agisse de pathologies dentaires ou systémiques, les microbiotes pourront servir de biomarqueurs et faciliteront les thérapies ciblées et la médecine personnalisée pour une meilleure gestion des patients en pratique clinique. La miniaturisation des séquenceurs de la taille d'une clé USB (technologie de séquençage par nanopores) pourrait les faire rentrer dans les cabinets dentaires dans les années à venir. Quant à la masse d'informations qu'ils génèrent, elle nécessite le développement d'algorithmes appropriés pour en extraire une information cliniquement pertinente. Sur ce point, les derniers progrès en sciences de l'information (réseaux neuronaux, apprentissage profond) pourraient encore étendre les possibilités offertes par les NGS.

RÉFÉRENCES

1. Kilian M, Chapple ILC, Hannig M, Marsh PD, Meuric V, Pedersen AML, et al. The oral microbiome – an update for oral healthcare professionals. *Br Dent J.* nov 2016;221(10):657-66.
2. Lederberg J, McCray AT. 'Ome Sweet 'Omics-- A Genealogical Treasury of Words. *The Scientist.* avr 2001;15(7):8-10.
3. Socransky SS, Haffajee AD, Cugini MA, Smith C, Kent RL. Microbial complexes in subgingival plaque. *J Clin Periodontol.* févr 1998;25(2):134-44.
4. Turnbaugh PJ, Ley RE, Hamady M, Fraser-Liggett CM, Knight R, Gordon JI. The human microbiome project. *Nature.* 18 oct 2007;449(7164):804-10.
5. Pérez-Chaparro PJ, Gonçalves C, Figueiredo LC, Faveri M, Lobão E, Tamashiro N, et al. Newly identified pathogens associated with periodontitis: a systematic review. *J Dent Res.* sept 2014;93(9):846-58.
6. Bearfield C, Davenport ES, Sivapathasundaram V, Allaker RP. Possible association between amniotic fluid micro-organism infection and microflora in the mouth. *BJOG Int J Obstet Gynaecol.* mai 2002;109(5):527-33.
7. Aagaard K, Ma J, Antony KM, Ganu R, Petrosino J, Versalovic J. The Placenta Harbors a Unique Microbiome. *Sci Transl Med.* 21 mai 2014;6(237):237ra65-237ra65.
8. Stout MJ, Conlon B, Landeau M, Lee I, Bower C, Zhao Q, et al. Identification of intracellular bacteria in the basal plate of the human placenta in term and preterm gestations. *Am J Obstet Gynecol.* mars 2013;208(3):226.e1-7.
9. Collado MC, Rautava S, Aakko J, Isolauri E, Salminen S. Human gut colonisation may be initiated in utero by distinct microbial communities in the placenta and amniotic fluid. *Sci Rep.* 22 mars 2016;6:23129.
10. Reh binder EM, Lødrup Carlsen KC, Staff AC, Angell IL, Landrø L, Hilde K, et al. Is amniotic fluid of women with uncomplicated term pregnancies free of bacteria? *Am J Obstet Gynecol.* sept 2018;219(3):289.e1-289.e12.
11. Martín V, Mañes-Lázaro R, Rodríguez JM, Maldonado-Barragán A. *Streptococcus lactarius* sp. nov., isolated from breast milk of healthy women. *Int J Syst Evol Microbiol.* mai 2011;61(Pt 5):1048-52.
12. Mason MR, Chambers S, Dabdoub SM, Thikkurissy S, Kumar PS. Characterizing oral microbial communities across dentition states and colonization niches. *Microbiome.* 10 2018;6(1):67.
13. Hegde S, Munshi AK. Influence of the maternal vaginal microbiota on the oral microbiota of the newborn. *J Clin Pediatr Dent.* 1998;22(4):317-21.
14. Gomez A, Nelson KE. The Oral Microbiome of Children: Development, Disease, and Implications Beyond Oral Health. *Microb Ecol.* 2017;73(2):492-503.
15. Dzidic M, Collado MC, Abrahamsson T, Artacho A, Stensson M, Jenmalm MC, et al. Oral microbiome development during childhood: an ecological succession influenced by postnatal factors and associated with tooth decay. *ISME J.* sept 2018;12(9):2292-306.
16. Fejerskov O, Nyvad B, Larsen MJ. Human experimental caries models: intra-oral environmental variability. *Adv Dent Res.* juill 1994;8(2):134-43.
17. Aas JA, Paster BJ, Stokes LN, Olsen I, Dewhirst FE. Defining the normal bacterial flora

of the oral cavity. *J Clin Microbiol.* nov 2005;43(11):5721-32.

18. Simón-Soro A, Tomás I, Cabrera-Rubio R, Catalan MD, Nyvad B, Mira A. Microbial geography of the oral cavity. *J Dent Res.* juill 2013;92(7):616-21.
19. Yamashita Y, Takeshita T. The oral microbiome and human health. *J Oral Sci.* 2017;59(2):201-6.
20. Chen H, Jiang W. Application of high-throughput sequencing in understanding human oral microbiome related with health and disease. *Front Microbiol.* 2014;5:508.
21. Takeshita T, Kageyama S, Furuta M, Tsuboi H, Takeuchi K, Shibata Y, et al. Bacterial diversity in saliva and oral health-related conditions: the Hisayama Study. *Sci Rep.* 24 févr 2016;6:22164.
22. Willis JR, González-Torres P, Pittis AA, Bejarano LA, Cozzuto L, Andreu-Somavilla N, et al. Citizen science charts two major «stomatotypes» in the oral microbiome of adolescents and reveals links with habits and drinking water composition. *Microbiome.* 6 déc 2018;6(1):218.
23. Zaura E, Brandt BW, Prodan A, Teixeira de Mattos MJ, Imangaliyev S, Kool J, et al. On the ecosystemic network of saliva in healthy young adults. *ISME J.* 2017;11(5):1218-31.
24. Arumugam M, Raes J, Pelletier E, Le Paslier D, Yamada T, Mende DR, et al. Enterotypes of the human gut microbiome. *Nature.* 12 mai 2011;473(7346):174-80.
25. Boutin S, Hagenfeld D, Zimmermann H, El Sayed N, Höpker T, Greiser HK, et al. Clustering of Subgingival Microbiota Reveals Microbial Disease Ecotypes Associated with Clinical Stages of Periodontitis in a Cross-Sectional Study. *Front Microbiol* [Internet]. 1 mars 2017 [cité 23 avr 2018];08. Disponible sur: <http://journal.frontiersin.org/article/10.3389/fmicb.2017.00340/full>
26. Chen L, Qin B, Du M, Zhong H, Xu Q, Li Y, et al. Extensive description and comparison of human supra-gingival microbiome in root caries and health. *PloS One.* 2015;10(2):e0117064.
27. Diaz PI, Zilm PS, Rogers AH. *Fusobacterium nucleatum* supports the growth of *Porphyromonas gingivalis* in oxygenated and carbon-dioxide-depleted environments. *Microbiol Read Engl.* févr 2002;148(Pt 2):467-72.
28. Tan KH, Seers CA, Dashper SG, Mitchell HL, Pyke JS, Meuric V, et al. *Porphyromonas gingivalis* and *Treponema denticola* exhibit metabolic symbioses. *PLoS Pathog.* mars 2014;10(3):e1003955.
29. Mark Welch JL, Rossetti BJ, Rieken CW, Dewhirst FE, Borisy GG. Biogeography of a human oral microbiome at the micron scale. *Proc Natl Acad Sci.* 9 févr 2016;113(6):E791-800.
30. Zijngge V, van Leeuwen MBM, Degener JE, Abbas F, Thurnheer T, Gmür R, et al. Oral biofilm architecture on natural teeth. *PloS One.* 24 févr 2010;5(2):e9321.
31. Mark Welch JL, Rossetti BJ, Rieken CW, Dewhirst FE, Borisy GG. Biogeography of a human oral microbiome at the micron scale. *Proc Natl Acad Sci U S A.* 9 févr 2016;113(6):E791-800.
32. Soga Y, Maeda Y, Ishimaru F, Tanimoto M, Maeda H, Nishimura F, et al. Bacterial substitution of coagulase-negative staphylococci for streptococci on the oral mucosa after hematopoietic cell transplantation. *Support Care Cancer Off J Multinatl Assoc Support Care Cancer.* juill 2011;19(7):995-1000.

33. Cho I, Blaser MJ. The human microbiome: at the interface of health and disease. *Nat Rev Genet.* 13 mars 2012;13(4):260-70.
34. Marsh PD. Are dental diseases examples of ecological catastrophes? *Microbiol Read Engl.* févr 2003;149(Pt 2):279-94.
35. Espinoza JL, Harkins DM, Torralba M, Gomez A, Highlander SK, Jones MB, et al. Supragingival Plaque Microbiome Ecology and Functional Potential in the Context of Health and Disease. *mBio.* 27 nov 2018;9(6).
36. Loe H, Theilade E, Jensen SB. Experimental gingivitis in man. *J Periodontol.* juin 1965;36:177-87.
37. Tonetti MS, Greenwell H, Kornman KS. Staging and grading of periodontitis: Framework and proposal of a new classification and case definition. *J Periodontol.* 2018;89(S1):S159-72.
38. Haubek D, Ennibi O-K, Poulsen K, Vaeth M, Poulsen S, Kilian M. Risk of aggressive periodontitis in adolescent carriers of the JP2 clone of *Aggregatibacter (Actinobacillus) actinomycetemcomitans* in Morocco: a prospective longitudinal cohort study. *Lancet Lond Engl.* 19 janv 2008;371(9608):237-42.
39. Mombelli A, Casagni F, Madianos PN. Can presence or absence of periodontal pathogens distinguish between subjects with chronic and aggressive periodontitis? A systematic review. *J Clin Periodontol.* 2002;29 Suppl 3:10-21; discussion 37-38.
40. Eke PI, Dye BA, Wei L, Thornton-Evans GO, Genco RJ, CDC Periodontal Disease Surveillance workgroup: James Beck (University of North Carolina, Chapel Hill, USA), Gordon Douglass (Past President, American Academy of Periodontology), Roy Page (University of Washin. Prevalence of periodontitis in adults in the United States: 2009 and 2010. *J Dent Res.* oct 2012;91(10):914-20.
41. Bourgeois DM, Roland E, Desfontaine J. Caries prevalence 1987–1998 in 12-year-olds in France. *Int Dent J.* 2004;54(4):193-200.
42. Pérez-Chaparro PJ, Gonçalves C, Figueiredo LC, Faveri M, Lobão E, Tamashiro N, et al. Newly identified pathogens associated with periodontitis: a systematic review. *J Dent Res.* sept 2014;93(9):846-58.
43. Hajishengallis G, Darveau RP, Curtis MA. The keystone-pathogen hypothesis. *Nat Rev Microbiol.* oct 2012;10(10):717-25.
44. Hajishengallis G, Liang S, Payne MA, Hashim A, Jotwani R, Eskin MA, et al. Low-abundance biofilm species orchestrates inflammatory periodontal disease through the commensal microbiota and complement. *Cell Host Microbe.* 17 nov 2011;10(5):497-506.
45. Griffen AL, Becker MR, Lyons SR, Moeschberger ML, Leys EJ. Prevalence of *Porphyromonas gingivalis* and periodontal health status. *J Clin Microbiol.* nov 1998;36(11):3239-42.
46. Meuric V, Le Gall-David S, Boyer E, Acuña-Amador L, Martin B, Fong SB, et al. Signature of Microbial Dysbiosis in Periodontitis. *Appl Environ Microbiol.* 15 2017;83(14).
47. Dabdoub SM, Tsigarida AA, Kumar PS. Patient-specific analysis of periodontal and peri-implant microbiomes. *J Dent Res.* déc 2013;92(12 Suppl):168S-75S.
48. Koyanagi T, Sakamoto M, Takeuchi Y, Maruyama N, Ohkuma M, Izumi Y. Comprehensive microbiological findings in peri-implantitis and periodontitis. *J Clin*

Periodontol. mars 2013;40(3):218-26.

49. Kumar PS, Mason MR, Brooker MR, O'Brien K. Pyrosequencing reveals unique microbial signatures associated with healthy and failing dental implants. *J Clin Periodontol.* mai 2012;39(5):425-33.
50. Zheng H, Xu L, Wang Z, Li L, Zhang J, Zhang Q, et al. Subgingival microbiome in patients with healthy and ailing dental implants. *Sci Rep.* 16 juin 2015;5:10948.
51. Ganesan SM, Joshi V, Fellows M, Dabdoub SM, Nagaraja HN, O'Donnell B, et al. A tale of two risks: smoking, diabetes and the subgingival microbiome. *ISME J.* 2017;11(9):2075-89.
52. Scher JU, Ubeda C, Equinda M, Khanin R, Buischi Y, Viale A, et al. Periodontal disease and the oral microbiota in new-onset rheumatoid arthritis. *Arthritis Rheum.* oct 2012;64(10):3083-94.
53. Corrêa JD, Calderaro DC, Ferreira GA, Mendonça SMS, Fernandes GR, Xiao E, et al. Subgingival microbiota dysbiosis in systemic lupus erythematosus: association with periodontal status. *Microbiome.* 20 mars 2017;5(1):34.
54. Graves DT, Alshabab A, Albiero ML, Mattos M, Corrêa JD, Chen S, et al. Osteocytes play an important role in experimental periodontitis in healthy and diabetic mice through expression of RANKL. *J Clin Periodontol.* 2018;45(3):285-92.
55. Wu Y-Y, Xiao E, Graves DT. Diabetes mellitus related bone metabolism and periodontal disease. *Int J Oral Sci.* 26 juin 2015;7(2):63-72.
56. Xiao E, Mattos M, Vieira GHA, Chen S, Corrêa JD, Wu Y, et al. Diabetes Enhances IL-17 Expression and Alters the Oral Microbiome to Increase Its Pathogenicity. *Cell Host Microbe.* juill 2017;22(1):120-128.e4.
57. Ussar S, Fujisaka S, Kahn CR. Interactions between host genetics and gut microbiome in diabetes and metabolic syndrome. *Mol Metab.* sept 2016;5(9):795-803.
58. Xiao W, Li S, Pacios S, Wang Y, Graves DT. Bone Remodeling Under Pathological Conditions. *Front Oral Biol.* 2016;18:17-27.
59. Abusleme L, Moutsopoulos NM. IL-17: overview and role in oral immunity and microbiome. *Oral Dis.* oct 2017;23(7):854-65.
60. D'Aiuto F, Gkranias N, Bhowruth D, Khan T, Orlandi M, Suvan J, et al. Systemic effects of periodontitis treatment in patients with type 2 diabetes: a 12 month, single-centre, investigator-masked, randomised trial. *Lancet Diabetes Endocrinol.* 2018;6(12):954-65.
61. de Smit MJ, Westra J, Brouwer E, Janssen KMJ, Vissink A, van Winkelhoff AJ. Periodontitis and Rheumatoid Arthritis: What Do We Know? *J Periodontol.* sept 2015;86(9):1013-9.
62. Queiroz-Junior CM, Madeira MFM, Coelho FM, Costa VV, Bessoni RLC, Sousa LF da C, et al. Experimental arthritis triggers periodontal disease in mice: involvement of TNF- α and the oral Microbiota. *J Immunol Baltim Md 1950.* 1 oct 2011;187(7):3821-30.
63. Corrêa JD, Saraiva AM, Queiroz-Junior CM, Madeira MFM, Duarte PM, Teixeira MM, et al. Arthritis-induced alveolar bone loss is associated with changes in the composition of oral microbiota. *Anaerobe.* juin 2016;39:91-6.
64. Zhang X, Zhang D, Jia H, Feng Q, Wang D, Liang D, et al. The oral and gut microbiomes are perturbed in rheumatoid arthritis and partly normalized after treatment. *Nat*

Med. août 2015;21(8):895-905.

65. Chen B, Zhao Y, Li S, Yang L, Wang H, Wang T, et al. Variations in oral microbiome profiles in rheumatoid arthritis and osteoarthritis with potential biomarkers for arthritis screening. *Sci Rep.* 20 nov 2018;8(1):17126.
66. López P, de Paz B, Rodríguez-Carrio J, Hevia A, Sánchez B, Margolles A, et al. Th17 responses and natural IgM antibodies are related to gut microbiota composition in systemic lupus erythematosus patients. *Sci Rep.* 5 avr 2016;6:24072.
67. Fabbri C, Fuller R, Bonfá E, Guedes LKN, D'Alleva PSR, Borba EF. Periodontitis treatment improves systemic lupus erythematosus response to immunosuppressive therapy. *Clin Rheumatol.* 1 avr 2014;33(4):505-9.
68. van der Meulen TA, Harmsen HJM, Vila AV, Kurilshikov A, Liefers SC, Zhernakova A, et al. Shared gut, but distinct oral microbiota composition in primary Sjögren's syndrome and systemic lupus erythematosus. *J Autoimmun.* 1 févr 2019;97:77-87.
69. Meuric V, Lainé F, Boyer E, Le Gall-David S, Oger E, Bourgeois D, et al. Periodontal status and serum biomarker levels in HFE hemochromatosis patients. A case series study. *J Clin Periodontol.* sept 2017;44(9):892-7.
70. Boyer E, Gall-David SL, Martin B, Fong SB, Loréal O, Deugnier Y, et al. Increased transferrin saturation is associated with subgingival microbiota dysbiosis and severe periodontitis in genetic haemochromatosis. *Sci Rep.* 19 oct 2018;8(1):15532.
71. Mar JS, LaMere BJ, Lin DL, Levan S, Nazareth M, Mahadevan U, et al. Disease Severity and Immune Activity Relate to Distinct Interkingdom Gut Microbiome States in Ethnically Distinct Ulcerative Colitis Patients. *mBio.* 16 2016;7(4).
72. Xun Z, Zhang Q, Xu T, Chen N, Chen F. Dysbiosis and Ecotypes of the Salivary Microbiome Associated With Inflammatory Bowel Diseases and the Assistance in Diagnosis of Diseases Using Oral Bacterial Profiles. *Front Microbiol* [Internet]. 2018 [cité 31 janv 2019];9. Disponible sur: <https://www.frontiersin.org/articles/10.3389/fmicb.2018.01136/full>
73. Jepsen S, Caton JG, Albandar JM, Bissada NF, Bouchard P, Cortellini P, et al. Periodontal manifestations of systemic diseases and developmental and acquired conditions: Consensus report of workgroup 3 of the 2017 World Workshop on the Classification of Periodontal and Peri-Implant Diseases and Conditions. *J Clin Periodontol.* 2018;45(S20):S219-29.

1.2 La maladie parodontale

La parodontite est une maladie inflammatoire chronique de la cavité buccale. Elle résulte d'interactions complexes entre : i) les bactéries d'un microbiote en situation de dysbiose, ii) les réponses immunitaires de l'hôte, et iii) des facteurs environnementaux et nutritionnels qui favorisent les perturbations inflammatoires et immunologiques [13]. Cet ensemble conduit à la destruction des tissus environnants les dents (voir la Figure 1.2). Décrite dans les années 1970 [14], la pathophysiologie de la maladie parodontale ne cesse d'être affinée : si les principaux acteurs cellulaires impliqués dans la maladie ont peu changé, la compréhension du rôle de chacun et de leurs interactions moléculaires a considérablement progressé [15].

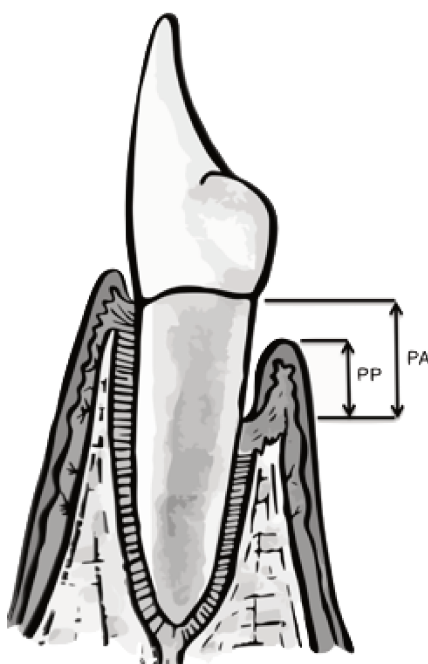


FIGURE 1.2 – Dent atteinte de parodontite. PP : profondeur de la poche parodontale, distance entre la crête gingivale et le fond du sillon gingivo-dentaire ; PA : perte d'attache tissulaire, distance entre la jonction émail-cément et le fond du sillon gingivo-dentaire.

La prise en compte de l'ensemble du microbiote sous-gingival dans l'étiopathogénie est une évolution notable. Différentes hypothèses se sont en effet succédées à propos du rôle de la plaque bactérienne dans les pathologies orales que sont les maladies carieuse et parodontale : hypothèse de la plaque spécifique [16], de la plaque non spécifique [17], et de la plaque écologique [18]. Cette dernière, toujours d'actualité, replace la flore bactérienne dans son environnement. La communauté bactérienne vit au sein d'une niche écologique, d'un écosystème. Elle évolue dans le temps, façonnée par son adaptation aux variations des différents facteurs environnementaux, qu'ils

soient physico-chimiques (pH, température, pression d'oxygène, etc.) ou liés à l'hôte (inflammation, alimentation, etc.).

Le modèle actuel de la maladie parodontale met ainsi l'accent sur une action de groupe, une synergie polymicrobienne, plutôt que sur des agents pathogènes individuels [19]. Le modèle introduit aussi la notion de dysbiose pour le microbiote buccal. Initialement apparu pour le microbiote digestif, le terme de dysbiose désigne un état de déséquilibre au sein de l'écosystème hôte-microbiote (entre les bactéries qui composent le microbiote, ou entre le microbiote et son hôte). Dans tous les cas, cette situation est préjudiciable pour l'hôte. Les auteurs du modèle ne désignent ni la dysbiose, ni la réponse inflammatoire de l'hôte comme élément déclencheur, mais pointent le renforcement réciproque entre ces deux composantes, qui induit alors la parodontite. D'après eux, l'apparition d'une communauté pathogène suppose néanmoins que certaines espèces bien spécifiques (dites « *pathogènes clés* ») aient perturbé les interactions hôte-microbiote. Plusieurs bactéries restent ainsi considérées comme très favorables au déclenchement de cette dysbiose, tandis que d'autres espèces commencent à émerger comme de potentiels pathogènes parodontaux [20]; leur degré d'implication dans la parodontite devant encore être affiné².

La complexité du modèle étiopathogénique de la parodontite découle directement de l'amélioration des outils d'analyse, car ils permettent d'étudier la communauté bactérienne dans son ensemble, et de façon plus précise. Cependant, comment définir la dysbiose dans le cas de la parodontite? Comme indiqué précédemment, le terme est utilisé dans différentes entités cliniques et recouvre plusieurs observations microbiologiques [21]: changement de composition, apparition ou abondance d'espèces considérées comme pathogènes, prédominance d'une espèce bien particulière, ou diminution d'espèces protectrices, associées à un état sain, etc. Tirant parti des possibilités offertes par la bioinformatique, nous avons donc mené une analyse à grande échelle d'échantillons de microbiote sous-gingival, déjà publiés et librement accessibles. Provenant de différentes études et protocoles, ils ont tous en commun d'être des données de séquençage du gène de l'ARNr 16S. En les regroupant dans le même circuit d'analyse, nous avons tenté d'identifier une signature de la dysbiose, à la fois liée à la parodontite et indépendante de la méthodologie utilisée dans chaque étude d'origine. L'article présenté dans la section suivante est le résultat de cette analyse.

1.2.1 Signature of Microbial Dysbiosis in Periodontitis, *Applied and Environmental Microbiology* 2017

La standardisation des études sur le microbiote est toujours en construction. Elle est nécessaire, car de nombreux biais sont susceptibles de se produire au long du protocole d'analyse (prélèvement, conservation, extraction de l'ADN, amplification, séquençage, filtres qualité, etc.). La mise en accès libre des données brutes de séquen-

2. voir à ce propos le travail présenté dans la section 2.2 [Periodontal pathogens and clinical parameters in periodontitis](#), *Molecular Oral Microbiology* 2019 page 37

çage, bien que faisant partie des politiques éditoriales de la plupart des revues scientifiques, n'est pas systématiquement réalisée. Cela est dommageable, car, tandis que les comparaisons entre études se heurtent aux différences de méthodologie, le regroupement des échantillons peut permettre de surpasser ces différences et donner lieu à des études à plus large échelle.

Dans notre étude, 647 échantillons de microbiote sous-gingival (422 provenant de sujets sains, 196 provenant de patients atteints de parodontite, et 29 provenant de sites sains chez des patients) récupérés, pour la grande majorité, dans différents articles³, ainsi que 779 échantillons de microbiote provenant d'autres sites (plaque supra-gingivale, salive, carie dentinaire et vagin, pris comme témoins externes) ont été analysés ensemble selon le même procédé bioinformatique. La visualisation de la diversité inter-échantillon (*beta* diversité, figure 1 de l'article) permet de constater que, malgré les différences de protocoles entre chaque étude dont ils sont issus, les échantillons ont une forte tendance à se regrouper selon le site de prélèvement. Puis, ils se regroupent, dans une moindre mesure, selon le statut de santé : sain ou atteint de parodontite, pour les échantillons sous-gingivaux.

La plupart des mesures classiquement utilisées pour caractériser la diversité des microbiotes provient de champs disciplinaires extérieurs à la biologie : écologie (Jaccard, Bray-Curtis) [22, 23], théories de l'information (Shannon-Weaver) [24], étude des populations (Simpson) [25]. D'autres outils ont été développés spécifiquement pour les bactéries, comme les distances UniFrac qui intègrent dans leurs calculs de diversité la distance pylogénétique qui sépare les espèces présentes dans chaque échantillon [26]. Malgré tout, ces indices sont parfois insuffisants pour distinguer les microbiotes issus de sites sains et ceux issus de sites malades. Bien que 90 % des échantillons de patients avec parodontite se classaient dans le même cluster, celui-ci comportait également une forte proportion d'échantillons de sujets sains (cluster 5, figure 2 de l'article). D'autres outils ont donc été développés pour définir le microbiote, dont l'identification du *core microbiome* et l'analyse des réseaux bactériens, qui ont été utilisés dans ce travail. Le principal écueil dans l'utilisation de ces outils, fréquemment rencontrés dans les publications sur le microbiote, est le nombre limité d'échantillons. Dans ce travail, nous avons donc pu nous affranchir de cette limitation et spécifier des paramètres plus stricts : par exemple, le seuil de prévalence permettant de constituer le *core microbiome*, habituellement à 50 %, et qui a ici été réglé à 95 %.

L'analyse du *core microbiome* et des réseaux bactériens chez les sujets sains et malades (figure 4 de l'article) nous a ainsi permis d'identifier des genres bactériens associés à un état sain ou malade et de proposer des ratios, calculés à partir des abondances de ces différents genres. En testant ces ratios sur leur capacité à classer les patients selon leur statut (figure 5 de l'article) et leur corrélation avec la profondeur de la poche prélevée (figure 6 de l'article), nous avons sélectionné deux calculs, qui nous ont paru refléter le degré de dysbiose du microbiote sous-gingival :

3. Seuls les échantillons de 24 patients provenaient de notre propre collection.

Eubacterium + Campylobacter + Treponema + Tannerella
Veillonella + Neisseria + Rothia + Corynebacterium + Actinomyces

Et dans sa version simplifiée :

Porphyromonas + Treponema + Tannerella
Rothia + Corynebacterium

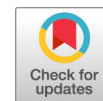
Il faut d'ailleurs souligner que les tests de corrélation entre les ratios et la profondeur du sillon gingivo-dentaire prélevé ont été réalisés avec des échantillons de microbiote sous-gingival qui n'ont pas servi à construire les *core microbiome* et nos réseaux bactériens. Ils n'ont donc pas servi à élaborer les ratios mais ont permis de tester leur pertinence.

Nous proposons donc ces ratios comme outils de mesure de la dysbiose bactérienne sous-gingivale et biomarqueurs potentiels. Dans le cadre des associations entre maladie parodontale et maladies générales, ils peuvent se révéler utile pour caractériser le microbiote sous-gingival de sujets avec différents états de santé. Nous les avons d'ailleurs utilisés pour étudier la dysbiose du microbiote sous-gingival de patients atteints de surcharge en fer d'origine génétique⁴.

Mon rôle dans ce travail a principalement été de perfectionner les étapes de bioinformatique. Dans un premier temps, récupérer, depuis différentes bases de données (NCBI, GenBank, MG-RAST), de grandes quantités de données brutes de séquençage (1 426 échantillons de microbiote au total). Ces données étaient issues de chacun des articles inclus, ainsi que du « *Human Microbiome Project* » (HMP). Puis, j'ai chargé l'ensemble de ces échantillons dans l'outil web « *Visualization and Analysis of Microbial Population Structures* » (VAMPS, <https://vamps.mbl.edu/>) pour permettre un traitement uniforme sur l'ensemble des échantillons : contrôle qualité, assignation taxonomique, calculs de diversité, etc. J'ai ensuite participé à l'analyse des résultats — notamment les statistiques de corrélation avec les paramètres cliniques de sévérité de la parodontite —, et à la finalisation de la figure 6 de l'article.

Cet article a été publié dans *Applied and Environmental Microbiology* le 5 mai 2017. Il est disponible en accès ouvert dans les archives ouvertes HAL (<https://hal.archives-ouvertes.fr/hal-01560240v1>) et sur PubMed Central (<https://www.ncbi.nlm.nih.gov/pmc/articles/PMC5494626/>).

4. Voir à ce propos le travail présenté dans la section 2.2 *Periodontal pathogens and clinical parameters in periodontitis*, *Molecular Oral Microbiology* 2019 en page 37.



Signature of Microbial Dysbiosis in Periodontitis

Vincent Meuric,^{a,b} Sandrine Le Gall-David,^b Emile Boyer,^{a,b} Luis Acuña-Amador,^c Bénédicte Martin,^b Shao Bing Fong,^b Frederique Barloy-Hubler,^c Martine Bonnaure-Mallet^{a,b}

CHU Rennes, Pôle Odontologie, Rennes, France^a; Université de Rennes 1, EA 1254, INSERM 1241, Equipe de Microbiologie, Rennes, France^b; CNRS, UMR 6290, IGDR, Rennes, France^c

ABSTRACT Periodontitis is driven by disproportionate host inflammatory immune responses induced by an imbalance in the composition of oral bacteria; this instigates microbial dysbiosis, along with failed resolution of the chronic destructive inflammation. The objectives of this study were to identify microbial signatures for health and chronic periodontitis at the genus level and to propose a model of dysbiosis, including the calculation of bacterial ratios. Published sequencing data obtained from several different studies (196 subgingival samples from patients with chronic periodontitis and 422 subgingival samples from healthy subjects) were pooled and subjected to a new microbiota analysis using the same Visualization and Analysis of Microbial Population Structures (VAMPS) pipeline, to identify microbiota specific to health and disease. Microbiota were visualized using CoNet and Cytoscape. Dysbiosis ratios, defined as the percentage of genera associated with disease relative to the percentage of genera associated with health, were calculated to distinguish disease from health. Correlations between the proposed dysbiosis ratio and the periodontal pocket depth were tested with a different set of data obtained from a recent study, to confirm the relevance of the ratio as a potential indicator of dysbiosis. Beta diversity showed significant clustering of periodontitis-associated microbiota, at the genus level, according to the clinical status and independent of the methods used. Specific genera (*Veillonella*, *Neisseria*, *Rothia*, *Corynebacterium*, and *Actinomyces*) were highly prevalent (>95%) in health, while other genera (*Eubacterium*, *Campylobacter*, *Treponema*, and *Tannerella*) were associated with chronic periodontitis. The calculation of dysbiosis ratios based on the relative abundance of the genera found in health versus periodontitis was tested. Nonperiodontitis samples were significantly identifiable by low ratios, compared to chronic periodontitis samples. When applied to a subgingival sample set with well-defined clinical data, the method showed a strong correlation between the dysbiosis ratio, as well as a simplified ratio (*Porphyromonas*, *Treponema*, and *Tannerella* to *Rothia* and *Corynebacterium*), and pocket depth. Microbial analysis of chronic periodontitis can be correlated with the pocket depth through specific signatures for microbial dysbiosis.

IMPORTANCE Defining microbiota typical of oral health or chronic periodontitis is difficult. The evaluation of periodontal disease is currently based on probing of the periodontal pocket. However, the status of pockets “on the mend” or sulci at risk of periodontitis cannot be addressed solely through pocket depth measurements or current microbiological tests available for practitioners. Thus, a more specific microbiological measure of dysbiosis could help in future diagnoses of periodontitis. In this work, data from different studies were pooled, to improve the accuracy of the results. However, analysis of multiple species from different studies intensified the bacterial network and complicated the search for reproducible microbial signatures. Despite the use of different methods in each study, investigation of the microbiota at the genus level showed that some genera were prevalent (up to 95% of the sam-

Received 23 February 2017 Accepted 2 May 2017

Accepted manuscript posted online 5 May 2017

Citation Meuric V, Le Gall-David S, Boyer E, Acuña-Amador L, Martin B, Fong SB, Barloy-Hubler F, Bonnaure-Mallet M. 2017. Signature of microbial dysbiosis in periodontitis. *Appl Environ Microbiol* 83:e00462-17. <https://doi.org/10.1128/AEM.00462-17>.

Editor Andrew J. McBain, University of Manchester

Copyright © 2017 American Society for Microbiology. All Rights Reserved.

Address correspondence to Vincent Meuric, vincent.meuric@univ-rennes1.fr.

F.B.-H. and M.B.-M. contributed equally to this work.

ples) in health or disease, allowing the calculation of bacterial ratios (i.e., dysbiosis ratios). The correlation between the proposed ratios and the periodontal pocket depth was tested, which confirmed the link between dysbiosis ratios and the severity of the disease. The results of this work are promising, but longitudinal studies will be required to improve the ratios and to define the microbial signatures of the disease, which will allow monitoring of periodontal pocket recovery and, conceivably, determination of the potential risk of periodontitis among healthy patients.

KEYWORDS chronic periodontitis, health, microbiota, dysbiosis ratio

Chronic periodontitis (CP) is a type of chronic inflammation characterized by alveolar bone loss, with intermittent periods of remission and relapse. CP is currently considered an infection, mainly due to increases in bacteria in the sulcus, leading to the formation of a periodontal pocket (for review, see references 1 and 2). The major pathogen linked to CP is *Porphyromonas gingivalis*, with bacterial partners such as *Treponema denticola* and *Tannerella forsythia*. These three bacteria have been considered the major pathogenic “red complex” since 1998 (3). However, recent advances from metagenomic studies have developed a new model of periodontal disease pathogenesis. CP does not result from individual pathogens but rather from polymicrobial synergy and dysbiosis (4) associated with a dysregulated immune response inducing inflammation-mediated tissue damage (5). Host genetic components have also been implicated in CP, with multiple genes contributing cumulatively to the host’s overall disease risk (or protection) through effects on the host immune response and the microbiome (6). Since the Human Microbiome Project (HMP) (7), microbiota have been analyzed based on partial sequencing of the 16S rRNA gene, with different numbers of healthy and CP samples. However, comparisons between studies are difficult because of the differences in the methods used (i.e., clinical examination and diagnosis of periodontitis and oral health, sample collection protocols, DNA extraction protocols, and analysis of hypervariable regions of the 16S rRNA gene). Because there is growing interest in the human microbiome, despite the difficulties mentioned earlier, the use of independent studies to look for “signal in the noise” should proceed as suggested previously (8), through reanalysis of all data with the same protocol. The difference between periodontal health-associated and disease-associated microbiota should be larger than the technical variations of the different studies, which would enable the identification of microbial signatures using next-generation sequencing (NGS) technologies. The first objective of this study was to explore the disease-associated changes in the subgingival microbiota at the genus level, using a unique Visualization and Analysis of Microbial Population Structure (VAMPS) pipeline (9), for beta diversity (Bray-Curtis dissimilarity) with a large number of samples (from 6 different studies) and to confirm that the microbiota identified did not cluster according to the methods used (primer or study type). Subgingival microbiota from patients with diagnosed chronic periodontitis (196 samples) and from healthy subjects (422 samples), as well as external control samples (from dentine caries, supragingival plaque, and the midvagina), were included. The second objective was to determine a dysbiosis ratio of bacteria that could predict health or disease severity from the subgingival samples and finally to test the ratio with an independent cohort of patients with well-described periodontal pocket measurements.

RESULTS

Microbial community structure analysis. Using a matrix correlation analysis, the possible clustering of microbiota according to the nature of the primers used, the site of sampling, or the study investigated was explored. Despite various studies, the analyzed data clustered into five groups according to the clinical status (healthy or CP) or the sampling site, as shown by the three-dimensional (3D) principal-coordinate analysis (PCoA) plots (Fig. 1). Healthy subgingival samples were primarily spread into two main clusters; control samples were clearly separated into two other clusters, corresponding to saliva and dentine caries/vagina, while the majority of CP samples

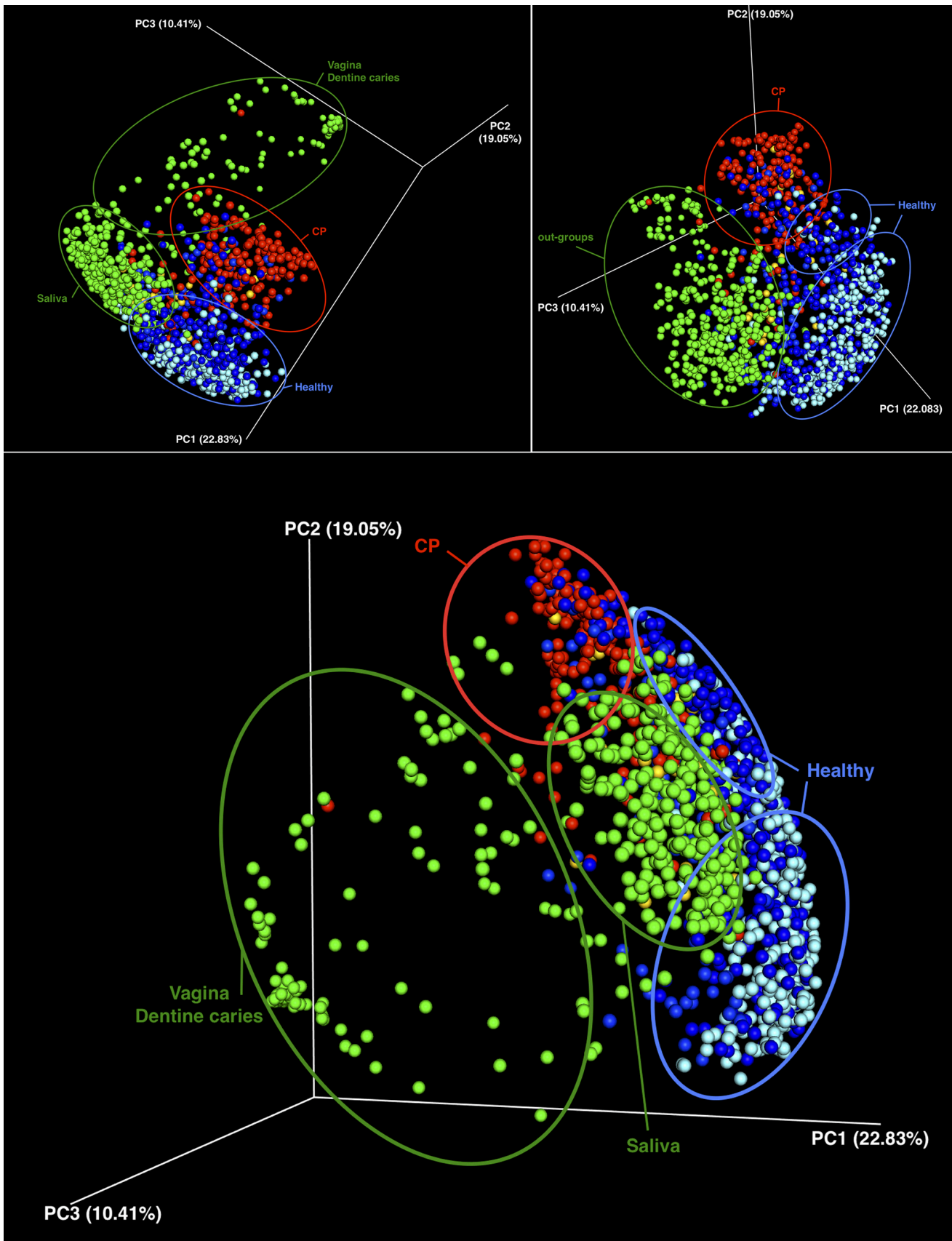


FIG 1 Different views of 3D PCoA plots illustrating the beta diversity of bacterial populations as a function of sampling site and diagnosis. Light blue, supragingival samples; dark blue, healthy subgingival samples; green, outgroups (saliva, midvagina, and dentine caries samples); red, CP samples. Percentages represent percent explained variance.

Downloaded from <http://aem.asm.org/> on November 19, 2018 by guest

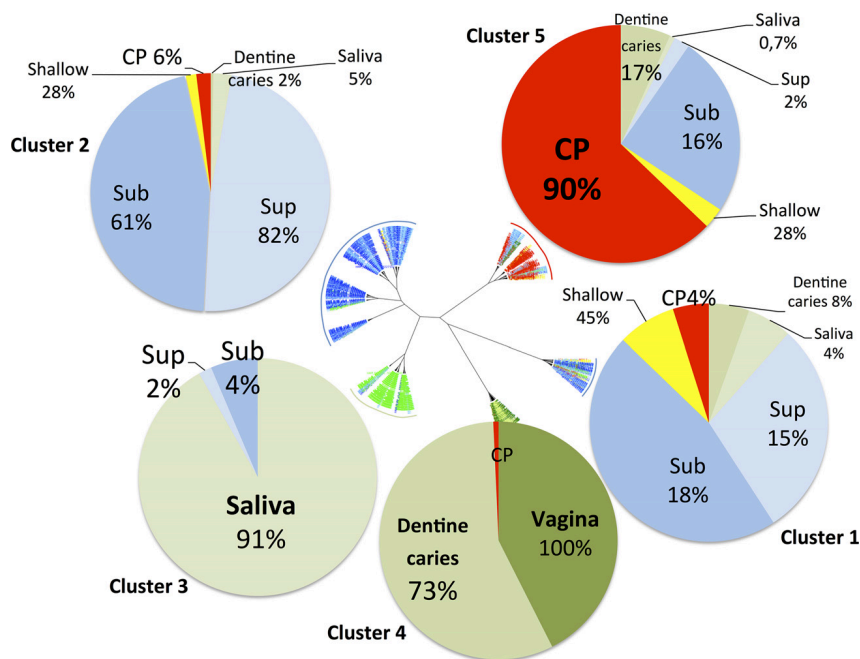


FIG 2 Unrooted tree displaying genus Bray-Curtis beta-diversity clustering of microbiota and pie charts related to the sample origins within each cluster. The distribution of microbiota in each cluster is represented by pie charts, with different colors representing different sampling sites (supragingival [Sup] in light blue, saliva in light green, dentine caries in medium green, and midvagina in dark green) and diagnosis for subgingival (Sub) samples (healthy in dark blue, shallow in yellow, and CP in red). Percentages correspond to the number of samples from a specific sampling site in a given cluster relative to the total number of samples from the same sampling site.

were found in a fifth cluster. Two-dimensional (2D) beta-diversity analysis showed the precise distribution of the samples in the five clusters (Fig. 2). The search for an association between clusters and primers and/or study type showed that the fourth cluster was associated with V3V4 16S rRNA primers (correlation $r = 0.537$; $P < 0.001$) and with the study by Kianoush et al. (10), which used those specific primers (correlation $r = 0.608$; $P < 0.001$). No other correlations with primers were found. The two healthy clusters (clusters 1 and 2) were characterized by subgingival and supragingival samples in similar proportions (Fig. 2, light blue and dark blue sections). Focusing on healthy subgingival samples, the main difference between the two healthy clusters (clusters 1 and 2) was in the distribution of samples from the HMP study and from the other studies in the clusters; 225/323 samples from the HMP study were clustered in healthy cluster 2, while healthy cluster 1 was richer in samples derived from the other studies (44/99 samples). Cluster 3 was characterized by saliva, as 91% of the saliva samples (258/284 samples) were grouped in this cluster (correlation $r = 0.892$; $P < 0.001$) (Fig. 2). Cluster 4 was characterized by dentine caries samples (73% [80/110 samples]; correlation $r = 0.603$; $P < 0.001$) and midvagina samples (100% [60/60 samples]; correlation $r = 0.638$; $P < 0.001$). Finally, cluster 5 contained 90% of the CP samples (176/196 samples; correlation $r = 0.708$; $P < 0.001$).

It is interesting to note that 10% of the CP samples were found in the two healthy clusters (19/196 samples) and contained similar microbiota (analyzed on the basis of beta diversity), at the genus level, as dentine caries samples and/or midvagina samples (1/196 samples). Conversely, 16% of the healthy subgingival samples (69/422 samples) and 17% of the dentine caries samples (19/110 samples) were found in cluster 5.

Microbiota richness and alpha diversity in subgingival samples. A cluster comparison showed that the sampling depth (number of reads sequenced) was greater in healthy subgingival clusters 1 and 2 than in cluster 5. Nevertheless, no significant difference between healthy subgingival samples and CP samples of cluster 5 was found (Fig. 3). The observed richness (S) was lower in the CP samples of cluster 5 than in the

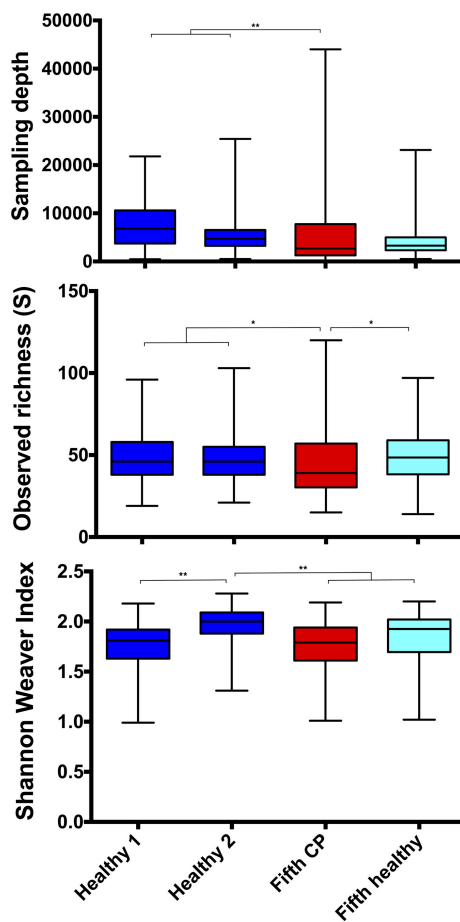


FIG 3 Alpha diversity index values. Comparisons of microbiota sampling depth, observed richness (number of different taxa per sample), and diversity (Shannon-Weaver index) in subgingival samples of healthy clusters 1 and 2 (dark blue) and either CP samples (red) or healthy subgingival samples (light blue) of cluster 5 were performed. *, $P < 0.05$; **, $P < 0.01$.

samples of healthy clusters 1 and 2 and the healthy subgingival samples of cluster 5 (Fig. 3). However, the Shannon-Weaver diversity index values showed that the diversity of healthy cluster 2 was significantly greater than the diversity of healthy cluster 1 and that of all samples from cluster 5, which were similar.

Patterns of microbial communities in subgingival samples (genus level). Genera that were present in at least 95% of all healthy subgingival samples or 95% of the CP samples from cluster 5 are presented in Fig. 4A and B, respectively. Results showed that healthy subgingival samples were dominated by 8 major genera, i.e., *Fusobacterium*, *Actinomyces*, *Streptococcus*, *Neisseria*, *Capnocytophaga*, *Prevotella*, *Corynebacterium*, and *Rothia*, and 6 minor genera, i.e., *Leptotrichia*, *Veillonella*, *Porphyromonas*, *Granulicatella*, *Kingella*, and *Gemella*. Associations were found between *Fusobacterium* and *Prevotella*, *Actinomyces*, and *Rothia* and between *Leptotrichia* and *Porphyromonas*. Common genera found in CP samples were less abundant, with 4 major genera, *Treponema*, *Porphyromonas*, *Prevotella*, and *Fusobacterium*, followed by *Streptococcus*, *Eubacterium*, *Tannerella*, and *Campylobacter* genera. Only one association was found, between *Eubacterium* and *Treponema*, while *Fusobacterium* and *Treponema* presented a negative correlation.

Calculation of dysbiosis ratios of bacteria. The dysbiosis ratios of the genera found mainly in CP samples (*Eubacteria*, *Campylobacter*, *Treponema*, and *Tannerella*) to the genera found mainly in healthy samples (*Veillonella*, *Neisseria*, *Rothia*, *Corynebacterium*, and *Actinomyces*) were significantly different among the samples according to their diagnosis. The dysbiosis ratios for healthy subgingival samples (from the HMP, $n = 323$,

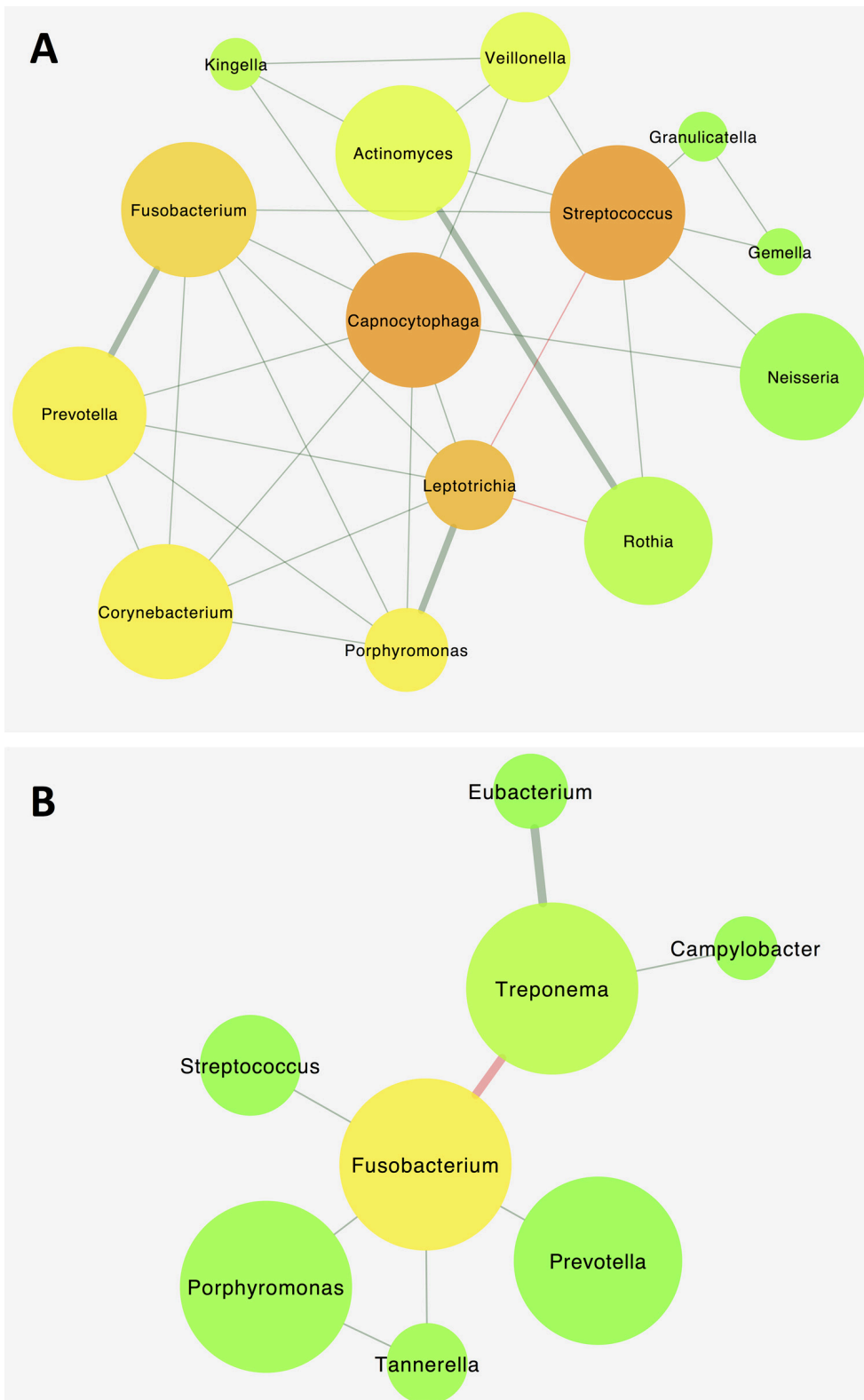


FIG 4 Patterns of subgingival microbial communities. (A) Patterns of genera present in at least 95% of all healthy subgingival samples. (B) Patterns of genera present in at least 95% of all CP samples from cluster 5. Edges represent 1 (thin line) or 2 or 3 (thick line) significant correlations between genera (green, positive; red, negative). Node colors represent the numbers of partners, ranging from 1 (green) to 7 (dark orange). Node sizes represent the abundance of each taxon.

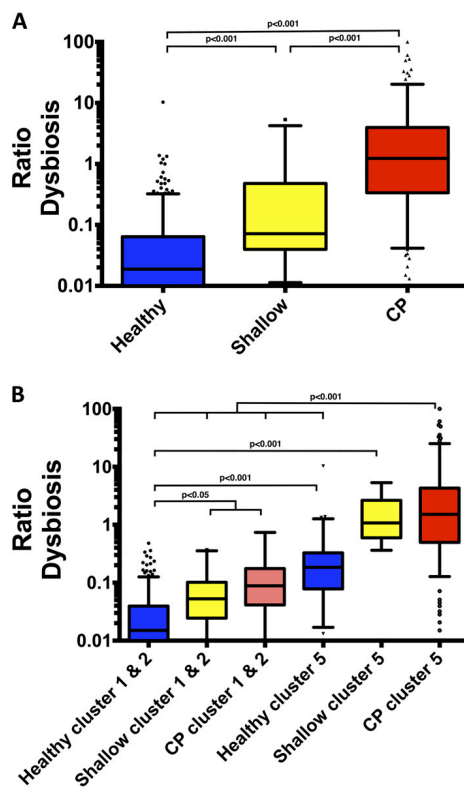


FIG 5 Subgingival dysbiosis ratios of *Eubacterium*, *Campylobacter*, *Treponema*, and *Tannerella* to *Veillonella*, *Neisseria*, *Rothia*, *Corynebacterium*, and *Actinomyces*. (A) Comparisons between healthy, shallow, and CP samples from all clusters. (B) Comparisons between clusters 1 and 2 and cluster 5 for healthy, shallow, and CP samples.

ratio of 0.016; from the other studies, $n = 99$, ratio of 0.021) yielded a median ratio of 0.018; the samples from shallow sites had a ratio of 0.071, and the CP samples had a ratio of 1.229 ($P < 0.001$) (Fig. 5A).

Although different clustering was achieved through beta-diversity analysis, no significant difference in the ratios of clusters 1 and 2 according to the clinical status (healthy, shallow, or CP) was found. Pooling of samples according to clinical status was performed, and the resulting ratios were compared to the ratios for cluster 5, as shown in Fig. 5B.

The dysbiosis ratio found for CP samples from cluster 5 (ratio of 1.510) was significantly greater than the ratios for the majority of samples from clusters 1 and 2 (healthy subgingival samples, ratio of 0.015; shallow samples, ratio of 0.052; CP samples, ratio of 0.088) and was also significantly greater than the ratio for healthy subgingival samples (ratio of 0.184) from cluster 5 ($P < 0.001$). In clusters 1 and 2, the dysbiosis ratios for CP samples were similar to the ratios for shallow sites. These two groups were significantly different from the healthy subgingival samples ($P < 0.05$) in the same cluster.

Healthy subgingival samples ($n = 69$) belonging to cluster 5 exhibited a dysbiosis ratio (ratio of 0.184) significantly different from that for the other healthy subgingival samples (ratio of 0.015) and also from that for the majority of the CP samples (cluster 5) (ratio of 1.510). These results confirmed the possible difference of these healthy subgingival microbiota ($P < 0.001$) from those of healthy clusters 1 and 2. Their ratio was not significantly different from the CP sample ratios in clusters 1 and 2, which could be considered "on the mend."

Validation of the dysbiosis ratio. A different data set, from Bizzarro et al. (11) and containing well-described samples (pocket depths of 2 to 8 mm), was used as an external control to confirm the relevance of the bacterial dysbiosis ratio. The dysbiosis

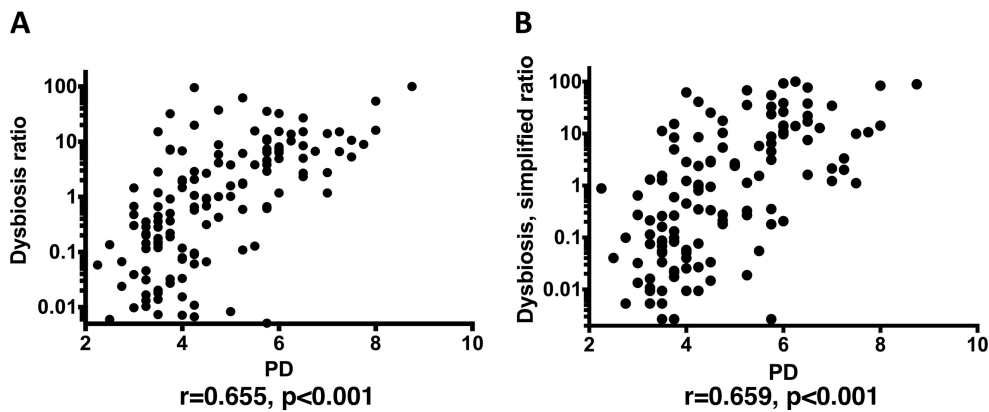


FIG 6 Correlation between pocket depth (PD) and dysbiosis. Samples from Bizzarro et al. (11) were analyzed by VAMPS, followed by calculation of the dysbiosis ratios. (A) Ratios of *Eubacterium*, *Campylobacter*, *Treponema*, and *Tannerella* to *Veillonella*, *Neisseria*, *Rothia*, *Corynebacterium*, and *Actinomyces*. (B) Simplified ratios of *Porphyromonas*, *Treponema*, and *Tannerella* to *Rothia* and *Corynebacterium*.

ratio at the genus level was correlated with the periodontal pocket depth ($r = 0.655$; $P < 0.001$) (Fig. 6A). These results, based on data for 37 patients (147 samples collected at different times, with different procedures for periodontal treatment), confirmed the link between dysbiosis and the depth of the periodontal pocket. The simplified ratio of *Porphyromonas*, *Treponema*, and *Tannerella* to *Rothia* and *Corynebacterium* showed a similar correlation ($r = 0.659$; $P < 0.001$) (Fig. 6B).

DISCUSSION

Many studies have been published since the Human Microbiome Project in 2009, increasing the volume of microbiota data available for the research community. However, comparisons between studies are challenging, at least at the species level, because of the use of different methods. This issue is a real limitation to understanding disease, as is the small number of samples in each study. Additionally, findings are more complicated for healthy subgingival samples, which usually represent less than one-half of the samples included in the studies (12, 13). This work is a taxon-based analysis, at the genus level, of sequence reads from several studies. Studying a large number of samples minimized individual variations and overcame technical variations by increasing the effective sample size. Such an analysis had already been proposed in a recent study of the microbiota in obesity (8). Studies with described healthy samples (sulci of ≤ 3 mm) and CP samples (pocket depths of ≥ 5 mm) and available raw sequence data in data banks were chosen. Data from the HMP resources (two different pairs of primers used) were added to increase the number of healthy subgingival samples with available microbiota data from 99 samples to 422 samples. The different microbiota clustered either by sampling site, such as the outgroups used as controls for this study (saliva samples in cluster 3 and dentine caries and vagina samples, which are both rich in *Lactobacillus*, in cluster 4), or by clinical status, such as subgingival samples (healthy samples in clusters 1 and 2 and CP samples in cluster 5). CP sites either can show greater microbial diversity and observed richness, compared with healthy subgingival sites (14, 15), or can present no significant difference in microbial diversity, as reported for health versus periodontitis (16). Thus, the large number of samples surpasses the technical variations, at least at the genus level, with the primers used in the different studies, and the difference between periodontal health and disease is larger than the technical variations, as described by Kirst et al. (16). No difference between the healthy subgingival and supragingival samples was found when beta-diversity analysis was performed at the genus level, as described previously (17). Ninety percent of the CP samples were found in cluster 5. To define cluster 5 as a "periodontitis cluster" by beta diversity was appealing. However, cluster 5 also contained healthy subgingival samples, indicating that further investigations are necessary to understand and to develop prediction markers for chronic periodontitis.

A core community (genera present in at least 50% of the samples) is usually identified in publications and provides a basis for disease diagnosis, prevention, and therapeutic targets (18, 19). However, the variability of genera expands as the sample size increases, thus limiting its use for establishing an easy microbiological marker for dysbiosis. In this work, genera present at higher prevalence in at least 95% of the samples were used to determine the genera implicated in health or in favor of the disease. The genera used to calculate the dysbiosis ratio in favor of periodontitis were *Treponema*, *Campylobacter*, *Eubacterium*, and *Tannerella*. These genera were identified at high levels and high prevalence in CP samples, compared to healthy samples. The genera include well-identified species (*Tannerella forsythia*, *Treponema denticola*, *C. rectus*, and *E. nodatum*) that are strongly associated with disease (3, 20–22). It should be noted that some species, such as the newly cultivated *Tannerella* clone BU063 (23, 24), which is thought to be health associated, are also found in active periodontal sites (25); therefore, this species is still controversial. Despite a significant difference in the abundance of the *Porphyromonas* genus (including *P. gingivalis*, which is strongly associated with periodontitis) between healthy samples (3.35%) and CP samples (13%), the genus was excluded in the first dysbiosis ratio because of its similar prevalence rates. Because the lowest abundance value among genera accounting for the CP calculations was that for *Campylobacter* (1.9%), this value was chosen as a cutoff value to minimize the number of genera used for the health calculations, i.e., *Rothia*, *Corynebacterium*, *Actinomyces*, *Veillonella*, and *Neisseria*. *Capnocytophaga* and *Leptotrichia* were not included because of their high rates of prevalence in CP samples (more than 90%; data not shown). Species belonging to the genus *Rothia* have been repeatedly described as being members of oral communities associated with periodontal health (26–31) or at least as being more predominant in health (28). In the same way, *Corynebacterium* appeared to be more associated with healthy subgingival biofilm (32, 33). Moreover, *Rothia* and *Corynebacterium* were among the bacteria that showed the greatest increases after periodontal treatment (34), while a study suggested that *Corynebacterium* might be considered a putative periodontal protector (35). *Veillonella* and *Actinomyces* have been negatively correlated with clinical markers in CP (36), and *Neisseria* was found in inactive sites (25). The calculated dysbiosis ratios distinguish clearly healthy subgingival samples from CP samples.

Shallow samples were divided into two groups, which can be easily explained based on the origin of the samples (healthy subgingival sites in mouths presenting chronic periodontitis). Two-thirds of the samples had low ratios (clusters 1 and 2) and could be considered microbiologically healthy. The remaining one-third of the samples (cluster 5) presented high ratios, certainly due to contamination of the sampling sites by bacteria from surrounding CP sites, and could be considered at risk of periodontitis. Thus, shallow samples may represent an intermediate stage in disease development, as proposed by Griffen et al. (14).

Healthy subgingival samples were divided into three groups. Two of the groups (clusters 1 and 2) presented the same low ratios and described an absence of dysbiosis. The third group had a higher dysbiosis ratio, similar to those for shallow sites and CP samples from clusters 1 and 2 but significantly lower than those for CP or shallow samples from cluster 5. Because healthy patients from the HMP were defined as patients with pockets depths of <4 mm, some of them could have explained this high-ratio group; however, healthy patients from other studies (19/99 subjects) were also included in this group. This result is similar to those of Zhou et al., in which a few healthy subjects with indicators of disease, such as increases in *Treponema*, were detected (37). Therefore, patients who presented with relatively high ratios could be considered at risk of periodontitis.

Conversely, a few CP samples with deep periodontal pockets (i.e., ≥ 5 mm) had low dysbiosis ratios. An hypothesis of appropriate host responses (such as a stronger immune response and/or better hygiene) could explain this discrepancy between the dysbiosis ratios and the diagnoses; these patients might be microbiologically on the mend, as revealed by both the clustering and the dysbiosis ratios. Another hypothesis

is a sampling issue between the top and base of the periodontal pocket (to be discussed later). To study the hypothesis of microbiota on the mend and the calculated dysbiosis ratios, a recent study presenting follow-up findings after treatment, with well-defined depths of periodontal pockets, was performed (11). The study was conducted with a different set of primers (for V5V7) and allowed testing of the dysbiosis ratios at the genus level with a new set of primers that had not been used to determine the ratios. Consequently, this comparative analysis can be considered a validation experiment for the ratios. A strong correlation between the dysbiosis ratios and the pocket depths was observed, thus highlighting the value of calculating the dysbiosis ratio (using the selected genera of our study) as a microbial signature to evaluate the microbiota of chronic periodontitis.

A major concern at the beginning of this work was the capacity to identify species with multiple data sets. However, the V1V2 and V5V7 primers used in three studies were not suitable for species identification. At the genus level, as reported by Bizzarro et al. (11), the proposed dysbiosis ratio (even as a simplified dysbiosis ratio) is a good microbial signature calculated using the online VAMPS software. Indeed, *Rothia* and *Corynebacterium* were the major healthy genera found and, although *Porphyromonas* was found in both health and disease, its abundance increased significantly in disease (from 3.34% to 13%). The result was interesting because it was found to be similar to the precedent ratio (correlation with pocket depth, $r = 0.659$; $P < 0.001$). However, the simplified ratio needed more adjustment, because 43 of 196 CP samples presented neither of the two healthy genera and a value of 0.1% was attributed for the calculation (see Materials and Methods ["Calculation of dysbiosis ratios of bacteria" section]).

Finally, using ratios, some data points still showed discrepancies in predicting the periodontal status. The variability in microbial composition and spatial distribution could explain these results. Deep periodontal pockets in CP patients may present gradients of oxygen tension, pH, and nutrients, as well as host defense factors, from the base of the pocket to the top (opening). This may explain why some genera (*Porphyromonas* and *Treponema*) are typically found at the base of the pocket (38, 39). However, the sampling could induce bias even after careful removal of the supragingival plaque. Healthy genera may be found predominantly at the top (opening) of the pocket, with the genera more closely associated with CP being located at the base of the pocket. Indeed, while the architecture of the periodontal pocket has not yet been clearly studied with the use of NGS analysis, the importance of the biogeography of the microbiome on the micron scale was clearly shown recently (40).

In conclusion, this study aimed to define ratios of bacteria as microbial signatures, after the analysis of publicly available raw data from different studies, independent of the technical methods used to generate the data. These ratios allowed the differentiation of healthy and diseased microbiota in the majority of samples. Standardized protocols for sampling and complete metadata in public data banks are necessary to study dysbiosis in oral health and to improve the proposed dysbiosis ratios. The addition of specific perioprotectors and potential specific pathogens to the dysbiosis calculations could also be promising. Longitudinal studies are necessary to predict exact pockets that are microbiologically on the mend or sulci with a risk of periodontitis.

MATERIALS AND METHODS

Microbiome data sets for comparison. Read sequences from healthy and CP subgingival samples from five different studies, i.e., those by Abusleme et al. (12), Kirst et al. (16), Griffen et al. (14) (shallow site samples also included), Zhou et al. (41), and Camelo-Castillo et al. (13), were retrieved from either the NCBI Sequence Read Archive (SRA) or the metagenomics (MG)-RAST server (Table 1). Twenty-four samples from patients with chronic periodontitis who were recruited between June 2010 and September 2011 at the University Hospital (Rennes, France), which were analyzed using V3V4 primers, were added (E. Boyer, S. Le Gall-David, Y. Deugnier, M. Bonnaure-Mallet, and V. Meuric, unpublished data). Each data set was manually imported into VAMPS (<https://vamaps.mbl.edu>), while numerous healthy subgingival samples were added from the HMP (two different subgingival data sets, using V1V3 and V3V5 primers, available in VAMPS [9]). Three mouth control microbiota data sets from the HMP (saliva and supragingival, both V1V3 and V3V5 regions, available in VAMPS) and dentine caries data from the study by

TABLE 1 Subgingival microbiota samples used in this study

Authors	Accession no.	No. of subgingival microbiota samples				16S rRNA gene regions
		Health	CP		Follow up after treatment	
			Shallow ^a	Diagnosis		
Abusleme et al. (12)	GenBank SRA SRA051864	10		44		V1V2
Kirst et al. (16)	GenBank BioProject PRJNA269205	25		25		V1V3
Griffen et al. (14)	GenBank SRA SRP009299	29	29	29		V1V2 and V4
Camelo-Castillo et al. (13)	MG-RAST 12161	22		60		V1V3
Zhou et al. (37)	GenBank SRA SRA062091	13		18		V1V3
Boyer et al. (unpublished)	In progress ^b			24		V3V4
HMP (7)		119				V1V3
HMP (7)		204				V3V5
Bizzarro et al. (11)	GenBank BioProject PRJNA289294			37 ^c	110 ^c	V5V7

^aSites defined as healthy in patients with periodontitis (14).

^bData are available on VAMPS (data set designated Y_Hemoparo).

^cData on the CP microbiota from patients with follow-up findings after treatment were used to confirm the dysbiosis ratio hypothesis (11).

Kianoush et al. (10) (V3V4 regions; BioProject accession no. [PRJEB5178](#)) were used. One midvaginal microbiome data set from the HMP (V1V3 region, available in VAMPS) was used as an external mouth control. Finally, the data set from the study by Bizzarro et al. (11), containing well-described sample pocket depths (from 2 to 8 mm), was used to independently challenge the relevance of the dysbiosis ratio of bacteria involved in periodontitis.

Ecology diversity and taxonomic identifications. Reads from the different data sets were analyzed with VAMPS, using default parameters for taxonomic assignment to the genus level through the Global Alignment for Sequence Taxonomy (GAST) process and using the Ribosomal Database Project (RDP) classification to produce the best taxonomic assignment for each read. Reads identified as *Archaea*, *Eukarya*, or organelle and unknown reads were excluded from further analysis. The frequency of each taxonomic assignment in the data set was reported as a percentage (number of reads with the taxonomic assignment relative to the total number of reads in the data set). Alpha diversity, as the observed richness, and Shannon-Weaver index values were determined from the raw data sets. Differences between microbiota structures (beta diversity) were assessed using a 2D PCoA tree based on the Bray-Curtis distances, through VAMPS. Samples were divided into five clusters (clusters 1 to 5); visualizations were performed using Figtree software (version 1.4.2), and 3D PCoA plots were generated using Emperor software. Relative abundances were studied when the average abundance was above 1% in at least one sample. Assessments of significant patterns of microbial cooccurrence or mutual exclusion at the genus level were performed using Cytoscape 3.2.1 (42) and the CoNet plugin (43). Only genera found in the great majority (at least 95%) of the healthy subgingival samples or the CP samples (from cluster 5) are represented.

Calculation of dysbiosis ratios of bacteria. To measure the dysbiosis, a first ratio, based on the relative abundance of genera highly prevalent (>95%) in CP samples (*Eubacterium*, *Campylobacter*, *Treponema*, and *Tannerella*) versus genera highly prevalent (>95%) in healthy microbiota (*Veillonella*, *Neisseria*, *Rothia*, *Corynebacterium*, and *Actinomyces*), was calculated. The ratios were normalized between samples using GraphPad Prism 6 software before comparisons. A second simplified ratio of *Porphyromonas*, *Treponema*, and *Tannerella* versus *Rothia* and *Corynebacterium* was also tested. When no specific genus was detected, a value of 0.1% was attributed (because "not detected" does not mean "absence").

Statistical analysis. Normality tests for data distribution were performed. Data were studied with the Spearman correlation test for correlations of biological origins, primers used, published sample origins, and microbiota clusters. Observed richness (number of taxa per sample), Shannon-Weaver index values, and dysbiosis ratios of the genera found in disease to the genera found in health were analyzed with a Kruskal-Wallis test (nonparametric analysis of variance). Tests were carried out using GraphPad Prism 6 software and were considered significant with *P* values of <0.05. The significant patterns of microbial cooccurrence and mutual exclusion were analyzed as described by Faust et al. (43); a compilation of statistical analyses (Spearman and Pearson correlations and Bray-Curtis and Kullback-Leibler dissimilarity measures) was used, with a threshold set at 0.5. The data matrix was randomized by 100 row-wise permutations. The *P* values were adjusted with the Benjamini-Hochberg false discovery rate (FDR) correction for the number of tests, retaining only *P* values of <0.05. Finally, the ratios of genera and pocket depths were controlled for normality, followed by the Spearman correlation test.

ACKNOWLEDGMENTS

V.M., F.B.-H., and M.B.-M. conceived and designed the research, V.M. performed the sampling, S.L.G.-D. performed the molecular biological analyses, V.M., S.L.G.-D., E.B., L.A.-A., B.M., S.B.F., and M.B.-M. performed the bioinformatic and statistical analyses and wrote the manuscript, and M.B.-M. supervised the project.

We declare no competing financial interests.

REFERENCES

- Teles R, Teles F, Frias-Lopez J, Paster B, Haffajee A. 2013. Lessons learned and unlearned in periodontal microbiology. *Periodontol* 2000 62: 95–162. <https://doi.org/10.1111/prd.12010>.
- Kilian M, Chapple IL, Hannig M, Marsh PD, Meuric V, Pedersen AM, Tonetti MS, Wade WG, Zaura E. 2016. The oral microbiome: an update for oral healthcare professionals. *Br Dent J* 221:657–666. <https://doi.org/10.1038/sj.bdj.2016.865>.
- Socransky SS, Haffajee AD, Cugini MA, Smith C, Kent RL, Jr. 1998. Microbial complexes in subgingival plaque. *J Clin Periodontol* 25:134–144. <https://doi.org/10.1111/j.1600-051X.1998.tb02419.x>.
- Hajishengallis G. 2015. Periodontitis: from microbial immune subversion to systemic inflammation. *Nat Rev Immunol* 15:30–44. <https://doi.org/10.1038/nri3785>.
- Hajishengallis G, Darveau RP, Curtis MA. 2012. The keystone-pathogen hypothesis. *Nat Rev Microbiol* 10:717–725. <https://doi.org/10.1038/nrmicro2873>.
- Hajishengallis G, Moutsopoulos NM, Hajishengallis E, Chavakis T. 2016. Immune and regulatory functions of neutrophils in inflammatory bone loss. *Semin Immunol* 28:146–158. <https://doi.org/10.1016/j.smim.2016.02.002>.
- Peterson J, Garges S, Giovanni M, McInnes P, Wang L, Schloss JA, Bonazzi V, McEwen JE, Wetterstrand KA, Deal C, Baker CC, Di Francesco V, Howcroft TK, Karp RW, Lunsford RD, Wellington CR, Belachew T, Wright M, Giblin C, David H, Mills M, Salomon R, Mullins C, Akolkar B, Begg L, Davis C, Grandison L, Humble M, Khalsa J, Little AR, Peavy H, Pontzer C, Portnoy M, Sayre MH, Starke-Reed P, Zakhari S, Read J, Watson B, Guyer M. 2009. The NIH Human Microbiome Project. *Genome Res* 19: 2317–2323. <https://doi.org/10.1101/gr.096651.109>.
- Sze MA, Schloss PD. 2016. Looking for a signal in the noise: revisiting obesity and the microbiome. *mBio* 7:e01018-16. <https://doi.org/10.1128/mBio.01018-16>.
- Huse SM, Mark Welch DB, Voorhis A, Shipunova A, Morrison HG, Eren AM, Sogin ML. 2014. VAMPS: a website for visualization and analysis of microbial population structures. *BMC Bioinformatics* 15:41. <https://doi.org/10.1186/1471-2105-15-41>.
- Kianoush N, Adler CJ, Nguyen KA, Browne GV, Simonian M, Hunter N. 2014. Bacterial profile of dentine caries and the impact of pH on bacterial population diversity. *PLoS One* 9:e92940. <https://doi.org/10.1371/journal.pone.0092940>.
- Bizzarro S, Laine ML, Buijs MJ, Brandt BW, Crielaard W, Loos BG, Zaura E. 2016. Microbial profiles at baseline and not the use of antibiotics determine the clinical outcome of the treatment of chronic periodontitis. *Sci Rep* 6:20205. <https://doi.org/10.1038/srep20205>.
- Abusleme L, Dupuy AK, Dutzan N, Silva N, Burlinson JA, Strausbaugh LD, Gamonal J, Diaz PI. 2013. The subgingival microbiome in health and periodontitis and its relationship with community biomass and inflammation. *ISME J* 7:1016–1025. <https://doi.org/10.1038/ismej.2012.174>.
- Camelo-Castillo AJ, Mira A, Pico A, Nibali L, Henderson B, Donos N, Tomas I. 2015. Subgingival microbiota in health compared to periodontitis and the influence of smoking. *Front Microbiol* 6:119. <https://doi.org/10.3389/fmicb.2015.00119>.
- Griffen AL, Beall CJ, Campbell JH, Firestone ND, Kumar PS, Yang ZK, Podar M, Leys EJ. 2012. Distinct and complex bacterial profiles in human periodontitis and health revealed by 16S pyrosequencing. *ISME J* 6:1176–1185. <https://doi.org/10.1038/ismej.2011.191>.
- Socransky SS, Haffajee AD, Smith C, Dibart S. 1991. Relation of counts of microbial species to clinical status at the sampled site. *J Clin Periodontol* 18:766–775. <https://doi.org/10.1111/j.1600-051X.1991.tb00070.x>.
- Kirst ME, Li EC, Alfant B, Chi YY, Walker C, Magnusson I, Wang GP. 2015. Dysbiosis and alterations in predicted functions of the subgingival microbiome in chronic periodontitis. *Appl Environ Microbiol* 81:783–793. <https://doi.org/10.1128/AEM.02712-14>.
- Ning J, Beiko RG. 2015. Phylogenetic approaches to microbial community classification. *Microbiome* 3:47. <https://doi.org/10.1186/s40168-015-0114-5>.
- Shade A, Handelsman J. 2012. Beyond the Venn diagram: the hunt for a core microbiome. *Environ Microbiol* 14:4–12. <https://doi.org/10.1111/j.1462-2920.2011.02585.x>.
- Jalanka-Tuovinen J, Salonen A, Nikkila J, Immonen O, Kekkonen R, Lahti L, Palva A, de Vos WM. 2011. Intestinal microbiota in healthy adults: temporal analysis reveals individual and common core and relation to intestinal symptoms. *PLoS One* 6:e23035. <https://doi.org/10.1371/journal.pone.0023035>.
- Laine ML, Moustakis V, Koumakis L, Potamias G, Loos BG. 2013. Modeling susceptibility to periodontitis. *J Dent Res* 92:45–50. <https://doi.org/10.1177/0022034512465435>.
- Byrne SJ, Dashper SG, Darby IB, Adams GG, Hoffmann B, Reynolds EC. 2009. Progression of chronic periodontitis can be predicted by the levels of *Porphyromonas gingivalis* and *Treponema denticola* in subgingival plaque. *Oral Microbiol Immunol* 24:469–477. <https://doi.org/10.1111/j.1399-302X.2009.00544.x>.
- Haffajee AD, Teles RP, Socransky SS. 2006. Association of *Eubacterium nodatum* and *Treponema denticola* with human periodontitis lesions. *Oral Microbiol Immunol* 21:269–282. <https://doi.org/10.1111/j.1399-302X.2006.00287.x>.
- Leys EJ, Lyons SR, Moeschberger ML, Rumpf RW, Griffen AL. 2002. Association of *Bacteroides forsythus* and a novel *Bacteroides* phylotype with periodontitis. *J Clin Microbiol* 40:821–825. <https://doi.org/10.1128/JCM.40.3.821-825.2002>.
- Vartoukian SR, Moazzez RV, Paster BJ, Dewhirst FE, Wade WG. 2016. First cultivation of health-associated *Tannerella* sp. HOT-286 (BU063). *J Dent Res* 95:1308–1313. <https://doi.org/10.1177/0022034516651078>.
- Yost S, Duran-Pinedo AE, Teles R, Krishnan K, Frias-Lopez J. 2015. Functional signatures of oral dysbiosis during periodontitis progression revealed by microbial metatranscriptome analysis. *Genome Med* 7:27. <https://doi.org/10.1186/s13073-015-0153-3>.
- Moore LV, Moore WE, Cato EP, Smibert RM, Burmeister JA, Best AM, Ranney RR. 1987. Bacteriology of human gingivitis. *J Dent Res* 66: 989–995. <https://doi.org/10.1177/00220345870660052401>.
- Aas JA, Paster BJ, Stokes LN, Olsen I, Dewhirst FE. 2005. Defining the normal bacterial flora of the oral cavity. *J Clin Microbiol* 43:5721–5732. <https://doi.org/10.1128/JCM.43.11.5721-5732.2005>.
- Colombo AP, Boches SK, Cotton SL, Goodson JM, Kent R, Haffajee AD, Socransky SS, Hasturk H, Van Dyke TE, Dewhirst F, Paster BJ. 2009. Comparisons of subgingival microbial profiles of refractory periodontitis, severe periodontitis, and periodontal health using the human oral microbe identification microarray. *J Periodontol* 80:1421–1432. <https://doi.org/10.1902/jop.2009.090185>.
- Bik EM, Long CD, Armitage GC, Loomer P, Emerson J, Mongodin EF, Nelson KE, Gill SR, Fraser-Liggett CM, Relman DA. 2010. Bacterial diversity in the oral cavity of 10 healthy individuals. *ISME J* 4:962–974. <https://doi.org/10.1038/ismej.2010.30>.
- Heuer W, Stiesch M, Abraham WR. 2011. Microbial diversity of supra- and subgingival biofilms on freshly colonized titanium implant abutments in the human mouth. *Eur J Clin Microbiol Infect Dis* 30:193–200. <https://doi.org/10.1007/s10096-010-1068-y>.
- Moutsopoulos NM, Chalmers NI, Barb JJ, Abusleme L, Greenwell-Wild T, Dutzan N, Paster BJ, Munson PJ, Fine DH, Uzel G, Holland SM. 2015. Subgingival microbial communities in leukocyte adhesion deficiency and their relationship with local immunopathology. *PLoS Pathog* 11: e1004698. <https://doi.org/10.1371/journal.ppat.1004698>.
- Paster BJ, Boches SK, Galvin JL, Ericson RE, Lau CN, Levanos VA, Saharabudhe A, Dewhirst FE. 2001. Bacterial diversity in human subgingival plaque. *J Bacteriol* 183:3770–3783. <https://doi.org/10.1128/JB.183.12.3770-3783.2001>.
- Ling Z, Liu X, Luo Y, Yuan L, Nelson KE, Wang Y, Xiang C, Li L. 2013. Pyrosequencing analysis of the human microbiota of healthy Chinese undergraduates. *BMC Genomics* 14:390. <https://doi.org/10.1186/1471-2164-14-390>.
- Laksmana T, Kittichotirat W, Huang Y, Chen W, Jorgensen M, Bumgarner R, Chen C. 2012. Metagenomic analysis of subgingival microbiota following non-surgical periodontal therapy: a pilot study. *Open Dent J* 6:255–261. <https://doi.org/10.2174/1874210601206010255>.
- Zorina OA, Petrukhina NB, Basova AA, Shibaeva AV, Trubnikova EV, Shevelev AB. 2014. Identification of key markers of normal and pathogenic microbiota determining health of periodontium by NGS-sequencing 16S-rDNA libraries of periodontal swabs. *Stomatologia* (Mosk) 93:25–31. <https://doi.org/10.17116/stomat201493625-31>. (In Russian.)
- Teles R, Sakellari D, Teles F, Konstantinidis A, Kent R, Socransky S, Haffajee A. 2010. Relationships among gingival crevicular fluid biomarkers, clinical parameters of periodontal disease, and the subgingival

- microbiota. *J Periodontol* 81:89–98. <https://doi.org/10.1902/jop.2009.090397>.
37. Zhou Y, Mihindukulasuriya KA, Gao H, La Rosa PS, Wylie KM, Martin JC, Kota K, Shannon WD, Mitreva M, Sodergren E, Weinstock GM. 2014. Exploration of bacterial community classes in major human habitats. *Genome Biol* 15:R66. <https://doi.org/10.1186/gb-2014-15-5-r66>.
38. Zijngé V, van Leeuwen MB, Degener JE, Abbas F, Thurnheer T, Gmur R, Harmsen HJ. 2010. Oral biofilm architecture on natural teeth. *PLoS One* 5:e9321. <https://doi.org/10.1371/journal.pone.0009321>.
39. Kigure T, Saito A, Seida K, Yamada S, Ishihara K, Okuda K. 1995. Distribution of *Porphyromonas gingivalis* and *Treponema denticola* in human subgingival plaque at different periodontal pocket depths examined by immunohistochemical methods. *J Periodont Res* 30:332–341. <https://doi.org/10.1111/j.1600-0765.1995.tb01284.x>.
40. Mark Welch JL, Rossetti BJ, Rieken CW, Dewhirst FE, Borisy GG. 2016. Biogeography of a human oral microbiome at the micron scale. *Proc Natl Acad Sci U S A* 113:E791–E800. <https://doi.org/10.1073/pnas.1522149113>.
41. Zhou M, Rong R, Munro D, Zhu C, Gao X, Zhang Q, Dong Q. 2013. Investigation of the effect of type 2 diabetes mellitus on subgingival plaque microbiota by high-throughput 16S rDNA pyrosequencing. *PLoS One* 8:e61516. <https://doi.org/10.1371/journal.pone.0061516>.
42. Shannon P, Markiel A, Ozier O, Baliga NS, Wang JT, Ramage D, Amin N, Schwikowski B, Ideker T. 2003. Cytoscape: a software environment for integrated models of biomolecular interaction networks. *Genome Res* 13:2498–2504. <https://doi.org/10.1101/gr.1239303>.
43. Faust K, Sathirapongsasuti JF, Izard J, Segata N, Gevers D, Raes J, Huttenhower C. 2012. Microbial co-occurrence relationships in the human microbiome. *PLoS Comput Biol* 8:e1002606. <https://doi.org/10.1371/journal.pcbi.1002606>.

1.3 Fer, bactéries et cavité buccale

Dans le sillon gingival sain, ou la poche parodontale formée dans les sites parodontaux atteints par la parodontite, le microbiote est baigné en permanence dans le fluide gingival. Cette communauté est influencée par des facteurs environnementaux : pH, température, oxygène, . . . mais aussi par la présence de fer. Celui-ci est un nutriment indispensable au bon fonctionnement de la plupart des formes de vie. Permettant le transport et l'échange d'électrons grâce à ses deux formes ioniques ($\text{Fe}^{2+} \leftrightarrow \text{Fe}^{3+} + 1 \text{e}^-$), c'est un élément essentiel pour le fonctionnement des enzymes impliquées dans les réactions d'oxydo-réduction. Qu'il s'agisse des micro-organismes, des plantes ou des animaux, invertébrés comme vertébrés, le fer assure ainsi un rôle de composant catalytique dans de nombreuses réactions biochimiques de la vie cellulaire. Parmi les fonctions qui impliquent des protéines liées au fer chez l'Homme, citons le transport et le stockage d'oxygène (hémoglobine et myoglobine), la production d'énergie (cytochrome c), la détoxification (cytochrome P450, catalase) ou la synthèse d'hormones et de neurotransmetteurs. Il est aussi utilisé par les enzymes qui génèrent les dérivés réactifs de l'oxygène et de l'azote (notamment la NADPH oxydase NOX, et l'oxyde nitrique synthase NOS) dans le cadre de la phagocytose, une fonction majeure de l'immunité innée. Plus récemment, il s'est révélé être l'acteur principal d'une nouvelle forme de mort cellulaire non apoptotique, la ferroptose [27].

1.3.1 Un enjeu nutritionnel pour les bactéries et leur hôte

Chez l'adulte, le fer représente 35 à 45 mg par kilogramme de poids corporel [28]. Si les deux tiers se trouvent dans l'hémoglobine des globules rouges circulants et en cours de maturation, une grande partie est stockée dans le foie (1 000 mg) et les macrophages (600 mg). Viennent ensuite les muscles et les autres tissus pour les 10 % à 15 % restants [29]. Ce sont les macrophages qui fournissent la majeure partie du fer utilisable en dégradant l'hémoglobine des érythrocytes sénescents. Un processus indispensable puisque l'érythropoïèse nécessite 20 mg par jour, là où seulement 1 à 2 mg de fer est absorbé par l'intestin grâce à l'alimentation [28]. Cet apport alimentaire, malgré ses fluctuations, doit néanmoins permettre de couvrir les pertes journalières. Le maintien d'un équilibre dans le métabolisme du fer est donc indispensable pour un organisme sain.

L'homéostasie du fer dans l'organisme humain est assurée par un système endocrinien. Dans celui-ci, l'hepcidine, une hormone principalement synthétisée par le foie et codée par le gène *HAMP*, sert à la fois de senseur et de régulateur du taux de fer systémique (voir la Figure 1.3). Des taux croissants de fer dans le sang, et dans le stock hépatique, favorisent sa production. L'hepcidine agit alors en bloquant l'export sanguin de fer par la dégradation de la ferroportine (le transporteur du fer cellulaire), ce qui a pour effet de réduire l'afflux de fer provenant des réserves et de bloquer l'absorption ultérieure de fer alimentaire. Lorsque les taux de fer dans le corps diminuent, la produc-

tion d'hepcidine est réduite en conséquence, ce qui permet la reprise de l'absorption du fer et l'augmentation de ses niveaux dans le plasma. Sa concentration plasmatique peut ainsi rester stable, entre 12 et 25 $\mu\text{mol.L}^{-1}$ (soit entre 0,5 et 1,7 mg.L^{-1}).

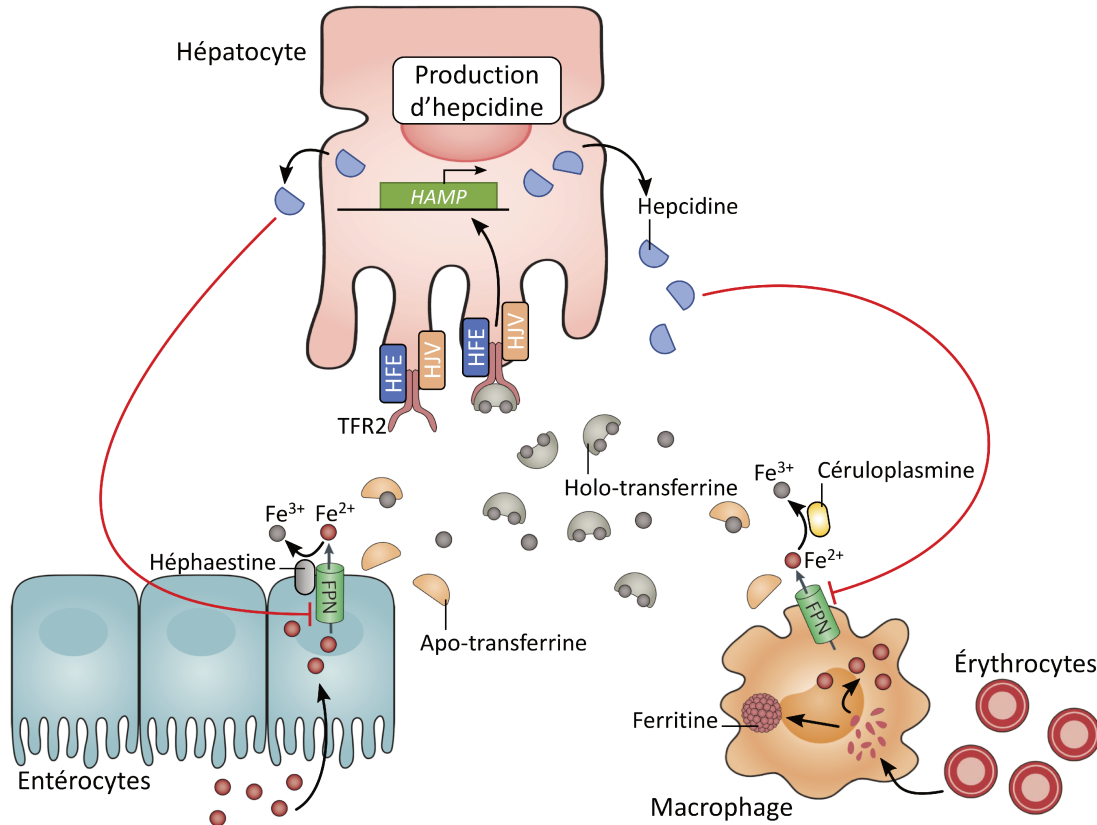


FIGURE 1.3 – Les entérocytes et les macrophages exportent, par le biais de la ferropontine (FPN), le fer ferreux (Fe^{2+}) issu, respectivement, de l'alimentation et du recyclage des érythrocytes sénescents (ce dernier pouvant également être stocké dans la ferritine). Après cet export plasmatique, le fer doit être oxydé sous sa forme ferrique (Fe^{3+}) pour être pris en charge par la transferrine. Au niveau des entérocytes, c'est l'héphaestine membranaire située à proximité de la ferropontine qui remplit cette fonction, tandis que le fer exporté par les macrophages est oxydé par la céruloplasmine circulant dans le sang. La transferrine peut lier jusqu'à deux atomes de fer pour former l'holo-transferrine, qui peut alors distribuer le fer dans l'organisme. La liaison de l'holo-transferrine par le récepteur membranaire TFR2 permet aux hépatocytes de détecter les variations du niveau de fer plasmatique. La transduction du signal qui résulte de cette liaison, et qui requiert les protéines HFE et l'hémojuvéline (HJV), active l'expression du gène *HAMP* codant pour l'hepcidine. Cette dernière, sécrétée dans le plasma, inhibe l'export sanguin du fer en liant la ferropontine, ce qui aboutit à son internalisation et à sa dégradation.

Chez les micro-organismes comme les bactéries, le fer est également impliqué dans nombre de processus cellulaires : production d'énergie, réplication génétique, protection contre le stress oxydatif, etc. Les bactéries ont ainsi des besoins en fer de l'ordre de

la micromole (10^{-6} mole.L⁻¹, soit 55 µg.L⁻¹ pour pouvoir se développer [30]. Les bactéries qui composent le microbiote humain et susceptibles d'infecter leur hôte, rencontrent donc un obstacle : la concentration du fer présent dans les fluides de l'organisme et librement accessible aux micro-organismes — c'est à dire, non lié à une protéine chaperonne — ne concerne qu'une proportion extrêmement faible de la concentration totale en fer. En effet, elle se situe aux alentours de l'attomole (10^{-18} mole.L⁻¹, soit 55 ag.L⁻¹) [31]. Les bactéries doivent donc mettre en place des stratégies d'acquisition du fer lié aux protéines chaperonnes⁵.

1.3.2 Séquestration immunitaire du fer

Sous forme ionique, le fer est hautement réactif. Au sein des tissus biologiques, il est donc pris en charge par des protéines qui agissent comme des chélateurs. Qu'il soit intracellulaire ou dans le milieu extra-cellulaire, la grande majorité du fer du corps humain se trouve ainsi lié à des protéines, qui sont dédiées à son transport (transferrine), son stockage (ferritine) ou à son utilisation (hémoglobine, myoglobine, etc.). La fixation du fer par ces protéines est réalisée grâce à des structures spécifiques : l'hème, un noyau de base pour de nombreuses molécules biologiques, ou les clusters fer-soufre, formés grâce aux résidus cystéines présents dans la composition en acides aminés des protéines [32]. Par ailleurs, l'environnement aérobie et le pH neutre du sérum garantissent l'insolubilité du fer extra-cellulaire et donc sa faible biodisponibilité pour d'éventuels agents pathogènes [33].

Cet accaparement du fer par l'organisme est ainsi apparu pour plusieurs auteurs comme une stratégie de l'hôte pour limiter l'infection. En privant de fer d'éventuels pathogènes, alors que ceux-ci en ont pour la plupart une dépendance absolue pour leur survie, l'organisme exercerait une immunité nutritionnelle [34, 35]. Dans le sang, la transferrine, protéine chargée de son transport, lie le fer avec une affinité extrêmement élevée [33]. Dans de nombreux fluides corporels (salive, larmes, lait maternel), la lactoferrine est capable de fixer le fer même en cas de faible pH, ce qui est fréquemment le cas des tissus infectés ou inflammés. Elle aurait également une activité bactéricide directe en agissant sur la perméabilité membranaire après s'être liée aux lipopolysaccharides des bactéries à Gram négatif [36]. Relarguée par les polynucléaires neutrophiles, elle est considérée comme faisant partie de l'immunité innée. Sa présence inhibe par exemple la formation de biofilm par *Pseudomonas aeruginosa* chez des patients atteints de mucoviscidose [37]. En modèle animal, l'administration orale de lactoferrine chez des souris diminue la présence d'endotoxines au niveau intestinal [38]. Plusieurs autres protéines ayant cette capacité de fixation et de transport du fer voient leur concentration augmentée en réponse à des cytokines proinflammatoires ou à une infection : la sidérocaldine, l'haptoglobine, l'hémopexine, etc. [32].

L'hypothèse d'une séquestration immunitaire du fer attribue également un rôle à l'hepcidine dans le cas d'une infection. En effet, il a été observé que sa concentration

5. Voir plus loin la section 1.3.3 Stratégies bactériennes d'acquisition en page 13.

présentait une hausse considérable au cours d'une infection et d'une inflammation aiguë. Elle n'atteint cependant pas les concentrations requises pour exercer une activité antimicrobienne, celle-ci ayant uniquement pu être démontrée *in vitro*. Toutefois, cette augmentation est responsable de l'une des caractéristiques de l'inflammation : une hypoferrémie, qui se développe quelques heures après l'apparition des stimuli infectieux ou immunitaires [39]. Cette hypoferrémie découle assez logiquement des fortes concentrations d'hepcidine qui ont pour effet majeur la séquestration du fer dans les macrophages. Car, bien que privés de leur capacité à exporter le fer, ils continuent néanmoins à recycler les globules rouges sénescents. Ce mécanisme n'est ainsi pas sans coût pour l'organisme, puisque s'il se prolonge, il peut donner lieu à une anémie inflammatoire causée par le manque d'apport de fer dans la moelle osseuse [40].

Pour d'autres auteurs, il est excessif d'attribuer un rôle d'immunité innée à l'hepcidine, arguant notamment du fait que, les baisses de concentration plasmatique en fer occasionnées par la forte production d'hepcidine n'affecteraient pas les mécanismes microbiens de transport du fer [32]. Au cours de l'infection, le fer voit sa concentration plasmatique diminuer jusqu'à 1 à 3 $\mu\text{mol.L}^{-1}$ (soit entre 0,05 et 0,15 mg.L^{-1}). Mais il reste lié aux protéines chaperonnes, ce qui le rend tout aussi inaccessible qu'à des concentrations physiologiques. Les chélateurs et transporteurs bactériens du fer étant adaptés à des conditions très variables de concentration en fer, l'hypoferrémie induite par l'hepcidine n'aurait ainsi que peu ou pas d'impact sur leur activité. La forte production d'hepcidine aurait cependant le rôle important de limiter au maximum la présence de fer libre, généré dans les tissus endommagés par les destructions cellulaires. D'une part, parce qu'il est facilement assimilable par les micro-organismes, et d'autre part, parce qu'il amplifierait les lésions tissulaires. Ce fer libre contribue effectivement, par la réaction de Fenton, à la production d'espèces réactives de l'oxygène (dont le radical hydroxyle HO^{\bullet} hautement réactif), lesquelles vont générer un stress oxydatif [41].

1.3.3 Stratégies bactériennes d'acquisition

Les tissus biologiques d'un hôte n'offrent donc que peu de fer libre et facilement accessible pour les micro-organismes. La carence nutritionnelle, liée à cette relative absence de fer libre, génère un stress pour les organismes bactériens. Au cours de l'évolution, ce stress est devenu un marqueur pour les bactéries, leur signalant la présence des tissus de l'hôte. Cette détection leur permet d'adapter leur stratégie d'acquisition du fer, par le biais d'une régulation transcriptionnelle. Celle-ci est principalement induite par le facteur Fur (Ferric uptake regulator) que l'on retrouve dans la majorité des bactéries, et qui contribue à la virulence des pathogènes [42, 43]. D'autres bactéries, comme *Staphylococcus aureus*, ont également développé des systèmes de détection spécifiques des protéines de leur hôte, fonctionnant grâce à la reconnaissance de l'hème [44, 45]. Ainsi, ces senseurs permettent à la bactérie de s'adapter à son milieu et déclenchent l'expression des systèmes permettant l'acquisition de fer lié aux protéines de l'hôte.

Des mécanismes mis en œuvre pour contourner l'immunité nutritionnelle sont présents dans la plupart des agents pathogènes. Les protéines impliquées peuvent varier d'une bactérie à l'autre, mais les stratégies sont communes : entrer en compétition avec l'hôte grâce à des chélateurs de très haute affinité, ou cibler les protéines porteuses de fer. Les sidérophores appartiennent à la première catégorie. Ces peptides sont capables de lier le fer avec des constantes d'association telles qu'ils peuvent concurrencer la transferrine et la lactoferrine [33]. Sécrétés par les bactéries, ils sont ensuite récupérés, une fois chargés en fer, par des récepteurs membranaires spécifiques puis importés dans le cytoplasme. Les sidérophores sont des éléments essentiels pour le développement des bactéries qui les produisent. Des souches mutantes, ayant perdu leur capacité à en produire, montrent systématiquement une virulence amoindrie dans des modèles animaux d'infection [33, 43].

En plus de concurrencer la transferrine et la lactoferrine, certaines bactéries, comme les espèces du genre *Neisseria* par exemple, sont également capables de reconnaître ces protéines, *via* des récepteurs spécifiques. Dans cette stratégie, il s'agit véritablement de détourner le fer contenu dans ces protéines. Et dans le cas de *Neisseria*, la liaison est spécifique de la transferrine humaine, indiquant une adaptation à un hôte en particulier [46]. Plus généralement, ce mécanisme d'acquisition implique des molécules qui vont reconnaître les protéines de l'hôte transportant le fer, puis les altérer de façon à récupérer le fer qu'elles contiennent. D'autres systèmes ciblent la molécule d'hème. Il s'agit alors pour les bactéries d'extraire l'hème hors des hémoprotéines (telles que l'hémoglobine ou l'hémopexine), à nouveau grâce à des récepteurs spécifiques. Ces derniers peuvent être exprimés en surface ou sécrétés dans le milieu extra-cellulaire, et sont alors appelés hémophores [47]. Une fois chargés en hème, les hémophores importent leur acquisition dans le cytoplasme bactérien, et, après l'action d'enzymes, le fer sera libéré. Comme dans le cas des sidérophores, les mutations affectant les systèmes d'acquisition par hémophores réduisent la pathogénicité bactérienne dans des modèles animaux d'infection, signant ainsi leur rôle en tant que facteur de virulence [33, 43].

1.3.4 Le fer dans la cavité buccale

Plusieurs études ont entrepris de doser la concentration de métaux, dont le fer, dans la salive. Cela dans le but de découvrir de nouveaux biomarqueurs de maladies buccales [48, 49] ou d'analyser le relargage lié aux appareils orthodontiques métalliques [50]. Chez le sujet sain, si les valeurs moyennes de concentration salivaire du fer varient grandement selon la méthode de quantification employée (de 0,03 à 1 mg.L⁻¹), les variations inter-individuelles sont également très importantes [48].

D'autres études ont rapporté des dosages salivaires des protéines porteuses de fer. La transferrine est présente à hauteur de 1 à 1,5 mg.L⁻¹, toujours chez le sujet sain [51]; des valeurs supérieures à 10 mg.L⁻¹ indiquent généralement une contamination par du sang dans la salive prélevée. La concentration en ferritine est bien plus faible

que celle de la transferrine : elle a été estimée à environ 5 à 10 $\mu\text{g.L}^{-1}$ [52]. Enfin, l'hepcidine fait aussi partie des composants produits par les glandes salivaires [53]. Cependant, les valeurs rapportées dans les études varient grandement là aussi (de 1 à 650 $\mu\text{g.L}^{-1}$) [52, 53].

Le sillon gingivo-dentaire est, lui, irrigué par le fluide gingival. Ce fluide étant issu d'un exsudat sérique, il contient plusieurs protéines possédant du fer. La transferrine et l'albumine sont ainsi des composants majeurs du fluide gingival [54]. Cette dernière est d'ailleurs la protéine la plus riche en hème au sein du fluide gingival [54, 55]. Au total, la concentration en fer moyenne est estimée à 1 mg.L^{-1} dans un fluide gingival sain, ce qui correspond aux valeurs normales de sa concentration plasmatique, et à la fourchette haute des estimations de sa concentration salivaire. Le fer dans le fluide gingival peut atteindre 5 mg.L^{-1} chez les patients atteints de parodontite [56]. Les sources potentielles de fer sont plus importantes lors d'un état inflammatoire, du fait de la vasodilatation et des saignements gingivaux qui l'accompagnent [57].

1.3.5 Pathogènes parodontaux et fer

Les bactéries du biofilm sous-gingival sont, elles aussi, en compétition, avec l'hôte et entre elles, pour la liaison du fer et usent des stratégies précédemment décrites pour son absorption. La surexpression des fonctions liées à l'acquisition et au transport du fer est l'une des signatures transcriptomiques d'un microbiote pathogénique [58]. Bien que le modèle actuel de la pathogenèse de la parodontite encourage à réévaluer le rôle de chaque bactérie dans l'équilibre hôte-microbiote [59], *P. gingivalis* est toujours considéré comme un pathogène majeur de la parodontite et il reste donc le mieux documenté.

La capacité de *P. gingivalis* à pouvoir se fournir en fer a un impact décisif sur sa croissance et sa virulence [60]. La bactérie est également auxotrophe pour le noyau protoporphyrine IX (PPIX), la voie métabolique permettant la biosynthèse *de novo* de cette molécule étant incomplète [61]. Les milieux de culture utilisés pour l'étude de *P. gingivalis* sont ainsi supplémentés avec de l'hème, de l'hémoglobine ou encore du sang, ce qui permet d'apporter à la fois du fer et de la PPIX [62]. Chez l'hôte, ces deux éléments, fer et PPIX, peuvent être obtenus à partir des hémoprotéines : la protoporphyrine étant la structure centrale de l'hème, formant un anneau organique qui lie le fer en son centre.

La principale source de fer, et de PPIX, pour *P. gingivalis* est donc l'hémoglobine [63]. Lorsque des érythrocytes sont présents dans son milieu, la bactérie utilisera d'abord des hémagglutinines pour se maintenir à proximité de ces cellules. Puis, l'action suivante sera de les lyser pour libérer l'hémoglobine qu'elles contiennent [64]. Ensuite, *P. gingivalis* possède des protéases qui permettront la dissociation et l'extraction de la molécule d'hème. Enfin, des mécanismes de transport prennent en charge l'hème pour l'internaliser. Plusieurs opérons codant pour ce type de transport ont été identifiés (*hmu*, *hus*, *lht*) [65–67]. Les acteurs majeurs de cette capture de l'hème sont

les gingipaïnes. Ces protéases, sécrétées ou situées à la surface de la bactérie, sont un élément majeur de la virulence de *P. gingivalis*. Véritables couteaux suisses, elles possèdent des domaines hémagglutinines, mais peuvent également lyser les globules rouges et se lier à l'hémoglobine [68]. De plus, elles sont capables de se lier avec une haute affinité à l'hème en vue de l'extraire [69]. Impliquées dans les destructions tissulaires de l'hôte, elles peuvent également agir sur la perméabilité vasculaire, induisant un saignement localisé et retardant la coagulation [70].

Hormis l'hémoglobine des érythrocytes, la transferrine est également une source importante de fer pour *P. gingivalis*. Composant majeur du fluide gingival, la transferrine a l'avantage d'être présente en l'absence de saignements gingivaux. Plusieurs études *in vitro* ont mis en évidence la croissance de la bactérie avec la transferrine comme seule source de fer dans le milieu de culture [71–73]. Les travaux menés sur le mécanisme d'absorption ont montré une liaison rapide et spécifique de la bactérie à la transferrine humaine [73]. Cette liaison est par ailleurs accrue lorsque le milieu est déplété en fer, suggérant une adaptation de la bactérie aux différentes sources de fer disponibles à sa portée. Toutefois, le ou les récepteurs impliqués dans cette liaison n'ont pas encore été identifiés. En revanche, l'étude de souches mutantes a permis de mettre en lumière le rôle des gingipaïnes dans la prise en charge de la transferrine, une fois cette dernière fixée [74, 75]. La transferrine serait donc clivée, libérant ainsi les atomes de fer qu'elle transporte. Ces derniers sont ensuite capturés et importés dans le cytoplasme de la bactérie.

Comme indiqué précédemment, dans un contexte pathologique, c'est l'ensemble du microbiote qui surexprime les mécanismes d'acquisition du fer [58]. Plusieurs d'entre eux ont pu être identifiés chez des espèces associées, à des degrés divers, avec la maladie parodontale. *T. denticola* peut collecter le fer dont il a besoin à partir de la lactoferrine [76]. Il possède également des hémagglutinines, des hémolysines et la capacité à oxyder la molécule d'hème, ce qui suggère sa capacité à utiliser l'hémoglobine de l'hôte [77, 78]. Des récepteurs spécifiques de l'hème ont, de plus, été identifiés sur sa membrane externe : HbpA et HbpB [79]. *T. denticola* possède enfin une activité fer réductase, ce qui lui permettrait de récupérer le fer capturé par des sidérophores sécrétés par d'autres bactéries (*T. denticola* n'ayant pas la capacité d'en produire) [80, 81]. Le métatranscriptome du biofilm présent dans un site gingival malade montre une régulation à la hausse des gènes impliqués dans l'hémolyse et le transport du fer chez *Tannerella forsythia* [82]. Par ailleurs, une étude a récemment montré la présence d'hémophores homologues chez *P. gingivalis* (HmuY, appartenant à l'opéron *hmu*) et *T. forsythia* (Tfo) ; ceux-ci présentent néanmoins des différences structurales et d'efficacité [83].

Prevotella intermedia exprime une interpaïne, une protéase à cystéine comme les gingipaïnes de *P. gingivalis*, qui dégrade l'hémoglobine, relarguant ainsi l'hème [84]. *In vitro*, la croissance de *P. intermedia* peut ainsi être stimulée avec de l'hémoglobine humaine, cette dernière étant liée par un récepteur membranaire spécifique [85]. L'interpaïne pourrait également récupérer l'hème liée à l'albumine. Par contre, *P. intermedia* ne semble pas pouvoir utiliser la transferrine ou la lactoferrine [86]. *Campylobacter rec-*

tus, enfin, est également capable d'assimiler le fer de la transferrine pour assurer sa croissance [87]. Contrairement à *P. gingivalis*, le mécanisme de capture impliquerait une réductase, la libération de fer par la transferrine étant favorisée lorsqu'il se trouve sous sa forme réduite Fe^{2+} .

L'équilibre de l'homéostasie du fer est tenu : une carence, comme une surcharge en fer sont néfastes pour l'organisme. Les troubles de l'homéostasie du fer font partie des maladies les plus courantes chez l'Homme [29]. L'anémie résultant de la carence en fer est un problème de santé mondial. À l'origine d'anomalies du développement chez l'enfant, elle touche particulièrement les populations défavorisées et les pays en voie de développement [88]. De l'autre côté du balancier, il apparaît qu'une surcharge en fer puisse être un élément de susceptibilité vis-à-vis de certaines maladies infectieuses. Plusieurs cas d'infections bactériennes, par ailleurs rarement rencontrées, ont été observées chez des personnes atteinte d'une maladie de surcharge en fer d'origine génétique, l'hémochromatose héréditaire [89, 90]. Un cas en particulier a retenu l'attention médiatique : l'infection d'un chercheur par *Yersinia pestis*, après avoir été exposé à une souche de laboratoire pourtant considérée comme avirulente [91]. Atteint d'hémochromatose héréditaire (le diagnostic sera établi après la découverte à l'autopsie de niveaux anormalement élevés de ferritine plasmatique et de saturation de la transferrine), il semble que la surcharge en fer ait permis à la bactérie de se développer, malgré sa mutation la rendant déficiente pour un sidérophore qui cible le fer de la transferrine [92].

1.4 Hémochromatose héréditaire et maladie parodontale

L'hémochromatose est une pathologie caractérisée par une hyperabsorption digestive de fer aboutissant à une surcharge ferrique dans l'organisme. Le terme d'hémochromatose est apparu en 1889, à l'initiative de Friedrich von Recklinghausen [93]. Ce médecin allemand, également connu pour sa description de la neurofibromatose, imputa à un pigment sanguin la coloration particulière de la cirrhose pigmentaire qui avait été initialement décrite en 1865 par Armand Trousseau, médecin à l'hôpital Saint-Antoine [94]. Le versant génétique de la maladie a été mis en évidence par une équipe rennaise en 1977 [95]. L'hémochromatose perd alors son caractère idiopathique pour devenir héréditaire. La découverte du gène en cause dans la pathologie, *HFE*, est bien plus récente, puisqu'elle date de 1996 [96].

Du point de vue épidémiologique, l'hémochromatose héréditaire est le syndrome de surcharge ferrique le plus couramment rencontré chez les individus caucasiens [97]. Les mutations majeures du gène *HFE*, qui est situé sur le chromosome 6, sont C282Y (p.Cys282Tyr) et H63D (p.His63Asp). La fréquence de la mutation C282Y est variable chez les européens (6,2 % en moyenne), avec une plus forte prévalence chez les descendants des populations d'Europe du Nord puisqu'elle concerne une personne sur dix [98, 99]. Les fréquences les plus fortes sont situées en Bretagne et en Irlande, tandis que les populations non caucasiennes ne la portent que très peu, voire pas du tout.

La mutation H63D se retrouve, elle, dans toutes les populations, avec une fréquence plus importante [100]. Parmi les génotypes d'*HFE*, seule l'homozygotie C282Y est associée à la maladie, avec toutefois une pénétrance incomplète (la prévalence de la maladie étant bien inférieure à celle, déduite, de l'homozygotie) [99]. L'hétérozygotie C282Y/H63D, elle, peut entraîner une forme atténuée de surcharge en fer [101].

La protéine HFE joue un rôle dans ce mécanisme par son interaction avec le récepteur à la transferrine TFR2 (voir la Figure 1.3) [102]. HFE participerait à la détection du coefficient de saturation de la transferrine, ce qui permettrait à l'hépatocyte de réguler sa production d'hepcidine selon le niveau de fer circulant [103]. Cependant, le mécanisme de la régulation de la production d'hepcidine recèle encore probablement des zones d'ombres.

L'hémochromatose reste d'abord quiescente et demeure au début une simple prédisposition génétique. Des perturbations biologiques, liées à un déficit d'hepcidine, peuvent ensuite apparaître de façon isolée. En premier lieu, une augmentation du coefficient de saturation de la transferrine, c'est-à-dire une augmentation du taux d'occupation des sites de fixation qui accueillent le fer (deux par protéine). Ses valeurs normales sont comprises entre 20 % et 45 %. Au-delà, la quantité de fer à prendre en charge excède la capacité des transferrines circulantes et des formes anormales de fer (non lié à la transferrine) peuvent apparaître. La ferritine circulante, qui représente normalement une quantité infime du fer circulant, augmente à son tour. Sa concentration est pathologique au-delà de 300 $\mu\text{g.L}^{-1}$ chez l'homme et 200 $\mu\text{g.L}^{-1}$ chez la femme [104]. Des signes cliniques plus marqués, ou des complications viscérales, pouvant mener au diagnostic apparaissent plutôt vers l'âge de 35 à 40 ans chez les hommes et 45 à 50 ans chez les femmes. Ces symptômes sont liés à une accumulation progressive de fer depuis la naissance [100].

Lorsque la maladie s'exprime pleinement, on peut observer des atteintes hépatique (hépatomégalie et cirrhose), cutanée (hyperpigmentation grisâtre, brune qui correspond à l'évolution de l'accumulation de fer dans la peau), ostéoarticulaire (arthropathie, déminéralisation osseuse), endocrinienne (diabète, hypogonadisme), cardiaque (cardiomyopathie et insuffisance cardiaque). Le tableau « historique » de la maladie (diabète, cirrhose et pigmentation cutanée) est cependant de moins en moins rencontré, grâce au diagnostic précoce. Le traitement a pour but de diminuer la charge ferrique de l'organisme en effectuant des saignées, ou phlébotomies, répétées. Leur fréquence est déterminée par le taux de ferritine sérique et varie d'une par semaine à une tous les 3 mois [99].

Historiquement impliqué dans la recherche sur les bases génétiques et la physiopathologie de l'hémochromatose héréditaire [95, 105, 106], le CHU de Rennes est le Centre de Référence national des surcharges en Fer rares d'origine génétique (CR-Fer, <https://centre-reference-fer-rennes.org/>). Site coordonnateur, il est en lien avec dix autres Centres de Compétences répartis sur le territoire national. La Bretagne étant particulièrement touchée en terme de prévalence de la maladie, le CRFer accueille également un grand nombre de patients pour leur suivi et leur traitement au sein du

service des Maladies du foie.

La présence, au sein de notre hôpital, de spécialistes de cette maladie, et d'une cohorte importante de patients, nous a amené à entamer une collaboration entre les services des Maladies du foie et de Parodontologie. En effet, au vu i) du facteur favorable que représente le fer pour le développement des pathogènes parodontaux, ii) de l'âge d'expression des signes cliniques de la parodontite et de l'hémochromatose, iii) des notions d'atteintes inflammatoires ostéoarticulaires, et iv) de la susceptibilité de ces patients à certains micro-organismes, il a paru pertinent d'évaluer leur statut parodontal. Un projet d'étude clinique a donc été déposé en 2009 pour réaliser un examen dentaire et parodontal chez des patients atteints d'hémochromatose liée à une homozygotie C282Y sur le gène *HFE*. Ces patients, suivis au CRFer, ont été vus au moment de leur diagnostic, ou au cours de leur prise en charge thérapeutique. De cette façon, nous disposons également du bilan sanguin, réalisé le jour même, et relatif au statut fer du patient : concentrations plasmatiques de fer, de transferrine, de ferritine et coefficient de saturation de la transferrine. Ces valeurs ont ensuite été analysées en regard des paramètres cliniques et parodontaux. L'étude clinique transversale qui résulte de ce travail est présentée dans la section suivante.

1.4.1 Periodontal status and serum biomarkers levels in *HFE* hemochromatosis patients. A case-series study, *Journal of Clinical Periodontology* 2017

Dans cette étude, 84 patients homozygotes pour la mutation C282Y du gène *HFE* ont été examinés au moment de leur séjour dans le service des Maladies du foie du CHU de Rennes. Pour quatorze d'entre eux, le diagnostic d'hémochromatose héréditaire était récent (moins d'un an et demi) et la thérapeutique initiale débutait. Les 73 autres sujets suivaient leur traitement par saignées régulières. L'objectif thérapeutique est d'atteindre puis de maintenir un taux de ferritine plasmatique $\leq 50 \mu\text{g.L}^{-1}$. Les patients nouvellement diagnostiqués présentent souvent des taux extrêmement élevés de ferritine (parfois supérieurs à $1\ 000 \mu\text{g.L}^{-1}$).

La première révélation de l'examen parodontal était la prévalence de la parodontite, qui concernait 100 % de cette population. En se basant sur la classification des maladies parodontales développée par le *Center for Disease Control and Prevention* et l'*American Academy of Periodontology* et publiée en 2012 [107], un peu plus de la moitié des patients (54,8 %) présentait une parodontite sévère, et seulement un présentait une parodontite légère. Ces différents degrés d'atteinte parodontale ne s'accompagnaient pas de variation significative dans le sexe ratio, le tabagisme, la fréquence de visite chez le dentiste traitant ou l'ancienneté du diagnostic de l'hémochromatose.

En comparant les marqueurs sériques du statut fer des patients, il est apparu que le coefficient de saturation de la transferrine était significativement augmenté chez les personnes avec une parodontite sévère par rapport à ceux présentant une parodontite légère ou modérée ($55,1 \% \pm 18 \%$ contre $47,2 \% \pm 17,9 \%$, $p = 0,029$, tableau 2



de l'article). Il est à noter que ce coefficient de saturation ne fait pas partie des critères du traitement par saignées, malgré l'association démontrée entre saturation de la transferrine et la concentration de fer non lié à la transferrine [108]. Or, des valeurs pathologiques de la saturation de la transferrine peuvent persister en dépit du retour à la normalité du taux de ferritine ; de plus, le rôle attribué au fer non lié à la transferrine dans les dommages tissulaires semble être prépondérant dans l'hémochromatose [104].

Par régression logistique, il s'est enfin avéré que le risque était significatif pour les patients de présenter une parodontite sévère en cas de saturation anormale de la transferrine ($> 45\%$) : odds-ratio = 5,49 – IC 95 % [1,85-16,28] $p = 0,002$; et ce, en prenant en compte les variables confondantes que sont l'âge, le sexe, le tabagisme, l'indice de plaque dentaire, la fréquence de visite chez le dentiste et l'ancienneté du diagnostic de l'hémochromatose. Nous avons conclu que les personnes souffrant d'hémochromatose héréditaire étaient une population à risque pour la parodontite, et que la sévérité de cette dernière était associée à la surcharge en fer. Cette étude est la première à faire un lien entre les deux pathologies, mais il est à noter que des manifestations orales liées à l'hémochromatose ont déjà fait l'objet d'un rapport de cas publié en 1972 [109]. La principale information de l'article était une forme rare de pigmentation bleue-grise de la muqueuse gingivale, se rapprochant de la pigmentation cutanée typiquement liée à l'hémochromatose. De façon intéressante, les auteurs rapportaient également une parodontite sévère, résistante au traitement, et de nombreuses dents mobiles chez la patiente.

Mon rôle dans ce travail a été de gérer les données cliniques, et de mettre en œuvre leur analyse statistique dans un logiciel open-source fonctionnant en ligne de commande (RStudio). J'ai ainsi réalisé : la mise en forme et l'import des données, l'analyse par variable, puis l'analyse de l'association entre paramètres cliniques parodontaux et fer. Celle-ci a été menée avec des statistiques univariées, et enfin avec des modèles de régression linéaire et logistique.

Cet article a été publié dans le *Journal of Clinical Periodontology* le 6 juin 2017. Il est disponible en accès ouvert dans les archives HAL (<https://hal.archives-ouvertes.fr/hal-01614700>).

Periodontal status and serum biomarker levels in HFE haemochromatosis patients. A case-series study

Vincent Meuric^{1,2}  | Fabrice Lainé^{2,3} | Emile Boyer^{1,2} | Sandrine Le Gall-David² | Emmanuel Oger³ | Denis Bourgeois⁴  | Philippe Bouchard^{5,6} | Edouard Bardou-Jacquet^{2,7} | Valérie Turmel³ | Martine Bonnaure-Mallet^{1,2†} | Yves Deugnier^{3,7†}

¹CHU Rennes, Service d'Odontologie et de Chirurgie Buccale, Rennes, France

²EA 1254/CIMIAD (Control of Iron Metabolism and Iron-Associated Diseases), Université Rennes 1, UMR 1241, Rennes, France

³INSERM, CIC 1414, Rennes, France

⁴Université de Lyon 1, Lyon, France

⁵Department of Periodontology, Service of Odontology, Denis Diderot University, Rothschild Hospital, U.F.R. of Odontology, Paris, France

⁶EA 2496 Laboratory Orofacial Pathologies, Imagery and Biotherapies, Dental School and Life imaging Platform (PIV), University Paris Descartes Sorbonne Paris Cité, Montrouge, France

⁷CHU Rennes, Service des maladies du Foie, Rennes, France

Correspondence

Martine Bonnaure-Mallet, EA 1254/CIMIAD UMR1241, UFR Odontologie - Université de Rennes 1, Rennes, France.

Email: martine.bonnaure@univ-rennes1.fr

Funding information

The study was funded by the Comité de la Recherche Clinique of the University Hospital of Rennes and the University of Rennes 1

Abstract

Aim: To investigate the association between periodontal status and serum biomarkers in patients with *HFE* haemochromatosis.

Material and Methods: This clinical case series included 84 *HFE*-C282Y homozygous patients. Periodontal evaluation was performed using clinical attachment level, probing depth, gingival bleeding index, visible plaque index and gingival index. Serum markers of iron metabolism were collected from medical records. The relationship between serum biomarkers of iron burden and the severity of periodontitis was investigated.

Results: The study population consisted of 47 men and 37 women, routinely treated in the Unit of Hepatology, University Hospital, Rennes. All patients presented with periodontitis (mild: $n = 1$, moderate: $n = 37$ and severe: $n = 46$). There was a positive association between transferrin saturation $>45\%$ and the severity of periodontitis (adjusted odds ratio = 5.49, $p = .002$).

Conclusion: Severe periodontitis is associated with the severity of iron burden in patients with *HFE*-related hereditary haemochromatosis. Dental examination should be included in the initial assessment of all these patients.

KEYWORDS

haemochromatosis, iron burden, periodontitis, transferrin saturation

1 | INTRODUCTION

In France, 45% of adults over 40 years of age have at least one tooth with localized periodontitis (Bourgeois, Bouchard, & Mattout, 2007). Severe forms of periodontitis (i.e. with periodontal pockets ≥ 5 mm) affect 11.2% of adults worldwide (Kassebaum et al., 2014). Periodontitis is associated with risk factors, including age, gender (Harris & Glassell, 2011; Silva-Boghossian, Luiz, & Colombo, 2011), tobacco smoking (Bagaitkar et al., 2011; Kumar & Faizuddin, 2011) and obesity (Linden, Patterson, Evans, & Kee, 2007; Morita et al., 2011). Recent studies indicate that bacteria involved in periodontitis could be associated

with systemic diseases, including diabetes (Ide, Hoshuyama, Wilson, Takahashi, & Higashi, 2011), rheumatoid arthritis (Hayashi, Gudino, Gibson, & Genco, 2010; Sezer et al., 2013) and atherosclerotic cardiovascular disease. Diabetes and arthritis are classical features in patients with haemochromatosis (Powell, Seckington, & Deugnier, 2016).

HFE-related hereditary haemochromatosis (*HFE*-HH), the most common form of genetic iron overload in Caucasians, is mainly due to homozygosity for a major mutation, p.Cys282Tyr (C282Y), on the *HFE* gene which is involved in the production of a key regulator of plasma iron, hepcidin. The allelic frequency of the C282Y mutation is 6.2% in the general European population, but it can reach 12% in Brittany or United Kingdom (Jouanolle et al., 1998; Powell et al., 2016). C282Y homozygosity is responsible for a hepcidin-deficient state leading to

†These authors participated equally in the study.

an increase in serum transferrin saturation, which potentially results in increased body iron stores (EASL guidelines 2011). The classical treatment of *HFE-HH* patients is venesection to remove iron excess.

Iron lies at the centre of a battle for nutritional resource between higher organisms and their microbial pathogens. The iron status of human hosts affects the pathogenicity of numerous infections (Drakesmith & Prentice, 2012). It has been reported that non-transferrin-bound iron, an abnormal biochemical form of iron that occurs when transferrin saturation exceeds 45%, could modulate bacterial growth and virulence (Jolivet-Gougeon et al., 2008). Most cases of *HFE-HH* are diagnosed during adulthood, between 40 and 50 years of age. Iron burden might represent a favourable background for the development of periodontitis. First, iron is both an essential growth factor and a regulator of the virulence of *Porphyromonas gingivalis* and *Prevotella intermedia*, two common periodontal pathogens (Byrne, Potempa, Olczak, & Smalley, 2013). Second, as hepcidin is known for its antimicrobial activity (Ganz, 2013), low hepcidin production could be a favourable factor for the development of periodontal disease. Finally, bone loss is a frequent complication of *HFE-HH* (Guggenbuhl et al., 2005), which is likely to aggravate alveolar bone damage in periodontitis.

The main goal of this study was to investigate the association between periodontal status and serum biomarker levels in *HFE-HH* patients and to seek a putative relationship between markers of iron burden and the severity of periodontitis in these patients.

2 | PATIENTS AND METHODS

2.1 | Participants

A case-series study was carried out after approval by the local ethical committee (CPP Ouest V - 10/02-744). All participants were recruited, either during phlebotomy therapy or at diagnosis, in the unit of hepatology, University hospital, Rennes, between June 2011 and June 2012. They gave an informed written consent and were instructed on the prevention and treatment of periodontitis, as well as on oral hygiene procedures.

Inclusion criteria were homozygosity for the *HFE* C282Y mutation, age between 35 and 65 years and the presence of at least 10 natural teeth. Non-inclusion criteria were pregnancy, presence of another systemic disease (e.g. diabetes), periodontal therapy within the last 12 months and treatment with either systemic antibiotics or drugs known to cause gingival hyperplasia (i.e. hydantoins, ciclosporin, diltiazem, dihydropyridine) within the last 3 months. In the absence of data on periodontitis in *HFE-HH* patients, the number of patients to be included was based on the precision ($\pm 10\%$) of the estimation of prevalence of periodontitis (50%) in the French population (Bourgeois et al., 2007).

2.2 | Interview and collection of clinical and laboratory data

Clinical data recorded at the time of dental examination included body mass index (BMI), smoking status (non-smoker and current or former

Clinical relevance

Scientific rationale for the study: *HFE*-related hereditary haemochromatosis (*HFE-HH*) is the most common form of genetic iron overload in Caucasians. As iron is an essential growth factor and a regulator of the virulence of *Porphyromonas gingivalis* and *Prevotella intermedia*, two common periodontal pathogens, increased severity of periodontitis was hypothesized in *HFE-HH* patients.

Principal findings: *HFE-HH* patients presented severe form of periodontitis associated with high transferrin saturation.

Practical Implications: Dental examination should be included in the initial assessment of all *HFE-HH* patients.

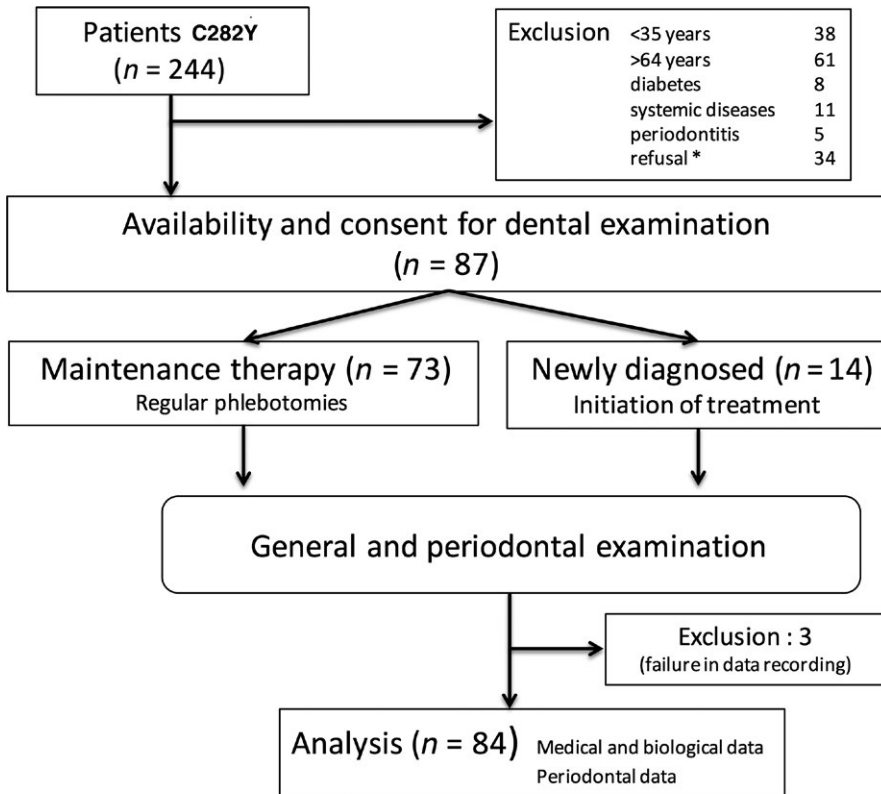
smoker), teeth-brushing habits (once, twice or more per day) and dental visits per year (<1 or ≥ 1). Serum ferritin, iron, and transferrin levels and transferrin saturation were collected from medical charts using routine procedures at the time of both diagnosis of haemochromatosis and dental examinations. The time elapsed between the diagnosis of haemochromatosis and dental examination was also registered.

2.3 | Evaluation of periodontal status

Full-mouth periodontal examination was performed by one examiner (VM), using a sterile U.S Williams PDT sensor probe at a pressure of 20 g (ZILA-PRO-DENTEC) positioned parallel to the long axis of the tooth. The following parameters were evaluated: probing depth (PD) as the distance (mm) between the gingival margin and the bottom of periodontal pocket; clinical attachment level (CAL) as the distance (mm) between the cemento-enamel junction and the bottom of periodontal pocket. Each of the following sites was recorded mesio-, mid- and disto-buccal, and mesio-, mid- and disto-lingual from all present teeth except for third molars. Gingival condition was diagnosed using the gingival bleeding index (GBI), gingival index (GI) (Loe, 1967; Schatzle et al., 2003) and visible plaque index (VPI) (McClanahan, Bartizek, & Biesbrock, 2001; Silness & Loe, 1964).

2.4 | Definition of periodontal case

To evaluate the presence and severity of periodontitis, case definitions developed by the Center for Disease Control and Prevention and the American Academy of Periodontology (CDC/AAP) were used: mild periodontitis was defined as " ≥ 2 interproximal sites with CAL ≥ 3 mm, and ≥ 2 interproximal sites with PD ≥ 4 mm (not on same tooth) or one site with PD ≥ 5 mm; moderate periodontitis as ≥ 2 interproximal sites with CAL ≥ 4 mm (not on same tooth), or ≥ 2 interproximal sites with PD ≥ 5 mm (not on same tooth); severe periodontitis as ≥ 2 interproximal sites with CAL ≥ 6 mm (not on same tooth) and ≥ 1 interproximal site with PD ≥ 5 mm" (Eke, Page, Wei, Thornton-Evans, & Genco, 2012).



* 14 declared current gum bleeding

FIGURE 1 Flow chart of participant recruitment

2.5 | Statistical analysis

Data management and statistical analysis were performed using R (version 3.3.1). Results of descriptive analysis are presented as frequencies and mean \pm standard deviation (SD). Distribution of continuous variables was assessed using the Shapiro–Wilk test. To analyse the association between the severity of periodontitis and the level of serum biomarkers, Student's *t*- and Mann–Whitney tests were used as appropriate. The chi-squared test was used for the analysis of categorical variables. $p < .05$ was considered as significant. The association between the severity of periodontitis (mild or moderate versus severe periodontitis) and transferrin saturation greater than 45% was assessed using logistic regression analysis adjusted for confounding variables (age, gender, smoking habit, plaque index, dental visit and time elapsed between the diagnosis of haemochromatosis and dental examination). Results are presented as odds ratio (OR) and 95% confidence intervals (CI).

3 | RESULTS

3.1 | Characteristic of HFE-HH patients

The review of charts from the 244 C282Y homozygous patients regularly phlebotomized in the unit of hepatology resulted in the identification of 87 patients fulfilling inclusion criteria (Figure 1). From these,

aged from 35 to 64 years (mean age 50.7 ± 8.4 years), 54% were males.

At the time of the diagnosis of haemochromatosis, one-third of the participants presented with chronic asthenia, 29.8% with osteoarthritis, 5.8% with clinical and biochemical liver disease and 2.4% with cardiopathy. Two males had hypogonadism. Mean serum ferritin (SF) levels were 815 ± 728 $\mu\text{g/L}$ (range: 86–4,021, normal range: 20–150 $\mu\text{g/L}$ in pre-menopausal women and 20–400 $\mu\text{g/L}$ in postmenopausal women and men), transferrin saturation was greater than 60% (normal range: 20–40) in 75% of patients and mean hepatic iron concentration assessed by MRI was 195 ± 79 $\mu\text{mol/g}$ dry liver (upper limit of normal = 36). All patients had normal C-reactive protein levels (i.e. <5 mg/L). Twenty-six patients had liver biopsy. Two presented significant fibrosis (bridging fibrosis or cirrhosis). Liver biopsy was not performed in the other patients because of serum ferritin levels $<1,000$ $\mu\text{g/L}$, which indicates the absence of cirrhosis (Guyader et al., 1999).

During the initial treatment of iron excess by weekly phlebotomy, the amount of removed iron ranged from 0.5 to 24 g (mean 4.6 ± 3.9 g).

At the time of dental examination, 82.2% of patients were already treated by regular phlebotomies and 17.8% had not been previously phlebotomized. Serum ferritin was 174.5 ± 418.1 $\mu\text{g/L}$, serum iron 26.7 ± 9.1 $\mu\text{mol/L}$, serum transferrin 2.1 ± 0.3 g/L and transferrin saturation $51.5 \pm 18.3\%$. All patients had normal serum C-reactive

TABLE 1 Distribution of periodontal clinical parameters and general characteristics of the population in accordance with the severity of periodontitis (N = 84). Significant results in bold

Periodontal Clinical Parameters	Total N = 84, 100% Mean ± SD	Type of Periodontitis		p-values
		Mild (n = 1) to moderate (n = 37) 45.2% Mean ± SD	Severe (n = 46) 54.8% Mean ± SD	
CAL				
Mean (mm)	2.82 ± 0.68	2.45 ± 0.32	3.13 ± 0.74	.0001
CAL ≥ 3 mm (%)	50.1 ± 17.4	40.2 ± 14.6	58.2 ± 15.2	.0001
CAL ≥ 5 mm (%)	10.3 ± 11.8	3.7 ± 2.8	15.8 ± 13.6	.0001
PD				
Mean (mm)	2.29 ± 0.35	2.06 ± 0.21	2.49 ± 0.34	.0001
PD ≥ 4 mm (%)	11.9 ± 9.7	5.6 ± 3.4	17.1 ± 10.1	.0001
PD ≥ 6 mm (%)	0.9 ± 1.7	0.1 ± 0.3	1.6 ± 2.1	.0001
GBI	0.40 ± 0.30	0.29 ± 0.20	0.48 ± 0.30	.001
PI	0.18 ± 0.20	0.16 ± 0.20	0.20 ± 0.25	.879
GI	0.40 ± 0.30	0.30 ± 0.21	0.47 ± 0.29	.005
Body mass index (kg/m ²)	25.46 ± 3.61	25.64 ± 3.24	25.35 ± 3.88	.798
Time elapsed from HFE-HH diagnosis	10.4 ± 7.6	11 ± 6.7	9.9 ± 8.4	.277
Gender				
Male	47 (55.9)	23 (48.9)	24 (51.1)	.443
Female	37 (44.1)	15 (40.5)	22 (59.5)	
Smoking habits				
Non-smoker	30 (35.7)	12 (31.6)	18 (39.1)	.472
Current or former	54 (64.3)	26 (68.4)	28 (60.9)	
Frequency of dentist visits				
< 1/years	17 (20.2)	7 (18.4)	10 (21.7)	.752
≥1/year	67 (79.8)	31 (85.6)	36 (78.3)	

protein. The mean time that had elapsed between the diagnosis of haemochromatosis and dental examination was calculated as 10.1 ± 7.65 years.

3.2 | Prevalence and severity of periodontitis

All patients underwent complete periodontal examination. Based on the CDC/AAP case definition, all presented periodontitis, and 44% and 54.8% had moderate and severe periodontitis, respectively (Table 1). Characteristics of patients did not differ according to the severity of periodontitis. Proportions of sites per mouth with CAL ≥ 3 mm, CAL ≥ 5 mm and PD ≥ 4 mm were 50.1 ± 17.4, 10.3 ± 11.8 and 11.9 ± 9.7 percentage, respectively. Individuals with severe periodontitis showed the worst values of PD, CAL, as well as for bleeding on probing and GI, with statistically significant differences ($p < .001$) when compared to those with mild-to-moderate periodontitis. There was no difference between both groups with respect to visible plaque. Men and women with HFE-HH were equally affected in terms of both frequency and severity of periodontitis. All patients reported brushing their teeth at least once daily and 80% reported visiting the dentist at least once a year. Sixty-four percentage were current or former smokers.

3.3 | Periodontitis severity and serum iron biomarkers at the time of dental examination

As indicated in Table 2, transferrin saturation was significantly higher in the group with severe periodontitis when compared to the group with mild or moderate periodontitis (55.1% versus 47.2% - $p = .029$). Subjects with transferrin saturation ≥45% had a fourfold higher risk (OR = 4.27 - 95% CI = 1.68–11.37, $p = .003$) of severe periodontitis than those with transferrin saturation <45%. After adjustment for confounding variables, this risk remained elevated (OR = 5.49 - 95% CI = 1.85–16.28, $p = .002$).

4 | DISCUSSION

HFE-HH is a hepcidin-deficient disease resulting in parenchymal iron overload. It is associated with complications commonly found in patients with periodontitis (i.e. diabetes and bone loss). The relationship between iron metabolism and periodontitis was previously investigated, and no significant serum iron and serum hepcidin modification was found (Carvalho et al., 2016) in patients with periodontitis compared to healthy subjects. To the best of our knowledge, the present

TABLE 2 Serum biomarkers levels (mean \pm SD) in the 84 *HFE*-HH patients in accordance with the severity of periodontitis. Significant results in bold

Measure of periodontitis	Serum biomarkers			
	Iron ($\mu\text{mol/L}$)	Transferrin (g/L)	Transferrin saturation (%)	Ferritin ($\mu\text{g/L}$)
Mild/Moderate	25 \pm 9	2.2 \pm 0.3	47.2 \pm 17.9	136.2 \pm 227.6
Severe	27.8 \pm 9.2	2.1 \pm 0.3	55.1 \pm 18	205 \pm 524.4
<i>p</i> -value	.234	.101	.029	.916
Statistical test	<i>t</i> test	<i>t</i> test	Mann-Whitney test	Mann-Whitney test

study is the first to explore the periodontal status of patients with haemochromatosis.

Serum ferritin level is considered a reliable indicator of body iron stores. However, it can overestimate iron burden in chronic inflammatory conditions such as periodontitis or chronic liver disease. A relationship between serum CRP and ferritin levels has been reported in periodontitis (Chakraborty, Tewari, Sharma, & Narula, 2014), but, in the present series, it is unlikely that inflammation could explain, even partly, the rise in serum ferritin levels as serum CRP levels were normal in all patients and initial serum ferritin levels were markedly elevated and well correlated with the amount of iron removed. Then, we can assume that serum ferritin levels were truly representative of iron excess and validated the iron-overloaded status of the patients studied.

It is noteworthy that all patients had increased body iron stores at the time of the diagnosis of haemochromatosis and all had periodontitis at the time of dental examination, which was performed after iron removal in 74 of 87 patients.

To investigate whether indicators of body iron stores were associated with the severity of periodontal disease, the population was divided into two groups (mild and moderate compared to severe periodontitis). General characteristics of both groups were similar with respect to general and iron-related features except for transferrin saturation at the time of dental examination, which was significantly increased in the group with severe periodontitis. The risk of severe periodontitis was 5.49 times greater when transferrin saturation exceeded 45%, even after adjustment for age, gender, smoking habits, plaque index and time elapsed between the diagnosis of haemochromatosis and dental examination. The threshold of 45% was chosen because it corresponds to the threshold above which non-transferrin-bound iron, a highly toxic form of iron, occurs (Brissot, Ropert, Le Lan, & Loreal, 2012).

Periopathogens live within periodontal pockets in a complex, mixed and interacting microbial community bathed in the gingival crevicular fluid, an anaerobic and inflammatory environment. Iron concentration is increased in the crevicular fluid of periodontal diseased sites (Wang, Greenwell, & Bissada, 1990). Iron regulates 10%–20% of bacterial genes and is necessary for bacterial growth. It also favours the virulence of numerous bacteria, some of which are periopathogens (Khan, Fisher, & Khakoo, 2007). As soon as transferrin saturation exceeds 45%, non-transferrin-bound iron is increased in patients with haemochromatosis (Loreal et al., 2000). This highly reactive form of iron may be more bioavailable for bacteria. Moreover, the relative hepcidin-deficient state characterizing *HFE*-HH may enhance bacterial virulence and/or

proliferation because hepcidin has a physiological antimicrobial effect. These data are in line with a direct role of iron in chronic periodontal infection (Byrne et al., 2013; Lewis, 2010; Xie & Zheng, 2012).

Finally, bone loss is a common feature in human *HFE*-HH, with a frequency ranging from 25.3% to 34.2% (Guggenbuhl et al., 2005). It results from both increased bone resorption due to elevated osteoclast activity and decreased osteoid thickness due to diminished osteoblast activity (Conte et al., 1989). In *Hfe*^{-/-} male mice, a phenotype of osteoporosis develops associating low bone mass and altered bone microarchitecture with a relationship between bone iron load and the increase in the number of osteoclasts (Guggenbuhl et al., 2011). This supports our findings that all of *HFE*-HH patients had periodontitis—of whom 54.8% presented a severe form of the disease with an average of 15% of sites having CAL \geq 5 mm.

The present study has three main limitations. First, it is a case series with no control group available, which precludes assessment of whether the prevalence of periodontitis is really increased in *HFE*-HH as suggested by the finding that all *HFE*-HH patients had periodontitis compared to 50% in the general French population (Bourgeois et al., 2007). Second, only one dental odontologist was implicated and it may be conceivable that he tended to overestimate periodontal damage. However, this senior associate professor in the periodontal department is well trained in routine examination of patients with periodontitis (ICC > 0.9) and used a widely accepted definition of periodontitis (Eke et al., 2012). This should not have influenced the main result indicating that severity of periodontitis was independently associated with increased transferrin saturation. Third, although significant, adjusted Odd ratios lacked precision as indicated by wide confidence intervals. In addition, some possible confounders, for example socio-economic status, were not taken into account.

In conclusion, the present study suggests that the severity of periodontitis is increased in *HFE*-HH patients and demonstrated an association between the severity of periodontitis and the degree of iron burden, especially elevated transferrin saturation. Dental examination should be part of the initial management of these patients.

ACKNOWLEDGEMENTS

The authors are indebted to the medical and nursing staff of the Liver Unit for participating in the recruitment and follow-up of patients, to Christian Merry for technical assistance and to Stuart Byrom (INSERM, CIC 1414) for reviewing the English language of the manuscript.

CONFLICT OF INTEREST

The authors declare that they have no conflict of interest in connection with this article.

REFERENCES

- Bagaitkar, J., Daep, C. A., Patel, C. K., Renaud, D. E., Demuth, D. R., & Scott, D. A. (2011). Tobacco smoke augments *Porphyromonas gingivalis*-*Streptococcus gordonii* biofilm formation. *PLoS One*, 6, e27386.
- Bourgeois, D., Bouchard, P., & Mattout, C. (2007). Epidemiology of periodontal status in dentate adults in France, 2002-2003. *Journal of Periodontal Research*, 42, 219-227.
- Brissot, P., Ropert, M., Le Lan, C., & Loreal, O. (2012). Non-transferrin bound iron: A key role in iron overload and iron toxicity. *Biochimica et Biophysica Acta*, 1820, 403-410.
- Byrne, D. P., Potempa, J., Olczak, T., & Smalley, J. W. (2013). Evidence of mutualism between two periodontal pathogens: Co-operative haem acquisition by the HmuY haemophore of *Porphyromonas gingivalis* and the cysteine protease interpain A (InpA) of *Prevotella intermedia*. *Molecular Oral Microbiology*, 28, 219-229.
- Carvalho, R. C., Leite, S. A., Rodrigues, V. P., Pereira, A. F., Ferreira, T. C., Nascimento, F. R., ... Pereira, A. L. (2016). Chronic periodontitis and serum levels of hepcidin and hemoglobin. *Oral Diseases*, 22, 75-76.
- Chakraborty, S., Tewari, S., Sharma, R. K., & Narula, S. C. (2014). Effect of non-surgical periodontal therapy on serum ferritin levels: An interventional study. *Journal of Periodontology*, 85, 688-696.
- Conte, D., Caraceni, M. P., Duriez, J., Mandelli, C., Corghi, E., Cesana, M., ... Bianchi, P. A. (1989). Bone involvement in primary hemochromatosis and alcoholic cirrhosis. *The American Journal of Gastroenterology*, 84, 1231-1234.
- Drakesmith, H., & Prentice, A. M. (2012). Hepcidin and the iron-infection axis. *Science*, 338, 768-772.
- Eke, P. I., Page, R. C., Wei, L., Thornton-Evans, G., & Genco, R. J. (2012). Update of the case definitions for population-based surveillance of periodontitis. *Journal of Periodontology*, 83, 1449-1454.
- Ganz, T. (2013). Systemic iron homeostasis. *Physiological Reviews*, 93, 1721-1741.
- Guggenbuhl, P., Deugnier, Y., Boisdet, J. F., Rolland, Y., Perdriger, A., Pawlotsky, Y., & Chales, G. (2005). Bone mineral density in men with genetic hemochromatosis and HFE gene mutation. *Osteoporosis International*, 16, 1809-1814.
- Guggenbuhl, P., Fergelot, P., Doyard, M., Libouban, H., Roth, M. P., Gallois, Y., ... Chappard, D. (2011). Bone status in a mouse model of genetic hemochromatosis. *Osteoporosis International*, 22, 2313-2319.
- Guyader, D., Gandon, Y., Sapey, T., Turlin, B., Mendler, M. H., Brissot, P., & Deugnier, Y. (1999). Magnetic resonance iron-free nodules in genetic hemochromatosis. *The American Journal of Gastroenterology*, 94, 1083-1086.
- Harris, E. F., & Glassell, B. E. (2011). Sex differences in the uptake of orthodontic services among adolescents in the United States. *American Journal of Orthodontics and Dentofacial Orthopedics*, 140, 543-549.
- Hayashi, C., Gudino, C. V., Gibson, F. C. 3rd, & Genco, C. A. (2010). Review: Pathogen-induced inflammation at sites distant from oral infection: Bacterial persistence and induction of cell-specific innate immune inflammatory pathways. *Molecular Oral Microbiology*, 25, 305-316.
- Ide, R., Hoshuyama, T., Wilson, D., Takahashi, K., & Higashi, T. (2011). Periodontal disease and incident diabetes: a seven-year study. *Journal of Dental Research*, 90, 41-46.
- Jolivet-Gougeon, A., Loreal, O., Ingels, A., Danic, B., Ropert, M., Bardou-Jacquet, E., ... Brissot, P. (2008). Serum transferrin saturation increase is associated with decrease of antibacterial activity of serum in patients with HFE-related genetic hemochromatosis. *The American Journal of Gastroenterology*, 103, 2502-2508.
- Jouanolle, A. M., Fergelot, P., Raoul, M. L., Gandon, G., Roussey, M., Deugnier, Y., ... David, V. (1998). Prevalence of the C282Y mutation in Brittany: Penetrance of genetic hemochromatosis? *Annales de Genetique*, 41, 195-198.
- Kassebaum, N. J., Bernabe, E., Dahiya, M., Bhandari, B., Murray, C. J., & Marcenes, W. (2014). Global burden of severe periodontitis in 1990-2010: A systematic review and meta-regression. *Journal of Dental Research*, 93, 1045-1053.
- Khan, F. A., Fisher, M. A., & Khakoo, R. A. (2007). Association of hemochromatosis with infectious diseases: Expanding spectrum. *International Journal of Infectious Diseases*, 11, 482-487.
- Kumar, V., & Faizuddin, M. (2011). Effect of smoking on gingival microvasculature: A histological study. *Journal of Indian Society of Periodontology*, 15, 344-348.
- Lewis, J. P. (2010). Metal uptake in host-pathogen interactions: Role of iron in *Porphyromonas gingivalis* interactions with host organisms. *Periodontology 2000*, 52, 94-116.
- Linden, G., Patterson, C., Evans, A., & Kee, F. (2007). Obesity and periodontitis in 60-70-year-old men. *Journal of Clinical Periodontology*, 34, 461-466.
- Loe, H. (1967). The Gingival Index, the Plaque Index and the Retention Index Systems. *Journal of Periodontology*, 38(Suppl), 610-616.
- Loreal, O., Gosriwatana, I., Guyader, D., Porter, J., Brissot, P., & Hider, R. C. (2000). Determination of non-transferrin-bound iron in genetic hemochromatosis using a new HPLC-based method. *Journal of Hepatology*, 32, 727-733.
- McClanahan, S. F., Bartizek, R. D., & Biesbrock, A. R. (2001). Identification and consequences of distinct Loe-Silness gingival index examiner styles for the clinical assessment of gingivitis. *Journal of Periodontology*, 72, 383-392.
- Morita, I., Okamoto, Y., Yoshii, S., Nakagaki, H., Mizuno, K., Sheiham, A., & Sabbah, W. (2011). Five-year incidence of periodontal disease is related to body mass index. *Journal of Dental Research*, 90, 199-202.
- Powell, L. W., Seckington, R. C., & Deugnier, Y. (2016). Haemochromatosis. *Lancet*, 388, 706-716.
- Schatzle, M., Loe, H., Lang, N. P., Heitz-Mayfield, L. J., Burgin, W., Anerud, A., & Boysen, H. (2003). Clinical course of chronic periodontitis. III. Patterns, variations and risks of attachment loss. *Journal of Clinical Periodontology*, 30, 909-918.
- Sezer, U., Erciyas, K., Ustun, K., Pehlivan, Y., Senyurt, S. Z., Aksoy, N., ... Onat, A. M. (2013). Effect of chronic periodontitis on oxidative status in patients with rheumatoid arthritis. *Journal of Periodontology*, 84, 785-792.
- Silness, J., & Loe, H. (1964). Periodontal disease in pregnancy. II. Correlation between oral hygiene and periodontal condition. *Acta Odontologica Scandinavica*, 22, 121-135.
- Silva-Boghossian, C. M., Luiz, R., & Colombo, A. P. (2011). Risk indicators for increased periodontal probing depth in subjects attending a public dental school in Brazil. *Oral Health & Preventive Dentistry*, 9, 289-299.
- Wang, H. L., Greenwell, H., & Bissada, N. F. (1990). Crevicular fluid iron changes in treated and untreated periodontally diseased sites. *Oral Surgery, Oral Medicine, and Oral Pathology*, 69, 450-456.
- Xie, H., & Zheng, C. (2012). OxyR activation in *Porphyromonas gingivalis* in response to a hemin-limited environment. *Infection and Immunity*, 80, 3471-3480.

How to cite this article: Meuric V, Lainé F, Boyer E, et al. Periodontal status and serum biomarker levels in HFE haemochromatosis patients. A case-series study. *J Clin Periodontol*. 2017;44:892-897. <https://doi.org/10.1111/jcpe.12760>

1.5 Problématique et objectifs

La conclusion de l'article précédent — association entre l'hémochromatose héréditaire et la maladie parodontale — a été prise comme point de départ pour le travail de cette thèse, qui a pour objectif de comprendre comment la surcharge en fer affecte l'équilibre hôte-microbiote. En se référant à la littérature existante sur le sujet, et qui a été introduite plus haut, plusieurs pistes peuvent être envisagées. D'une part, en cas de surcharge, il semble que les micro-organismes puissent profiter de la plus grande disponibilité du fer. D'autre part, ces mêmes micro-organismes sont susceptibles de tirer partie des dérèglements immunitaires de l'hôte liés à une homéostasie déficiente [32]. En outre, la surcharge en fer a également un impact sur le phénotype osseux, comme en témoigne l'ostéoporose fréquemment rencontrée chez les patients atteints d'hémochromatose et probablement liée à un défaut du métabolisme osseux [110, 111].

Pour répondre à la problématique, le travail a été divisé en deux volets qui sont développés dans les chapitres qui suivent. Un volet humain, qui a consisté à explorer le microbiote sous-gingival de patients atteints d'hémochromatose héréditaire, pour évaluer l'état de dysbiose de leur microbiote, et son association avec le statut fer des patients. Puis, un volet animal, dans lequel nous avons utilisé deux modèles expérimentaux murins. Le premier est un modèle reproduisant l'hémochromatose chez la souris, que nous avons cherché à caractériser au niveau buccal, du point de vue osseux et microbiologique. Le second est un modèle de parodontite induite, où nous avons évalué l'impact buccal de différentes souches bactériennes de *P. gingivalis*. Pour finir, ces deux modèles ont été croisés pour étudier la mécanistique de l'association. Ce point sera abordé dans le chapitre [Perspectives](#) en page 49, car les échantillons issus de cette expérimentation sont toujours en cours d'analyse.

1.6 Références

- [1] S. Finegold, V. Sutter, and G. Mathisen. Normal indigenous flora. In D. Hentges, editor, *Human Intestinal Microflora in Health and Disease*, pages 3–31. Academic Press, New York, N.Y., 1983. ISBN 978-0-12-341280-5.
- [2] N. Larsen, G. J. Olsen, B. L. Maidak, M. J. McCaughey, R. Overbeek, T. J. Macke, T. L. Marsh, and C. R. Woese. The ribosomal database project. *Nucleic Acids Res.*, 21(13) :3021–3023, July 1993. ISSN 0305-1048. doi : 10.1093/nar/21.13.3021.
- [3] J. P. Gray and R. P. Herwig. Phylogenetic analysis of the bacterial communities in marine sediments. *Appl Environ Microbiol*, 62(11) :4049–4059, November 1996. ISSN 0099-2240.
- [4] J. Borneman and E. W. Triplett. Molecular microbial diversity in soils from eastern Amazonia : Evidence for unusual microorganisms and microbial population shifts associated with deforestation. *Appl Environ Microbiol*, 63(7) :2647–2653, July 1997. ISSN 0099-2240.
- [5] B. Bor, J. S. McLean, K. R. Foster, L. Cen, T. T. To, A. Serrato-Guillen, F. E. Dewhirst, W. Shi, and X. He. Rapid evolution of decreased host susceptibility drives a stable relationship between ultrasmall parasite TM7x and its bacterial host. *Proc Natl Acad Sci U S A*, 115(48) :12277–12282, November 2018. ISSN 1091-6490. doi : 10.1073/pnas.1810625115.
- [6] K. H. Wilson and R. B. Blitchington. Human colonic biota studied by ribosomal DNA sequence analysis. *Appl Environ Microbiol*, 62(7) :2273–2278, July 1996. ISSN 0099-2240.
- [7] P. B. Eckburg, E. M. Bik, C. N. Bernstein, E. Purdom, L. Dethlefsen, M. Sargent, S. R. Gill, K. E. Nelson, and D. A. Relman. Diversity of the human intestinal microbial flora. *Science*, 308(5728) :1635–1638, June 2005. ISSN 1095-9203. doi : 10.1126/science.1110591.
- [8] N. Tomašev, X. Glorot, J. W. Rae, M. Zielinski, H. Askham, A. Saraiva, A. Mottram, C. Meyer, S. Ravuri, I. Protsyuk, A. Connell, C. O. Hughes, A. Karthikesalingam, J. Cornebise, H. Montgomery, G. Rees, C. Laing, C. R. Baker, K. Peterson, R. Reeves, D. Hassabis, D. King, M. Suleyman, T. Back, C. Nielson, J. R. Ledsam, and S. Mohamed. A clinically applicable approach to continuous prediction of future acute kidney injury. *Nature*, 572(7767) :116–119, August 2019. ISSN 1476-4687. doi : 10.1038/s41586-019-1390-1.
- [9] R. C. Williams and S. Offenbacher. Periodontal medicine : The emergence of a new branch of periodontology. *Periodontol 2000*, 23 :9–12, June 2000. ISSN 0906-6713.

- [10] J. Beck, R. Garcia, G. Heiss, P. S. Vokonas, and S. Offenbacher. Periodontal Disease and Cardiovascular Disease. *J Periodontol*, 67 Suppl 10S :1123–1137, October 1996. ISSN 1943-3670. doi : 10.1902/jop.1996.67.10s.1123.
- [11] S. Offenbacher, V. Katz, G. Fertik, J. Collins, D. Boyd, G. Maynor, R. McKaig, and J. Beck. Periodontal Infection as a Possible Risk Factor for Preterm Low Birth Weight. *J Periodontol*, 67 Suppl 10S :1103–1113, October 1996. ISSN 1943-3670. doi : 10.1902/jop.1996.67.10s.1103.
- [12] W. A. Soskolne. Epidemiological and clinical aspects of periodontal diseases in diabetics. *Ann Periodontol*, 3(1) :3–12, July 1998. ISSN 1553-0841. doi : 10.1902/annals.1998.3.1.3.
- [13] R. J. Lamont, H. Koo, and G. Hajishengallis. The oral microbiota : Dynamic communities and host interactions. *Nat Rev Microbiol*, 16(12) :745–759, December 2018. ISSN 1740-1534. doi : 10.1038/s41579-018-0089-x.
- [14] R. C. Page and H. E. Schroeder. Pathogenesis of inflammatory periodontal disease. A summary of current work. *Lab Invest*, 34(3) :235–249, March 1976. ISSN 0023-6837.
- [15] G. Hajishengallis and J. M. Korostoff. Revisiting the Page & Schroeder model : The good, the bad and the unknowns in the periodontal host response 40 years later. *Periodontol 2000*, 75(1) :116–151, October 2017. ISSN 09066713. doi : 10.1111/prd.12181.
- [16] W. J. Loesche and S. A. Syed. Bacteriology of Human Experimental Gingivitis : Effect of Plaque and Gingivitis Score. *Infect Immun*, 21(3) :830–839, September 1978. ISSN 0019-9567, 1098-5522.
- [17] E. Theilade. The non-specific theory in microbial etiology of inflammatory periodontal diseases. *J Clin Periodontol*, 13(10) :905–911, 1986. ISSN 1600-051X. doi : 10.1111/j.1600-051X.1986.tb01425.x.
- [18] P. D. Marsh. Are dental diseases examples of ecological catastrophes? *Microbiology*, 149(Pt 2) :279–294, February 2003. ISSN 1350-0872. doi : 10.1099/mic.0.26082-0.
- [19] G. Hajishengallis and R. J. Lamont. Beyond the red complex and into more complexity : The polymicrobial synergy and dysbiosis (PSD) model of periodontal disease etiology. *Mol Oral Microbiol*, 27(6) :409–419, December 2012. ISSN 2041-1014. doi : 10.1111/j.2041-1014.2012.00663.x.
- [20] P. J. Pérez-Chaparro, C. Gonçalves, L. C. Figueiredo, M. Faveri, E. Lobão, N. Tamashiro, P. Duarte, and M. Feres. Newly identified pathogens associated with periodontitis : A systematic review. *J Dent Res*, 93(9) :846–858, September 2014. ISSN 1544-0591. doi : 10.1177/0022034514542468.

- [21] S. W. Olesen and E. J. Alm. Dysbiosis is not an answer. *Nat Microbiol*, 1 :16228, November 2016. ISSN 2058-5276. doi : 10.1038/nmicrobiol.2016.228.
- [22] P. Jaccard. The distribution of the flora in the alpine zone. *New phytologist*, 11 (2) :37–50, 1912. ISSN 1469-8137.
- [23] J. R. Bray and J. T. Curtis. An ordination of the upland forest communities of southern Wisconsin. *Ecological Monographs*, 27(4) :325–349, 1957. ISSN 0012-9615.
- [24] C. E. Shannon and W. Weaver. *The Mathematical Theory of Communication*. University of Illinois press, Urbana, Etats-Unis d'Amérique, 1963. ISBN 978-0-252-72548-7.
- [25] E. H. Simpson. Measurement of Diversity. *Nature*, 163(4148) :688–688, April 1949. ISSN 1476-4687. doi : 10.1038/163688a0.
- [26] C. Lozupone and R. Knight. UniFrac : A new phylogenetic method for comparing microbial communities. *Appl Environ Microbiol*, 71(12) :8228–8235, 2005.
- [27] S. J. Dixon, K. M. Lemberg, M. R. Lamprecht, R. Skouta, E. M. Zaitsev, C. E. Gleason, D. N. Patel, A. J. Bauer, A. M. Cantley, W. S. Yang, B. Morrison, and B. R. Stockwell. Ferroptosis : An iron-dependent form of nonapoptotic cell death. *Cell*, 149(5) :1060–1072, May 2012. ISSN 1097-4172. doi : 10.1016/j.cell.2012.03.042.
- [28] J. D. Cook, W. E. Barry, C. Hershko, G. Fillet, and C. A. Finch. Iron kinetics with emphasis on iron overload. *Am J Pathol*, 72(2) :337–344, August 1973. ISSN 0002-9440.
- [29] N. C. Andrews. Disorders of Iron Metabolism. *N Engl J Med*, 341(26) :1986–1995, December 1999. ISSN 0028-4793. doi : 10.1056/NEJM199912233412607.
- [30] E. D. Weinberg. Roles of Iron in Host-Parasite Interactions. *J Infect Dis*, 124(4) : 401–410, October 1971. ISSN 0022-1899. doi : 10.1093/infdis/124.4.401.
- [31] J. J. Bullen. The Significance of Iron in Infection. *Rev Infect Dis*, 3(6) :1127–1138, November 1981. ISSN 0162-0886. doi : 10.1093/clinids/3.6.1127.
- [32] T. Ganz and E. Nemeth. Iron homeostasis in host defence and inflammation. *Nat Rev Immunol*, 15(8) :500–510, August 2015. ISSN 1474-1741. doi : 10.1038/nri3863.
- [33] D. J. Bullen and E. Griffiths, editors. *Iron and Infection : Molecular, Physiological and Clinical Aspects*. Wiley, Chichester ; New York, 2nd edition edition, May 1999. ISBN 978-0-471-93940-5.

- [34] E. D. Weinberg. Nutritional Immunity : Host's Attempt to Withhold Iron From Microbial Invaders. *JAMA*, 231(1) :39–41, January 1975. ISSN 0098-7484. doi : 10.1001/jama.1975.03240130021018.
- [35] J. E. Cassat and E. P. Skaar. Iron in Infection and Immunity. *Cell Host Microbe*, 13(5) :509–519, May 2013. ISSN 1931-3128. doi : 10.1016/j.chom.2013.04.010.
- [36] B. J. Appelmelk, Y. Q. An, M. Geerts, B. G. Thijs, H. A. de Boer, D. M. MacLaren, J. de Graaff, and J. H. Nuijens. Lactoferrin is a lipid A-binding protein. *Infect Immun*, 62(6) :2628–2632, June 1994. ISSN 0019-9567, 1098-5522.
- [37] P. K. Singh, M. R. Parsek, E. P. Greenberg, and M. J. Welsh. A component of innate immunity prevents bacterial biofilm development. *Nature*, 417(6888) : 552–555, May 2002. ISSN 0028-0836. doi : 10.1038/417552a.
- [38] E. A. Griffiths, L. C. Duffy, F. L. Schanbacher, H. Qiao, D. Dryja, A. Leavens, J. Rossman, G. Rich, D. Dirienzo, and P. L. Ogra. In vivo effects of bifidobacteria and lactoferrin on gut endotoxin concentration and mucosal immunity in Balb/c mice. *Dig Dis Sci*, 49(4) :579–589, April 2004. ISSN 0163-2116.
- [39] G. Nicolas, C. Chauvet, L. Viatte, J. L. Danan, X. Bigard, I. Devaux, C. Beaumont, A. Kahn, and S. Vaulont. The gene encoding the iron regulatory peptide hepcidin is regulated by anemia, hypoxia, and inflammation. *J Clin Invest*, 110(7) :1037–1044, October 2002. ISSN 0021-9738. doi : 10.1172/JCI15686.
- [40] L. T. Goodnough, E. Nemeth, and T. Ganz. Detection, evaluation, and management of iron-restricted erythropoiesis. *Blood*, 116(23) :4754–4761, December 2010. ISSN 0006-4971, 1528-0020. doi : 10.1182/blood-2010-05-286260.
- [41] M. Boshuizen, K. van der Ploeg, L. von Bonsdorff, B. J. Biemond, S. S. Zeerleder, R. van Bruggen, and N. P. Juffermans. Therapeutic use of transferrin to modulate anemia and conditions of iron toxicity. *Blood Rev*, July 2017. ISSN 1532-1681. doi : 10.1016/j.blre.2017.07.005.
- [42] K. Hantke. Regulation of ferric iron transport in *Escherichia coli* K12 : Isolation of a constitutive mutant. *Mol Gen Genet*, 182(2) :288–292, 1981. ISSN 0026-8925. doi : 10.1007/bf00269672.
- [43] C. Ratledge and L. G. Dover. Iron metabolism in pathogenic bacteria. *Annu Rev Microbiol*, 54 :881–941, 2000. ISSN 0066-4227. doi : 10.1146/annurev.micro.54.1.881.
- [44] J. H. Crosa, A. R. Mey, and S. M. Payne. *Iron Transport in Bacteria*. American Society of Microbiology, Washington (D.C.), January 2004. ISBN 978-1-55581-654-4 978-1-55581-292-8. doi : 10.1128/9781555816544.
- [45] D. L. Stauff and E. P. Skaar. The heme sensor system of *Staphylococcus aureus*. *Contrib Microbiol*, 16 :120–135, 2009. ISSN 1420-9519. doi : 10.1159/000219376.

- [46] N. Noinaj, N. C. Easley, M. Oke, N. Mizuno, J. Gumbart, E. Boura, A. N. Steere, O. Zak, P. Aisen, E. Tajkhorshid, R. W. Evans, A. R. Gorringer, A. B. Mason, A. C. Steven, and S. K. Buchanan. Structural basis for iron piracy by pathogenic *Neisseria*. *Nature*, 483(7387) :53–58, February 2012. ISSN 1476-4687. doi : 10.1038/nature10823.
- [47] C. Wandersman and P. Delepelaire. Bacterial Iron Sources : From Siderophores to Hemophores. *Annu Rev Microbiol*, 58(1) :611–647, 2004. doi : 10.1146/annurev.micro.58.030603.123811.
- [48] M. Herman, M. Golasik, W. Piekoszewski, S. Walas, M. Napierala, M. Wyganowska-Swiatkowska, A. Kurhanska-Flisykowska, A. Wozniak, and E. Florek. Essential and Toxic Metals in Oral Fluid—a Potential Role in the Diagnosis of Periodontal Diseases. *Biol Trace Elem Res*, 173(2) :275, 2016. doi : 10.1007/s12011-016-0660-0.
- [49] S. R. Shetty, S. Babu, S. Kumari, P. Shetty, S. Hegde, and A. Karikal. Status of trace elements in saliva of oral precancer and oral cancer patients. *J Cancer Res Ther*, 11(1) :146–149, 2015 Jan-Mar. ISSN 1998-4138. doi : 10.4103/0973-1482.137973.
- [50] R. B. Lages, E. C. Bridi, C. A. Pérez, and R. T. Basting. Salivary levels of nickel, chromium, iron, and copper in patients treated with metal or esthetic fixed orthodontic appliances : A retrospective cohort study. *J Trace Elem Med Biol*, 40 : 67–71, March 2017. ISSN 0946-672X. doi : 10.1016/j.jtemb.2016.12.011.
- [51] Y.-J. Kim, Y.-K. Kim, and H.-S. Kho. Effects of smoking on trace metal levels in saliva. *Oral Dis*, 16(8) :823–830, 2010. ISSN 1601-0825. doi : 10.1111/j.1601-0825.2010.01698.x.
- [52] L.-N. Guo, Y.-Z. Yang, and Y.-Z. Feng. Serum and salivary ferritin and Hepsidin levels in patients with chronic periodontitis and type 2 diabetes mellitus. *BMC Oral Health*, 18(1) :63, October 2018. ISSN 1472-6831. doi : 10.1186/s12903-018-0524-4.
- [53] D. Cicek, A. F. Dağlı, S. Aydin, F. B. Dogan, S. B. Dertlioğlu, H. Uçak, and B. Demir. Does hepcidin play a role in the pathogenesis of aphthae in Behçet's disease and recurrent aphthous stomatitis? *J Eur Acad Dermatol Venereol*, 28 (11) :1500–1506, 2014. ISSN 1468-3083. doi : 10.1111/jdv.12326.
- [54] M. A. Curtis, J. A. Sterne, S. J. Price, G. S. Griffiths, S. K. Coulthurst, J. M. Wilton, and N. W. Johnson. The protein composition of gingival crevicular fluid sampled from male adolescents with no destructive periodontitis : Baseline data of a longitudinal study. *J Periodont Res*, 25(1) :6–16, January 1990. ISSN 0022-3484.

- [55] J. G. Tew, D. R. Marshall, J. A. Burmeister, and R. R. Ranney. Relationship between gingival crevicular fluid and serum antibody titers in young adults with generalized and localized periodontitis. *Infect Immun*, 49(3) :487–493, September 1985. ISSN 0019-9567, 1098-5522.
- [56] S. Mukherjee. The Role of Crevicular Fluid Iron in Periodontal Disease. *J Periodontol*, 56(11S) :22–27, 1985. ISSN 1943-3670. doi : 10.1902/jop.1985.56.11s.22.
- [57] J. W. Smalley and T. Olczak. Haem acquisition mechanisms of *Porphyromonas gingivalis* - strategies used in polymicrobial community in a haem-limited host environment. *Mol Oral Microbiol*, December 2015. ISSN 2041-1014. doi : 10.1111/omi.12149.
- [58] A. E. Duran-Pinedo, T. Chen, R. Teles, J. R. Starr, X. Wang, K. Krishnan, and J. Frias-Lopez. Community-wide transcriptome of the oral microbiome in subjects with and without periodontitis. *ISME J*, 8(8) :1659–1672, August 2014. ISSN 1751-7370. doi : 10.1038/ismej.2014.23.
- [59] G. Hajishengallis. Periodontitis : From microbial immune subversion to systemic inflammation. *Nat Rev Immunol*, 15(1) :30–44, January 2015. ISSN 1474-1741. doi : 10.1038/nri3785.
- [60] D. Grenier, V. Goulet, and D. Mayrand. The capacity of *Porphyromonas gingivalis* to multiply under iron-limiting conditions correlates with its pathogenicity in an animal model. *J Dent Res*, 80(7) :1678–1682, July 2001. ISSN 0022-0345.
- [61] R. E. Schifferle, S. A. Shostad, M. T. Bayers-Thering, D. W. Dyer, and M. E. Neiders. Effect of protoporphyrin IX limitation on *Porphyromonas gingivalis*. *J Endod*, 22(7) :352–355, July 1996. ISSN 0099-2399. doi : 10.1016/S0099-2399(96)80216-0.
- [62] C. Wyss. Growth of *Porphyromonas gingivalis*, *Treponema denticola*, *T. pectinovorum*, *T. socranskii*, and *T. vincentii* in a chemically defined medium. *J Clin Microbiol*, 30(9) :2225–2229, September 1992. ISSN 0095-1137, 1098-660X.
- [63] T. Olczak, W. Simpson, X. Liu, and C. A. Genco. Iron and heme utilization in *Porphyromonas gingivalis*. *FEMS Microbiol Rev*, 29(1) :119–144, January 2005. ISSN 0168-6445. doi : 10.1016/j.femsre.2004.09.001.
- [64] J. W. Smalley and T. Olczak. Heme acquisition mechanisms of *Porphyromonas gingivalis* – strategies used in a polymicrobial community in a heme-limited host environment. *Mol Oral Microbiol*, 32(1) :1–23, 2017. ISSN 2041-1014. doi : 10.1111/omi.12149.
- [65] J.-L. Gao, K.-A. Nguyen, and N. Hunter. Characterization of a Hemophore-like Protein from *Porphyromonas gingivalis*. *J Biol Chem*, 285(51) :40028–40038, December 2010. ISSN 0021-9258, 1083-351X. doi : 10.1074/jbc.M110.163535.

- [66] T. Olczak, A. Sroka, J. Potempa, and M. Olczak. *Porphyromonas Gingivalis* HmuY and HmuR : Further characterization of a novel mechanism of heme utilization. *Arch Microbiol*, 189(3) :197–210, March 2008. ISSN 0302-8933. doi : 10.1007/s00203-007-0309-7.
- [67] S. G. Dashper, A. Hendtlass, N. Slakeski, C. Jackson, K. J. Cross, L. Brownfield, R. Hamilton, I. Barr, and E. C. Reynolds. Characterization of a novel outer membrane hemin-binding protein of *Porphyromonas gingivalis*. *J Bacteriol*, 182(22) : 6456–6462, November 2000. ISSN 0021-9193. doi : 10.1128/jb.182.22.6456-6462.2000.
- [68] N. Li and C. A. Collyer. Gingipains from *Porphyromonas gingivalis* – Complex domain structures confer diverse functions. *Eur J Microbiol Immunol (Bp)*, 1(1) : 41–58, March 2011. ISSN 2062-509X. doi : 10.1556/EuJMI.1.2011.1.7.
- [69] J. P. Lewis, J. A. Dawson, J. C. Hannis, D. Muddiman, and F. L. Macrina. Hemoglobinase Activity of the Lysine Gingipain Protease (Kgp) of *Porphyromonas gingivalis* W83. *J Bacteriol*, 181(16) :4905–4913, August 1999. ISSN 0021-9193, 1098-5530.
- [70] T. Imamura. The role of gingipains in the pathogenesis of periodontal disease. *J Periodontol*, 74(1) :111–118, January 2003. ISSN 0022-3492. doi : 10.1902/jop.2003.74.1.111.
- [71] S. Shizukuishi, K. Tazaki, E. Inoshita, K. Kataoka, T. Hanioka, and A. Amano. Effect of concentration of compounds containing iron on the growth of *Porphyromonas gingivalis*. *FEMS Microbiol Lett*, 131(3) :313–317, September 1995. ISSN 0378-1097. doi : 10.1111/j.1574-6968.1995.tb07793.x.
- [72] E. Inoshita, K. Iwakura, A. Amano, H. Tamagawa, and S. Shizukuishi. Effect of transferrin on the growth of *Porphyromonas gingivalis*. *J Dent Res*, 70(9) :1258–1261, 1991.
- [73] K. Tazaki, E. Inoshita, A. Amano, T. Hanioka, H. Tamagawa, and S. Shizukuishi. Interaction of *Porphyromonas gingivalis* with transferrin. *FEMS Microbiol Lett*, 131(2) :161–166, September 1995. ISSN 0378-1097. doi : 10.1111/j.1574-6968.1995.tb07771.x.
- [74] A. Sroka, M. Sztukowska, J. Potempa, J. Travis, and C. A. Genco. Degradation of Host Heme Proteins by Lysine- and Arginine-Specific Cysteine Proteinases (Gingipains) of *Porphyromonas gingivalis*. *J Bacteriol*, 183(19) :5609–5616, October 2001. ISSN 0021-9193, 1098-5530. doi : 10.1128/JB.183.19.5609-5616.2001.
- [75] V. Brochu, D. Grenier, K. Nakayama, and D. Mayrand. Acquisition of iron from human transferrin by *Porphyromonas gingivalis* : A role for Arg- and Lys-gingipain activities. *Oral Microbiol Immunol*, 16(2) :79–87, April 2001. ISSN 0902-0055.

- [76] T. M. Staggs, M. K. Greer, J. B. Baseman, S. C. Holt, and V. V. Tryon. Identification of lactoferrin-binding proteins from *Treponema pallidum* subspecies *pallidum* and *Treponema denticola*. *Mol Microbiol*, 12(4) :613–619, May 1994. ISSN 0950-382X. doi : 10.1111/j.1365-2958.1994.tb01048.x.
- [77] D. Grenier. Characteristics of hemolytic and hemagglutinating activities of *Treponema denticola*. *Oral Microbiol Immunol*, 6(4) :246–249, August 1991. ISSN 0902-0055.
- [78] L. Chu, W. Kennell, and S. C. Holt. Characterization of hemolysis and hemoxidation activities by *Treponema denticola*. *Microb Pathog*, 16(3) :183–195, March 1994. ISSN 0882-4010. doi : 10.1006/mpat.1994.1019.
- [79] X. Xu and D. Kolodrubetz. Construction and analysis of hemin binding protein mutants in the oral pathogen *Treponema denticola*. *Res Microbiol*, 153(9) :569–577, November 2002. ISSN 0923-2508.
- [80] D. Scott, E. C. Chan, and R. Siboo. Iron acquisition by oral hemolytic spirochetes : Isolation of a hemin-binding protein and identification of iron reductase activity. *Can J Microbiol*, 42(10) :1072–1079, October 1996. ISSN 0008-4166. doi : 10.1139/m96-137.
- [81] L. Chu, M. Song, and S. C. Holt. Effect of iron regulation on expression and hemin-binding function of outer-sheath proteins from *Treponema denticola*. *Microb Pathog*, 16(5) :321–335, May 1994. ISSN 0882-4010. doi : 10.1006/mpat.1994.1033.
- [82] S. Yost, A. E. Duran-Pinedo, R. Teles, K. Krishnan, and J. Frias-Lopez. Functional signatures of oral dysbiosis during periodontitis progression revealed by microbial metatranscriptome analysis. *Genome Med*, 7(1), April 2015. ISSN 1756-994X. doi : 10.1186/s13073-015-0153-3.
- [83] M. Bielecki, S. Antonyuk, R. W. Strange, J. W. Smalley, P. Mackiewicz, M. Śmiga, P. Stępień, M. Olczak, and T. Olczak. *Tannerella Forsythia* Tfo belongs to *Porphyromonas gingivalis* HmuY-like family of proteins but differs in heme-binding properties. *Biosci Rep*, 38(5), October 2018. ISSN 1573-4935. doi : 10.1042/BSR20181325.
- [84] D. P. Byrne, S. P. Manandhar, J. Potempa, and J. W. Smalley. Breakdown of albumin and haemalbumin by the cysteine protease interpain A, an albuminase of *Prevotella intermedia*. *BMC Microbiol*, 15, September 2015. ISSN 1471-2180. doi : 10.1186/s12866-015-0516-3.
- [85] K. P. Leung, P. S. Subramaniam, M. Okamoto, H. Fukushima, and C. H. Lai. The binding and utilization of hemoglobin by *Prevotella intermedia*. *FEMS Microbiol Lett*, 162(2) :227–233, May 1998. ISSN 0378-1097. doi : 10.1111/j.1574-6968.1998.tb13003.x.

- [86] K.-P. Leung and S. P. Folk. Effects of porphyrins and inorganic iron on the growth of *Prevotella intermedia*. *FEMS Microbiol Lett*, 209(1) :15–21, March 2002. ISSN 0378-1097. doi : 10.1111/j.1574-6968.2002.tb11103.x.
- [87] D. Grenier and S.-I. Tanabe. Transferrin as a source of iron for *Campylobacter rectus*. *J Oral Microbiol*, 3, 2011. ISSN 2000-2297. doi : 10.3402/jom.v3i0.5660.
- [88] K. Schümann and N. W. Solomons. Perspective : What Makes It So Difficult to Mitigate Worldwide Anemia Prevalence? *Adv Nutr*, 8(3) :401–408, May 2017. ISSN 2161-8313. doi : 10.3945/an.116.013847.
- [89] T. K. Bergmann, K. Vinding, and H. Hey. Multiple hepatic abscesses due to *Yersinia enterocolitica* infection secondary to primary haemochromatosis. *Scand J Gastroenterol*, 36(8) :891–895, August 2001. ISSN 0036-5521. doi : 10.1080/003655201750313450.
- [90] J. C. Barton and R. T. Acton. Hemochromatosis and *Vibrio vulnificus* wound infections. *J Clin Gastroenterol*, 43(9) :890–893, October 2009. ISSN 1539-2031. doi : 10.1097/MCG.0b013e31819069c1.
- [91] K. M. Frank, O. Schneewind, and W.-J. Shieh. Investigation of a researcher's death due to septicemic plague. *N Engl J Med*, 364(26) :2563–2564, June 2011. ISSN 1533-4406. doi : 10.1056/NEJMc1010939.
- [92] L. E. Quenee, T. M. Hermanas, N. Ciletti, H. Louvel, N. C. Miller, D. Elli, B. Blaylock, A. Mitchell, J. Schroeder, T. Krausz, J. Kanabrocki, and O. Schneewind. Hereditary Hemochromatosis Restores the Virulence of Plague Vaccine Strains. *J Infect Dis*, 206(7) :1050–1058, October 2012. ISSN 0022-1899. doi : 10.1093/infdis/jis433.
- [93] F. von Recklinghausen. Über hämochromatose. In *Tagebl Der 62 Versamml Deutscher Naturforscher Und Ärzte in Heidelberg*, volume 62, pages 324–325, Heidelberg, 1889.
- [94] A. Trousseau. Glycosurie, diabète sucré. *Clinique Médicale de l'Hôtel-Dieu de Paris*, 2 :663–698, 1865.
- [95] M. Simon, M. Bourel, B. Genetet, and R. Fauchet. Idiopathic Hemochromatosis : Demonstration of Recessive Transmission and Early Detection by Family HLA Typing. *New England Journal of Medicine*, 297(19) :1017–1021, November 1977. ISSN 0028-4793. doi : 10.1056/NEJM197711102971901.
- [96] J. N. Feder, A. Gnirke, W. Thomas, Z. Tsuchihashi, D. A. Ruddy, A. Basava, F. Dormishian, R. Domingo, M. C. Ellis, A. Fullan, L. M. Hinton, N. L. Jones, B. E. Kimmel, G. S. Kronmal, P. Lauer, V. K. Lee, D. B. Loeb, F. A. Mapa, E. McClelland, N. C. Meyer, G. A. Mintier, N. Moeller, T. Moore, E. Morikang, C. E. Prass, L. Quintana, S. M. Starnes, R. C. Schatzman, K. J. Brunke, D. T. Drayna, N. J.

- Risch, B. R. Bacon, and R. K. Wolff. A novel MHC class I-like gene is mutated in patients with hereditary haemochromatosis. *Nat Genet*, 13(4) :399–408, August 1996. doi : 10.1038/ng0896-399.
- [97] L. W. Powell, R. C. Seckington, and Y. Deugnier. Haemochromatosis. *Lancet*, 388 (10045) :706–716, August 2016. ISSN 1474-547X. doi : 10.1016/S0140-6736(15)01315-X.
- [98] J. O’Neil and L. Powell. Clinical aspects of hemochromatosis. *Semin Liver Dis*, 25(4) :381–391, November 2005. ISSN 0272-8087. doi : 10.1055/s-2005-923310.
- [99] Y. Deugnier, F. Lainé, C. Le Lan, E. Bardou-Jacquet, A.-M. Jouanolle, and P. Brissot. Hémochromatoses et autres surcharges hépatiques en fer. *EMC - Traité d’Hépatologie*, 7-007-B-22 :1–12, January 2011. ISSN 11551976. doi : 10.1016/S1155-1976(11)40364-8.
- [100] R. Moirand, D. Guyader, P. Brissot, and Y. Deugnier. Hémochromatose. *EMC - Traité d’Hépatologie*, 7-200-A-10 :1–15, 2000. ISSN 1155-1976.
- [101] J. C. Barton and C. Q. Edwards. HFE Hemochromatosis. In M. P. Adam, H. H. Ardinger, R. A. Pagon, S. E. Wallace, L. J. Bean, K. Stephens, and A. Amemiya, editors, *GeneReviews®*. University of Washington, Seattle, Seattle (WA), 1993.
- [102] Q. Wu, H. Wang, P. An, Y. Tao, J. Deng, Z. Zhang, Y. Shen, C. Chen, J. Min, and F. Wang. HJV and HFE Play Distinct Roles in Regulating Hepcidin. *Antioxid Redox Signal*, 22(15) :1325–1336, May 2015. ISSN 1557-7716. doi : 10.1089/ars.2013.5819.
- [103] A. Roetto, A. Totaro, A. Piperno, A. Piga, F. Longo, G. Garozzo, A. Cali, M. De Gobbi, P. Gasparini, and C. Camaschella. New mutations inactivating transferrin receptor 2 in hemochromatosis type 3. *Blood*, 97(9) :2555–2560, May 2001. ISSN 0006-4971. doi : 10.1182/blood.v97.9.2555.
- [104] P. Brissot, M. Ropert, C. Le Lan, and O. Loréal. Non-transferrin bound iron : A key role in iron overload and iron toxicity. *Biochim Biophys Acta*, 1820(3) :403–410, March 2012. ISSN 0006-3002. doi : 10.1016/j.bbagen.2011.07.014.
- [105] P. Brissot, R. Moirand, A. M. Jouanolle, D. Guyader, J. Y. Le Gall, Y. Deugnier, and V. David. A genotypic study of 217 unrelated probands diagnosed as "genetic hemochromatosis" on "classical" phenotypic criteria. *J Hepatol*, 30(4) :588–593, April 1999. ISSN 0168-8278. doi : 10.1016/s0168-8278(99)80188-3.
- [106] T. Cavey, C. Latour, M.-L. Island, P. Leroyer, P. Guggenbuhl, H. Coppin, M.-P. Roth, C. Bendavid, P. Brissot, M. Ropert, and O. Loréal. Spleen iron, molybdenum, and manganese concentrations are coregulated in hepcidin-deficient and secondary iron overload models in mice. *FASEB J*, page fj201801381RR, July 2019. ISSN 1530-6860. doi : 10.1096/fj.201801381RR.

- [107] P. I. Eke, R. C. Page, L. Wei, G. Thornton-Evans, and R. J. Genco. Update of the case definitions for population-based surveillance of periodontitis. *J Periodontol*, 83(12) :1449–1454, December 2012. ISSN 1943-3670. doi : 10.1902/jop.2012.110664.
- [108] O. Loréal, I. Gosriwatana, D. Guyader, J. Porter, P. Brissot, and R. C. Hider. Determination of non-transferrin-bound iron in genetic hemochromatosis using a new HPLC-based method. *J Hepatol*, 32(5) :727–733, May 2000. ISSN 0168-8278.
- [109] T. G. Frantzis, P. J. Sheridan, C. M. Reeve, and L. L. Young. Oral manifestations of hemochromatosis. Report of a case. *Oral Surg Oral Med Oral Pathol*, 33(2) : 186–190, February 1972. ISSN 0030-4220.
- [110] N. Guañabens and A. Parés. Osteoporosis in chronic liver disease. *Liver Int*, 38 (5) :776–785, 2018. ISSN 1478-3231. doi : 10.1111/liv.13730.
- [111] M. Doyard, D. Chappard, P. Leroyer, M.-P. Roth, O. Loréal, and P. Guggenbuhl. Decreased Bone Formation Explains Osteoporosis in a Genetic Mouse Model of Hemochromatosis. *PLoS One*, 11(2) :e0148292, 2016. ISSN 1932-6203. doi : 10.1371/journal.pone.0148292.

Chapitre 2

Observations chez l'Homme

Sommaire

2.1 Increased transferrin saturation is associated with subgingival microbiota dysbiosis and severe periodontitis in genetic haemochromatosis, <i>Scientific Reports</i> 2018	34
2.2 Periodontal pathogens and clinical parameters in periodontitis, <i>Molecular Oral Microbiology</i> 2019	37
2.3 Références	40

La recherche chez l'Homme avait deux objectifs. Le premier était de déterminer si la surcharge en fer, liée à l'hémochromatose héréditaire, pouvait influencer le microbiote. Pour cela, des échantillons de microbiote sous-gingival ont été collectés lors de l'examen clinique des patients atteints d'hémochromatose héréditaire présentés précédemment¹. Ces échantillons ont été traités par biologie moléculaire, puis par séquençage du gène de l'ARNr 16S bactérien. Une étude par bioinformatique a ensuite été réalisée pour évaluer la biodiversité des échantillons, et l'association entre le statut fer des patients et la composition de leur microbiote. Le résultat de ce travail est présenté dans la section suivante.

Le second objectif était d'étudier la dysbiose bactérienne du microbiote sous-gingival de ces mêmes patients, et notamment le ratio de dysbiose mentionné précédemment². Ce ratio ayant été développé à partir de sujets très majoritairement sans pathologie systémique³, nous souhaitions tester sa validité chez les patients atteints d'hémochromatose héréditaire. Étant donné que nous disposions du statut parodontal précis de ces patients, nous avons pu évaluer précisément, par des modèles de régression linéaire multiple, l'association entre le ratio de dysbiose et la sévérité de leur parodontite. Le résultat de ce travail est présenté dans la section 2.2 du présent chapitre, en page 37.

2.1 Increased transferrin saturation is associated with sub-gingival microbiota dysbiosis and severe periodontitis in genetic haemochromatosis, *Scientific Reports* 2018

Comme indiqué précédemment, les patients présentés dans l'étude clinique parue dans le *Journal of Clinical Periodontology* ont fait, pour la plupart, l'objet d'un prélèvement de microbiote sous-gingival. Celui-ci a été collecté dans les deux sites parodontaux les plus atteints par la maladie parodontale, c'est à dire présentant les valeurs les plus fortes lors du sondage parodontal. Après extraction de l'ADN bactérien, les régions V3-V4 du gène de l'ARNr 16S ont été amplifiées puis séquencées par Illumina MiSeq®. L'analyse bioinformatique des fichiers issus du séquençage a été réalisée jusqu'au niveau taxonomique des genres bactériens avec l'outil web VAMPS, complétée par QIIME (version 1.9.1) pour une analyse au niveau taxonomique des espèces. Les bases de données de référence qui ont été utilisées sont : RDP (version 11), et la « *Human Oral Microbiome Database* » (HOMD version 14.51, <http://homd.org>).

Une fois exclus les patients n'ayant pas fait l'objet d'un prélèvement, ceux dont il manquait certaines données démographiques ou relatives au statut fer et ceux dont

1. Voir la section 1.4.1 *Periodontal status and serum biomarkers levels in HFE hemochromatosis patients. A case-series study*, *Journal of Clinical Periodontology* 2017 en page 19.

2. Voir la section 1.2.1 *Signature of Microbial Dysbiosis in Periodontitis*, *Applied and Environmental Microbiology* 2017 en page 7.

3. Parmi les 196 échantillons de patients ayant une parodontite, 24 correspondaient à nos propres échantillons issus de patients présentant une hémochromatose.

les échantillon n'étaient pas exploitables, le groupe d'étude était constitué de 66 patients. Après un rappel des paramètres cliniques de la maladie parodontale chez nos patients, une analyse de l'*alpha* diversité (richesse et variété d'espèces au sein de chaque échantillon) et de la *beta* diversité (variations entre les différents échantillons) a été menée. Enfin, une analyse des réseaux de co-occurrences bactériens — qui compile plusieurs tests de corrélation et d'association entre les abondances des genres bactériens — a été réalisée sur le *core* microbiote. Tout cela, en lien avec les données fer disponibles, et notamment avec le coefficient de saturation de la transferrine, puisque celui-ci apparaissait comme étant un facteur de risque pour une parodontite sévère dans l'étude précédente. Les patients ont donc été séparés en deux groupes : saturation de la transferrine normale ($\leq 45\%$, « *normal TSAT* », 21 patients), et saturation de la transferrine élevée ($> 45\%$, « *high TSAT* », 45 patients).

Bien qu'il s'agissait d'une sous-population, les patients présentaient les mêmes caractéristiques que celles présentées dans l'étude dont ils étaient issus. Ils étaient tous atteints de parodontite, et celle-ci était significativement plus sévère (d'après la classification de 2012 [1]) pour les patients qui présentaient une saturation de la transferrine pathologique, malgré leur prise en charge par saignées régulières. Les paramètres cliniques détaillés dans le tableau 1 de l'article montrent une augmentation significative de la perte d'attache (« *clinical attachment loss, CAL* »), et une tendance à des poches parodontales plus profondes (« *pocket probing depth, PPD* »).

Les mesures classiques de la diversité du microbiote que sont l'*alpha* et la *beta* diversité — présentées respectivement dans les figures 1 et 2 de l'article — ne présentaient pas de différence selon la saturation de la transferrine. D'après ces mesures, la composition du microbiote était assez semblable entre ces deux groupes. Cela était confirmé par un test d'abondance différentiel, présenté en figure 3 de l'article. L'algorithme d'analyse discriminante linéaire utilisé (« *Linear discriminant analysis with Effect Size, LEfSe* [2]) ne relevait que peu de taxons avec une abondance significativement différente entre les deux groupes, et ceux-ci ne comptaient que pour une faible proportion du microbiote total. Ce constat était cependant cohérent avec nos précédents travaux sur le microbiote sous-gingival qui avaient abouti au ratio de dysbiose : les mesures classiquement utilisées distinguent déjà de façon imparfaite les microbiotes de sujets sain et malade ; leur résolution est donc insuffisante pour distinguer des microbiotes provenant de sujets malades à différentes sévérités.

Finalement, les réseaux de co-occurrence bactériens (présentés dans la figure 4 de l'article) permettaient d'observer deux profils de microbiote différents selon la surcharge en fer circulant. Bien que l'on y retrouvait les mêmes genres bactériens, ceux-ci s'associaient de façon extrêmement différente entre les deux groupes. Ces variations structurelles et l'intégration de la saturation de la transferrine dans les réseaux nous ont permis de formuler l'hypothèse suivante : l'augmentation progressive de la saturation de la transferrine pourrait profiter aux espèces susceptibles de pouvoir l'utiliser comme source de fer (dont les espèces pathogènes appartenant aux genres *Porphyromonas* et *Treponema*). Cette sélection d'espèces potentiellement pathogènes pour le parodonte serait un facteur favorisant la dysbiose. Au-delà de 45 % de saturation,

toute augmentation supplémentaire ne constituerait cependant plus un avantage sélectif pour ces bactéries, compte tenu de l'apparition de fer non lié à la transferrine⁴, qui pourrait être acquis sans facteur de virulence particulier. Cet événement viendrait alors pérenniser une situation de déséquilibre hôte-microbiote et pourrait également contribuer aux dommages tissulaires, du fait de la toxicité de ces formes particulières de fer [4].

Cet article a été publié dans *Scientific Reports* le 19 octobre 2018. Il est disponible en accès ouvert sur le site de l'éditeur (<https://www.nature.com/articles/s41598-018-33813-0>) et dans les archives HAL (<https://hal.archives-ouvertes.fr/hal-01903064>).

4. Sa concentration est évaluée à 1 à 3 $\mu\text{mol.L}^{-1}$ dans les dosages plasmatiques [3]

SCIENTIFIC REPORTS

OPEN

Increased transferrin saturation is associated with subgingival microbiota dysbiosis and severe periodontitis in genetic haemochromatosis

Emile Boyer^{1,2}, Sandrine Le Gall-David¹, Bénédicte Martin¹, Shao Bing Fong¹, Olivier Loréal¹, Yves Deugnier^{3,4}, Martine Bonnaure-Mallet^{1,2} & Vincent Meuric^{1,2}

Genetic haemochromatosis (GH) is responsible for iron overload. Increased transferrin saturation (TSAT) has been associated with severe periodontitis, which is a chronic inflammatory disease affecting tissues surrounding the teeth and is related to dysbiosis of the subgingival microbiota. Because iron is essential for bacterial pathogens, alterations in iron homeostasis can drive dysbiosis. To unravel the relationships between serum iron biomarkers and the subgingival microbiota, we analysed samples from 66 GH patients. The co-occurrence analysis of the microbiota showed very different patterns according to TSAT. Healthy and periopathogenic bacterial clusters were found to compete in patients with normal TSAT ($\leq 45\%$). However, significant correlations were found between TSAT and the proportions of *Porphyromonas* and *Treponema*, which are two genera that contain well-known periopathogenic species. In patients with high TSAT, the bacterial clusters exhibited no mutual exclusion. Increased iron bioavailability worsened periodontitis and promoted periopathogenic bacteria, such as *Treponema*. The radical changes in host-bacteria relationships and bacterial co-occurrence patterns according to the TSAT level also suggested a shift in the bacterial iron supply from transferrin to NTBI when TSAT exceeded 45%. Taken together, these results indicate that iron bioavailability in biological fluids is part of the equilibrium between the host and its microbiota.

Periodontitis is a chronic inflammatory disease that affects tissues surrounding the teeth. It is strongly associated with the major pathogenic “red complex”, including *Porphyromonas gingivalis*, *Tannerella forsythia* and *Treponema denticola*¹ and thus is considered an infection. Recent advances in the pathogenesis of periodontal disease have suggested that polymicrobial synergy and microbiota dysbiosis together with a dysregulated immune response can induce inflammation-mediated damage in periodontal tissues^{2–4}. Interestingly, currently periodontitis is associated with a growing number of systemic diseases, including cardiovascular diseases, adverse pregnancy outcomes, diabetes^{5–7} and hereditary haemochromatosis⁸.

Genetic haemochromatosis (GH), which is related to the HFE gene p.Cys282Tyr mutation, is the most common form of inherited iron overload disease in European population descendants^{9,10}. In plasma, iron is associated with transferrin to increase its bioavailability for cells. Transferrin saturation (TSAT) is the ratio between the total number of iron-binding sites on patient plasma transferrin and the number of binding sites occupied by iron. Normally, TSAT ranges between 20% and 45%. Systemic iron metabolism is controlled by hepcidin, whose expression level is adapted to TSAT to regulate the plasma iron levels. Due to an alteration in the HFE-linked transduction signalling pathway, GH is characterized by a hepcidin-deficiency state. The resulting iron egress from macrophages and enterocytes leads to an increased TSAT level. When TSAT exceeds 45%, non-transferrin-bound iron (NTBI), which is an abnormal biochemical form of iron, occurs in the plasma. NTBI consists mostly of iron

¹Univ Rennes, INSERM, INRA, CHU Rennes, Institut NuMeCan (Nutrition, Metabolism and Cancer), Rennes, F-35000, France. ²CHU de Rennes, Service d’Odontologie, Rennes, 35033, France. ³CHU de Rennes, Service des Maladies du Foie, Rennes, 35033, France. ⁴CIC 1414, Inserm, Rennes, 35033, France. Correspondence and requests for materials should be addressed to E.B. (email: emile.boyer@univ-rennes1.fr)

Measures of periodontitis	Transferrin saturation		p-value
	Normal ($\leq 45\%$) (n = 21)	High ($> 45\%$) (n = 45)	
Degree of periodontitis (severe)	7 (33.3)	31 (68.9)	0.006^a
<i>CAL measures</i>			
Proportion of sites/mouth CAL ≥ 3 mm (%)	42.03 (3.66)	55.41 (2.39)	<0.001^b
Proportion of sites/mouth CAL ≥ 5 mm (%)	8.36 (2.28)	13.01 (2.05)	0.016^b
Mean CAL (mm)	2.63 (0.13)	2.99 (0.11)	0.006^b
<i>PPD measures</i>			
Proportion of sites/mouth PPD ≥ 4 mm (%)	10.19 (1.40)	14.90 (1.69)	0.184 ^b
Proportion of sites/mouth PPD ≥ 6 mm (%)	0.92 (0.32)	1.15 (0.30)	0.676 ^b
Mean PPD (mm)	2.22 (0.06)	2.40 (0.06)	0.152 ^b

Table 1. Periodontitis measures of patients in accordance with their TSAT levels. CAL, clinical attachment loss; PPD, pocket probing depth. The degree of periodontitis is presented as numbers (percentages). The CAL and PPD measures are presented as percentages (standard errors (SE)) or means (SE). Bold p-values indicate significant ^a χ^2 or ^bMann-Whitney tests.

associated with citrate or ADP and is involved in oxidative stress through reactive oxygen species generation^{11–13}. NTBI especially targets the liver and heart, which explains why the classical form of GH is responsible for hepatic cirrhosis and diabetes¹⁴. However, currently most GH patients are asymptomatic or present with chronic fatigue, abnormal serum transaminase levels, rheumatism and osteoporosis^{15,16} in the absence of cirrhosis and diabetes. To avoid iron toxicity, cells synthesize ferritin to store excess iron. Consequently, the plasma ferritin levels reflect the tissue iron stores. Standard treatment is based on phlebotomy therapy to first clear out and then avoid reconstitution of iron excess. The primary international guidelines advise that the serum ferritin levels should be lower than 50 $\mu\text{g/L}$ as the gold standard for both initial treatment and maintenance therapy^{17–20}.

In a previous study, we investigated the periodontal statuses of GH patients. Unexpectedly, we found that all of the patients had periodontitis. Furthermore, we observed a significant link between the periodontitis severity and increased TSAT; patients with a TSAT level greater than 45% had a five times greater risk of severe periodontitis⁸. Iron overload may strongly impact bacterial behaviour²¹. Indeed, iron is an essential growth factor and can act as a virulence factor for *P. gingivalis*, which is considered one of the major keystone pathogens driving dysbiosis in periodontitis^{2,22}. In addition, excess iron in the sera has been reported to decrease serum antibacterial activity in GH patients²³. Furthermore, alteration of the gut microbiota has been reported in *Hfe*^{-/-} mice, with the gut microbiota of the *Hfe*^{-/-} mice significantly distinct from that of the wild-type mice. The authors suggested that genetic modification of iron metabolism could influence the composition of potentially probiotic bacterial species²⁴.

Therefore, we hypothesized that the alteration of iron metabolism induced by the HFE C282Y gene mutation could modify and drive the subgingival microbiota towards dysbiosis, which could participate in the periodontitis severity. The aim of this study was to investigate a putative association between the subgingival microbiota and serum iron biomarkers in GH patients from our previous study.

Results

At the time of the dental examination, 21 patients had normal TSAT ($\leq 45\%$) and 45 patients had high TSAT ($> 45\%$). Among the 45 patients with high TSAT, 19 had serum ferritin levels $\leq 50 \mu\text{g/L}$ and 26 had serum ferritin levels $> 50 \mu\text{g/L}$. As shown in Table 1, 33.3% of the patients with normal TSAT presented severe periodontitis versus 68.9% of those with high TSAT (χ^2 , $p = 0.006$). A significant increase in all clinical attachment loss (CAL) measures was observed in the patients with high TSAT. Although not significant, we observed a trend towards increased pocket probing depth (PPD) measures in patients with high TSAT. Moreover, no significant differences in demographic data were found between the patients with normal and high TSAT (Supplementary Table S1).

In the high TSAT patients, no difference in the periodontitis severity was observed according to the serum ferritin levels: 68.4% versus 69.2% presented severe periodontitis (χ^2 , $p = 0.954$). Moreover, no significant difference was found in the PPD or CAL measures according to the serum ferritin levels (see Supplementary Table S2). Therefore, the rest of the study centred on the groups with normal and high TSAT levels.

Alpha and beta diversity analyses showed no clustering according to TSAT. We explored the community structures of the subgingival microbiotas between the TSAT groups using *alpha* and *beta* diversity metrics. The rarefaction curves shown in Fig. 1A reached approximately 60 genus level taxa with 15,000 sampled sequences with no differences between the TSAT groups. No difference was found in the species richness (Sobs) or Shannon-Weaver diversity index according to the TSAT level (Fig. 1B,C). The *beta* diversity analysis did not show any patient clustering according to the TSAT level using the Bray-Curtis (PERMANOVA, $p = 0.141$) (Fig. 2A,B) and weighted UniFrac metrics (PERMANOVA, $p = 0.153$) (Fig. 2C,D).

Differences in the relative abundances of specific taxa according to the TSAT level. We used the linear discriminant analysis with effect size (LEfSe) algorithm to investigate the impact of the TSAT level on

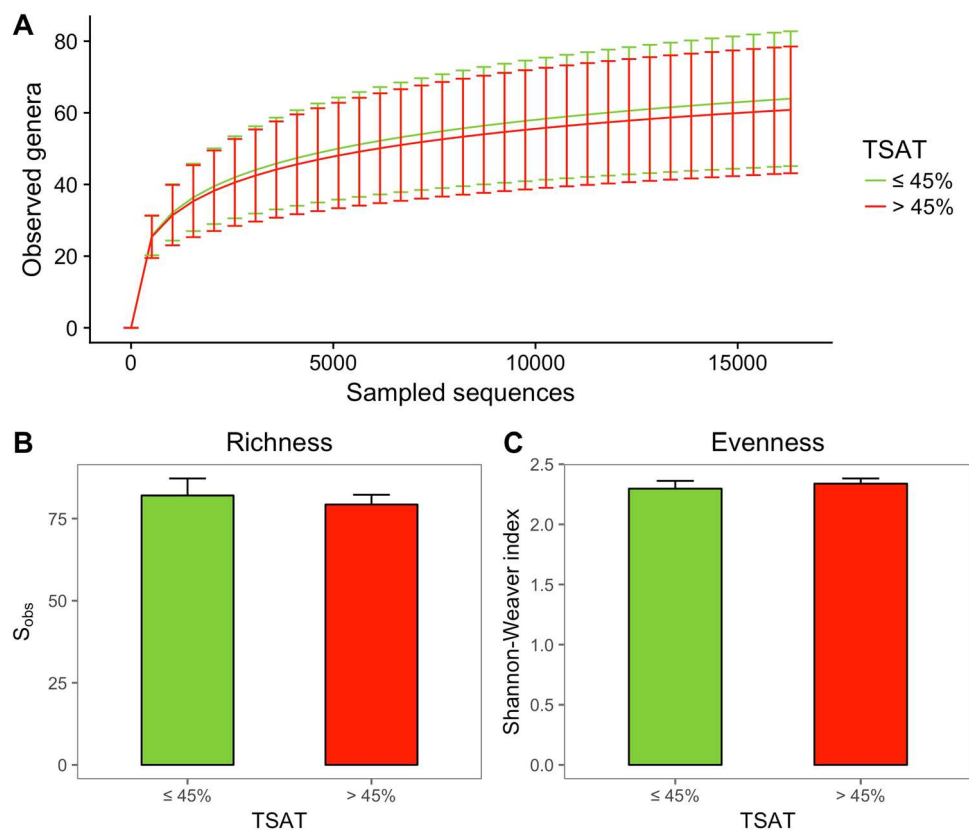


Figure 1. Alpha diversity analysis of subgingival microbiota samples. (A) Rarefaction curves. The data are presented as the mean \pm standard deviation. (B) Richness index S_{obs} . The data are presented as the mean \pm standard error. (C) Shannon-Weaver evenness index. The data are presented as the mean \pm standard error. The results are presented according to the study groups: normal transferrin saturation (TSAT) ($\leq 45\%$; $n = 21$) and high TSAT ($> 45\%$; $n = 45$). Alpha diversity metrics were calculated after subsampling to obtain equal numbers of sequences per library. Mann-Whitney and Student's t test returned no significant differences in alpha diversity measures between the normal and high TSAT samples ($p > 0.05$).

the subgingival bacterial composition. In patients with normal TSAT, *Streptococcus constellatus*, *Campylobacter lari*, *Atopobium vaginae*, *Treponema zuelzaruae* and *Porphyromonas somerae* were found with significantly elevated proportions in the subgingival microbiota (Fig. 3). *S. constellatus* had the strongest linear discriminant analysis (LDA) score.

In patients with high TSAT, the *Desulfobulbus* genus and all taxonomic levels to which it belonged showed increased relative levels and the strongest LDA scores; the unclassified *Desulfobulbus* sp. were also increased. Family *Peptostreptococcaceae* [XI] and the species *Prevotella marshii*, *Treponema medium*, *Neisseria bacilliformis*, *Streptococcus mutans* and *Treponema lecithinolyticum* were also increased in patients with high TSAT. The average relative abundances of taxa with LDA scores $< |3|$ were low ($< 0.24\%$ of the microbiota).

Co-occurrence network analysis identified distinct bacterial patterns according to the TSAT level.

Co-occurrence tests were performed to investigate interactions among the subgingival core microbiota at the genus level and their relationships with the TSAT and serum ferritin levels. Two co-occurrence network analyses between normal and high TSAT patients were constructed with genera that had prevalence rates of 50% and 70% in the samples. Similar co-occurrence patterns were found within the high and normal TSAT networks with prevalence rates between 50% and 70%. The co-occurrence patterns with a bacterial prevalence rate of 70% are presented in Fig. 4. Thirty-four genera were shared by both patterns. Three genera were found specifically in the pattern from patients with normal TSAT (*Bhargavaea*, *Escherichia-Shigella* and *Pseudoalteromonas*). In the samples from patients with normal TSAT, the major genera were *Fusobacterium* (relative abundance = 24.17%), *Prevotella* (12.20%), *Sphingomonas* (6.89%), *Porphyromonas* (6.26%) and *Streptococcus* (6.13%). In the samples from the high TSAT patients, *Fusobacterium* (25.40%), *Prevotella* (12.06%), *Porphyromonas* (7.32%), *Treponema* (6.85%), *Tannerella* (6.31%) and *Streptococcus* (6.15%) were predominant.

In the normal TSAT group (Fig. 4A), the network showed two distinct bacterial clusters. In each cluster, genera were positively and strongly associated with each other (green edges). A clear mutual exclusion was observed between the two clusters (red edges). Classic and putative periopathogens, including *Porphyromonas*, *Treponema*, *Tannerella* and *Filifactor*, were located in cluster 1, whereas frequently health-associated genera, such as *Rothia* and *Corynebacterium*, were located in cluster 2. Moreover, *Porphyromonas* and *Treponema* presented a positive

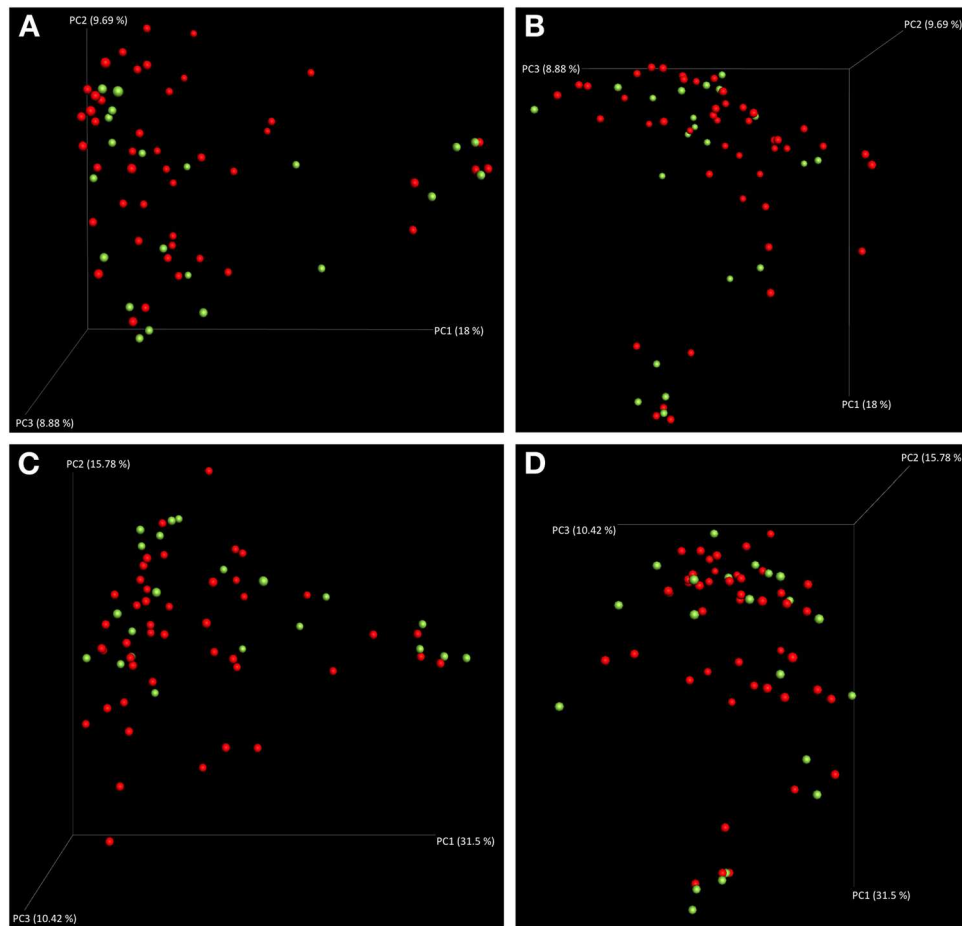


Figure 2. Beta diversity analysis illustrating the community structure of the subgingival microbiota. (A,B) Different views of the 3D PCoA plots calculated with Bray-Curtis metrics. (C,D) Different views of the 3D PCoA plots calculated with weighted UniFrac metrics. Green, TSAT \leq 45%; red, TSAT $>$ 45%.

correlation with TSAT as a continuous variable with three significant similarity measures. The serum ferritin levels were positively linked with *Corynebacterium*.

The high TSAT network (Fig. 4B) had less numerous co-occurrences and very few mutual exclusions (64 edges versus 144 in the normal TSAT group). Genera still gathered in clusters, but no opposition was found. Cluster 1 contained genera usually described in periodontitis, including *Porphyromonas*, *Treponema*, *Tannerella* and *Filifactor*. The TSAT level was positively associated with *Catonella* and *Mogibacterium* but with a lower strength, since only the Bray-Curtis dissimilarity returned significant co-occurrences. Similarity measures returned no association between the serum ferritin levels and the subgingival core microbiota, which explained why ferritin did not appear in the high TSAT network.

Correlation matrices identified different relationships between the subgingival microbiota and clinical parameters.

Associations between bacteria and bioclinical data for both GH and periodontitis were evaluated using Spearman's correlation matrices. Plots were computed with genera identified in the co-occurrence patterns, TSAT and serum ferritin, and extent/severity measures of periodontitis (Figs 5 and 6).

In patients with normal TSAT, the inter-bacterial correlations showed two clusters (green squares in Fig. 5A). As shown in the co-occurrence bacterial network (Fig. 4A), we observed positive correlations within each cluster and negative correlations between the two clusters.

For the serum iron biomarkers, correlations at the genus level were confirmed between *Porphyromonas* (6.26%) and *Treponema* (3.86%) with the TSAT level ($r = 0.52$ and $r = 0.54$, respectively; $p < 0.05$). At the species level, *Porphyromonas endodontalis* (2.53%), *Treponema sp.* (1.87%) and *T. forsythia* (3.20%) were correlated with the TSAT level ($r = 0.48$, $r = 0.50$ and $r = 0.44$, respectively; $p < 0.05$), as shown in Fig. 5B–D. No significant association was found between the serum ferritin levels and bacteria. For the periodontitis measures, at the genus level *Aggregatibacter* (0.58%), *Campylobacter* (3.17%), *Capnocytophaga* (2.39%) and *Cardiobacterium* (0.51%) presented significant negative correlations with the PPD measures. *Capnocytophaga* and *Cardiobacterium* also presented significant negative correlations with the CAL measures (Fig. 5A).

In patients with high TSAT, very few negative correlations were found between the bacterial clusters (green squares in Fig. 6A), as observed in the co-occurrence bacterial network (Fig. 4B).

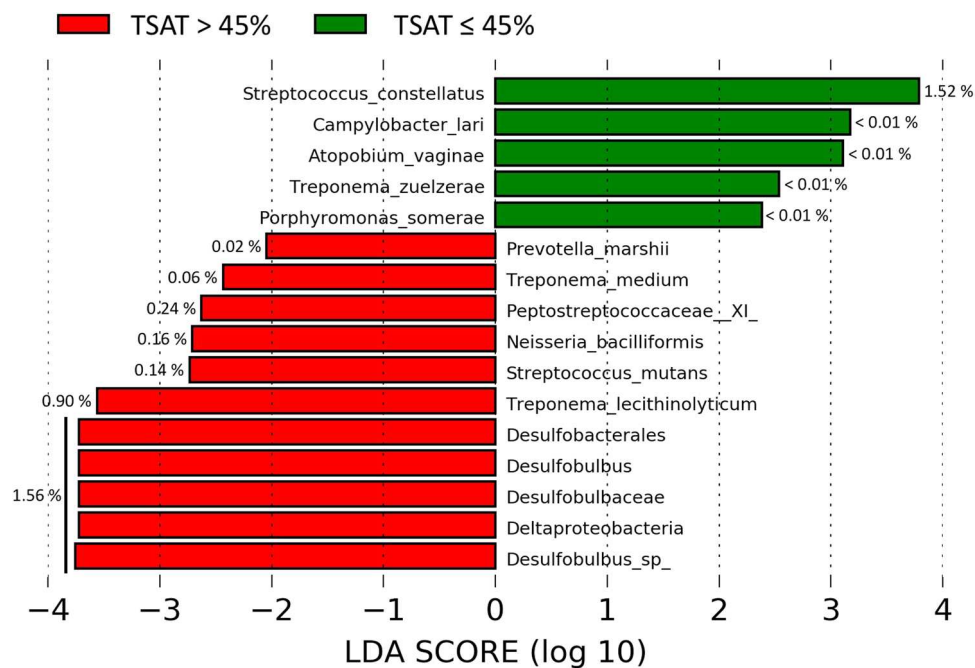


Figure 3. Analysis of taxa relative abundances according to the TSAT level. Taxa showing significant differences in the LEfSe analysis. The percentages are the average relative abundances of the corresponding taxa in the related TSAT group.

With respect to serum iron biomarkers, at the genus level, the TSAT level was positively associated with *Kingella* (0.52%) and negatively associated with *Tannerella* (6.31%) and *Treponema* (6.85%) ($r = 0.46$, $r = -0.51$ and $r = -0.32$, respectively; $p < 0.01$) (Fig. 6A). At the species level, *Campylobacter sp.* (0.93%), *Prevotella sp.* (2.48%) and *T. forsythia* (5.52%) were significantly associated with the TSAT level ($r = 0.33$, $r = 0.31$ and $r = -0.46$, respectively; $p < 0.05$). The serum ferritin levels were significantly correlated with *Aggregatibacter* (0.94%), *Campylobacter* (4.56%), *Capnocytophaga* (1.35%), *Kingella* (0.52%), *Leptotrichia* (1.49%) and *Streptococcus* (6.15%) ($r = 0.31$, $r = 0.39$, $r = 0.41$, $r = 0.31$, $r = 0.34$ and $r = 0.41$, respectively; $p < 0.05$) (Fig. 6A). At the species level, *Campylobacter sp.* (0.93%), *Leptotrichia sp.* (0.61%), *Prevotella denticola* (0.99%), *Prevotella intermedia* (0.97%), *Prevotella melaninogenica* (0.55%), *Streptococcus anginosus* (0.68%) and *Streptococcus gordonii* (0.91%) were associated with ferritin ($r = 0.31$ to $r = 0.37$, $p < 0.05$). Periodontitis measures were positively associated at the genus level with *Eubacterium* (1.58%) and *Desulfobulbus* (1.56%) and negatively associated with *Campylobacter* (4.56%), *Capnocytophaga* (1.35%), *Gemella* (0.62%), *Kingella* (0.52%) and *Neisseria* (2.04%) (Fig. 6A). These genera were low-abundant taxa except for *Campylobacter*. The highly abundant (7.32%) and prevalent (detected in 97.8% of patients with high TSAT) *Porphyromonas* genus was significantly correlated with all periodontitis measures. The two highest coefficients were obtained for the proportion of sites with CAL ≥ 5 mm ($r = 0.51$, $p < 0.001$) and the proportion of sites with PPD ≥ 4 mm ($r = 0.44$, $p = 0.002$). Significant correlations were also found between the proportion of sites with PPD ≥ 4 mm and *Treponema* and *Tannerella* ($r = 0.33$ and $r = 0.36$, respectively; $p < 0.05$). At the species level, *P. gingivalis* (3.08%), *P. endodontalis* 3.30%) and *Treponema sp.* (3.61%) were significantly correlated with the mean PPD ($r = 0.43$, $r = 0.35$ and $r = 0.40$, respectively; $p < 0.05$) (Fig. 6B–D) and the proportion of sites with PPD ≥ 4 mm ($r = 0.50$, $r = 0.31$ and $r = 0.41$, respectively; $p < 0.05$) (Fig. 6E–G).

Discussion

Periodontitis is associated with an inflammatory process related to modifications of the subgingival biofilm⁴. In normal subjects, inflammation leads to iron sequestration within macrophages, which deprives bacteria of iron²⁵. In GH patients with abnormally high TSAT, iron bioavailability is increased in biological fluids, including those of the oral cavity, resulting in an increased risk of severe periodontitis⁸. Additionally, evidence of the presence of iron deposits in oral tissues of haemochromatosis patients can be found in the literature^{26–30}. Currently, most patients with haemochromatosis are pauci-symptomatic, and the skin and mucosal pigmentation related to iron deposits has become exceptional. However, the presence of asymptomatic iron deposits in oral tissues cannot be excluded.

In the present study, 66 GH patients were sampled to analyse their subgingival microbiotas. As expected, an increased risk of severe periodontitis was observed in patients with a TSAT level $>45\%$ together with a significant increase in CAL measures and higher but not significant PPD measures (Table 1). In contrast, no differences in the periodontal status were observed in relation to the serum ferritin level, which could be explained by the physiological role of both markers. Indeed, TSAT provides an insight into iron bioavailability in the plasma, whereas

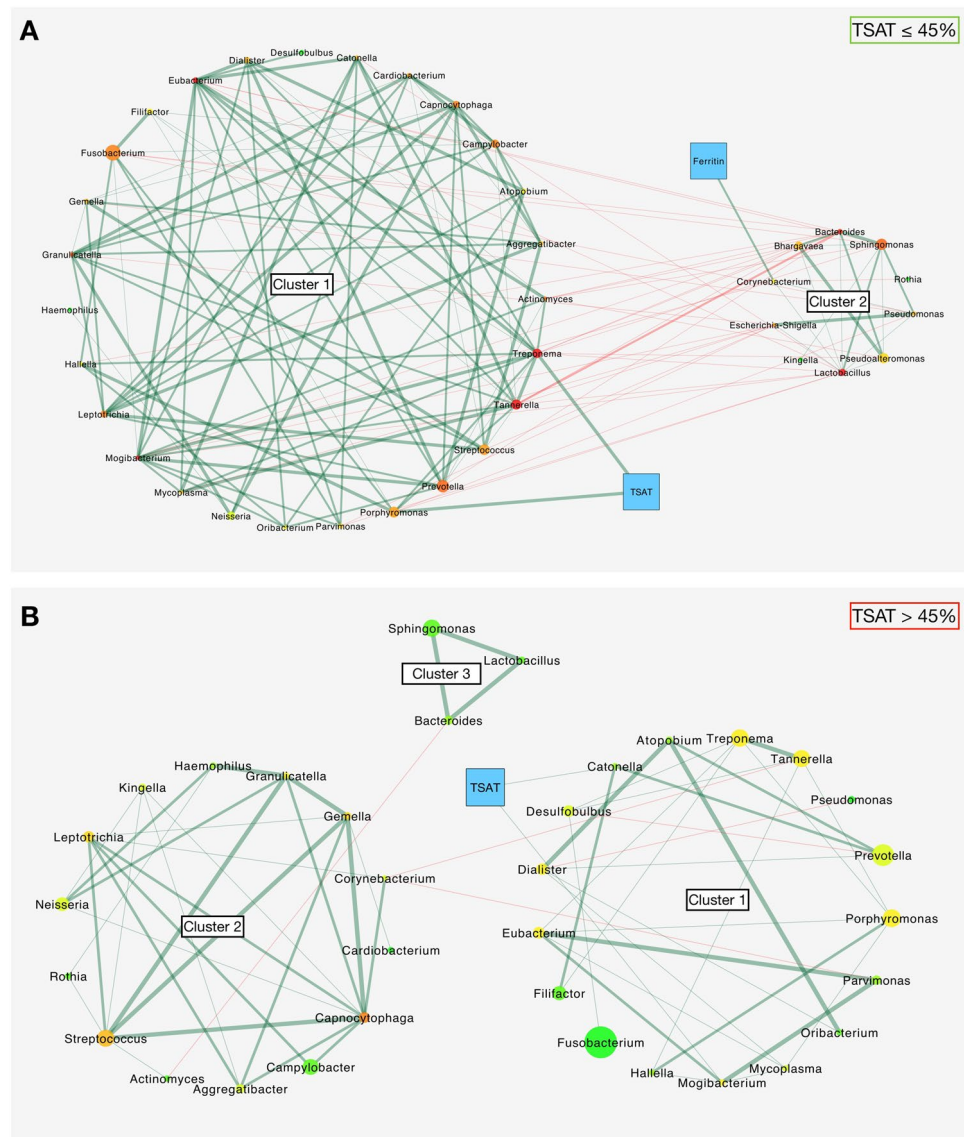


Figure 4. Bacterial co-occurrence patterns with serum iron biomarkers according to the TSAT level. **(A)** Co-occurrence patterns of genera present in at least 70% of patients with normal TSAT ($n = 21$); a total of 37 bacterial nodes, TSAT, ferritin and 144 edges are represented. **(B)** Co-occurrence patterns of genera present in at least 70% of patients with high TSAT ($n = 45$); a total of 34 bacterial nodes, TSAT and 64 edges are represented. The edges represent 1 (thin line) or 2 or 3 (thick line) significant co-occurrence tests between nodes (green, positive; red, negative). The bacterial node colours represent the number of partners ranging from 1 (light green) to 11 (red); the serum iron biomarkers are shown in blue. The bacterial node sizes represent the mean relative abundance of each taxon.

serum ferritin quantifies the total body iron stores. Notably, increased TSAT is associated with the occurrence of NTBI, which is considered a main factor of both iron accumulation and iron-related organ damage in GH^{11–13}. Therefore, TSAT was considered the only relevant iron-related biomarker in the present study.

First, the *alpha* and *beta* diversity analyses did not show any significant differences between patients with normal and high TSAT regardless of the metric used. This result could be explained by the fact that the samples had similar origins; the sampling site and host disease status were the same for all samples (subgingival and periodontitis/GH, respectively). As noted in a previous meta-analysis, *beta* diversity allows clustering of samples from different sampling sites and to a lesser extent from opposite conditions (i.e., healthy versus periodontitis)³¹. Despite sharing a high degree of similarity at the community level, significant differences were detected when relative abundance comparisons were conducted between the normal and high TSAT groups using the LefSe algorithm. *S. constellatus*, which was more abundant in patients with normal TSAT, has been isolated from a wide range of sites and infections and is considered a commensal component of the oral microbiota³², although it is part of the orange complex according to the Socransky classification¹. In patients with high TSAT, the increased taxa with major LDA scores were *Desulfobulbus* and *Desulfobulbus sp.* Although not known as a periopathogen, this genus

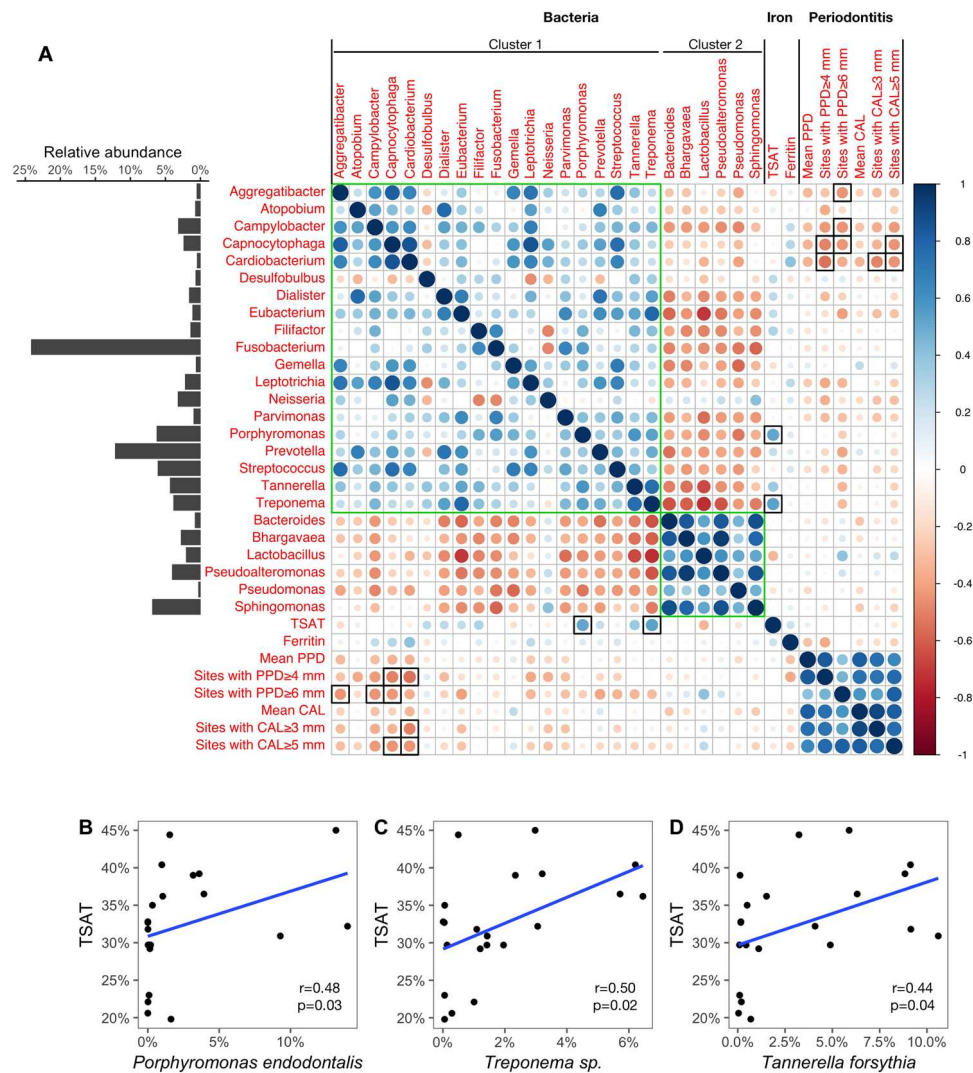


Figure 5. Correlations between microbiota and clinical parameters in patients with normal TSAT ($\leq 45\%$). **(A)** Correlation matrix among genera found in the co-occurrence network of patients with normal TSAT, serum iron biomarkers and periodontitis measures computed with Spearman's test. Genera from the co-occurrence network that had an average relative abundance $\geq 0.5\%$ were used to generate the correlation matrix. Green squares indicate clusters identified in the co-occurrence network. Black squares indicate significant Spearman's correlations between genera and clinical parameters ($p < 0.05$). The average relative abundances of genera are presented in the bar chart on the left side of the matrix. Spearman's coefficient values are depicted using the colour gradient scale. **(B–D)** Scatterplots of significant correlations between species level taxa and TSAT. Blue lines plot the linear regression slopes.

deserves more attention; for instance, Camelo-Castillo *et al.* showed an association between *Desulfobulbus* and the periodontitis severity^{33,34}. The increased taxa also included *T. lecithinolyticum*, which was associated with periodontitis^{35,36} and was detected in endodontic lesions³⁷. Because the periodontal status is led by TSAT⁸, the results from the LEfSe analysis can also reflect the periodontal disease severity. Consequently, we investigated the structures of the microbial communities and their relationships with serum iron biomarkers according to the host iron bioavailability status.

Co-occurrence network comparisons between patients with normal and high TSAT were initially realized at bacterial prevalence rates of 50% (corresponding to the minimal fraction required to compute the core microbiome in the QIIME pipeline) and 70%. In both the normal and high TSAT patients, very similar patterns were found regardless of the prevalence cut-offs used. The number of genera was reduced in the 70% bacterial prevalence patterns, but this discrepancy concerned only low abundance genera, and the 70% cut-off was chosen for network representation. Most of the represented genera, including the main potential periopathogens, were present in the patterns of both the normal and high TSAT patients. This observation remained consistent with the findings of the core microbiota analyses, since all samples originated from patients with similar conditions and from similar sampling sites (i.e., subgingival samples from periodontitis patients). However, the inter-relationships between the different bacterial clusters and the serum iron biomarkers differed according to

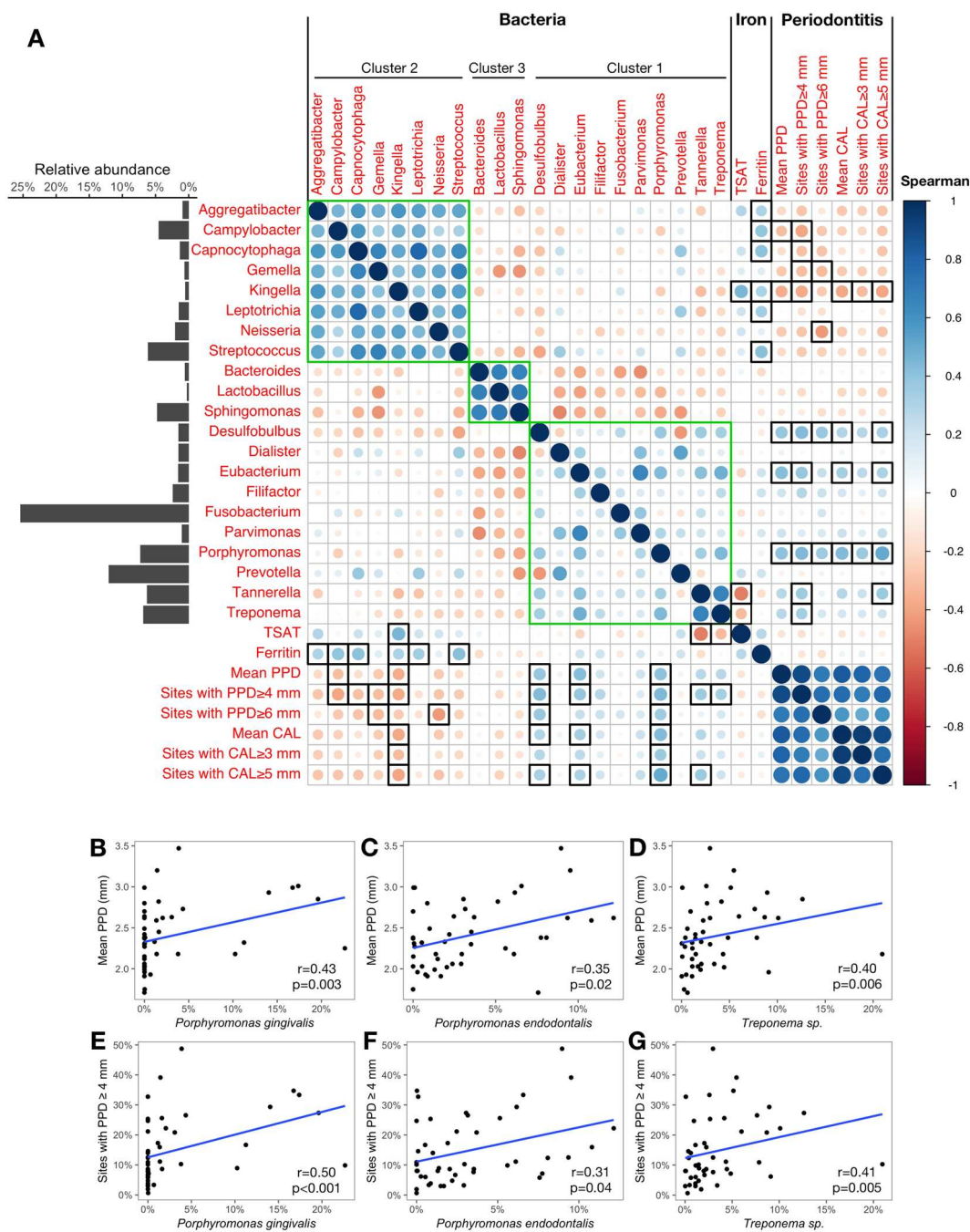


Figure 6. Correlations between microbiota and clinical parameters in patients with high TSAT (>45%). (A) Correlation matrix among genera found in the co-occurrence network of patients with high TSAT, serum iron biomarkers and periodontitis measures computed with Spearman’s test. Genera from the co-occurrence network that had an average relative abundance $\geq 0.5\%$ were used to generate the correlation matrix. Green squares indicate clusters identified in the co-occurrence network. Black squares indicate significant Spearman’s correlations between genera and clinical parameters ($p < 0.05$). The average relative abundances of genera are presented in the bar chart on the left side of the matrix. Spearman’s coefficient values are depicted using the colour gradient scale. (B–G) Scatterplots of significant correlations between species level taxa and periodontitis measures. Blue lines plot the linear regression slopes.

the TSAT level (Fig. 4). Therefore, the co-occurrence network analysis indicated a shift in bacterial dynamics when the TSAT exceeded 45%, suggesting a change in host-microbiota dynamics when the iron bioavailability was increased.

In patients with normal TSAT, two bacterial clusters were found to compete. Cluster 1 included *Porphyromonas* and *Treponema*, which are well known to contain periopathogenic species¹, whereas cluster 2 included genera implicated in periodontal health, such as *Rothia* and *Corynebacterium*^{38,39}. Moreover, all association measures

revealed significant although moderate positive relationships between the relative proportions of *Porphyromonas* and *Treponema* and the TSAT level in both the co-occurrence network and the correlation matrix (Figs 4A and 5A). In addition, the relative abundances of *P. endodontalis* and *T. forsythia*, which are two species also described as periopathogenic⁴⁰, as well as *Treponema sp.* were the only species associated with the TSAT level.

In patients with high TSAT, the co-occurrence pattern was characterized by a lack of mutual exclusion between clusters and presented less numerous relationships than that of the normal TSAT patients. Neither the TSAT nor the serum ferritin level showed correlations with any genera, since only the Bray-Curtis dissimilarity returned significant results. This finding may raise questions concerning the significance of the correlations found in the matrix between the serum iron biomarkers and several genera. The correlation matrix showed that the clusters seemed to have an opposite impact on periodontal disease. Genera that contained major and putative periopathogens species, such as *Porphyromonas*, *Tannerella*, *Treponema*, *Prevotella*, *Eubacterium*, *Desulfobulbus* and *Filifactor*^{1,33,41}, constituted cluster 1 and were positively associated with periodontitis measurements. This result is in accordance with previous studies on the subgingival microbiota in periodontitis patients^{31,42,43} and suggests the presence of a disease-associated dysbiotic microbiota in patients with high TSAT. Conversely, taxa from cluster 2 were negatively associated with the periodontitis measures.

Transferrin is a major player in iron homeostasis⁴⁴. Below 45% saturation, transferrin allows adequate iron delivery to cells. However, bacteria can also access this primary source of bioavailable iron in the host. Indeed, Goulet *et al.* detected the presence of transferrin fragments in subgingival samples from patients with periodontitis, suggesting bacterial or host-related degradation⁴⁵. In addition, an increase in the transferrin concentration in the gingival crevicular fluid was observed in patients with periodontitis⁴⁶. The significant correlations between *Porphyromonas*, *Treponema*, and TSAT in patients with TSAT \leq 45% support previous studies showing the ability of *Porphyromonas* and *Treponema* species to acquire iron from transferrin^{45,47–52}. Moreover, iron provided by *Porphyromonas* through transferrin degradation by gingipains⁴⁹ could supply the biofilm and other periopathogens with iron. Similar nutritional cooperation has been observed between *Treponema* species and *P. gingivalis*⁵³. These associations between *Porphyromonas*, *Treponema* and TSAT could explain the occurrence of periodontitis in all of these patients.

Increased TSAT $>$ 45% can lead to the formation of abnormal forms of iron in the plasma, such as NTBI, which is considered the key factor of iron toxicity and organ damage in GH¹¹. NTBI is a highly bioavailable form of iron, and its uptake by bacteria can benefit the entire microbial community, as suggested by a bacterial co-occurrence network with no mutual exclusion. These data could explain the severity of the periodontitis observed in these patients.

As a whole, this study supports the association between the iron burden, especially elevated transferrin saturation, and the periodontitis severity⁸. Elevation of circulating transferrin-bound iron could facilitate dysbiosis through favouring keystone pathogens, such as *Porphyromonas* and *Treponema*⁵⁴. Once TSAT is high and NTBI occurs, iron acquisition is no longer a challenge. The whole dysbiotic microbiota of these patients is in favour of severe periodontitis, and correlations between periodontal measures and classical periopathogens have been found.

The limitations of this study include its relatively small sample size, although clinical GH related to C282Y homozygosity remains a rare disease⁵⁵. In addition, this study is a case series with no control group available to compare the microbiota of non-GH iron-overloaded patients with normal and high TSAT. Whether the TSAT increase itself or the presence of NTBI in the gingival crevicular fluid plays a role in the occurrence of dysbiosis should be explored. In the gingival sulcus or pocket formed by periodontitis, bacteria are constantly bathed in the gingival crevicular fluid formed by the serum exudate or blood during inflammatory periods. Therefore, iron overload related to GH and variations in TSAT are probably locally reflected in the ecological niche inhabited by the subgingival microbiota.

Moreover, NTBI and labile plasma iron – its highly reactive component – contribute to the production of reactive oxygen species through the Fenton reaction^{12,56}. This reaction may take place in the liver, pancreas, bones and heart and participates in the lesions observed in GH⁵⁷. As indicated earlier, mucosal pigmentation in the oral cavity similar to that observed on the skin has also been reported in GH patients, suggesting a local impact of the disease²⁶. Cellular NTBI-related toxicity in oral tissues cannot be excluded and may participate in an inflammatory state beneficial to periopathogens³ and to a dysbiotic community. Regardless of whether it acts directly by providing iron to bacteria, indirectly via its pro-inflammatory effect or through both mechanisms, future studies should include measurement of NTBI in the serum and gingival crevicular fluid.

In addition, we cannot rule out the impact of a lower iron content in macrophages from GH patients due to hepcidin deficiency. Ferroportin (the cellular iron exporter protein regulated by hepcidin) is overexpressed on macrophage membranes and thus favours an iron-poor phenotype⁵⁸. This macrophage phenotype may alter its innate immunity function and contribute to microbiota dysbiosis. However, the concomitant inflammatory process localized in periodontal tissues could modify this picture. Finally, hepcidin is reported to have direct though small antibacterial activity⁵⁹, and we cannot exclude that a low hepcidin level may directly modulate the oral microbiota.

In this study, we explored associations between the subgingival microbiota, periodontal status and serum iron biomarkers in GH patients with periodontitis. We showed changes in the periodontal status and microbial dynamics according to iron bioavailability as reflected by TSAT. Our data demonstrate that increased TSAT is associated with oral dysbiosis characterized by elevated proportions of periopathogens, which may participate in periodontitis severity. This result and the finding of significant correlations between periopathogenic bacteria and the TSAT level in patients with normal TSAT may suggest a shift in the bacterial iron supply from transferrin to NTBI when NTBI occurs. Taken together, these results indicate that iron bioavailability more than the total body iron stores is part of the equilibrium between the host and its microbiota.

Methods

Participants. The participants corresponded to a sub-cohort of the 84 GH patients previously studied by Meuric *et al.*⁸. The demographic data (age, gender ratio, body mass index, smoking habits and frequency of dental visits) of this sub-cohort can be found in Supplementary Table S1. This case series study was approved by the local ethics committee (CPP Ouest V - 10/02-744). The informed consent for study participation has been obtained from all patients and all research was performed in accordance with relevant guidelines and regulations. These subjects were recruited in the Hepatology Department of the University Hospital of Rennes based on C282Y homozygosity and benefited from a full-mouth periodontal examination, including PPD, CAL, gingival bleeding index, gingival index, plaque score and evaluation of periodontitis severity according to the case definitions from the Centers for Disease Control and Prevention and the American Association of Periodontology⁶⁰. The exclusion criteria were pregnancy, presence of another systemic disease, periodontal therapy within the last 12 months and treatment with either systemic antibiotics or drugs known to cause gingival hyperplasia within the last 3 months. Two biomarkers of iron metabolism (the serum ferritin and TSAT levels) were collected at the time of the dental examination together with the clinical data. The 66 patients for whom frozen gingival fluid was available were the sample participants of the present study.

Sample Collection. For each subject, sterile endodontic paper points (Henry Schein, France) were inserted into the deepest periodontal pocket for 30 seconds after supra-gingival plaque removal. The material was transferred to a sterile tube with 100 μ L of sterile distilled water and kept at 4 °C overnight before DNA extraction.

DNA extraction and sequencing. DNA extraction from the supernatants was performed using the QIAamp DNA Mini Kit (Qiagen, France) according to the manufacturer's recommendations. The DNA was kept frozen at -80 °C prior to amplification. The V3-V4 regions of the 16S rRNA gene were amplified with the primers 338F (5'-ACTCCTACGGGAGGCAGCAG-3')⁶¹ and 802R (5'-TACN VGGGTATCTAATCC-3')⁶² using 25 amplification cycles with an annealing temperature of 45 °C. The PCR products were sequenced with the Illumina MiSeq at the Get-PlaGe facility (Toulouse, France)³¹.

Microbiological analysis. Taxonomy at the genus level was assigned using the "Visualization and Analysis of Microbial Population Structures" (VAMPS) analysis pipeline web tool⁶³. Default parameters were used for assignment at the genus level with the "Ribosomal Database Project" (RDP release 11) classification⁶⁴. Through the VAMPS process, the best taxonomic hit was assigned for each read. Reads identified as Archaea, Eukarya, Organelle and unknown were excluded from the analysis. *Alpha* rarefaction and diversity were evaluated using the Observed Species metric (Sobs) and the Shannon-Weaver index⁶⁵. *Beta* diversity was calculated using Bray-Curtis⁶⁶ and UniFrac distances⁶⁷. Genera were removed if their relative abundances did not reach 1% in at least one sample or if their mean relative abundances did not reach 0.5% in at least one group (normal or high TSAT) to avoid significant statistical changes with no biological relevance. Genera that had significant differences in presence/relative abundance between healthy and periodontitis subjects in previous studies^{33,68-70} were marked as genera of interest for a species-level taxonomic assignment. This assignment was made using the "Quantitative Insights Into Microbial Ecology" (QIIME version 1.9.1) package software⁷¹ with a curated database constructed with the "Human Oral Microbiome Database" (HOMD version 14.51)⁷² and full-length 16S rRNA gene sequences of all species belonging to the genera of interest present in the RDP.

Statistics. The data were analysed using R (version 3.3.3)⁷³ with the RStudio software⁷⁴. Statistical tests were chosen following Shapiro-Wilk normality test results for the data distribution and were considered significant for $p < 0.05$. Demographic data, periodontal cases and the extent and severity measures of periodontitis were compared using the χ^2 and Mann-Whitney tests. The observed richness was analysed using the Mann-Whitney test, and the Shannon-Weaver index was analysed using Student's t test. The 3D principal coordinates analysis (PCoA) plots were generated using Emperor (version 0.9.51)⁷⁵. The PERMANOVA test was performed to compare *beta* diversity metrics. LDA was computed using the LEfSe algorithm in Galaxy (<http://huttenhower.sph.harvard.edu/galaxy/>) with the default parameters⁷⁶. Assessments of significant patterns of microbial co-occurrence or mutual exclusion at the genus level of the core microbiota (prevalence $\geq 50\%$) were performed using Cytoscape (version 3.2.1)⁷⁷ with the CoNet plugin⁷⁸. Only genera found in at least 70% of the normal TSAT or in 70% of the high TSAT samples were represented. Four similarity measures were calculated: the Bray Curtis and Kullback-Leibler non-parametric dissimilarity indices and the Pearson and Spearman rank correlations. The threshold for the similarity measures was set at 0.5, and only edges with merged *p-values* < 0.05 (Benjamini-Hochberg correction) were kept. Genera from the co-occurrence networks that had an average relative abundance $\geq 0.5\%$ were used to generate correlation matrices (calculated using Spearman's test and plotted using the 'corrplot' package for R⁷⁹) between the genera relative abundance and bioclinical parameters with both excess iron and periodontitis treated as continuous variables. Additional correlations between species level taxa and clinical data were also computed with Spearman's test.

Ethics approval and consent to participate. A case-series study was conducted after approval by the local ethics committee (CPP Ouest V - 10/02-744). All participants were recruited either during phlebotomy therapy or at diagnosis in the unit of Hepatology, University Hospital, Rennes, between June 2011 and June 2012. The patients gave informed written consent for the dental examination and subgingival sampling. They were instructed on the prevention and treatment of periodontitis as well as on oral hygiene procedures. All research methods were performed in accordance with the relevant guidelines and regulations.

Availability of Data and Materials

The sequence data were submitted to the NCBI Sequence Read Archive (<https://www.ncbi.nlm.nih.gov/Traces/study/>) under BioProject accession number PRJNA416501. Due to the low sequence counts, the Hemoparo37 and Hemoparo43 samples were withdrawn from the study. The metadata and datasets (OTU tables) supporting the conclusions of this article are included within the article as additional files (see Supplementary Tables S3 and S4, respectively).

References

- Socransky, S. S., Haffajee, A. D., Cugini, M. A., Smith, C. & Kent, R. L. Microbial complexes in subgingival plaque. *Journal of Clinical Periodontology* **25**, 134–144 (1998).
- Hajishengallis, G., Darveau, R. P. & Curtis, M. A. The keystone-pathogen hypothesis. *Nature Reviews. Microbiology* **10**, 717–725, <https://doi.org/10.1038/nrmicro2873> (2012).
- Hajishengallis, G. Periodontitis: from microbial immune subversion to systemic inflammation. *Nature Reviews. Immunology* **15**, 30–44, <https://doi.org/10.1038/nri3785> (2015).
- Kilian, M. *et al.* The oral microbiome - an update for oral healthcare professionals. *British Dental Journal* **221**, 657–666, <https://doi.org/10.1038/sj.bdj.2016.865> (2016).
- Linden, G. J., Herzberg, M. C. & working group 4 of the joint EFP/AAP workshop. Periodontitis and systemic diseases: a record of discussions of working group 4 of the Joint EFP/AAP Workshop on Periodontitis and Systemic Diseases. *Journal of Periodontology* **84**, S20–23, <https://doi.org/10.1902/jop.2013.1340020> (2013).
- Monsarrat, P. *et al.* Clinical research activity in periodontal medicine: a systematic mapping of trial registers. *Journal of Clinical Periodontology* **43**, 390–400, <https://doi.org/10.1111/jcpe.12534> (2016).
- Williams, R. C. & Offenbacher, S. Periodontal medicine: the emergence of a new branch of periodontology. *Periodontology 2000* **23**, 9–12 (2000).
- Meuric, V. *et al.* Periodontal status and serum biomarker levels in HFE hemochromatosis patients. A case series study. *Journal of Clinical Periodontology*, <https://doi.org/10.1111/jcpe.12760> (2017).
- Merryweather-Clarke, A. T., Pointon, J. J., Shearman, J. D. & Robson, K. J. Global prevalence of putative haemochromatosis mutations. *Journal of Medical Genetics* **34**, 275–278 (1997).
- Powell, L. W., Seckington, R. C. & Deugnier, Y. Haemochromatosis. *Lancet (London, England)* **388**, 706–716, [https://doi.org/10.1016/S0140-6736\(15\)01315-X](https://doi.org/10.1016/S0140-6736(15)01315-X) (2016).
- Brissot, P., Ropert, M., Le Lan, C. & Loréal, O. Non-transferrin bound iron: a key role in iron overload and iron toxicity. *Biochimica Et Biophysica Acta* **1820**, 403–410, <https://doi.org/10.1016/j.bbagen.2011.07.014> (2012).
- Crichton, R. Iron Deficiency, Iron Overload and Therapy. In *Iron Metabolism*, 376–417, 4 edn, <https://doi.org/10.1002/9781118925645.ch11> (John Wiley & Sons, Ltd, Chichester, UK, 2016).
- Loréal, O. *et al.* Determination of non-transferrin-bound iron in genetic hemochromatosis using a new HPLC-based method. *Journal of Hepatology* **32**, 727–733 (2000).
- O'Neil, J. & Powell, L. Clinical aspects of hemochromatosis. *Seminars in Liver Disease* **25**, 381–391, <https://doi.org/10.1055/s-2005-923310> (2005).
- Guggenbuhl, P. *et al.* Bone mineral density in men with genetic hemochromatosis and HFE gene mutation. *Osteoporosis international: a journal established as result of cooperation between the European Foundation for Osteoporosis and the National Osteoporosis Foundation of the USA* **16**, 1809–1814, <https://doi.org/10.1007/s00198-005-1934-0> (2005).
- Guggenbuhl, P., Brissot, P. & Loréal, O. Miscellaneous non-inflammatory musculoskeletal conditions. Haemochromatosis: the bone and the joint. *Best Practice & Research. Clinical Rheumatology* **25**, 649–664, <https://doi.org/10.1016/j.berh.2011.10.014> (2011).
- Bacon, B. R. *et al.* Diagnosis and management of hemochromatosis: 2011 practice guideline by the American Association for the Study of Liver Diseases. *Hepatology (Baltimore, Md.)* **54**, 328–343, <https://doi.org/10.1002/hep.24330> (2011).
- Bismuth, M. & Peynaud-Debayle, E. Haute Autorité de Santé (HAS) - Prise en charge de l'hémochromatose liée au gène HFE (hémochromatose de type 1), https://www.has-sante.fr/portail/jcms/c_432802/fr/prise-en-charge-de-l-hemochromatose-liee-au-gene-hfe-hemochromatose-de-type-1 (2005).
- European Association For The Study Of The Liver. EASL clinical practice guidelines for HFE hemochromatosis. *Journal of Hepatology* **53**, 3–22, <https://doi.org/10.1016/j.jhep.2010.03.001> (2010).
- Swinkels, D. W. & Jorna, A. T. M. & Raymakers, R. a. P. Synopsis of the Dutch multidisciplinary guideline for the diagnosis and treatment of hereditary haemochromatosis. *The Netherlands Journal of Medicine* **65**, 452–455 (2007).
- Schaible, U. E. & Kaufmann, S. H. E. Iron and microbial infection. *Nature Reviews Microbiology* **2**, 946–953, [http://www.nature.com.gate1.inist.fr/nrmicro/journal/v2/n12/full/nrmicro1046.html](http://www.nature.com/gate1.inist.fr/nrmicro/journal/v2/n12/full/nrmicro1046.html), <https://doi.org/10.1038/nrmicro1046> (2004).
- Byrne, D. P., Potempa, J., Olczak, T. & Smalley, J. W. Evidence of mutualism between two periodontal pathogens: co-operative haem acquisition by the HmuY haemophore of *Porphyromonas gingivalis* and the cysteine protease interpain A (InpA) of *Prevotella intermedia*. *Molecular Oral Microbiology* **28**, 219–229, <https://doi.org/10.1111/omi.12018> (2013).
- Jolivet-Gougeon, A. *et al.* Serum transferrin saturation increase is associated with decrease of antibacterial activity of serum in patients with HFE-related genetic hemochromatosis. *The American Journal of Gastroenterology* **103**, 2502–2508, <https://doi.org/10.1111/j.1572-0241.2008.02036.x> (2008).
- Buhnik-Rosenblau, K., Moshe-Belizowski, S., Danin-Poleg, Y. & Meyron-Holtz, E. G. Genetic modification of iron metabolism in mice affects the gut microbiota. *Biomaterials: An International Journal on the Role of Metal Ions in Biology, Biochemistry, and Medicine* **25**, 883–892, <https://doi.org/10.1007/s10534-012-9555-5> (2012).
- Ratledge, C. & Dover, L. G. Iron metabolism in pathogenic bacteria. *Annual Review of Microbiology* **54**, 881–941, <https://doi.org/10.1146/annurev.micro.54.1.881> (2000).
- Frantzis, T. G., Sheridan, P. J., Reeve, C. M. & Young, L. L. Oral manifestations of hemochromatosis. Report of a case. *Oral Surgery, Oral Medicine, and Oral Pathology* **33**, 186–190 (1972).
- McCarthy, P. L. & Shklar, G. *Diseases of the oral mucosa: diagnosis, management, therapy*. (McGraw-Hill, New York, 1964).
- Finch, S. C. & Finch, C. A. Idiopathic hemochromatosis, an iron storage disease: A. Iron metabolism in hemochromatosis. *Medicine* **34**, 381–430 (1955).
- Conn, H. J., Darrow, M. & Emmel, V. *Staining procedures used by the biological stain commission*. 2 edn., (Williams & Wilkins Company, Baltimore, 1960).
- Gorlin, R. & Goldman, H. *Thoma's Oral Pathology*. 6 edn., 2 (The C.V. Mosby Company, St. Louis, 1970).
- Meuric, V. *et al.* Signature of Microbial Dysbiosis in Periodontitis. *Applied and Environmental Microbiology* **83**, <https://doi.org/10.1128/AEM.00462-17> (2017).
- Wiley, R. A., Beighton, D., Winstanley, T. G., Fraser, H. Y. & Hardie, J. M. *Streptococcus intermedius*, *Streptococcus constellatus*, and *Streptococcus anginosus* (the *Streptococcus milleri* group): association with different body sites and clinical infections. *Journal of Clinical Microbiology* **30**, 243–244 (1992).
- Camelo-Castillo, A. *et al.* Relationship between periodontitis-associated subgingival microbiota and clinical inflammation by 16S pyrosequencing. *Journal of Clinical Periodontology* **42**, 1074–1082, <https://doi.org/10.1111/jcpe.12470> (2015).

34. Camelo-Castillo, A. J. *et al.* Subgingival microbiota in health compared to periodontitis and the influence of smoking. *Frontiers in Microbiology* **6**, <https://doi.org/10.3389/fmicb.2015.00119> (2015).
35. Moter, A. *et al.* Molecular epidemiology of oral treponemes in patients with periodontitis and in periodontitis-resistant subjects. *Journal of Clinical Microbiology* **44**, 3078–3085, <https://doi.org/10.1128/JCM.00322-06> (2006).
36. Wyss, C. *et al.* Treponema lecithinolyticum sp. nov., a small saccharolytic spirochaete with phospholipase A and C activities associated with periodontal diseases. *International Journal of Systematic Bacteriology* **49**(Pt 4), 1329–1339, <https://doi.org/10.1099/00207713-49-4-1329> (1999).
37. Siqueira, J. F. & Rôças, I. N. PCR-based identification of Treponema maltophilum, T amylovorum, T medium, and T lecithinolyticum in primary root canal infections. *Archives of Oral Biology* **48**, 495–502 (2003).
38. Ling, Z. *et al.* Pyrosequencing analysis of the human microbiota of healthy Chinese undergraduates. *BMC genomics* **14**, 390, <https://doi.org/10.1186/1471-2164-14-390> (2013).
39. Moutsopoulos, N. M. *et al.* Subgingival microbial communities in Leukocyte Adhesion Deficiency and their relationship with local immunopathology. *PLoS pathogens* **11**, e1004698, <https://doi.org/10.1371/journal.ppat.1004698> (2015).
40. Lourenço, T. G. B. *et al.* Microbial signature profiles of periodontally healthy and diseased patients. *Journal of Clinical Periodontology* **41**, 1027–1036, <https://doi.org/10.1111/jcpe.12302> (2014).
41. Pérez-Chaparro, P. J. *et al.* Newly identified pathogens associated with periodontitis: a systematic review. *Journal of Dental Research* **93**, 846–858, <https://doi.org/10.1177/0022034514542468> (2014).
42. Bizzarro, S. *et al.* Microbial profiles at baseline and not the use of antibiotics determine the clinical outcome of the treatment of chronic periodontitis. *Scientific Reports* **6**, 20205, <https://doi.org/10.1038/srep20205> (2016).
43. Byrne, S. J. *et al.* Progression of chronic periodontitis can be predicted by the levels of Porphyromonas gingivalis and Treponema denticola in subgingival plaque. *Oral Microbiology and Immunology* **24**, 469–477, <https://doi.org/10.1111/j.1399-302X.2009.00544.x> (2009).
44. Brissot, P. *et al.* Haemochromatosis. *Nature Reviews. Disease Primers* **4**, 18016, <https://doi.org/10.1038/nrdp.2018.16> (2018).
45. Goulet, V., Britigan, B., Nakayama, K. & Grenier, D. Cleavage of human transferrin by Porphyromonas gingivalis gingipains promotes growth and formation of hydroxyl radicals. *Infection and Immunity* **72**, 4351–4356, <https://doi.org/10.1128/IAI.72.8.4351-4356.2004> (2004).
46. Adonogianaki, E., Mooney, J. & Kinane, D. F. The ability of gingival crevicular fluid acute phase proteins to distinguish healthy, gingivitis and periodontitis sites. *Journal of Clinical Periodontology* **19**, 98–102 (1992).
47. Bramanti, T. E. & Holt, S. C. Roles of porphyrins and host iron transport proteins in regulation of growth of Porphyromonas gingivalis W50. *Journal of Bacteriology* **173**, 7330–7339 (1991).
48. Brochu, V., Grenier, D., Nakayama, K. & Mayrand, D. Acquisition of iron from human transferrin by Porphyromonas gingivalis: a role for Arg- and Lys-gingipain activities. *Oral Microbiology and Immunology* **16**, 79–87 (2001).
49. Grenier, D., Goulet, V. & Mayrand, D. The capacity of Porphyromonas gingivalis to multiply under iron-limiting conditions correlates with its pathogenicity in an animal model. *Journal of Dental Research* **80**, 1678–1682, <https://doi.org/10.1177/00220345010800071501> (2001).
50. Inoshita, E., Iwakura, K., Amano, A., Tamagawa, H. & Shizukuishi, S. Effect of transferrin on the growth of Porphyromonas gingivalis. *Journal of Dental Research* **70**, 1258–1261, <https://doi.org/10.1177/00220345910700090501> (1991).
51. Alderete, J. F., Peterson, K. M. & Baseman, J. B. Affinities of Treponema pallidum for human lactoferrin and transferrin. *Genitourinary Medicine* **64**, 359–363 (1988).
52. Wong, G. H., Steiner, B. & Graves, S. Effect of four serum components on survival of Treponema pallidum and its attachment to rabbit cells *in vitro*. *Genitourinary Medicine* **62**, 1–3 (1986).
53. Tan, K. H. *et al.* Porphyromonas gingivalis and Treponema denticola exhibit metabolic symbioses. *PLoS pathogens* **10**, e1003955, <https://doi.org/10.1371/journal.ppat.1003955> (2014).
54. Kurniyati, K. *et al.* A novel glycan modifies the flagellar filament proteins of the oral bacterium Treponema denticola. *Molecular Microbiology* **103**, 67–85, <https://doi.org/10.1111/mmi.13544> (2017).
55. Seckington, R. & Powell, L. *HFE-Associated Hereditary Hemochromatosis*. (University of Washington, Seattle, Seattle (WA), 2015).
56. Boshuizen, M. *et al.* Therapeutic use of transferrin to modulate anemia and conditions of iron toxicity. *Blood Reviews*, <https://doi.org/10.1016/j.blre.2017.07.005> (2017).
57. Brissot, P. Optimizing the diagnosis and the treatment of iron overload diseases. *Expert Review of Gastroenterology & Hepatology* **10**, 359–370, <https://doi.org/10.1586/17474124.2016.1119043> (2016).
58. Wang, L. *et al.* Attenuated inflammatory responses in hemochromatosis reveal a role for iron in the regulation of macrophage cytokine translation. *Journal of Immunology (Baltimore, Md.: 1950)* **181**, 2723–2731 (2008).
59. Ganz, T. Systemic iron homeostasis. *Physiological Reviews* **93**, 1721–1741, <https://doi.org/10.1152/physrev.00008.2013> (2013).
60. Eke, P. L., Page, R. C., Wei, L., Thornton-Evans, G. & Genco, R. J. Update of the case definitions for population-based surveillance of periodontitis. *Journal of Periodontology* **83**, 1449–1454, <https://doi.org/10.1902/jop.2012.110664> (2012).
61. Huse, S. M. *et al.* Exploring Microbial Diversity and Taxonomy Using SSU rRNA Hypervariable Tag Sequencing. *PLoS Genet* **4**, e1000255, <https://doi.org/10.1371/journal.pgen.1000255> (2008).
62. Claesson, M. J. *et al.* Comparative Analysis of Pyrosequencing and a Phylogenetic Microarray for Exploring Microbial Community Structures in the Human Distal Intestine. *PLoS One* **4**, e6669, <https://doi.org/10.1371/journal.pone.0006669> (2009).
63. Huse, S. M. *et al.* VAMPS: a website for visualization and analysis of microbial population structures. *BMC Bioinformatics* **15**, 41, <https://doi.org/10.1186/1471-2105-15-41> (2014).
64. Cole, J. R. *et al.* Ribosomal Database Project: data and tools for high throughput rRNA analysis. *Nucleic Acids Research* **42**, D633–642, <https://doi.org/10.1093/nar/gkt1244> (2014).
65. Shannon, C. E. & Weaver, W. *The mathematical theory of communication*. (Urbana, Etats-Unis d'Amérique, 1963).
66. Bray, J. R. & Curtis, J. T. An ordination of the upland forest communities of southern Wisconsin. *Ecological monographs* **27**, 325–349 (1957).
67. Lozupone, C. & Knight, R. UniFrac: a new phylogenetic method for comparing microbial communities. *Applied and environmental microbiology* **71**, 8228–8235, <http://aem.asm.org/content/71/12/8228.short> (2005).
68. Abusleme, L. *et al.* The subgingival microbiome in health and periodontitis and its relationship with community biomass and inflammation. *The ISME journal* **7**, 1016–1025, <https://doi.org/10.1038/ismej.2012.174> (2013).
69. Galimanas, V. *et al.* Bacterial community composition of chronic periodontitis and novel oral sampling sites for detecting disease indicators. *Microbiome* **2**, 32, <https://doi.org/10.1186/2049-2618-2-32> (2014).
70. Griffen, A. L. *et al.* Distinct and complex bacterial profiles in human periodontitis and health revealed by 16s pyrosequencing. *The ISME journal* **6**, 1176–1185, <https://doi.org/10.1038/ismej.2011.191> (2012).
71. Caporaso, J. G. *et al.* QIIME allows analysis of high-throughput community sequencing data. *Nature methods* **7**, 335–336, <http://www.nature.com/nmeth/journal/v7/n5/full/nmeth.f.303.html> (2010).
72. Chen, T. *et al.* The Human Oral Microbiome Database: a web accessible resource for investigating oral microbe taxonomic and genomic information. *Database* **2010**, baq013, <http://database.oxfordjournals.org/content/2010/baq013>, <https://doi.org/10.1093/database/baq013> (2010).
73. R. Core Team. R: A language and environment for statistical computing. *R foundation for Statistical Computing, Vienna, Austria*, <https://www.R-project.org/> (2015).

74. RStudio Team. RStudio: integrated development for R. *RStudio, Inc., Boston, MA*, <http://www.rstudio.com> (2016).
75. Vázquez-Baeza, Y., Pirrung, M., Gonzalez, A. & Knight, R. EMPeror: a tool for visualizing high-throughput microbial community data. *GigaScience* **2**, 16, <https://doi.org/10.1186/2047-217X-2-16> (2013).
76. Segata, N. *et al.* Metagenomic biomarker discovery and explanation. *Genome Biology* **12**, R60, <https://doi.org/10.1186/gb-2011-12-6-r60> (2011).
77. Shannon, P. *et al.* Cytoscape: a software environment for integrated models of biomolecular interaction networks. *Genome Research* **13**, 2498–2504, <https://doi.org/10.1101/gr.1239303> (2003).
78. Faust, K. & Raes, J. CoNet app: inference of biological association networks using Cytoscape. *F1000Research* **5**, 1519, <https://doi.org/10.12688/f1000research.9050.2> (2016).
79. Wei, T. & Simko, V. corrplot: Visualization of a Correlation Matrix, <https://cran.r-project.org/web/packages/corrplot/index.html> (2016).

Acknowledgements

The authors are indebted to the medical and nursing staff of the Liver Unit for participating in the recruitment and follow-up of patients. We thank the GeT-PlaGe facility and the NED team for sequencing the samples. We also thank Adina Pascu for her contribution to this work and the “Direction de la Recherche et de l’Innovation” at the University hospital of Rennes for their support. This study was funded by the “Comité de la Recherche Clinique” of the University Hospital of Rennes (2009-A00998-49) and by the University of Rennes 1.

Author Contributions

The project was conceived by E.B., V.M., S.L.G.D., Y.D. and M.B.M. The clinical material was collected by V.M. and M.B.M. All laboratory work was conducted by E.B., V.M. and S.L.G.D. The bioinformatics analysis was conducted by E.B., V.M. and S.L.G.D. E.B., B.M., S.L.G.D., S.B.F., O.L., Y.D., M.B.M. and V.M. interpreted the data and wrote the manuscript. All authors read and approved the final manuscript.

Additional Information

Supplementary information accompanies this paper at <https://doi.org/10.1038/s41598-018-33813-0>.

Competing Interests: The authors declare no competing interests.

Publisher’s note: Springer Nature remains neutral with regard to jurisdictional claims in published maps and institutional affiliations.



Open Access This article is licensed under a Creative Commons Attribution 4.0 International License, which permits use, sharing, adaptation, distribution and reproduction in any medium or format, as long as you give appropriate credit to the original author(s) and the source, provide a link to the Creative Commons license, and indicate if changes were made. The images or other third party material in this article are included in the article’s Creative Commons license, unless indicated otherwise in a credit line to the material. If material is not included in the article’s Creative Commons license and your intended use is not permitted by statutory regulation or exceeds the permitted use, you will need to obtain permission directly from the copyright holder. To view a copy of this license, visit <http://creativecommons.org/licenses/by/4.0/>.

© The Author(s) 2018

2.2 Periodontal pathogens and clinical parameters in periodontitis, *Molecular Oral Microbiology* 2019

La conclusion de l'article précédent était que le fer présent dans l'organisme, et en particulier le fer circulant, biodisponible, participe à l'équilibre hôte-microbiote. L'augmentation du niveau de fer, et l'apparition d'une surcharge sont susceptibles de perturber cet équilibre et favoriseraient une dysbiose du microbiote sous-gingival. Les réseaux de co-occurrence montraient une corrélation entre la saturation de la transferrine et les genres *Porphyromonas* et *Treponema*, qui contiennent des espèces pathogènes majeures pour le parodonte. Il était donc naturel de penser que le microbiote sous-gingival de ces patients présentait une dysbiose se rapprochant de la signature bactérienne présentée dans l'article publié dans *Applied and Environmental Microbiology*⁵. Cependant, nous pouvions aussi suspecter que la pathologie systémique des patients avait induite un autre modèle de dysbiose. Pour tester cette hypothèse, nous avons appliqué à ces échantillons le ratio de dysbiose développé dans cet article.

Le ratio de dysbiose ($\frac{\text{Porphyromonas} + \text{Treponema} + \text{Tannerella}}{\text{Rothia} + \text{Corynebacterium}}$ dans sa version simplifiée) a été conçu par comparaison entre des échantillons provenant de sites parodontaux sains ou malades. Un autre intérêt de son étude avec nos propres échantillons est de pouvoir évaluer son association avec des indices cliniques de la maladie parodontale, et donc avec sa sévérité. Grâce aux échantillons provenant d'une étude publiée par Bizzarro et coll., et qui n'avaient pas été utilisés pour concevoir le ratio de dysbiose, nous avons pu faire une première validation de ce dernier [5]. En effet, nous avons à disposition, dans les métadonnées, la profondeur de sondage des sites prélevées par Bizzarro et coll., et celle-ci présentait une corrélation significative avec le ratio. L'utilisation de nos propres échantillons nous a cependant permis d'aller plus loin : en disposant du statut parodontal complet de chaque patient, nous avons pu tester la capacité du ratio de dysbiose à être un biomarqueur de la maladie parodontale, à l'échelle de la cavité buccale.

Au fur et à mesure des publications sur le microbiote sous-gingival dans la parodontite, plusieurs espèces et genre bactériens ont fait l'objet d'une attention nouvelle. Détectés en plus grande abondance dans les sites malades, ils ont été identifiés comme potentiellement associés avec la maladie. Par opposition aux pathogènes classiquement décrits⁶, une revue systématique de 2014 a répertorié ces nouveaux pathogènes parodontaux potentiels selon leur nombre d'apparition dans la littérature [7]. Notre étude était donc l'occasion de pouvoir évaluer le degré d'implication de chacun dans la maladie parodontale. Pour cela, nous avons mesuré la force de l'association statistique entre la sévérité de la parodontite, et la présence de ces espèces bien spécifiques. Là encore, le fait de disposer de nombreuses métadonnées associées à chaque patient (âge, sexe, statut tabagique, etc.) est un avantage conséquent, car il a permis

5. Voir l'article présenté dans la section 1.2.1 *Signature of Microbial Dysbiosis in Periodontitis*, *Applied and Environmental Microbiology* 2017 en page 7.

6. Les complexes bactériens publiés par Socransky et coll. [6].

de réaliser des modèles statistiques de régression linéaire multiple. Ces derniers, en incluant ces variables confondantes, ont renforcé la pertinence des associations entre bactéries et maladie parodontale.

Le premier objectif de l'étude était de rechercher des taxons spécifiquement liés à la maladie parodontale, qu'ils soient classiquement décrits ou nouvellement identifiés. Dans cette population, atteinte par une parodontite majoritairement sévère, environ les deux tiers (64,4 %) des genres et espèces recherchés ont été détectés (tableau 2 de l'article). Malgré une bonne profondeur de séquençage, il n'est pas exclu que des taxons non détectés aient pu être présents, mais en quantité trop faible pour apparaître dans les résultats. La majorité des taxons décrits par Socransky et coll. (19/22) était présent dans les échantillons. Parmi ceux répertoriés par Pérez-Chaparro et coll., leur taux de détection croît avec le nombre de citation dont ils font l'objet dans la littérature (de 2 à 5 articles). Il faut noter que trois espèces n'étaient pas identifiables par notre méthodologie bioinformatique. Bien que cela représente une faible proportion des taxons recherchés, cela illustre les limites que peut rencontrer l'analyse du microbiote au niveau espèces, par le biais du 16S.

Deux critères, reflétant à la fois la sévérité et l'étendue globales de la maladie parodontale, ont été utilisés pour réaliser les tests de corrélation qui constituaient le deuxième objectif de l'étude. Il s'agissait de la profondeur moyenne des sondages parodontaux, et de la proportion de sites parodontaux présentant une profondeur de sondage ≥ 4 mm, calculées pour chaque patient. Il est ressorti de ces tests que seul un des taxons nouvellement identifiés était significativement corrélé avec la parodontite : *Desulfobulbus*. À l'inverse, plusieurs des taxons classiquement décrits présentaient des corrélations significatives.

Néanmoins, que ce soit par des corrélations ou confrontés à des variables confondantes dans des modèles statistiques, le ratio de dysbiose présentait les associations les plus fortes et les plus significatives avec la parodontite. Plusieurs hypothèses peuvent expliquer ce constat. L'abondance calculée au niveau du genre bactérien agrège les différentes espèces qu'il contient, qu'elles soient pathogènes ou non. L'analyse perd en spécificité mais devient alors plus robuste. Elle s'affranchit, en outre, de la prévalence des espèces bactériennes, qui atteint rarement les 100 %, même pour un pathogène majeur comme *P. gingivalis*. Enfin, le ratio prend en compte l'abondance de plusieurs genres, et se rapproche ainsi du modèle de synergie polymicrobienne qui prévaut aujourd'hui. Il faut également remarquer qu'il présente rarement une valeur nulle, ce qui simplifie sa normalisation lors d'une transformation logarithmique, avant intégration dans un modèle statistique.

Les modèles de régression linéaire multiple présentés dans les tableaux 4 et S1 de l'article montrent que, à niveau de fer égal, le ratio de dysbiose expliquait de façon significative la maladie parodontale des patients. Nous avons donc conclu que, i) la dysbiose du microbiote sous-gingivale de ces patients rejoignait la signature précédemment décrite, et ii) que le ratio de dysbiose apparaissait comme un biomarqueur de la santé parodontale.

Cet article a été publié dans *Molecular Oral Microbiology* le 29 novembre 2019. Il est disponible au format prépublication dans les archives HAL (<https://hal.archives-ouvertes.fr/hal-02394270>).

1

2 DR EMILE BOYER (Orcid ID : 0000-0002-0208-2084)

3 DR VINCENT MEURIC (Orcid ID : 0000-0001-5411-4001)

4

5

6 Article type : Original Article

7

8

9 **Periodontal pathogens and clinical parameters in chronic periodontitis**

10 **Running Title:** Dysbiosis in periodontitis

11 Emile Boyer¹; Bénédicte Martin¹; Sandrine Le Gall-David¹; Shao Bing Fong¹; Yves Deugnier²;

12 Martine Bonnaure-Mallet¹; Vincent Meuric¹

13 ¹INSERM, INRA, Univ Rennes 1, CHU de Rennes, Nutrition Metabolisms and Cancer, Rennes,

14 France

15 ²CIC 1414, Inserm, Rennes, 35033, France

16 **Corresponding author:**

17 Vincent Meuric

18 2, avenue du Professeur Léon Bernard, 35043 Rennes, France

19 Telephone number: +33 2 23 23 49 19 Fax number: +33 2 23 23 49 13

20 E-mail: vincent.meuric@univ-rennes1.fr

21

The peer review history for this article is available at <https://publons.com/publon/10.1111/omi.12274>

This article has been accepted for publication and undergone full peer review but has not been through the copyediting, typesetting, pagination and proofreading process, which may lead to differences between this version and the [Version of Record](#). Please cite this article as [doi: 10.1111/MOM.12274](https://doi.org/10.1111/MOM.12274)

This article is protected by copyright. All rights reserved

22 Abstract

23 *Background:* The use of Next Generation Sequencing and bioinformatics have revealed the
24 complexity and richness of the human oral microbiota. While some species are well known for their
25 periodontal pathogenicity, the molecular-based approaches for bacterial identification have raised
26 awareness about new putative periodontal pathogens. Although they are found increased in case of
27 periodontitis, there is currently a lack of data on their interrelationship with the periodontal measures.

28 *Methods:* We processed the sequencing data of the subgingival microbiota of 75 patients with
29 haemochromatosis and chronic periodontitis in order to characterize well-described and newly
30 identified subgingival periodontal pathogens. We used correlation tests and statistical models to
31 assess the association between the periodontal pathogens and mean pocket depth, and to determine the
32 most relevant bacterial biomarkers of periodontitis severity.

33 *Results:* Based on correlation test results, nine taxa were selected and included in the statistical
34 models. The multiple linear regression models adjusted for systemic and periodontal clinical variables
35 showed that mean pocket depth was negatively associated with *Aggregatibacter* and *Rothia*, and
36 positively associated with *Porphyromonas*. Furthermore, a bacterial ratio that was previously
37 described as a signature of dysbiosis in periodontitis,
38 $(\%Porphyromonas + \%Treponema + \%Tannerella) / (\%Rothia + \%Corynebacterium)$, was the most
39 significant predictor.

40 *Conclusion:* In this specific population, we found that the best model in predicting the mean pocket
41 depth was microbial dybiosis using the dysbiosis ratio taxa formula. While further studies are needed
42 to assess the validity of these results on the general population, such a dysbiosis ratio could be used in
43 the future to monitor the subgingival microbiota.

44 Keywords

45 Deep sequencing; potential periodontal pathogens; chronic periodontitis; dysbiosis.

46 **1 Introduction**

47
48 Periodontitis is a worldwide health problem and the 6th most common disease globally
49 (Frencken et al., 2017). It is a chronic inflammation produced in response to a disease-associated
50 multispecies bacterial community with intermittent episodes of remission and relapse, characterized
51 by alveolar bone loss. The current model of periodontitis pathogenesis implies a synergistic
52 polymicrobial community and a dysregulated host inflammatory response (G. Hajishengallis &
53 Lamont, 2012). Indeed, a dysbiosis of the complex and diverse oral microbiota (Paster et al., 2001)
54 that inhabits the sulcus is concomitant with the occurrence of a periodontal pocket. This
55 pathognomonic sign of the periodontitis can be quantified as pocket depth (PD) and clinical
56 attachment loss (CAL) (Lamont, Koo, & Hajishengallis, 2018).

57 Subgingival colonization by specific species, including the red complex bacterial species, i.e.,
58 *Porphyromonas gingivalis*, *Tannerella forsythia* and *Treponema denticola*, has been reported to be
59 related to PD and bleeding as determined by DNA-DNA checkerboard analysis (Socransky, Haffajee,
60 Cugini, Smith, & Kent, 1998). *P. gingivalis* is also considered as the keystone pathogen of the
61 disease, that is able to disrupt the immune system allowing for dysbiosis to arise (George
62 Hajishengallis, Darveau, & Curtis, 2012; Jiao, Hasegawa, & Inohara, 2014). The development of
63 contemporary molecular methods (Next Generation of Sequencing – NGS) has expanded the list of
64 potential periodontal pathogens. The review by Pérez-Chaparro *et al.* identified in the literature 29
65 species and one genus putatively implicated in chronic periodontitis that have been cited by at least
66 two different authors (Pérez-Chaparro et al., 2014). However, these results are usually based on health
67 *versus* disease comparisons. The relationship between periodontitis measures and these taxa are
68 lacking. Using NGS data from the literature, we have previously defined a bacterial ratio as a
69 signature of periodontitis that could score the dysbiosis of the subgingival microbiota (Meuric, Le
70 Gall-David, et al., 2017). However, its relationship with the global periodontal status remains to be
71 tested.

72 We have worked on a cohort of patients with chronic periodontitis and hemochromatosis, that
73 allowed us to show worsened periodontal measures in case of iron overload (Meuric, Lainé, et al.,
74 2017). An early study (with 66 patients) of their subgingival microbiota showed a potential impact of

75 iron through correlations between transferrin saturation and the abundance of *Porphyromonas* and
76 *Treponema* (Boyer et al., 2018). Nevertheless, an extensive characterization of their microbiota
77 (including dysbiosis) has not been performed yet, regarding occurrence, abundance and relationship
78 of well-known and newly identified potential periodontal pathogens with periodontal measures.

79 The purpose of this study is three-fold. 1: to characterize all the well-described and newly
80 identified periodontal pathogens (bacterial complexes described by Socransky *et al.* and reviewed by
81 Pérez-Chaparro *et al.*) in the deepest pocket using the NGS in patients with chronic periodontitis
82 (Pérez-Chaparro et al., 2014; Socransky et al., 1998). Two genera usually cited as implicated in
83 health, *Corynebacterium* and *Rothia*, are also analyzed, as a part of the bacterial dysbiosis ratio. 2: to
84 determine the association between the well-described, newly discovered periodontal pathogens and
85 the periodontitis severity through continuous measures (mean PD, sites with $PD \geq 4$ mm). 3: to propose
86 multiple regression linear models to refine the bacterial biomarkers of periodontitis severity adjusted
87 for demographic and clinical data (including iron overload).

88

89 2 Materials and methods

90 Participants and collection of clinical data

91 The participants corresponded to a group of 75 patients with hemochromatosis and chronic
92 periodontitis previously studied by Meuric *et al.* (Meuric, Lainé, et al., 2017). This case study series
93 was approved by the local ethical committee (CPP Ouest V - 10/02-744). The informed consent for
94 study participation has been obtained from all patients and all research was performed in accordance
95 with relevant guidelines and regulations. These patients were recruited at the University Hospital of
96 Rennes and benefited from a full-mouth periodontal examination, including PD, CAL, papillary
97 bleeding index, gingival index, plaque score (Barnett, Ciancio, & Mather, 1980; Lobene,
98 Weatherford, Ross, Lamm, & Menaker, 1986; Silness & Loe, 1964) and evaluation of periodontitis
99 severity according to the case definitions from the Centers for Disease Control and Prevention and the
100 American Association of Periodontology (CDC/AAP) (Eke, Page, Wei, Thornton-Evans, & Genco,
101 2012). For the 2018 classification, the algorithms considered the interdental CAL on two non-adjacent
102 teeth and tooth loss (Graetz et al., 2019; Tonetti, Greenwell, & Kornman, 2018). The exclusion
103 criteria were pregnancy, periodontal therapy within the last 12 months and treatment with either

104 systemic antibiotics or drugs known to cause gingival hyperplasia within the last 3 months. Clinical
105 data recorded at the time of dental examination included smoking status, alcohol consumption (non-
106 drinkers, former drinkers, occasional drinkers and regular drinkers evaluated quantitatively in
107 dose/day), number of dental visits per year and transferrin saturation. The assays of serum iron and
108 transferrin were performed on an automated analyzer AU2700 Olympus (Beckman Coulter). Serum
109 iron levels were measured by a standard colorimetric method that used
110 TPTZ[2,4,6-Tri-(2-pyridyl)-5-triazine] as a chromogen and serum transferrin concentrations were
111 quantified by immunoturbidimetry. Test procedures were conducted as described in the
112 manufacturer's standard operating manual. Total iron binding capacity (TIBC) was calculated using
113 the formula: (transferrin in g/l x 25) and transferrin saturation is calculated as follows: (iron in $\mu\text{mol/l}$
114 / TIBC) \times 100.

115 Sample collection

116 After supra-gingival plaque removal, sterile endodontic paper points (Henry Schein, France) were
117 inserted into one of the deepest periodontal pockets for 30s. The material was transferred into a sterile
118 tube with 100 μL of sterile distilled water and kept at 4°C overnight before DNA extraction.

119 DNA extraction and sequencing

120 DNA extraction from supernatants was performed using QIAamp DNA Mini Kit (Qiagen, France)
121 according to the manufacturer's recommendations. DNA was then kept frozen at -80°C until
122 amplification. The V3-V4 regions of the 16S rRNA gene were amplified with the primers 338F (5'-
123 ACTCCTACGGGAGGCAGCAG-3') (Huse et al., 2008) and 802R (5'-
124 TACNVGGGTATCTAATCC-3') (Claesson et al., 2009) using 25 amplification cycles with an
125 annealing temperature of 45°C. PCR products were sequenced with the Illumina MiSeq of the Get-
126 PlaGe platform (Toulouse, France). The sequence data were submitted to the NCBI Sequence Read
127 Archive (<https://www.ncbi.nlm.nih.gov/Traces/study/>) under BioProject accession number
128 PRJNA416501 and PRJNA517671.

129 Microbiological analysis

130 Taxonomy at the genus level was assigned using the "Visualization and Analysis of Microbial
131 Population Structures" (VAMPS) analysis pipeline web tool (Huse et al., 2014). Default parameters
132 were used for assignment to the genus level with the Ribosomal Database Project (RDP) classification
133 (Cole et al., 2014). Through the Global Alignment for Sequence Taxonomy (GAST) process of
134 VAMPS, the best taxonomic hit was assigned for each read. Reads identified as Archaea, Eukarya,
135 Organelle and unknown were excluded from further analysis. Taxonomy at the species level was
136 assigned using the "Quantitative Insights Into Microbial Ecology" (QIIME 1.9.1) package software
137 (Caporaso et al., 2010) with the default parameters (script: pick_open_reference_otus.py, uclust as the
138 clustering method) and the Human Oral Microbiome Database (HOMD, version 15.1) as the reference
139 database (Chen et al., 2010). The mean unassigned reads per sample was $6.4\% \pm 6.2\%$. These reads
140 have been excluded from further species analyses. To challenge the assignment capacities used in this
141 study, the V3V4 sequences of each taxon were extracted from the HOMD and entered in the
142 previously described pipeline. Only three species (*Mogibacterium timidum*, *Anaeroglobus geminatus*
143 and *Enterococcus faecalis*) could not be correctly classified by the pipeline, among all the putative
144 periodontal pathogens described.

145 Statistics

146 Data were studied using R (version 3.3.3) (R. Core Team, 2015) with the RStudio software (RStudio
147 Team, 2016). Statistical tests were considered significant for $p < 0.05$. Results of the descriptive
148 analysis are presented as mean \pm standard error (SE) and with prevalence (%). Distribution of
149 continuous variables was assessed using the Shapiro-Wilk test. The mean PD was analyzed according
150 to the demographic and clinical data using the Mann-Whitney test. Correlations between taxa relative
151 abundance and clinical parameters were calculated using Spearman correlation coefficient. Multiple
152 linear regression models were used to study the association between periodontal parameters (i.e. mean
153 PD and percentage of site with $PD \geq 4\text{mm}$) and bacterial taxa presenting a significant correlation
154 ($r \geq 0.20$, $p < 0.05$) or the dysbiosis ratio ($\% \text{ Porphyromonas} + \% \text{ Treponema} + \% \text{ Tannerella}$) / ($\% \text{ Rothia} + \% \text{ Corynebacterium}$) described in Meuric *et al.* 2017 (Meuric, Le Gall-David, et al., 2017),
156 adjusted for confounding factors including age, gender, smoking status, alcohol intake, plaque index,
157 transferrin saturation, gingival and bleeding index. The stepwise AIC algorithm was performed using

158 the 'MASS' package for R (Venables & Ripley, 2002). Final regression coefficients, standard errors
159 (SE) and statistics for each variable adjusted for confounding factors, with the characteristics of the
160 models (adjusted R², *p*-value) are presented.

161

162 3 Results

163 - Clinical data

164 Based on the CDC/AAP case definition (Eke et al., 2012), all patients presented periodontitis; 44.3 %
165 and 54.4 % had moderate and severe periodontitis, respectively. On average, 50.0 ± 1.96 % of sites per
166 mouth had CAL ≥ 3 mm, 10.7 ± 1.43 % of sites had CAL ≥ 5 mm, and 12.5 ± 1.15 % of sites had
167 PD ≥ 4 mm. The full description of the periodontal measures is available in Table S1. According to
168 the 2018 classification, and using CAL and tooth loss as the main available criteria, 3/75 (4%)
169 patients were classified as stage II, 59/75 (79%) as stage III and 13/75 (17%) as stage IV (Tonetti et
170 al., 2018). A minority (9/75, 12%) was classified as localized. The average age was 50.6 ± 8 years.
171 Males represented 56 %, and former or current smokers and drinkers were 62.6 % and 80 %,
172 respectively. Most of the patients visited their dentist at least once a year (78.6 %). Table 1 presents
173 the statistics exploring the potential impact of each demographic on the mean PD. The mean PD was
174 increased in former or current drinkers, compared to patients who had never experienced alcohol
175 abuse (*p*=0.028).

176

177 - Prevalence and proportion of bacteria

178 The average of reads per sample was 14 980 ± 740 (minimum = 5 298 reads). From the 74 genera and
179 species related to periodontitis and described by Socransky *et al.*, Pérez-Chaparro *et al.* and Meuric *et*
180 *al.*, 47 taxa (64.4 %) have been identified in this study (Table 2). All the bacteria belonging to the
181 orange and red complexes described by Socransky *et al.* were found. The lowest prevalence was
182 *Fusobacterium periodonticum* (6.4 %), while *Fusobacterium nucleatum* and *T. forsythia* were found
183 in all patients. For the 8 species which have been reported as highly implicated in periodontitis
184 (reported by ≥ 4 studies according to the systematic review of the literature by Pérez-Chaparro *et al.*),
185 five of them were found: i.e. *Porphyromonas endodontalis* (prevalence = 88.6 %),

186 *Treponema lecithinolyticum* (62 %), *Treponema medium* (55.7 %), *Filifactor alocis* (40.5 %) and
187 *Eubacterium saphenum* (11.4 %), while two were not detected (*Fretibacterium OT360* and
188 *Selenomonas sputigena*). For the taxa cited 3 times, the following were not detected: *Bacteroidales*
189 OT274, *Peptostreptococcus stomatis*, *Desulfobulbus* OT041 and phylum TM7. Species with lower
190 evidence of implication with periodontitis (cited only by two studies) or belonging to the purple or
191 green complex (*Actinomyces odontolyticus*, *Veillonella parvula* and *Eikenella corrodens* respectively)
192 were not, or hardly detected (Table 2). *Mogibacterium timidum*, *Anaeroglobus geminatus* and
193 *Enterococcus faecalis* were not found due to methodological limitations.

194 The most abundant genus was *Fusobacterium* (mean = 26.1±1.7 %) followed by *Prevotella* (12±1 %),
195 *Porphyromonas* (7±0.8 %), *Streptococcus* (5.8±0.7 %), *Treponema* (5.6±0.6 %) and *Tannerella*
196 (5.4±0.6 %). The most abundant species were *F. nucleatum* (15.3±1.4 %) followed by *T. forsythia*
197 (4.5±0.5 %), *P. endodontalis* (3.1±0.4 %), and *P. gingivalis* (2.8±0.6 %).

198

199 - Microbiological correlation with periodontal data

200 Analysis showed that the species exhibiting significant correlations with periodontal clinical data
201 were *P. gingivalis* (r=0.33 and 0.41, with mean PD and percentage of sites with PD≥4 mm,
202 respectively), *T. forsythia* (r=0.25 and 0.30, respectively), and *E. nodatum* (r=0.35 and 0.34,
203 respectively). *Desulfobulbus*, *Treponema* and *Porphyromonas* genera were also found significantly
204 correlated with these periodontal data. Significant inverse correlations were found for the taxa of
205 *Campylobacter*, *Aggregatibacter* and *Rothia*. No correlation was found between the sampled pocket
206 depth and any of the bacterial taxa. Finally, the calculated dysbiosis ratio corresponding to
207 $(\%Porphyromonas + \%Treponema + \%Tannerella) / (\%Rothia + \%Corynebacterium)$ showed the
208 highest correlation with mean PD (r=0.37, p=0.001) and with the percentage of sites with PD ≥ 4 mm
209 (r=0.35, p=0.0017), as compared with individual taxa. Table 3 presents all the significant results of
210 the correlation between bacterial/clinical data and mean PD, which were further used in the following
211 statistical experiments. As shown in Table 3, the periodontal indices rating the plaque, gingival
212 inflammation and bleeding on probing, were found significantly correlated with the mean PD.
213 Therefore, they were also used in the statistical models as confounding variables.

214

215 - Multiple linear regression analyses

216 The multiple linear regression was performed with the stepwise method which selects the most
217 significant variables affecting the mean pocket depth. After adjustment for age, sex, smoking status,
218 alcohol status, plaque index, transferrin saturation, bleeding index and gingival index, the mean PD
219 was found independently associated with *Aggregatibacter*, *Rothia* and *Porphyromonas* genera (β =-
220 0.053, -0.063 and 0.051, respectively, $p < 0.05$) in the first model (adjusted $R^2 = 0.3798$, $p < 0.001$). The
221 most significant data were obtained in the second model using the dysbiosis ratio and *Aggregatibacter*
222 as independent variables with $\beta = 0.062$ ($p < 0.001$) and $\beta = -0.053$ ($p < 0.01$) respectively and an adjusted
223 $R^2 = 0.4868$ ($p < 0.00001$) (Table 4). By using another periodontal measure as the outcome variable –
224 the percentage of sites with $PD \geq 4$ mm –, the dysbiosis ratio ($p < 0.001$ – Table S2) remained as the
225 most significant predictor.

226

227 4 Discussion

228 Owing to decades of oral microbiology studies, some species are well known for their
229 periodontal pathogenicity. Culture-independent and molecular-based approaches to bacterial
230 identification has highlighted new putative periodontal pathogens, that were found increased in
231 periodontitis patients. However, few studies assess the correlation between the severity of periodontal
232 disease and the abundance of these taxa. The identification of taxa that are significantly associated
233 with the periodontal status is the first step in the search for biomarkers that could predict the onset of
234 the disease.

235 Most of the periodontal pathogens were identified in the analyses due to the sequencing depth.
236 However, six species were not detected. *Bacteroidales* OT274, *Peptostreptococcus stomatis*,
237 *Desulfobulbus* OT041, *Fretibacterium* sp., TM7 and *Selenomonas Sputigena* could not be found while
238 they are highly cited (≥ 3 times) in the literature as being implicated in periodontitis. Only three
239 (*Mogibacterium timidum*, *Anaeroglobus geminatus* and *Enterococcus faecalis*) could not be identified
240 through the pipeline of assignment, due to methodological limitations. The lack of detection of
241 *Fretibacterium* is surprising since it was proposed as a diagnostic bacterial biomarker for periodontitis
242 screening in a Japanese population (Khemwong et al., 2019). Indeed, *Fretibacterium* was not detected
243 in our Caucasian population. As for the other five remaining taxa, we have confirmed that they were

244 not detected in this population. Thus, different population could carry different taxon associated with
245 periodontitis. However, previous works on periodontitis microbiota analysis through NGS have used a
246 binary approach (healthy or disease) to determine in which condition taxon are increased (Abusleme
247 et al., 2013; Kirst et al., 2015). In this study, we have performed correlation analyses between the
248 abundance of species considered as periodontal pathogens (from previous studies) and continuous
249 periodontal measures, in haemochromatosis patients with periodontitis to assess the current weight of
250 their implication in the disease. Adjusted regression models were then used to determine the best
251 bacterial biomarkers of periodontitis severity. Taxa already well described as implicated in the disease
252 were found correlated with the mean PD or the percentage of sites with $PD \geq 4$ mm: *P. gingivalis* and
253 *T. forsythia* (red complex) and *E. nodatum* (orange complex) (Socransky et al., 1998). From the
254 newly identified putative periodontal pathogen, only *Desulfobulbus* genus (Pérez-Chaparro et al.,
255 2014) was found correlated with the mean pocket depth. Correlation coefficients between periodontal
256 data and bacterial taxa remained inferior to 0.4, similarly to other microbiota analyses in chronic
257 periodontitis (Khemwong et al., 2019; Lourenço et al., 2014; Silva-Boghossian, Cesário, Leão, &
258 Colombo, 2018). Finding associations is especially more difficult when looking at the species level.
259 However, it is not surprising as this disease is a multifactorial pathology, as each taxon might be
260 partially implicated in the disease. For instance, *T. denticola* which belongs to the red complex
261 (Socransky et al., 1998), was not correlated with the mean PD. Nevertheless, the *Treponema* genus,
262 which contains *T. denticola* and other species highly suspected to be periodontal pathogens (i.e.
263 *T. vincentii*, *T. lecithinolyticum* and *T. medium*, as reported in the systematic review by Pérez-
264 Chaparro et al.), was found correlated with the PD measures.

265 Surprisingly, *Campylobacter* was negatively associated with the mean PD, while
266 *Campylobacter* species are mainly classified as periodontal pathogens (i.e.: *C. showae*, *C. gracilis*,
267 and *C. rectus* belonging to the orange complex and *C. concisus* to the green complex (Socransky et
268 al., 1998)). However, this repartition of species is controversial: *C. gracilis* belongs to the orange
269 complex, though it was found increased in healthy subjects (Henne, Fuchs, Kruth, Horz, & Conrads,
270 2014) and decreased in severe periodontitis (Macuch & Tanner, 2000). Finally, the *Campylobacter*
271 genus was still negatively associated with percentage of $PD \geq 4$ mm in the regression model.

272 This analytical approach is also interesting when focused on the prevalence or occurrence of
273 periodontal pathogens in patients. Taxa are not found in all patients. Even the prevalence of
274 *P. gingivalis*, which is well described as one of the keystone pathogens in the disease (George
275 Hajishengallis *et al.*, 2012), was only found at 62% in this study. Moreover, *P. gingivalis* has been
276 detected in 25% of healthy Caucasian (Griffen, Becker, Lyons, Moeschberger, & Leys, 1998), up to
277 40% in healthy Japanese (Kato, Imai, Ochiai, & Ogata, 2013) and not higher than 79% in chronic
278 periodontitis (Griffen *et al.*, 1998). The chronic nature and clinical course of the disease, with
279 alternating episodes of exacerbation and remission (Goodson, Tanner, Haffajee, Sornberger, &
280 Socransky, 1982), could explain that the bacteria are more difficult to detect. The single sampling
281 could also be a potential modifier of the microbiota and a limitation, as different periodontal pockets
282 in the same patient could show various microbiota composition. Long-term follow-up with regular
283 and multi-site sampling is certainly needed, which could address these issues. As such studies are
284 difficult to implement, a ratio of taxa was developed (Meuric, Le Gall-David, *et al.*, 2017) to explore
285 the periodontal dysbiosis responsible for chronic periodontitis (Kilian *et al.*, 2016). This dysbiosis
286 ratio showed the highest and the most significant correlation with mean PD in this study ($p=0.001$)
287 and could be calculated for each patient, whereas *P. gingivalis* could only be detected in 62% of the
288 patients. Thereafter, in the first multiple regression model, each taxon found significantly correlated
289 with mean PD was entered, while *Porphyromonas*, *Treponema*, *P. gingivalis*, *T. forsythia* and *Rothia*
290 were replaced in the second model by the dysbiosis ratio which is computed with their relative
291 abundance. The models were refined with the stepwise method (Venables & Ripley, 2002) adjusted
292 with the clinical and demographic data as for example, alcohol intake, which is considered as a risk
293 factor for periodontitis (Wang, Lv, Wang, & Jiang, 2016) and a worsened mean PD in our population.
294 Since the patients come from a sub-cohort of a previous study where high transferrin saturation
295 (specifically for the hemochromatosis disease) was implicated in explaining clinical severity of
296 periodontitis, we have added the transferrin saturation into the multiple linear regression models as a
297 confounding factor. As described previously, periodontitis through mean PD was associated with
298 transferrin saturation in the two models (Meuric, Lainé, *et al.*, 2017). For each dependent variable
299 (mean PD or percentage of sites with $PD \geq 4$ mm), the most significant result, appeared in the second
300 model with the dysbiosis ratio ($p<0.001$) which is compiled with majority of the periopathogens (*i.e.*:

301 *Porphyromonas*, *Treponema* and *Tannerella* genera) and the genera usually found in health (Meuric,
302 Le Gall-David, et al., 2017). This result is independent from the transferrin saturation (reflecting the
303 iron status of the hemochromatosis disease). Thus, the dysbiosis ratio confirmed its utility in
304 exploring the microbial dysbiosis to explain periodontal disease (Meuric, Le Gall-David, et al., 2017).
305 Similar microbial dysbiosis ratios have also been calculated in Crohn's disease (Gevers et al., 2014)
306 and in peri-implantitis (Kröger et al., 2018).

307 These results are based on a specific population suffering from haemochromatosis.
308 Extrapolations outside of this population need to be validated, though the iron status of the patients
309 has been included as a confounding variable in statistical models. Nonetheless, these results are in
310 accordance with the existing view that periodontitis or peri-implantitis are orchestrated by a bacterial
311 consortium rather than a single pathogen (Darveau, 2010).

312

313

314 **5 Conclusion**

315 In this study, we have confirmed that most of the well-described and newly identified
316 periodontal pathogens can be found in the deepest periodontal pocket of patients suffering from
317 haemochromatosis and periodontitis. Yet, only few taxa were correlated to mean pocket depth. The
318 relative abundance of these taxa was therefore used as a predictor, with confounding variables, in
319 multiple linear regression models that allowed for the prediction of mean pocket depth. While
320 *Porphyromonas*, *Aggregatibacter* and *Rothia* returned significant results, the previously described
321 dysbiosis ratio – $(\% \textit{Porphyromonas} + \% \textit{Treponema} + \% \textit{Tannerella}) / (\% \textit{Rothia} + \% \textit{Corynebacterium})$ – was the most reliable biomarker to predict periodontitis severity in our patients.
322 Longitudinal studies in patients with no systemic disease, as well as several sampling sites and time
323 points during the episodes of disease-active periodontitis should be considered to further validate and
324 generalize the findings of this study.
325

326 **Acknowledgments:** The authors are indebted to the medical and nursing staff for participating in the
327 recruitment and follow-up of patients. We thank the GeT-PlaGe facility and the NED team for
328 sequencing the samples. We also thank Adina Pascu (INSERM U1241) for her contribution to this
329 work and the “Direction de la Recherche et de l’Innovation” at the University hospital of Rennes for
330 their support. The study was funded by the Comité de la Recherche Clinique of the University
331 Hospital (2009-A00998-49) of Rennes and the University of Rennes 1. The authors report no conflicts
332 of interest related to this study.

333 **Data availability:** The sequence data were deposited to the NCBI Sequence Read Archive
334 (<https://www.ncbi.nlm.nih.gov/Traces/study/>) under BioProject accession numbers PRJNA416501
335 and PRJNA517671. The detailed periodontal and demographic data for every patient can be accessed
336 in Table S3.

337

338 **References**

- 339 Abusleme, L., Dupuy, A. K., Dutzan, N., Silva, N., Burleson, J. A., Strausbaugh, L. D., ... Diaz, P. I.
340 (2013). The subgingival microbiome in health and periodontitis and its relationship with community
341 biomass and inflammation. *The ISME Journal*, 7(5), 1016–1025.
342 <https://doi.org/10.1038/ismej.2012.174>
- 343 Barnett, M., Ciancio, S., & Mather, M. (1980). The Modified Papillary Bleeding Index—Comparison
344 with Gingival Index During the Resolution of Gingivitis. *Journal of Preventive Dentistry*, 6(2), 135–
345 138.
- 346 Boyer, E., Gall-David, S. L., Martin, B., Fong, S. B., Loréal, O., Deugnier, Y., ... Meuric, V. (2018).
347 Increased transferrin saturation is associated with subgingival microbiota dysbiosis and severe
348 periodontitis in genetic haemochromatosis. *Scientific Reports*, 8(1), 15532.
349 <https://doi.org/10.1038/s41598-018-33813-0>
- 350 Caporaso, J. G., Kuczynski, J., Stombaugh, J., Bittinger, K., Bushman, F. D., Costello, E. K., ...
351 others. (2010). QIIME allows analysis of high-throughput community sequencing data. *Nature*
352 *Methods*, 7(5), 335–336.
- 353 Chen, T., Yu, W.-H., Izard, J., Baranova, O. V., Lakshmanan, A., & Dewhirst, F. E. (2010). The
354 Human Oral Microbiome Database: A web accessible resource for investigating oral microbe
355 taxonomic and genomic information. *Database*, 2010, baq013.
356 <https://doi.org/10.1093/database/baq013>
- 357 Claesson, M. J., O’Sullivan, O., Wang, Q., Nikkilä, J., Marchesi, J. R., Smidt, H., ... O’Toole, P. W.
358 (2009). Comparative Analysis of Pyrosequencing and a Phylogenetic Microarray for Exploring
359 Microbial Community Structures in the Human Distal Intestine. *PLOS ONE*, 4(8), e6669.
360 <https://doi.org/10.1371/journal.pone.0006669>
- 361 Cole, J. R., Wang, Q., Fish, J. A., Chai, B., McGarrell, D. M., Sun, Y., ... Tiedje, J. M. (2014).
362 Ribosomal Database Project: Data and tools for high throughput rRNA analysis. *Nucleic Acids*
363 *Research*, 42(Database issue), D633-642. <https://doi.org/10.1093/nar/gkt1244>

- 364 Darveau, R. P. (2010). Periodontitis: A polymicrobial disruption of host homeostasis. *Nature Reviews*
365 *Microbiology*, 8(7), 481–490. <https://doi.org/10.1038/nrmicro2337>
- 366 Eke, P. I., Page, R. C., Wei, L., Thornton-Evans, G., & Genco, R. J. (2012). Update of the case
367 definitions for population-based surveillance of periodontitis. *Journal of Periodontology*, 83(12),
368 1449–1454. <https://doi.org/10.1902/jop.2012.110664>
- 369 Frencken, J. E., Sharma, P., Stenhouse, L., Green, D., Lavery, D., & Dietrich, T. (2017). Global
370 epidemiology of dental caries and severe periodontitis – a comprehensive review. *Journal of Clinical*
371 *Periodontology*, 44(S18), S94–S105. <https://doi.org/10.1111/jcpe.12677>
- 372 Gevers, D., Kugathasan, S., Denson, L. A., Vázquez-Baeza, Y., Van Treuren, W., Ren, B., ... Xavier,
373 R. J. (2014). The treatment-naïve microbiome in new-onset Crohn's disease. *Cell Host & Microbe*,
374 15(3), 382–392. <https://doi.org/10.1016/j.chom.2014.02.005>
- 375 Goodson, J. M., Tanner, A. C., Haffajee, A. D., Sornberger, G. C., & Socransky, S. S. (1982).
376 Patterns of progression and regression of advanced destructive periodontal disease. *Journal of*
377 *Clinical Periodontology*, 9(6), 472–481.
- 378 Graetz, C., Mann, L., Krois, J., Sälzer, S., Kahl, M., Springer, C., & Schwendicke, F. (2019).
379 Comparison of periodontitis patients' classification in the 2018 versus 1999 classification. *Journal of*
380 *Clinical Periodontology*. <https://doi.org/10.1111/jcpe.13157>
- 381 Griffen, A. L., Becker, M. R., Lyons, S. R., Moeschberger, M. L., & Leys, E. J. (1998). Prevalence of
382 *Porphyromonas gingivalis* and periodontal health status. *Journal of Clinical Microbiology*, 36(11),
383 3239–3242.
- 384 Hajishengallis, G., & Lamont, R. J. (2012). Beyond the red complex and into more complexity: The
385 polymicrobial synergy and dysbiosis (PSD) model of periodontal disease etiology. *Molecular Oral*
386 *Microbiology*, 27(6), 409–419. <https://doi.org/10.1111/j.2041-1014.2012.00663.x>
- 387 Hajishengallis, George, Darveau, R. P., & Curtis, M. A. (2012). The keystone-pathogen hypothesis.
388 *Nature Reviews. Microbiology*, 10(10), 717–725. <https://doi.org/10.1038/nrmicro2873>
- 389 Henne, K., Fuchs, F., Kruth, S., Horz, H.-P., & Conrads, G. (2014). Shifts in *Campylobacter* species

390 abundance may reflect general microbial community shifts in periodontitis progression. *Journal of*
391 *Oral Microbiology*, 6, 25874. <https://doi.org/10.3402/jom.v6.25874>

392 Huse, S. M., Dethlefsen, L., Huber, J. A., Welch, D. M., Relman, D. A., & Sogin, M. L. (2008).
393 Exploring Microbial Diversity and Taxonomy Using SSU rRNA Hypervariable Tag Sequencing.
394 *PLoS Genet*, 4(11), e1000255. <https://doi.org/10.1371/journal.pgen.1000255>

395 Huse, S. M., Mark Welch, D. B., Voorhis, A., Shipunova, A., Morrison, H. G., Eren, A. M., & Sogin,
396 M. L. (2014). VAMPS: A website for visualization and analysis of microbial population structures.
397 *BMC Bioinformatics*, 15, 41. <https://doi.org/10.1186/1471-2105-15-41>

398 Jiao, Y., Hasegawa, M., & Inohara, N. (2014). The Role of Oral Pathobionts in Dysbiosis during
399 Periodontitis Development. *Journal of Dental Research*, 93(6), 539–546.
400 <https://doi.org/10.1177/0022034514528212>

401 Kato, A., Imai, K., Ochiai, K., & Ogata, Y. (2013). Higher Prevalence of Epstein–Barr Virus DNA in
402 Deeper Periodontal Pockets of Chronic Periodontitis in Japanese Patients. *PLoS ONE*, 8(8), e71990.
403 <https://doi.org/10.1371/journal.pone.0071990>

404 Khemwong, T., Kobayashi, H., Ikeda, Y., Matsuura, T., Sudo, T., Kano, C., ... Izumi, Y. (2019).
405 *Fretibacterium* sp. Human oral taxon 360 is a novel biomarker for periodontitis screening in the
406 Japanese population. *PloS One*, 14(6), e0218266. <https://doi.org/10.1371/journal.pone.0218266>

407 Kilian, M., Chapple, I. L. C., Hannig, M., Marsh, P. D., Meuric, V., Pedersen, A. M. L., ... Zaura, E.
408 (2016). The oral microbiome – an update for oral healthcare professionals. *British Dental Journal*,
409 221(10), 657–666. <https://doi.org/10.1038/sj.bdj.2016.865>

410 Kirst, M. E., Li, E. C., Alfant, B., Chi, Y.-Y., Walker, C., Magnusson, I., & Wang, G. P. (2015).
411 Dysbiosis and alterations in predicted functions of the subgingival microbiome in chronic
412 periodontitis. *Applied and Environmental Microbiology*, 81(2), 783–793.
413 <https://doi.org/10.1128/AEM.02712-14>

414 Kröger, A., Hülsmann, C., Fickl, S., Spinell, T., Hüttig, F., Kaufmann, F., ... Kebschull, M. (2018).
415 The severity of human peri-implantitis lesions correlates with the level of submucosal microbial

416 dysbiosis. *Journal of Clinical Periodontology*, 45(12), 1498–1509. <https://doi.org/10.1111/jcpe.13023>

417 Lamont, R. J., Koo, H., & Hajishengallis, G. (2018). The oral microbiota: Dynamic communities and
418 host interactions. *Nature Reviews. Microbiology*, 16(12), 745–759. [https://doi.org/10.1038/s41579-](https://doi.org/10.1038/s41579-018-0089-x)
419 018-0089-x

420 Lobene, R. R., Weatherford, T., Ross, N. M., Lamm, R. A., & Menaker, L. (1986). A modified
421 gingival index for use in clinical trials. *Clinical Preventive Dentistry*, 8(1), 3–6.

422 Lourenço, T. G. B., Heller, D., Silva-Boghossian, C. M., Cotton, S. L., Paster, B. J., & Colombo, A.
423 P. V. (2014). Microbial signature profiles of periodontally healthy and diseased patients. *Journal of*
424 *Clinical Periodontology*, 41(11), 1027–1036. <https://doi.org/10.1111/jcpe.12302>

425 Macuch, P. J., & Tanner, A. C. (2000). Campylobacter species in health, gingivitis, and periodontitis.
426 *Journal of Dental Research*, 79(2), 785–792. <https://doi.org/10.1177/00220345000790021301>

427 Meuric, V., Lainé, F., Boyer, E., Le Gall-David, S., Oger, E., Bourgeois, D., ... Deugnier, Y. (2017).
428 Periodontal status and serum biomarker levels in HFE hemochromatosis patients. A case series study.
429 *Journal of Clinical Periodontology*, 44(9), 892–897. <https://doi.org/10.1111/jcpe.12760>

430 Meuric, V., Le Gall-David, S., Boyer, E., Acuña-Amador, L., Martin, B., Fong, S. B., ... Bonnaure-
431 Mallet, M. (2017). Signature of Microbial Dysbiosis in Periodontitis. *Applied and Environmental*
432 *Microbiology*, 83(14). <https://doi.org/10.1128/AEM.00462-17>

433 Paster, B. J., Boches, S. K., Galvin, J. L., Ericson, R. E., Lau, C. N., Levanos, V. A., ... Dewhirst, F.
434 E. (2001). Bacterial diversity in human subgingival plaque. *Journal of Bacteriology*, 183(12), 3770–
435 3783. <https://doi.org/10.1128/JB.183.12.3770-3783.2001>

436 Pérez-Chaparro, P. J., Gonçalves, C., Figueiredo, L. C., Faveri, M., Lobão, E., Tamashiro, N., ...
437 Feres, M. (2014). Newly identified pathogens associated with periodontitis: A systematic review.
438 *Journal of Dental Research*, 93(9), 846–858. <https://doi.org/10.1177/0022034514542468>

439 R. Core Team. (2015). R: A language and environment for statistical computing. *R Foundation for*
440 *Statistical Computing, Vienna, Austria*. Retrieved from <https://www.R-project.org/>

441 RStudio Team. (2016). RStudio: Integrated development for R. *RStudio, Inc., Boston, MA*. URL

442 [Http://Www.Rstudio.Com](http://www.Rstudio.Com).

443 Silness, J., & Loe, H. (1964). Periodontal disease in pregnancy. II. Correlation between oral hygiene
444 and periodontal condition. *Acta Odontologica Scandinavica*, 22, 121–135.

445 Silva-Boghossian, C. M., Cesário, P. C., Leão, A. T. T., & Colombo, A. P. V. (2018). Subgingival
446 microbial profile of obese women with periodontal disease. *Journal of Periodontology*, 89(2), 186–
447 194. <https://doi.org/10.1002/JPER.17-0236>

448 Socransky, S. S., Haffajee, A. D., Cugini, M. A., Smith, C., & Kent, R. L. (1998). Microbial
449 complexes in subgingival plaque. *Journal of Clinical Periodontology*, 25(2), 134–144.

450 Tonetti, M. S., Greenwell, H., & Kornman, K. S. (2018). Staging and grading of periodontitis:
451 Framework and proposal of a new classification and case definition. *Journal of Clinical*
452 *Periodontology*, 45 Suppl 20, S149–S161. <https://doi.org/10.1111/jcpe.12945>

453 Venables, W. N., & Ripley, B. D. (2002). *Modern Applied Statistics with S* (4th ed.). Retrieved from
454 <https://www.springer.com/gp/book/9780387954578>

455 Wang, J., Lv, J., Wang, W., & Jiang, X. (2016). Alcohol consumption and risk of periodontitis: A
456 meta-analysis. *Journal of Clinical Periodontology*, 43(7), 572–583.
457 <https://doi.org/10.1111/jcpe.12556>

458

Demographics	Mean PD (mm)	<i>p</i> -value
<i>Gender</i>		
Male (<i>n</i> = 42)	2.32 ± 0.06	
Female (<i>n</i> = 33)	2.29 ± 0.06	0.863
<i>Smoking status</i>		
Never (<i>n</i> = 28)	2.29 ± 0.04	
Former (<i>n</i> = 30) and Current (<i>n</i> = 17)	2.31 ± 0.06	0.81
<i>Alcohol status</i>		
Never (<i>n</i> = 15)	2.12 ± 0.07	
Former (<i>n</i> = 2) and Current (<i>n</i> = 58)	2.35 ± 0.05	0.028
<i>Frequency of dentist visits</i>		
Once or twice a year (<i>n</i> = 59)	2.32 ± 0.06	
Less than once a year (<i>n</i> = 16)	2.27 ± 0.09	0.535

Table 1: Mean probing depth (PD) according to demographic data. Data are presented as mean ± standard error (SE). Bold *p*-values indicate significant Mann-Whitney test.

Phylum	Genera	Species	HOT	Author	Year	Identified in	Mean % genera	Mean % species	+/-SE	Occurrence (%)
Actinobacteria	<i>Corynebacteria</i>			Meuric	2017	Health	0.143		0.028	83.5
Actinobacteria	<i>Rothia</i>			Meuric	2017	Health	0.215		0.050	73.4
Firmicutes	<i>Streptococcus</i>			Socransky	1998	yellow complex	5.782		0.728	100
Firmicutes	<i>Veillonella</i>	<i>parvula</i>	161	Socransky	1998	purple complex	ND			
Actinobacteria	<i>Actinomyces</i>						0.237		0.054	77.2
Actinobacteria	<i>Actinomyces</i>	<i>odontolyticus</i>	701	Socransky	1998	purple complex	ND			
Proteobacteria	<i>Eikenella</i>	<i>corrodens</i>	577	Socransky	1998	green complex	ND			
Bacteroidetes	<i>Capnocytophaga</i>						1.667		0.262	98.7
Bacteroidetes	<i>Capnocytophaga</i>	<i>gingivalis</i>	337	Socransky	1998	green complex		0.002	0.001	11.4
Bacteroidetes	<i>Capnocytophaga</i>	<i>sputigena</i>	775	Socransky	1998	green complex		0.509	0.087	83.5
Bacteroidetes	<i>Capnocytophaga</i>	<i>ochracea</i>	700	Socransky	1998	green complex		0.002	0.001	19.0
Bacteroidetes	<i>Campylobacter</i>						4.279		0.365	100.0
Bacteroidetes	<i>Campylobacter</i>	<i>concisus</i>	575	Socransky	1998	green complex		0.190	0.041	77.2
Bacteroidetes	<i>Porphyromonas</i>						7.054		0.833	98.7
Bacteroidetes	<i>Porphyromonas</i>	<i>gingivalis</i>	619	Socransky	1998	red complex		2.769	0.626	62.0
Spirochaetes	<i>Treponema</i>						5.591		0.584	100
Spirochaetes	<i>Treponema</i>	<i>denticola</i>	584	Socransky	1998	red complex		1.061	0.170	87.3
Bacteroidetes	<i>Tannerella</i>						5.368		0.584	100
Bacteroidetes	<i>Tannerella</i>	<i>forsythia</i>	613	Socransky	1998	red complex		4.522	0.531	100
Firmicutes	<i>Eubacterium</i>						1.415		0.200	97.6
Firmicutes	<i>Eubacterium</i>	<i>nodatum</i>	694	Socransky	1998	orange complex		0.177	0.043	62.0
Fusobacteria	<i>Fusobacterium</i>						26.140		1.733	100
Fusobacteria	<i>Fusobacterium</i>	<i>nucleatum</i>	200. 202. 420. 698	Socransky	1998	orange complex		15.292	1.458	100
Fusobacteria	<i>Fusobacterium</i>	<i>periodonticum</i>	201	Socransky	1998	orange complex		0.0003	0.0002	6.3
Firmicutes	<i>Parvimonas</i>						1.019		0.186	92.4
Firmicutes	<i>Parvimonas</i>	<i>micra</i>	111	Socransky	1998	orange complex		1.015	0.176	91.1
Bacteroidetes	<i>Prevotella</i>						12.006		1.043	100
Bacteroidetes	<i>Prevotella</i>	<i>intermedia</i>	643	Socransky	1998	orange complex		0.774	0.228	58.2

Bacteroidetes	<i>Prevotella</i>	<i>nigrescens</i>	693	Socransky	1998	orange complex	1.558	0.290	82.3
Firmicutes	<i>Streptococcus</i>	<i>constellatus</i>	576	Socransky	1998	orange complex	0.789	0.177	82.3
Proteobacteria	<i>Campylobacter</i>	<i>gracilis</i>	623	Socransky	1998	orange complex	1.363	0.202	92.4
Proteobacteria	<i>Campylobacter</i>	<i>rectus</i>	748	Socransky	1998	orange complex	1.740	0.240	94.9
Proteobacteria	<i>Campylobacter</i>	<i>showae</i>	763	Socransky	1998	orange complex	0.012	0.002	53.2
Proteobacteria	<i>Aggregatibacter</i>						0.851	0.167	86.1
Proteobacteria	<i>Aggregatibacter</i>	<i>actinomycetemcomitans</i>	531	Socransky	1998		0.027	0.012	17.7
Bacteroidetes	<i>Prevotella</i>	<i>denticola</i>	291	Perez-Chapparo	2014	2 studies	0.868	0.226	75.9
Bacteroidetes	<i>Alloprevotella</i>	<i>tannerae</i>	466	Perez-Chapparo	2014	2 studies	ND		
			124. 125. 126. 130. 133. 134. 136. 137. 138. 139. 146. 149. 388. 442. 478. 479. 481. 501. 639. 892. 919. 920. 936. 937						
Firmicutes	<i>Selenomonas</i>	<i>genus</i>		Perez-Chapparo	2014	2 studies	ND		
Firmicutes	<i>Johnsonella</i>	<i>oral taxon 166</i>	166	Perez-Chapparo	2014	2 studies	ND		
Firmicutes	<i>Eubacterium [X1] [G-3]</i>	<i>brachy</i>	557	Perez-Chapparo	2014	2 studies	0.005	0.001	30.4
Firmicutes	<i>Peptostreptococcaceae [XIII] [G-1]</i>	<i>oral taxon 113</i>	113	Perez-Chapparo	2014	2 studies	ND		
Firmicutes	<i>Lachnospiraceae [G-8]</i>	<i>oral taxon 500</i>	500	Perez-Chapparo	2014	2 studies	ND		
Firmicutes	<i>Dialister</i>						1.518	0.197	94.9
Firmicutes	<i>Dialister</i>	<i>pneumosintes</i>	736	Perez-Chapparo	2014	2 studies	ND		
Proteobacteria	<i>Acinetobacter</i>						0.081	0.030	45.6
Proteobacteria	<i>Acinetobacter</i>	<i>baumannii</i>	554	Perez-Chapparo	2014	2 studies	ND		
Proteobacteria	<i>Escherichia</i>						0.065	0.016	55.7
Proteobacteria	<i>Escherichia</i>	<i>coli</i>	574	Perez-Chapparo	2014	2 studies	ND		
Spirochaetes	<i>Treponema</i>	<i>phylogroup II</i>	584. 743	Perez-Chapparo	2014	2 studies	1.106	0.194	86.7
Synergistetes	<i>Fretibacterium</i>	<i>oral taxon 359</i>	359	Perez-Chapparo	2014	2 studies	ND		
TM7	<i>TM7 [G-1]</i>	<i>oral taxon 346. 349</i>	346. 349	Perez-Chapparo	2014	2 studies	ND		
SR1	<i>SR1 [G-1]</i>	<i>oral taxon 345</i>	345	Perez-Chapparo	2014	2 studies	ND		
Bacteroidetes	<i>Bacteroidales [G-2]</i>	<i>oral taxon 274</i>	274	Perez-Chapparo	2014	3 studies	ND		
Firmicutes	<i>Mogibacterium</i>						0.293	0.037	93.7
Firmicutes	<i>Mogibacterium</i>	<i>timidum</i>	0 42	Perez-Chapparo	2014	3 studies	ND		

Firmicutes	<i>Peptostreptococcus</i>							0.192	0.040	77.2
Firmicutes	<i>Peptostreptococcus</i>	<i>stomatis</i>	112	Perez-Chapparo	2014	3 studies	ND			
Firmicutes	<i>Anaeroglobus</i>	<i>geminatus</i>	121	Perez-Chapparo	2014	3 studies	ND			
Proteobacteria	<i>Desulfobulbus</i>							1.515	0.285	81.0
Proteobacteria	<i>Desulfobulbus</i>	<i>sp. oral taxon 041</i>	0 41	Perez-Chapparo	2014	3 studies	ND			
Spirochaetes	<i>Treponema</i>	<i>vincentii</i>	0 29	Perez-Chapparo	2014	3 studies		0.034	0.009	41.8
Synergistetes	<i>Fretibacterium</i>	<i>oral taxon 362</i>	362	Perez-Chapparo	2014	3 studies	ND			
Synergistetes	<i>Fretibacterium</i>	<i>fastidiosum</i>	363	Perez-Chapparo	2014	3 studies	ND			
TM7	<i>TM7 [G-5]</i>	<i>oral taxon 356</i>	356	Perez-Chapparo	2014	3 studies	ND			
Bacteroidetes	<i>Porphyromonas</i>	<i>endodontalis</i>	273	Perez-Chapparo	2014	4 studies		3.105	0.421	88.6
Firmicutes	<i>Enterococcus</i>	<i>faecalis</i>	604	Perez-Chapparo	2014	4 studies	ND			
Spirochaetes	<i>Treponema</i>	<i>lecithinolyticum</i>	653	Perez-Chapparo	2014	4 studies		0.696	0.158	62
Synergistetes	<i>Fretibacterium</i>	<i>oral taxon 360</i>	360	Perez-Chapparo	2014	4 studies	ND			
Firmicutes	<i>Eubacterium [XI] [G-5]</i>	<i>saphenum</i>	759	Perez-Chapparo	2014	5 studies		0.002	0.001	11.4
Firmicutes	<i>Filifactor</i>							2.202	0.305	97.5
Firmicutes	<i>Filifactor</i>	<i>alocis</i>	539	Perez-Chapparo	2014	5 studies		0.041	0.011	40.5
Firmicutes	<i>Selenomonas</i>	<i>sputigena</i>	151	Perez-Chapparo	2014	5 studies	ND			
Spirochaetes	<i>Treponema</i>	<i>medium</i>	667	Perez-Chapparo	2014	5 studies		0.044	0.010	55.7
Dysbiosis							Mean %	+/-SE	Occurrence	
Ratio	(% <i>Porphyromonas</i> + % <i>Treponema</i> + % <i>Tannerella</i>) / (% <i>Corynebacterium</i> + % <i>Rothia</i>)			Meuric	2017		61 816	+/- 19 257		100

Table 2: Taxonomy and dysbiosis ratio (PTT/RC) implicated in chronic periodontitis, with the mean, standard error (SE) and occurrence of the bacterial taxa and of the dysbiosis ratio in the present study. ND: not detected

Correlation with mean PD	Rho	p-value	Mean ± SE	Occurrence (%)
<i>Bacterial data</i>				
Dysbiosis ratio	0.37	0.001	3 573 ± 202	100
<i>E. nodatum</i>	0.35	0.01	0.18 ± 0.04	62
<i>P. gingivalis</i>	0.33	0.01	2.77 ± 0.63	62

<i>Desulfobulbus</i>	0.28	0.05	1.52 ± 0.29	81
<i>Treponema</i>	0.26	0.05	5.59 ± 0.58	100
<i>T. forsythia</i>	0.25	0.05	4.52 ± 0.53	100
<i>Porphyromonas</i>	0.23	0.05	7.05 ± 0.83	98.7
<i>Aggregatibacter</i>	-0.31	0.01	0.85 ± 0.17	86.1
<i>Campylobacter</i>	-0.27	0.05	4.28 ± 0.36	100
<i>Rothia</i>	-0.26	0.05	0.22 ± 0.05	73.4
<i>Clinical data</i>				
Plaque index	0.25	0.03	0.19 ± 0.03	
Gingival index	0.35	0.002	0.41 ± 0.03	
Papillary bleeding index	0.36	0.002	0.4 ± 0.03	

Table 3: Correlation between mean probing depth (PD) and bacterial or clinical data. Only significant correlations are presented.

Dysbiosis ratio: $(\%Porphyromonas + \%Treponema + \%Tannerella) / (\%Rothia + \%Corynebacterium)$; SE: standard error. Plaque index from Silness & Loe, 1964, Gingival index from Lobene *et al.* 1986 and Papillary bleeding index from Barnett *et al.* 1980.

Coefficients:	Estimate	Std. Error	t value	p-value
Model 1				
(Intercept)	1.484	0.221	6.730	3.54e-08
Transferrin saturation (binary)	0.198	0.076	2.612	0.05
Plaque index	-0.049	0.195	-0.252	NS
Papillary bleeding index	0.301	0.161	1.872	NS
log(<i>Aggregatibacter</i>)	-0.053	0.021	-2.492	0.05
log(<i>Rothia</i>)	-0.063	0.025	-2.482	0.05
log(<i>Porphyromnas</i>)	0.051	0.025	2.035	0.05
Model 2				
(Intercept)	1,280	0.147	8.686	4.39e-12
Log(Dysbiosis ratio)	0.062	0,016	3.791	0.001
Log(<i>Aggregatibacter</i>)	-0.053	0.018	-2.895	0.01
Papillary bleeding index	0.349	0.128	2.732	0.01
Transferrin saturation (binary)	0.159	0.069	2.309	0.05
Male	0.171	0.069	2.457	0.05
Alcohol	0.121	0.088	1.373	NS

Table 4: Multiple linear adjusted regression models with bacteria positively associated before or dysbiosis ratio and *Aggregatibacter* as predictors of **mean periodontal pocket depth**, adjusted for age, sex, smoking status, alcohol intake, transferrin saturation, plaque index, gingival index and bleeding index.

Characteristics of the model 1: multiple $R^2 = 0.4573$, adjusted $R^2 = 0.3798$, F-statistic = 5.899, P -value = 0.0001569. (42 degrees of freedom)

Characteristics of the model 2: multiple $R^2 = 0.5349$, adjusted $R^2 = 0.4868$, F-statistic = 11.12, P -value = 3.219e-08. (58 degrees of freedom)

2.3 Références

- [1] P. I. Eke, R. C. Page, L. Wei, G. Thornton-Evans, and R. J. Genco. Update of the case definitions for population-based surveillance of periodontitis. *J Periodontol*, 83 (12) :1449–1454, December 2012. ISSN 1943-3670. doi : 10.1902/jop.2012.110664.
- [2] N. Segata, J. Izard, L. Waldron, D. Gevers, L. Miropolsky, W. S. Garrett, and C. Huttenhower. Metagenomic biomarker discovery and explanation. *Genome Biol*, 12 (6) :R60, June 2011. ISSN 1474-760X. doi : 10.1186/gb-2011-12-6-r60.
- [3] O. Loréal, I. Gosriwatana, D. Guyader, J. Porter, P. Brissot, and R. C. Hider. Determination of non-transferrin-bound iron in genetic hemochromatosis using a new HPLC-based method. *J Hepatol*, 32(5) :727–733, May 2000. ISSN 0168-8278.
- [4] P. Brissot, M. Ropert, C. Le Lan, and O. Loréal. Non-transferrin bound iron : A key role in iron overload and iron toxicity. *Biochim Biophys Acta*, 1820(3) :403–410, March 2012. ISSN 0006-3002. doi : 10.1016/j.bbagen.2011.07.014.
- [5] S. Bizzarro, M. L. Laine, M. J. Buijs, B. W. Brandt, W. Crielaard, B. G. Loos, and E. Zaura. Microbial profiles at baseline and not the use of antibiotics determine the clinical outcome of the treatment of chronic periodontitis. *Sci Rep*, 6 :20205, February 2016. ISSN 2045-2322. doi : 10.1038/srep20205.
- [6] S. S. Socransky, A. D. Haffajee, M. A. Cugini, C. Smith, and R. L. Kent. Microbial complexes in subgingival plaque. *J Clin Periodontol*, 25(2) :134–144, February 1998. ISSN 1600-051X. doi : 10.1111/j.1600-051X.1998.tb02419.x.
- [7] P. J. Pérez-Chaparro, C. Gonçalves, L. C. Figueiredo, M. Faveri, E. Lobão, N. Tama-shiro, P. Duarte, and M. Feres. Newly identified pathogens associated with periodontitis : A systematic review. *J Dent Res*, 93(9) :846–858, September 2014. ISSN 1544-0591. doi : 10.1177/0022034514542468.

Chapitre 3

Modèles expérimentaux chez la souris

Sommaire

3.1	Alteration and loss of mandibular alveolar bone in <i>Hfe</i> knocked-out mice. A pilot study. Soumis dans <i>Journal of Clinical Periodontology</i> . . .	42
3.2	Oral dysbiosis model with <i>Porphyromonas gingivalis</i> is strain-dependent, soumis dans <i>Journal of Dental Research</i>	45
3.3	Références	47

La recherche menée chez l'animal a eu pour objectif de poursuivre la validation des résultats observés chez l'Homme, et d'élucider les mécanismes d'une association entre hémochromatose et parodontite. Elle s'est appuyée sur deux modèles murins. Le premier était une souris knock-out, délétée pour le gène *Hfe* (*Hfe*^{-/-}). Ce génotype, qui peut être produit par différentes manipulations génétiques, permet de reproduire chez l'animal le phénotype lié à l'hémochromatose héréditaire [1]. Les réserves corporelles de la souris sont augmentées du fait d'une forte diminution de l'hepcidine, et les signes cliniques précédemment décrits chez l'Homme, font leur apparition : augmentation de la saturation de la transferrine, accumulation de dépôts de fer dans le foie et dans la rate. Les souris *Hfe*^{-/-} font toujours l'objet d'expérimentation, à la fois pour poursuivre l'étude du métabolisme du fer, ainsi que pour élucider les symptômes qui composent le long tableau clinique de l'hémochromatose. Dans cette optique, nous avons procédé à la caractérisation du phénotype oral de ce modèle, et les résultats de cette analyse sont présentés dans la section suivante.

Le second modèle était une induction de la parodontite chez la souris, au moyen d'une inoculation de bactéries pathogènes dans la cavité orale. Ce modèle, décrit depuis 1994, est généralement mis en œuvre par l'administration de *P. gingivalis*, bien que quelques publications mentionnent l'utilisation de *T. denticola* ou de *T. forsythia* [2–4]. L'objectif final étant de croiser les deux modèles, il nous fallait au préalable tester ce protocole de parodontite induite, qui n'avait jusque là pas encore été utilisé dans le laboratoire. Les résultats de cette expérimentation de parodontite induite par différentes souches de *P. gingivalis*, sont présentés dans la section 3.2 de ce chapitre, en page 45.

3.1 Alteration and loss of mandibular alveolar bone in *Hfe* knocked-out mice. A pilot study. Soumis dans *Journal of Clinical Periodontology*

Le modèle murin *Hfe*^{-/-} a été l'une des preuves que la perte de fonction liée à HFE est à l'origine de l'hémochromatose héréditaire [5]. La meilleure compréhension de la maladie et sa prise en charge ont grandement diminué les symptômes dont souffrent les patients. Aujourd'hui, peu d'entre eux présentent une cirrhose ou un diabète lié à la surcharge en fer, et la pigmentation cutanée qui est à l'origine même du terme d'hémochromatose, est devenue exceptionnelle. Cependant, les patients peuvent encore présenter une fatigue chronique, ainsi que des atteintes ostéo-articulaires : rhumatismes et ostéoporose [6]. L'intérêt du modèle *Hfe*^{-/-} est donc toujours d'actualité, et les équipes de Rennes l'utilisent notamment pour comprendre la pathophysiologie de l'atteinte osseuse observée chez les patients [7].

Dans le cadre d'une expérimentation animale préliminaire, nous avons pu avoir accès à des échantillons provenant de la cavité buccale de souris *Hfe*^{-/-} et sauvages, âgées de six mois, et qui n'avaient reçu aucun traitement particulier. L'objectif du travail était double. Premièrement, évaluer le niveau d'os alvéolaire entourant les dents, afin

de détecter une éventuelle parodontite, et analyser la micro-architecture trabéculaire de la mandibule, afin de détecter d'éventuels signes d'une atteinte de type ostéoporose. Pour cela, une analyse morphométrique a été réalisée avec des logiciels dédiés, après acquisition des échantillons de mandibule par micro-tomographie. Deuxièmement, caractériser le microbiote oral de ces animaux en mettant à profit notre connaissance de la méthodologie précédemment employée avec des échantillons humains. Le microbiote digestif a également été prélevé afin d'approfondir des résultats présentés dans une étude de 2012 et obtenus par culture bactérienne d'échantillons de fèces [8].

Cet article a été soumis une première fois en juillet 2019 au *Journal of Clinical Periodontology*¹. Nous avons reçu la réponse des relecteurs fin août 2019, accompagnée d'une proposition de re-soumission après révisions. Si les relecteurs s'accordent sur l'importance et la pertinence de l'expérimentation, ils pointent néanmoins plusieurs éléments qui prêtent à corrections². L'une des limites de notre analyse est le nombre d'animaux disponibles dans le cadre de cette expérimentation préliminaire. Les relecteurs le soulignent à propos de l'étude du microbiote oral des animaux. Alors que la séparation entre le microbiote digestif de souris sauvages et *Hfe*^(-/-) apparaît nettement dans la figure 3a et 3c du manuscrit soumis, le zoom sur les échantillons oraux — présenté en figure 3b — peut inciter à disposer de plus d'échantillons pour pouvoir se prononcer définitivement. Néanmoins, les analyses de richesse, de diversité et d'abondance différentielle dans le microbiote oral ne rapportent pas de différence significative selon le génotype. Ce qui n'est pas forcément contradictoire avec les observations réalisées chez l'Homme. Les tests menés sur les mêmes données (*alpha* et *beta* diversité, ainsi que les abondances bactériennes) n'ont rapporté que peu de différences. Et bien que tous les patients aient été atteints d'hémochromatose, ils étaient malgré tout groupés selon la présence, ou non, d'une surcharge en fer.

La perte osseuse parodontale, bien que modérée, est en revanche indéniable. Sans exclure un impact de la surcharge en fer sur les bactéries du microbiote oral, il était donc intéressant d'élargir le champ d'investigation et de considérer la mandibule dans son entier. Et ce d'autant plus que nous disposions des fichiers complets issus de la capture par micro-tomographie, ce qui nous permettait un accès à l'ensemble de l'os reconstitué. En s'appuyant sur des méthodologies publiées et avec les logiciels appropriés, nous avons ainsi pu mettre en évidence une altération de la micro-architecture trabéculaire chez la souris *Hfe*^(-/-). Ces modifications sont similaires à celles observées sur leur tibia et leur fémur, qui sont des modèles d'étude plus classiques de l'ostéoporose. Cela permet donc de suspecter un phénotype ostéoporotique au niveau mandibulaire. En se projetant chez l'Homme, cela pourrait avoir un intérêt pour le dépistage : environ un tiers des patients atteints d'hémochromatose héréditaire souffrirait d'ostéoporose [9], et plusieurs études ont validé l'usage d'un orthopantomogramme pour sa détection [10]. De plus, cela suggère un déséquilibre dans l'homéostasie osseuse qui, dans les autres os analysés, se traduit par une augmentation des ostéoclastes ou une diminution de la fonction et du recrutement des ostéoblastes [7, 11].

1. Voir cette version du manuscrit dans l'annexe E, page 70.

2. Voir les commentaires de l'éditeur et des relecteurs en annexe F, page 101.

De façon globale, ces résultats viennent donc conforter la susceptibilité à la parodontite observée chez l'Homme, un élément relevé par les relecteurs. Une autre limite de notre analyse est son caractère principalement descriptif. En effet, les relecteurs, ainsi que l'éditeur, jugent nécessaire d'explorer des mécanismes mettant en jeu la réponse de l'hôte : équilibre RANKL/OPG, dosages immunologiques, analyses histologiques, etc. Bien qu'intéressantes, ces pistes ne peuvent malheureusement pas être mises en œuvre sur les individus présentés dans le manuscrit. Comme indiqué précédemment, ces derniers provenaient d'une expérimentation animale préliminaire, et les échantillons oraux qui en proviennent ont déjà tous été exploités. C'est pourquoi il était indispensable de réaliser une expérimentation à plus large échelle, en croisant les modèles de l'hémochromatose et de la parodontite induite. Malgré les délais imposés par la phase de reproduction de la colonie de souris *Hfe*^(-/-), cette expérimentation a pu être réalisée. Cependant, les échantillons qui en sont issus sont encore en cours d'analyse³.

Il a ainsi été décidé de proposer à nouveau à l'éditeur le manuscrit en un format plus court. Celui-ci, bien que n'explorant pas les mécanismes potentiels, vient tout de même étayer les observations chez l'Homme. Ce nouveau manuscrit, présenté ci-après, se concentre donc sur les résultats obtenus au niveau osseux. Il a été soumis le 14 novembre 2019⁴.

3. La description de l'expérimentation et des échantillons collectés est abordée dans le chapitre [Perspectives](#) en page 49

4. Voir l'accusé de réception en annexe [G](#), page 104



Alteration and loss of mandibular alveolar bone in *Hfe* knocked-out mice. A pilot study.

Journal:	<i>Journal of Clinical Periodontology</i>
Manuscript ID	CPE-11-19-8687
Manuscript Type:	Original Article Clinical Periodontology
Date Submitted by the Author:	14-Nov-2019
Complete List of Authors:	Boyer, Emile; Université de Rennes 1 - INSERM NuMeCan, EA1254/CIMIAD UMR1241 Robin, François; Université de Rennes 1 - INSERM NuMeCan, EA1254/CIMIAD UMR1241 Le gall-David, Sandrine; Université de Rennes 1 - INSERM NuMeCan, EA1254/CIMIAD UMR1241 Guggenbuhl, Pascal; Université de Rennes 1 - INSERM NuMeCan, EA1254/CIMIAD UMR1241 Loréal, Olivier; Université de Rennes 1 - INSERM NuMeCan, EA1254/CIMIAD UMR1241 Fong, Shao Bing; Université de Rennes 1 BONNAURE-MALLET, Martine; Université de Rennes 1, Equipe de Microbiologie UPRES-EA 1254 Meuric, Vincent; Université de Rennes 1 - INSERM NuMeCan, EA1254/CIMIAD UMR1241
Topic:	Aetiology
Main Methodology:	Animal Model
Keywords:	Alveolar Bone Loss, Haemochromatosis, Iron Overload, Mice

SCHOLARONE™
Manuscripts

1
2
3
4 Title: Alteration and loss of mandibular alveolar bone in *Hfe*
5
6 knocked-out mice. **A pilot study.**
7
8
9

10
11 Running title: Alveolar bone loss in *Hfe*^(+/-) mice
12
13
14

15
16
17 **Emile Boyer^{1*}, François Robin^{1†}, Sandrine Le Gall-David^{1†}, Pascal Guggenbuhl¹, Olivier**
18 **Loréal¹, Shao Bing Fong¹, Martine Bonnaure-Mallet¹, Vincent Meuric¹**
19

20
21
22
23 ¹ INSERM, INRA, Univ Rennes 1, CHU de Rennes, Nutrition Metabolisms and Cancer, Rennes,
24 France
25

26
27 † These authors contributed equally to this work
28

29 *** Corresponding author**
30

31 Emile Boyer, <https://orcid.org/0000-0002-0208-2084>.

32 Phone: +33 (0)2 23 23 49 19
33

34 Email: emile.boyer@univ-rennes1.fr
35
36
37
38
39

40 **Acknowledgments**

41
42 The authors would like to thank Patricia Leroyer for her valuable technical assistance, as
43 well as the teams of Prof. Daniel Chappard (GEROM research unit, Angers, France) for the
44 micro computed tomography, and the AEM2 facility (Rennes, France) for the elemental
45 analysis and metal metabolism. We thank the GeT-PlaGe facility and the NED team (Toulouse,
46 France) for sequencing the samples. This study was funded by the *Institut Français pour la*
47 *Recherche en Odontologie* (IFRO).
48
49
50
51
52
53
54
55
56
57
58
59
60

Abstract (200 words)

Aim: The *Hfe*^(-/-) mouse is the murine model of the *HFE*-related haemochromatosis, which is the most common inherited iron overload disease in northern European descents and was previously found associated with periodontitis. The aim of this study was to characterize the periodontal status and mandibular bone microarchitecture of *Hfe*^(-/-) mice.

Materials and methods: C57BL/6 mice knocked-out for the *Hfe* gene were analysed at 6 months-old regarding iron phenotype, alveolar bone loss and microarchitecture by morphometric analysis from micro-computed tomography, and compared with wild-type littermates.

Results: Alike in humans, the *Hfe*^(-/-) mice demonstrated an iron overload phenotype. Similar to human observations, the *Hfe*^(-/-) mice also exhibited alveolar bone loss. Alterations of the alveolar bone microarchitecture with reduced bone volume and increased trabecular separation was also found, suggesting an unbalanced bone homeostasis and osteoporosis phenotype.

Conclusions: The *Hfe*^(-/-) mice showed bone microarchitectural impairments and susceptibility to periodontal damage. These findings support the risk for periodontitis in haemochromatosis patients, and stress their need for special care. Further studies are also mandatory to explore the underlying mechanisms.

Keywords

Alveolar Bone Loss; Haemochromatosis; Iron Overload; Mice

Clinical Relevance (100 words)

Scientific rationale for study: Haemochromatosis patients with iron burden have shown an increased risk of severe periodontitis, specifically in the patients with high transferrin saturation rates.

Principal findings: Alterations in the alveolar bone of *Hfe*^(-/-) mice have been observed, with periodontal bone loss. Reduced alveolar bone and trabecular impairment were also found, suggesting an unbalanced bone homeostasis and osteoporosis phenotype.

Practical implications: These results support both the periodontal vulnerability observed in haemochromatosis patients, and their need for dental examination.

1. Introduction

Haemochromatosis is the most common inherited iron overload disease (Powell, Seckington, & Deugnier, 2016). The mutations leading to the clinical syndrome involved the *HFE* gene, which participates in the production of hepcidin, a regulatory protein engaged in the iron homeostasis. The substitution p.Cys282Tyr (C282Y) is the major *HFE* mutation that leads to a hepcidin-deficient state, which is responsible for excessive expression of ferroportin at the cell surfaces and the subsequent iron egress in the bloodstream. Iron deposition in the tissues, and especially the occurrence of highly reactive forms of iron, **are considered to drive the cell and tissue damages leading to the symptoms** (Brissot, Ropert, Le Lan, & Loréal, 2012).

Nowadays, most of the patients with hereditary haemochromatosis caused by the *HFE* gene (HH-HFE) are asymptomatic or present with chronic fatigue and musculoskeletal conditions. Recently, HH-HFE patients have also shown an increased risk of periodontitis in a case-series study (Meuric et al., 2017). **The iron burden appeared to be the driver for this increased risk, as severe periodontitis was predominant in the patients with high transferrin saturation rates.** Nonetheless, a bacterial interplay has also been mentioned because increased transferrin saturation was found associated with a dysbiosis of the subgingival microbiota, which is a leading cause of periodontitis (Boyer et al., 2018).

Animal models of hereditary haemochromatosis have been widely used to better understand the metabolism of iron, as well as the various iron overload related lesions and the pathogenesis of the disease. The *Hfe*^(-/-) mouse is the murine model of the HH-HFE disease (Fleming, Feng, & Britton, 2011). Alike humans, the *Hfe*^(-/-) mice demonstrate elevated transferrin saturation, increased iron concentration in blood and liver, as well as hepatic dysfunction and cardiac damage (Sukumaran et al., 2017).

However, the periodontal status of *Hfe*^(-/-) mice has not been characterized yet, **and detection of alveolar bone loss in these mice would support the human findings.** The aim of this study was therefore to assess the mandibular and teeth-surrounding alveolar bone of 6 months-old *Hfe*^(-/-) mice compared to wild-type animals, in order to complete the description of the *Hfe*^(-/-) animal model phenotype.

2. Materials and Methods

2.1. Animal model

The study was approved by the ethical committee of Rennes for animal experimentation. All experimented mice were males of a C57BL/6J background. *Hfe*^(-/-) mice were produced in the

1
2
3 animal facilities of UMS Biosit in Rennes (Arche). Controls consisted of Wild-Type (WT)
4 littermates. **At the time of weaning, the animals were separated in different cages according to**
5 **their genotype.** Animals were maintained under standard conditions of temperature, atmosphere
6 and light, and experimental procedures were performed in agreement with European law and
7 regulations. Mice were given free access to tap water and food (Teklad 19 % Protein Rodent
8 Diet). Mice were anaesthetised and sacrificed at 6 months for *Hfe*^(-/-) and controls (*n* = 5
9 mice/group). Blood was obtained from a trans-diaphragmatic intracardiac puncture and
10 sampled in sodium heparin tubes suitable for trace element analysis. Livers and mandibles were
11 dissected. Samples from liver were quickly frozen in liquid nitrogen and stored at -80°C to
12 perform the measurement of trace elements concentrations. The mandible was fixed in 70 %
13 ethanol 10 % formaldehyde for 24h at 4°C, and then stored in absolute acetone at 4°C until
14 micro-computed tomography (micro-CT).
15
16
17
18
19
20
21
22
23

24 **2.2. Plasma iron parameters**

25
26 The concentration of iron in the plasma and the unsaturated iron-binding capacity were
27 measured in the Biochemistry Laboratory of the University Rennes Hospital on Cobas 8000
28 analyzer (Roche). Plasma transferrin saturation was then calculated as (Iron plasma) / (Iron
29 plasma + UIBC) × 100.
30
31
32
33

34 **2.3. Trace elements**

35
36 Liver samples were desiccated for 15 hours at 120°C. Then, dried samples were weighed
37 and mineralized by nitric acid solution (Fischer Chemical – Optima Grade) in special
38 polypropylene tubes for 2 hours at 110°C in a heating block. Specimens were then preserved at
39 4°C until quantification of iron. Iron was measured by Inductively Coupled Plasma Mass
40 Spectrometry (ICP-MS), on a X-Series II from Thermo Scientific equipped with collision cell
41 technology (AEM2 facility, University of Rennes 1 and Biochemistry Laboratory of the
42 University Rennes Hospital) as previously described (Cavey et al., 2015).
43
44
45
46
47
48

49 **2.4. Micro-computed tomography**

50
51 Micro-CT was performed on the hemi-mandible in the GEROM research unit (Angers,
52 France) with a Skyscan 1272 (Bruker). The samples were placed in microtubes, filled with
53 water to prevent desiccation. The tubes were fixed on brass stubs with plasticine and scanned
54 with the following parameters: 9 µm resolution, Xray energy of 70 kV and 142 µA for 1.9 s
55 exposure, 0.2° rotation step, 5.000097 µm image pixel size. The data were reconstructed with
56 NRecon (v. 1.7.0.4, Bruker-MicroCT)
57
58
59
60

2.5. Quantification of alveolar bone loss

The DataViewer software (v. 1.5.6, Bruker-MicroCT) was used to visualise bone and produce the sagittal slices. All images were reoriented such that the cemento-enamel junction (CEJ) and the root apex (RA) appeared (Cho et al., 2016). Among the sagittal images, the image which showed the most recession of alveolar bone was selected for measurement. The distance from the alveolar bone crest (ABC) to the CEJ was measured in μm with the CTAn software (v. 1.18.8, Bruker-MicroCT) at two interdental sites: between the first and the second mandibular molars (M1M2) or between the second and the third mandibular molar (M2M3). As described elsewhere, the CEJ-ABC distance was the shortest distance from ABC to the line connecting the adjacent CEJs (Cho et al., 2016). Measurements of root lengths from the CEJ to the RA were also taken to assess the percentage of remaining alveolar bone using an equation previously described: Percent remaining bone (%) = $([\text{root length} - \text{CEJ-ABC}] / \text{root length}) \times 100$ (Park et al., 2007).

2.6. Characterization of alveolar bone microarchitecture

The bone microarchitecture of the hemi-mandible was characterized with the CTAnalyzer software (v. 1.18.8.0, Bruker-MicroCT), as described elsewhere (Bouvard, Gallois, Legrand, Audran, & Chappard, 2013). Briefly, each hemi-mandibular alveolar bone was measured on two types of 2D sections: five frontal sections through the middle of the pulp chamber of M1 were used to evaluate the thickness of alveolar bone (between the incisor and the M1 roots, five measurements per mouse) (see **Figure 2f**); eleven sagittal sections through the pulp chamber of M1, M2 and M3 were used to measure the trabecular characteristics of the bone. The volume of interest was an ellipse ($1080 \mu\text{m} \times 440 \mu\text{m}$) centred in the alveolar process between the M1 roots (see **Figure 2g**). The following parameters were measured by 2D morphometric analysis: the trabecular bone volume (BV/TV, in %), the trabecular thickness (Tb.Th, in μm), the trabecular separation (Tb.Sp, in μm) and the trabecular number (Tb.N, in mm^{-1}).

2.7. Statistics

Data were analysed using the R (v. 3.5.0) and RStudio softwares (v. 1.1.383, <https://www.rstudio.com/>). Non-parametric tests were used and considered significant for $p < 0.05$. The results were expressed as mean \pm standard error of the mean. The Mann-Whitney and Wilcoxon matched-pairs signed rank tests were used to compare means for quantitative

1
2
3 data related to iron and alveolar bone parameters. All plots were made with 'ggplot2' for
4 RStudio (Wickham, Chang, & RStudio, 2016).
5
6

7 **3. Results**

8 **3.1. Iron phenotype**

9
10
11 General and iron parameters are summarized in **Table 1**. The $Hfe^{(-/-)}$ mice were found to
12 have an iron overload phenotype with significantly higher transferrin saturation, plasma and
13 hepatic iron concentration than WT littermate mice ($p < 0.01$). No difference was found in the
14 body weight of mice between groups.
15
16
17

18 **3.2. Alveolar bone loss**

19
20
21 We observed a generalized alveolar bone loss in $Hfe^{(-/-)}$ mice. The average CEJ-ABC
22 distance was increased in $Hfe^{(-/-)}$ mice *versus* WT mice ($p < 0.05$) (**Figure 1a**). This variation
23 was higher in M1M2 region ($p < 0.05$) than in M2M3 region ($p < 0.10$). When the CEJ-ABC
24 distances were related to the molar roots length, we obtained the percentage of remaining bone
25 and significant differences were also found (**Figure 1b**). $Hfe^{(-/-)}$ mice had a decrease in
26 remaining bone compared to WT mice, in both M1M2 ($p < 0.05$) and M2M3 regions ($p < 0.05$).
27
28 No significant difference was found in the molar roots length between $Hfe^{(-/-)}$ and WT mice
29 (data not shown; $p > 0.05$).
30
31
32
33
34

35 **3.3. Alveolar bone microarchitecture**

36
37
38 When looking at the bone parameters of the mandible, significant differences were found
39 between $Hfe^{(-/-)}$ and WT (**Figure 2**). The thin bony slab between the incisor and the first molar
40 roots appeared to be significantly reduced in $Hfe^{(-/-)}$ mice *versus* WT ($p < 0.001$) (**Figure 2a**).
41
42 $Hfe^{(-/-)}$ mice had also significantly lower BV/TV ($p < 0.05$) and higher Tb.Sp ($p < 0.01$) than
43 WT mice (**Figure 2b, c**). We observed a trend towards decreasing Tb.N in $Hfe^{(-/-)}$ *versus* WT
44 ($p < 0.10$) (**Figure 2e**).
45
46
47

48 **4. Discussion**

49
50
51 Iron overload related to genetic haemochromatosis has deleterious effects on multiple organs
52 and sites. Bone disorders are now a subject of greater attention, because of the scarcity of the
53 classic signs of the disease (cirrhosis, diabetes and skin pigmentation). Available clinical data
54 show that HH-HFE patients are more likely to have osteoporosis (Guañabens & Parés, 2018).
55
56 In addition, a recent case-series study has reported a greater risk of severe periodontitis in these
57 patients (Meuric et al., 2017). However, the oral status of the mouse model of HH-HFE has not
58
59
60

1
2
3 yet been characterized. In this study, we investigated the periodontal and alveolar bone status
4 in the mandibles of *Hfe*^(-/-) mice, in comparison with WT littermates.
5
6

7 As previously described, the *Hfe*^(-/-) mice demonstrated an increased body iron level with
8 elevated transferrin saturation, hepatic and blood iron concentrations (Fleming et al., 2011). In
9 order to test the presence of periodontal defects, we first performed measurements of the
10 alveolar bone surrounding the mandibular molars. The CEJ-ABC distance measured in WT
11 mice were consistent with a previous study on mice at the same age (Damanaki et al., 2018).
12 Interestingly, this CEJ-ABC distance was significantly increased in *Hfe*^(-/-) mice. In addition,
13 the remaining alveolar bone surrounding teeth was significantly decreased in *Hfe*^(-/-). These
14 results indicated an alveolar bone loss in *Hfe*^(-/-) mice, although the C57BL/6 strain is not
15 considered susceptible to periodontitis (Baker, Dixon, & Roopenian, 2000).
16
17
18
19
20
21
22

23 Furthermore, these results support the relationship that was recently uncovered between HH-
24 HFE patients and periodontitis (Boyer et al., 2018; Meuric et al., 2017). In these studies, HH-
25 HFE patients were found to have a high prevalence of periodontitis. Moreover, the iron burden
26 was found associated with periodontitis severity and clinical attachment loss. Alike in humans,
27 the iron overloaded *Hfe*^(-/-) mice exhibited alveolar bone loss, thus supporting the relationship
28 between haemochromatosis and periodontitis. However, the question about the underlying
29 mechanisms remains to be seen. In a previous study, it has been proposed that an increased iron
30 bioavailability could promote periodontal pathogens and may drive a dysbiosis of the oral
31 microbiota (Boyer et al., 2018). While a direct effect of iron on microbiota needs to be validated
32 with further studies, complementary hypotheses may also be considered.
33
34
35
36
37
38
39
40

41 An imbalance in bone homeostasis could be involved in the periodontal susceptibility we
42 observed in the *Hfe* knock-out line. Indeed, previous studies have found osteoporosis in the
43 tibias of 12 months-old *Hfe*^(-/-) mice, and minor changes in bone microarchitecture was
44 observed at 6 months (Doyard et al., 2016; Guggenbuhl et al., 2011). Specifically, these minor
45 changes included a slight decrease in the BV/TV and, inconstantly, an enhanced Tb.Sp. In the
46 present study, the *Hfe*^(-/-) mice exhibited the same disorders in the mandibular bone. At only
47 six months old, they already had a significant reduction in mandibular BV/TV. This
48 microarchitectural impairment was confirmed by a significantly increased Tb.Sp as well. Taken
49 together with a decreased Tb.N, it could explain the reduced BV/TV and be interpreted as early
50 signs of osteoporosis. Moreover, we assessed the thickness of the mandibular alveolar bone as
51 shown in Bouvard *et al.* (Bouvard et al., 2013). In their study, the authors analysed the effects
52 of glucocorticoids on trabecular bone in mice. Although they used another line of mice (Swiss-
53
54
55
56
57
58
59
60

1
2
3 Webster), we found similar reduction in the thickness of the mandibular alveolar bone, thus
4 confirming an alteration in the mandibular bone of *Hfe*^(-/-) mice. In tibias, the disorganization
5 of the trabecular microarchitecture could be due to an impaired bone remodelling (Guggenbuhl
6 et al., 2011). One could hypothesize that the same process occurs in the mandibles, causing
7 susceptibility to alveolar bone loss.
8

9
10
11
12 Several studies also point out alterations of the immune response in *Hfe*^(-/-) mice.
13 Macrophages usually provide most of the usable iron by degrading haemoglobin. In HH-HFE,
14 they become the main source of excessive iron egress in the blood, and have shown attenuated
15 inflammatory phenotype (Wang et al., 2008). Although they are not involved in the iron
16 metabolism, neutrophils showed inefficient recruitment and upregulation of Th17 response in
17 *Hfe*^(-/-) mice (Benesova et al., 2012). While these findings remain to be validated in human,
18 such an impaired phenotype could have deleterious effects, considering the importance of the
19 neutrophils in the periodontal tissues. Moreover, a dysregulated inflammatory response may
20 have a negative impact on bone homeostasis through the RANKL/OPG ratio with an increased
21 bone resorption (Darveau, 2010)
22
23
24
25
26
27
28
29

30 In conclusion, we demonstrated alterations of the mandibular bone in *Hfe*^(-/-) mice at 6
31 months, with periodontal bone loss, reduced alveolar bone and trabecular impairment. These
32 results support a potential risk for periodontitis in haemochromatosis patients, underlining their
33 need for special care and attention. Dental examination should be part of the initial management
34 of these patients. The underlying mechanisms cannot be understood without further work on
35 the host's immune response and microbiota, but these findings emphasize the role of iron in
36 oral disorders.
37
38
39
40
41
42
43
44
45
46
47
48
49
50
51
52
53
54
55
56
57
58
59
60

1
2
3 Baker, P. J., Dixon, M., & Roopenian, D. C. (2000). Genetic control of susceptibility to
4 Porphyromonas gingivalis-induced alveolar bone loss in mice. *Infection and Immunity*, *68*(10),
5 5864–5868.
6
7

8
9 Benesova, K., Spasić, M. V., Schaefer, S. M., Stolte, J., Baehr-Ivacevic, T., Waldow, K., ...
10 Muckenthaler, M. U. (2012). Hfe Deficiency Impairs Pulmonary Neutrophil Recruitment in
11 Response to Inflammation. *PLOS ONE*, *7*(6), e39363. doi: 10.1371/journal.pone.0039363
12
13

14
15 Bouvard, B., Gallois, Y., Legrand, E., Audran, M., & Chappard, D. (2013). Glucocorticoids
16 reduce alveolar and trabecular bone in mice. *Joint, Bone, Spine: Revue Du Rhumatisme*, *80*(1),
17 77–81. doi: 10.1016/j.jbspin.2012.01.009
18
19

20
21 Boyer, E., Le Gall-David, S., Martin, B., Fong, S. B., Loréal, O., Deugnier, Y., ... Meuric,
22 V. (2018). Increased transferrin saturation is associated with subgingival microbiota dysbiosis
23 and severe periodontitis in genetic haemochromatosis. *Scientific Reports*, *8*(1), 15532. doi:
24 10.1038/s41598-018-33813-0
25
26

27
28 Brissot, P., Ropert, M., Le Lan, C., & Loréal, O. (2012). Non-transferrin bound iron: A key
29 role in iron overload and iron toxicity. *Biochimica Et Biophysica Acta*, *1820*(3), 403–410. doi:
30 10.1016/j.bbagen.2011.07.014
31
32

33
34 Cavey, T., Ropert, M., de Tayrac, M., Bardou-Jacquet, E., Island, M.-L., Leroyer, P., ...
35 Loréal, O. (2015). Mouse genetic background impacts both on iron and non-iron metals
36 parameters and on their relationships. *Biometals: An International Journal on the Role of Metal*
37 *Ions in Biology, Biochemistry, and Medicine*, *28*(4), 733–743. doi: 10.1007/s10534-015-9862-
38 8
39
40
41

42
43 Cho, Y.-J., Song, H. Y., Ben Amara, H., Choi, B.-K., Eunju, R., Cho, Y.-A., ... Koo, K.-T.
44 (2016). In Vivo Inhibition of *Porphyromonas gingivalis* Growth and Prevention of Periodontitis
45 With Quorum-Sensing Inhibitors. *Journal of Periodontology*, *87*(9), 1075–1082. doi:
46 10.1902/jop.2016.160070
47
48

49
50 Damanaki, A., Memmert, S., Nokhbehaim, M., Sanyal, A., Gnad, T., Pfeifer, A., &
51 Deschner, J. (2018). Impact of obesity and aging on crestal alveolar bone height in mice. *Annals*
52 *of Anatomy - Anatomischer Anzeiger*, *218*, 227–235. doi: 10.1016/j.aanat.2018.04.005
53
54

55
56 Darveau, R. P. (2010). Periodontitis: A polymicrobial disruption of host homeostasis. *Nature*
57 *Reviews Microbiology*, *8*(7), 481–490. doi: 10.1038/nrmicro2337
58

59
60 Doyard, M., Chappard, D., Leroyer, P., Roth, M.-P., Loréal, O., & Guggenbuhl, P. (2016).

1
2
3 Decreased Bone Formation Explains Osteoporosis in a Genetic Mouse Model of
4 Hemochromatosis. *PloS One*, 11(2), e0148292. doi: 10.1371/journal.pone.0148292

5
6
7 Fleming, R. E., Feng, Q., & Britton, R. S. (2011). Knockout Mouse Models of Iron
8 Homeostasis. *Annual Review of Nutrition*, 31(1), 117–137. doi: 10.1146/annurev-nutr-072610-
9 145117

10
11
12 Guañabens, N., & Parés, A. (2018). Osteoporosis in chronic liver disease. *Liver*
13 *International*, 38(5), 776–785. doi: 10.1111/liv.13730

14
15
16 Guggenbuhl, P., Fergelot, P., Doyard, M., Libouban, H., Roth, M.-P., Gallois, Y., ...
17 Chappard, D. (2011). Bone status in a mouse model of genetic hemochromatosis. *Osteoporosis*
18 *International: A Journal Established as Result of Cooperation between the European*
19 *Foundation for Osteoporosis and the National Osteoporosis Foundation of the USA*, 22(8),
20 2313–2319. doi: 10.1007/s00198-010-1456-2

21
22
23 Meuric, V., Lainé, F., Boyer, E., Le Gall-David, S., Oger, E., Bourgeois, D., ... Deugnier,
24 Y. (2017). Periodontal status and serum biomarker levels in *HFE* hemochromatosis patients. A
25 case series study. *Journal of Clinical Periodontology*, 44(9), 892–897. doi: 10.1111/jcpe.12760

26
27
28 Park, C. H., Abramson, Z. R., Taba, M., Jin, Q., Chang, J., Kreider, J. M., ... Giannobile,
29 W. V. (2007). Three-Dimensional Micro-Computed Tomographic Imaging of Alveolar Bone
30 in Experimental Bone Loss or Repair. *Journal of Periodontology*, 78(2), 273–281. doi:
31 10.1902/jop.2007.060252

32
33
34 Powell, L. W., Seckington, R. C., & Deugnier, Y. (2016). Haemochromatosis. *Lancet*
35 *(London, England)*, 388(10045), 706–716. doi: 10.1016/S0140-6736(15)01315-X

36
37
38 Sukumaran, A., Chang, J., Han, M., Mintri, S., Khaw, B.-A., & Kim, J. (2017). Iron overload
39 exacerbates age-associated cardiac hypertrophy in a mouse model of hemochromatosis.
40 *Scientific Reports*, 7(1), 5756. doi: 10.1038/s41598-017-05810-2

41
42
43 Wang, L., Johnson, E. E., Shi, H. N., Walker, W. A., Wessling-Resnick, M., & Cherayil, B.
44 J. (2008). Attenuated Inflammatory Responses in Hemochromatosis Reveal a Role for Iron in
45 the Regulation of Macrophage Cytokine Translation. *The Journal of Immunology*, 181(4),
46 2723–2731. doi: 10.4049/jimmunol.181.4.2723

47
48
49 Wickham, H., Chang, W., & RStudio. (2016). ggplot2: Create Elegant Data Visualisations
50 Using the Grammar of Graphics (Version 2.2.1). Retrieved from [https://cran.r-](https://cran.r-project.org/web/packages/ggplot2/index.html)
51 [project.org/web/packages/ggplot2/index.html](https://cran.r-project.org/web/packages/ggplot2/index.html)

1
2
3
4
5
6
7
8
9
10
11
12
13
14
15
16
17
18
19
20
21
22
23
24
25
26
27
28
29
30
31
32
33
34
35
36
37
38
39
40
41
42
43
44
45
46
47
48
49
50
51
52
53
54
55
56
57
58
59
60

For Peer Review

Parameters	WT	<i>Hfe</i> ^(-/-)	<i>p</i> -value
Body weight (g)	32.32 (1.10)	30.96 (1.08)	0.310
Hepatic iron concentration (μmol iron/liver g)	4.63 (0.39)	17.32 (2.54)	0.007**
Plasma iron concentration (μmol iron/L)	18.6 (0.67)	33.32 (2.06)	0.007**
Transferrin saturation (%)	37.88 (0.01)	82.72 (0.05)	0.007**

Table 1: General and iron parameters in *Hfe*^(-/-) and Wild-Type (WT) mice. Data are presented as mean (standard error) (*n* = 5 mice/group). Mann-Whitney, statistically significant at: ***p* < 0.01.

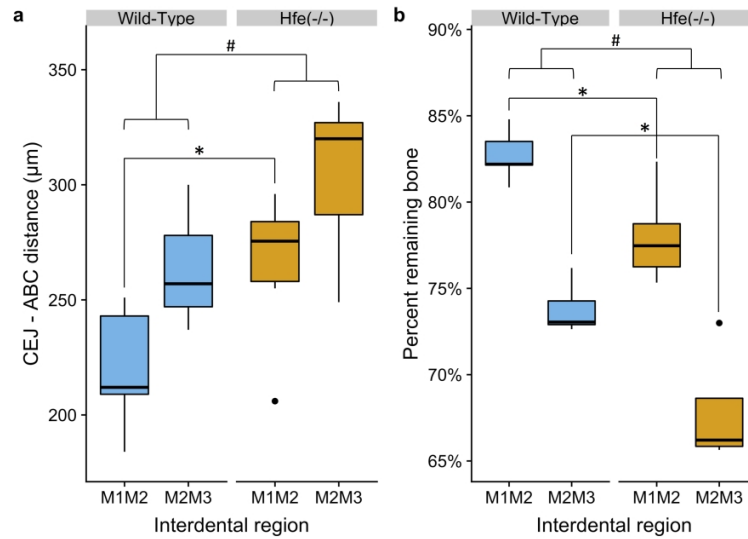
For Peer Review

1
2
3
4
5
6
7
8
9
10
11
12
13
14
15
16
17
18
19
20
21
22
23
24
25
26
27
28
29
30
31
32
33
34
35
36
37
38
39
40
41
42
43
44
45
46
47
48
49
50
51
52
53
54
55
56
57
58
59
60

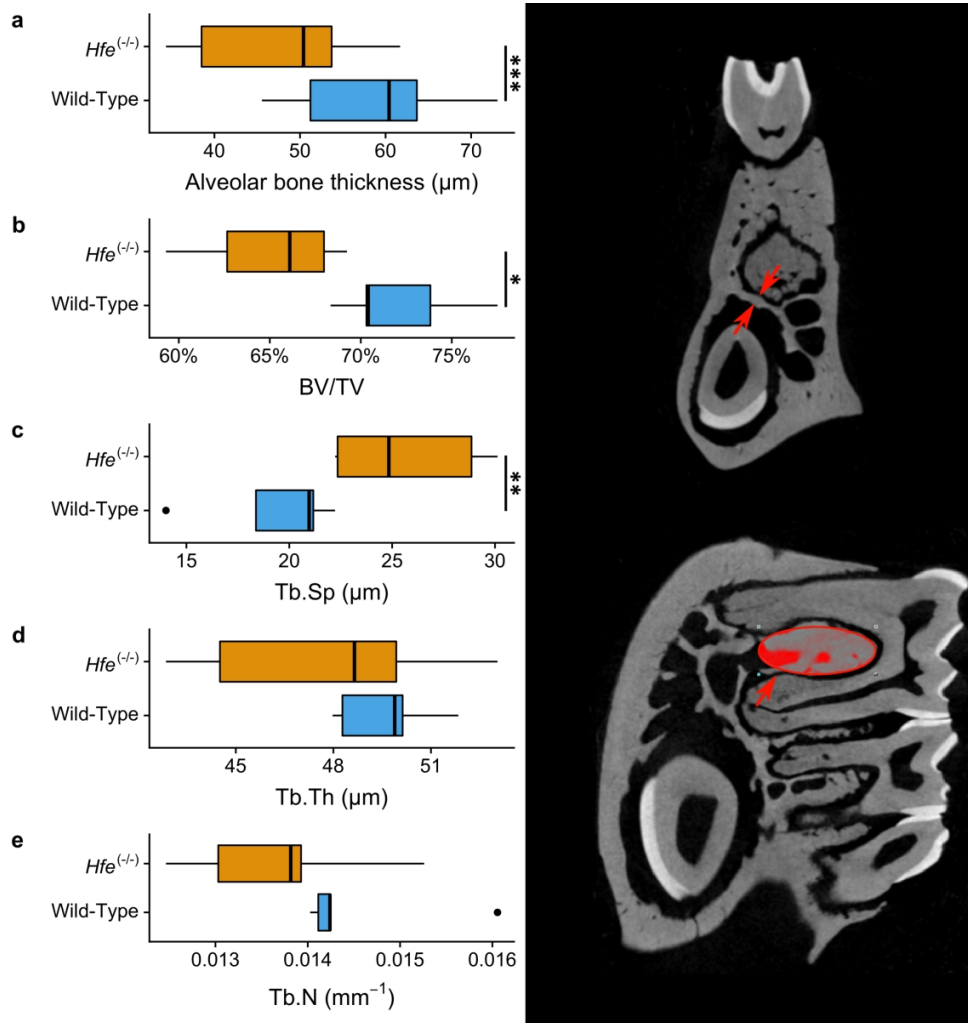
Figure 1: Alveolar bone loss in mice. Measurements of bone levels were made by comparing the distance from the cementoenamel junction (CEJ) to the alveolar bone crest (ABC) (**a**) and the percentage of remaining bone (**b**) at two interdental sites: between the first and second mandibular molars (M1M2) and between the second and the third mandibular molars (M2M3). Root lengths (from the CEJ to the root apex) were also measured to assess the percentage of remaining alveolar bone: Percent remaining bone (%) = $([\text{root length} - \text{CEJ-ABC}] / \text{root length}) \times 100$. *Hfe*^(-/-) and Wild-Type mice were 6 months old (*n* = 5 mice/group). Mann-Whitney, statistically significant at: **p* < 0.05; Wilcoxon matched-pairs, statistically significant at: #*p* < 0.05.

1
2
3
4
5
6
7
8
9
10
11
12
13
14
15
16
17
18
19
20
21
22
23
24
25
26
27
28
29
30
31
32
33
34
35
36
37
38
39
40
41
42
43
44
45
46
47
48
49
50
51
52
53
54
55
56
57
58
59
60

Figure 2: Characterization of alveolar bone structure. Following the microCT analysis of the hemi-mandibles of *Hfe^(-/-)* and Wild-Type mice ($n = 5$ mice/group, 6 months old), five frontal sections were used to evaluate the thickness of alveolar bone (**a**) between the incisor and molar roots (red arrows in **f**). Eleven sagittal sections of the alveolar process between the first molar roots were used to measure the bone volume fraction (Bone Volume/Tissue Volume) (**b**), the trabecular separation (Tb.Sp) (**c**), the trabecular thickness (Tb.Th) (**d**), and the trabecular number (Tb.N) (**e**) in the alveolar process between the roots of the first molar (red ellipse in **g**). Mann-Whitney, statistically significant at: $*p < 0.05$, $**p < 0.01$, $***p < 0.001$.



Alveolar bone loss in mice. Measurements of bone levels were made by comparing the distance from the cemento-enamel junction (CEJ) to the alveolar bone crest (ABC) (**a**) and the percentage of remaining bone (**b**) at two interdental sites: between the first and second mandibular molars (M1M2) and between the second and the third mandibular molars (M2M3). Root lengths (from the CEJ to the root apex) were also measured to assess the percentage of remaining alveolar bone: Percent remaining bone (%) = $([\text{root length} - \text{CEJ-ABC}] / \text{root length}) \times 100$. *Hfe*^(-/-) and Wild-Type mice were 6 months old ($n = 5$ mice/group). Mann-Whitney, statistically significant at: $*p < 0.05$; Wilcoxon matched-pairs, statistically significant at: $\#p < 0.05$.



Characterization of alveolar bone structure. Following the microCT analysis of the hemi-mandibles of *Hfe*^(-/-) and Wild-Type mice ($n = 5$ mice/group, 6 months old), five frontal sections were used to evaluate the thickness of alveolar bone (a) between the incisor and molar roots (red arrows in f). Eleven sagittal sections of the alveolar process between the first molar roots were used to measure the bone volume fraction (Bone Volume/Tissue Volume) (b), the trabecular separation (Tb.Sp) (c), the trabecular thickness (Tb.Th) (d), and the trabecular number (Tb.N) (e) in the alveolar process between the roots of the first molar (red ellipse in g). Mann-Whitney, statistically significant at: * $p < 0.05$, ** $p < 0.01$, *** $p < 0.001$.

3.2 Oral dysbiosis model with *Porphyromonas gingivalis* is strain-dependent, soumis dans *Journal of Dental Research*

Avant d'induire une parodontite à des animaux *Hfe*^(-/-), nous avons souhaité évaluer notre capacité à réaliser ce modèle chez des animaux sauvages. Le protocole originalement décrit par Baker et coll. en 1994 repose sur des administrations orales répétées de 100 µL d'une solution de PBS fortement concentrée en cellules de *P. gingivalis* (10⁹ CFU.mL⁻¹) [2]. Au nombre de trois, ces administrations sont précédées par un traitement antibiotique, le groupe contrôle recevant la même solution de PBS sans bactérie. Ce protocole a été repris de nombreuses fois dans la littérature avec quelques variantes, et a déjà permis d'établir des liens entre la maladie parodontale et des pathologies systémiques, comme le diabète et l'athérosclérose [12].

Dans le cadre de de cette première utilisation du modèle, nous avons également voulu tirer parti de la souchothèque du laboratoire et tester différentes souches de *P. gingivalis*. Notre choix s'est porté sur *P. gingivalis* W83, une souche isolée en Allemagne dans les années 1950 et qui est majoritairement utilisée dans les études, ainsi que sur *P. gingivalis* TDC60 qui est une souche plus récente (isolée au Japon dans les années 2000) et supposée être plus virulente que la précédente. Les auteurs à l'origine de son séquençage précisent que TDC60 est plus pathogène que W83 dans un modèle d'abcès chez la souris [13]. Cependant, son utilisation dans un modèle de parodontite induite par inoculation orale n'a, à notre connaissance, pas encore été publiée.

Ces deux souches ont donc été administrés aux animaux en vue de comparer, par micro-tomographie de la mandibule, le niveau de la perte osseuse induite. De plus, une analyse du microbiote oral a été effectuée, afin de préciser l'état de ce microbiote après l'inoculation de *P. gingivalis* et détecter un éventuel déséquilibre. Afin de mesurer l'effet de la bactérie seule sur l'équilibre hôte-microbiote, nous n'avons pas donné d'antibiotique en pré-traitement aux animaux, qui avaient donc un microbiote non altéré en début d'expérimentation. La phase d'infection a duré cinq semaines et chaque souris a reçu quinze administrations.

De façon étonnante, la souche W83 a engendré une perte osseuse alvéolaire plus importante que TDC60. La littérature sur le sujet aurait, en effet, tendance à suggérer l'inverse et met l'accent sur la pathogénicité de TDC60. Le génotype de *fimA*, le gène codant pour le fimbriae majeur de *P. gingivalis*, est souvent mis en avant lors de la comparaison des deux souches ; TDC60 possède le type II de *fimA*, tandis que W83 possède le type IV. Dans un modèle d'abcès cutané chez la souris, le type II se révèle plus virulent que le type IV [14]. De plus, des auteurs ont rapporté une plus forte prévalence du type II, par rapport au type IV, chez les patients atteints de parodontite [15]. Cependant, d'autres études ont montré que le type II était prédominant, que ce soit chez les sujets sains ou malades [16]. Une étude plus récente, enfin, a souligné l'absence de corrélation entre les paramètres cliniques de la parodontite et le génotype du fimbriae [17]. Ajouté au fait que la parodontite peut être initiée dans le modèle murin par un *P. gingivalis* mutant, ne possédant plus de fimbriae, il semble que d'autres

facteurs de virulence soient en cause et qu'ils nécessiteraient des investigations supplémentaires.

Parallèlement à ce constat, nous avons également pu observer que la perte osseuse causée par *P. gingivalis* W83 s'accompagnait d'une altération majeure du microbiote oral. Celle-ci peut être assimilée à une dysbiose : diminution significative de la richesse et de la diversité, perte de taxons habituellement présents à l'état sain, et apparition d'espèces retrouvées dans des situations pathologiques. L'apparition d'un tel déséquilibre n'est pas surprenant, compte tenu du modèle pathophysiologique actuel de la maladie parodontale. Même en faible quantité, l'inoculation d'un pathogène clé comme *P. gingivalis* rompt l'équilibre hôte-microbiote initial, et les dernières études sur le sujet soulignent son action de subversion des réponses de l'hôte et de promotion de l'inflammation [18]. En considérant le microbiote oral comme un reflet du degré de bouleversement immunitaire provoqué par *P. gingivalis*, il est néanmoins intéressant de constater la différence d'impact entre les deux souches, et surtout la persistance du déséquilibre induit par W83. La résilience du microbiote — observable, par exemple, après un traitement antibiotique — semble ainsi avoir été dépassée avec cette souche, car l'analyse a été réalisée un mois après la dernière inoculation. Se pose alors la question de l'impact de ce déséquilibre, à plus long terme et sur l'ensemble de l'organisme de l'animal.

Le manuscrit reproduit ci-après a été soumis au *Journal of Dental Research*, puis à *Molecular Oral Microbiology*. Après quelques échanges avec les éditeurs, il a été décidé de poursuivre les analyses avant de faire une nouvelle soumission. En effet, il nous a été demandé de fournir des données relatives à la colonisation de *P. gingivalis* qui pourraient être en relation avec les différences observées et citées plus haut. Des écouvillonnages buccaux ont été réalisés durant la phase d'exposition à *P. gingivalis*. Ils pourraient être exploités pour déterminer avec plus de précision la présence et l'abondance des deux souches dans la cavité buccale. Des tissus maxillaires issus de cette expérimentation sont encore exploitables et leur analyse histologique est également en cours de discussion. Celle-ci pourrait nous permettre de détecter un envahissement des tissus gingivaux par *P. gingivalis*.

Ce travail est donc encore en cours de préparation, et le manuscrit présenté ici est la version envoyée au *Journal of Dental Research* le 17 octobre 2019⁵.

5. Voir l'accusé de réception en annexe H, page 106

Journal of Dental Research

Oral dysbiosis model with *Porphyromonas gingivalis* is strain-dependent

Journal:	<i>Journal of Dental Research</i>
Manuscript ID	JDR-19-1065
Manuscript Type:	Research Reports
Date Submitted by the Author:	17-Oct-2019
Complete List of Authors:	Boyer, Emile; INSERM, U1241 Nutrition Metabolisms and Cancer; Rennes 1 University, Malherbe, Ludivine; UMR 7156 Leroyer, Patricia; INSERM, U1241 Nutrition Metabolisms and Cancer Fong, Shao Bing; INSERM, U1241 Nutrition Metabolisms and Cancer Loréal, Olivier; INSERM, U1241 Nutrition Metabolisms and Cancer Bonnaure, Martine; INSERM, U1241 Nutrition Metabolisms and Cancer Meuric, Vincent; CHU Rennes, Service d'odontologie et de chirurgie buccale; INSERM, U1241 Nutrition Metabolisms and Cancer
Keywords:	Periodontal disease(s)/periodontitis, Genomics, Microbiology
Abstract:	<i>Porphyromonas gingivalis</i> strain W83, one of the most widely investigated, is considered virulent in the context of periodontitis. The recently isolated <i>P. gingivalis</i> TDC60 has been reported to be highly pathogenic, though it has not been yet investigated in a mouse periodontitis model by oral gavage. Our aim was to compare the virulence of both strains by evaluating their impact on alveolar bone loss and the composition of oral microbiota. We inoculated by oral gavage C57BL/6 mice with one of the both <i>Porphyromonas</i> strains and compared to a sham-treated group, without antibiotics pre-treatment. The alveolar bone of treated mice and controls have been assessed, one month after the final inoculation, by microCT measurements. Moreover, at this time, we characterized their oral microbiota by 16S rRNA gene sequencing. While <i>P. gingivalis</i> W83 successfully initiate periodontitis, TDC60-treated mice only experience moderate lesions. Furthermore, only W83-treated mice exhibited a specific distinct microbiota, with significantly lower richness and evenness than other samples, and decreased proportions of taxa usually found in healthy individuals. This association between alveolar bone loss and a major persistent shift of the oral microbiota gives insights into virulence discrepancies among these strains.

SCHOLARONE™
Manuscripts

1
2
3
4
5
6
7
8
9
10
11
12
13
14
15
16
17
18
19
20
21
22
23
24
25
26
27
28
29
30
31
32
33
34
35
36
37
38
39
40
41
42
43
44
45
46
47
48
49
50
51
52
53
54
55
56
57
58
59
60

1
2
3
4 Title: Oral dysbiosis model with *Porphyromonas gingivalis*
5
6
7 is strain-dependent
8
9

10 **Emile Boyer^{1*}, Patricia Leroyer¹, Ludivine Malherbe², Shao Bing Fong¹, Olivier Loréal¹,**
11 **Martine Bonnaure-Mallet¹, Vincent Meuric¹**
12
13

14
15
16 ¹*INSERM, INRA, Univ Rennes 1, CHU de Rennes, Nutrition Metabolisms and Cancer, Rennes,*
17 *France.*
18

19
20 ²*Université de Strasbourg, CNRS, GMGM UMR 7156, 67000 Strasbourg, France.*
21
22

23
24 *** Corresponding author**
25

26 Emile Boyer, <https://orcid.org/0000-0002-0208-2084>.
27

28 Phone: +33 (0)2 23 23 49 19
29

30 Email: emile.boyer@univ-rennes1.fr
31
32

33
34
35 **Acknowledgments**
36

37 The authors would like to thank everyone at the Arche animal facility (UMS Biosit,
38 Université de Rennes 1, France), and the GEROM research unit (Pr Chappard, Angers, France)
39 for the micro-computed tomography. We also thank the GeT-PlaGe facility and the NED team
40 (Toulouse, France) for sequencing the samples. This study was funded by the *Institut Français*
41 *pour la Recherche en Odontologie* (IFRO).
42
43
44

45
46 Emile Boyer: Contributed to conception, design, data acquisition, analysis and
47 interpretation, performed all statistical analyses, and drafted the manuscript. Ludivine
48 Malherbe: Contributed to data acquisition, analysis and interpretation, and critically revised the
49 manuscript. Patricia Leroyer: Contributed to data acquisition, analysis and interpretation, and
50 critically revised the manuscript. Shao Bing Fong: Contributed to data acquisition, analysis and
51 interpretation, drafted and critically revised the manuscript. Olivier Loréal: Contributed to
52 conception, design, data acquisition, analysis and interpretation, and critically revised the
53 manuscript. Martine Bonnaure-Mallet: Contributed to conception, design, drafted and critically
54 revised the manuscript. Vincent Meuric: Contributed to conception, design, data acquisition,
55
56
57
58
59
60

1
2
3 analysis and interpretation, drafted and critically revised the manuscript. All authors gave their
4 final approval and agree to be accountable for all aspects of the work. The authors declare that
5 they have no conflict of interests.
6
7

8
9
10 **Abstract (250 words)**

11
12 *Porphyromonas gingivalis* strain W83, one of the most widely investigated, is considered
13 virulent in the context of periodontitis. The recently isolated *P. gingivalis* TDC60 has been
14 reported to be highly pathogenic, though it has not been yet investigated in a mouse
15 periodontitis model by oral gavage. Our aim was to compare the virulence of both strains by
16 evaluating their impact on alveolar bone loss and the composition of oral microbiota. We
17 inoculated by oral gavage C57BL/6 mice with one of the both *Porphyromonas* strains and
18 compared to a sham-treated group, without antibiotics pre-treatment. The alveolar bone of
19 treated mice and controls have been assessed, one month after the final inoculation, by microCT
20 measurements. Moreover, at this time, we characterized their oral microbiota by 16S rRNA
21 gene sequencing. While *P. gingivalis* W83 successfully initiate periodontitis, TDC60-treated
22 mice only experience moderate lesions. Furthermore, only W83-treated mice exhibited a
23 specific distinct microbiota, with significantly lower richness and evenness than other samples,
24 and decreased proportions of taxa usually found in healthy individuals. This association
25 between alveolar bone loss and a major persistent shift of the oral microbiota gives insights into
26 virulence discrepancies among these strains.
27
28
29
30
31
32
33
34
35
36
37
38
39
40
41
42

43 **Keywords:** Periodontitis; Animal Model; Mice; *Porphyromonas gingivalis* W83;
44 *Porphyromonas gingivalis* TDC60; Oral Microbiota; Alveolar Bone Loss.
45
46
47
48
49
50
51
52
53
54
55
56
57
58
59
60

1. Introduction

Periodontitis is a chronic inflammatory disease that affects tissues surrounding the teeth. Recent advances in the pathogenesis of periodontal disease have suggested that polymicrobial synergy and microbiota dysbiosis together with a dysregulated immune response can induce inflammation-mediated damage in periodontal tissues (Hajishengallis and Lamont 2012). *Porphyromonas gingivalis* is still considered as a major driver for the dysbiosis, especially due to its ability to initiate periodontitis in animal models.

Initially applied in a nonhuman primate model (Holt et al. 1988), *P. gingivalis* is widely used in murine models of periodontitis induced by oral gavage. Since its first description in 1994, this model allowed to explore the complex interactions between the bacteria and the host immunity (Baker et al. 1994). Various *P. gingivalis* strains were tested in studies, though the majority used *P. gingivalis* W50 or W83, which are very close strains (Chen et al. 2017). Variations in alveolar bone loss demonstrated the different virulence of *P. gingivalis* strains in mouse oral gavage model (Baker et al. 2000), and one could hypothesize that specific virulent clones of periodontal pathogens may cause more severe periodontitis.

Hajishengallis *et al.* showed that an indigenous bacterial community was required to induce the periodontitis, as *P. gingivalis* failed to induce bone loss into germ-free mice (Hajishengallis et al. 2011). The authors pinpointed the fact that the disease involved a disruption in the host-microbiota homeostasis caused by *P. gingivalis* inoculation. The discordance in bone loss obtained with different *P. gingivalis* strains could therefore be related to a variable ability to cause such imbalance. However, an extensive characterization of the oral microbiota after inoculation of *P. gingivalis* is lacking, despite the fact that molecular-based approaches to bacterial identification may give an easy access to its taxonomic composition, and could serve as a biomarker of the host homeostasis in oral cavity.

In this study, our aim was to compare the virulence of W83 and TDC60 *P. gingivalis* strains by evaluating their impact on alveolar bone loss and the composition of oral microbiota, after chronic inoculation by oral gavage, without antibiotics pretreatment. W83 is a widely studied strain isolated in the 1950s, while TDC60 was isolated in the 2000s from a severe human periodontal lesion and exhibited higher pathogenicity causing abscess in mice (Watanabe et al. 2011).

2. Methods

2.1. Animals

The study was approved by the ethical committee of Rennes for animal experimentation. All experimented mice were specific pathogen-free male C57BL/6JRj bred and raised at Janvier Labs (Saint-Berthevin, France). The animals were purchased at 6 weeks of age and kept in the animal colony at UMS Biosit in University of Rennes 1 (Arche), and given free access to tap water and food (Teklad 19 % Protein Rodent Diet). The animals were group-housed (three per cage) and maintained under standard conditions of temperature, atmosphere and light. All experimental procedures were performed in agreement with European law and regulations. This study conforms to the ARRIVE guidelines.

2.2. Bacteria

P. gingivalis strain W83 was directly obtained from the American Type Culture Collection (ATCC) and strain TDC60 was obtained from the Japan Collection of Microorganisms (Riken BioResource Research Center JCM). These strains are maintained at University of Rennes 1 frozen at -80°C in cryobeads. For the experiments, the bacteria were transferred and maintained on Columbia 3 agar plates supplemented with 5% (v/v) defibrinated horse blood (bioMérieux, France), $25\text{ mg}\cdot\text{L}^{-1}$ of hemin, and $10\text{ mg}\cdot\text{L}^{-1}$ of menadione. The cultures were incubated at 37°C in an anaerobic chamber Macs-VA500 (Don Whitley) flooded with 80% N_2 , 10% H_2 and 10% CO_2 .

2.3. Periodontitis mouse model by oral gavage

Following one-week acclimatization, the experiments started with 7 weeks old animals and were developed according to Baker *et al.* with slight modifications (Baker et al. 1994). Animals were randomly divided in three groups according to their treatment: Control, *P. gingivalis* W83 and *P. gingivalis* TDC60 ($n = 6$ mice/group). Animals were cohoused according to their group to avoid horizontal transmission (3 mice/cage). Prior to each infection, the bacteria were grown in enriched brain-heart infusion (BHIe) broth containing, per liter, 37 g of BHI powder (AES Chemunex, France), 5 g of yeast extract (Conda, Dutscher), 25 mg of hemin (Sigma), and 10 mg of menadione (Sigma), placed in an AnaeroPack™ rectangular jar (Mitsubishi Gas Chemical Co. Inc., Tokyo, Japan) with an AnaeroGen™ 3.5L (Mitsubishi Gas Chemical Co. Inc.) for 24 h at 37°C to reach mid exponential phase. The W83- and TDC60-infected groups received 10^9 CFU of live *P. gingivalis* of the corresponding strain, resuspended in 100 μL of PBS. The infection was made by direct inoculation of the oral cavity, three times a week, during five

1
2
3 weeks. Controls were sham-infected mice which received the PBS, but no *P. gingivalis*. The
4 oral administrations were made at the same time for all groups.
5
6

7 **2.4. Sample collection**

8
9 One month after the final oral gavage, mice were anaesthetised and sacrificed at 16 weeks
10 of age, and mandibles were dissected. One hemi-mandible was quickly frozen in liquid nitrogen
11 and stored at -80°C to perform the microbiota analyses. The other hemi-mandible was fixed in
12 70% ethanol 10% formaldehyde for 24h at 4°C , and then stored in absolute acetone at 4°C until
13 micro-computed tomography (micro-CT).
14
15
16
17

18 **2.5. Micro-computed tomography**

19
20 Micro-CT was performed on the hemi-mandible in the GEROM research unit (Angers,
21 France) with a Skyscan 1272 (Bruker). The samples were placed in microtubes, filled with
22 water to prevent desiccation. The tubes were fixed on brass stubs with plasticine and scanned
23 with the following parameters: 9 μm resolution, Xray energy of 70 kV and 142 μA for 1.9 s
24 exposure, 0.2° rotation step, 5.000097 μm image pixel size. The data were reconstructed with
25 NRecon (v. 1.7.0.4, Bruker-MicroCT)
26
27
28
29
30
31

32 **2.6. Quantification of alveolar bone loss**

33
34 The DataViewer software (v. 1.5.6, Bruker-MicroCT) was used to visualise bone and
35 produce the sagittal slices. All images were reoriented such that the cemento-enamel junction
36 (CEJ) and the root apex (RA) appeared (Cho et al. 2016). Among the sagittal images, the image
37 which showed the most recession of alveolar bone was selected for measurement. The distance
38 from the alveolar bone crest (ABC) to the CEJ was measured in μm with the CTAn software
39 (v. 1.18.8, Bruker-MicroCT) at two interdental sites: between the first and the second
40 mandibular molars (M1M2) or between the second and the third mandibular molar (M2M3).
41 As described elsewhere, the CEJ-ABC distance was the shortest distance from ABC to the line
42 connecting the adjacent CEJs (Cho et al. 2016). Measurements of root lengths from the CEJ to
43 the RA were also taken to assess the percentage of remaining alveolar bone using an equation
44 previously described: Percent remaining bone (%) = $([\text{root length} - \text{CEJ-ABC}] / \text{root length}) \times$
45 100 (Park et al. 2007).
46
47
48
49
50
51
52
53
54
55

56 **2.7. Extraction and amplification of bacterial DNA**

57
58 Total DNA was extracted from frozen hemi-mandible using the QIAamp DNA Mini Kit
59 (Qiagen, France) according to the manufacturer's recommendations. The DNA was then kept
60

1
2
3 frozen at -80°C prior to amplification. The V3-V4 regions of the 16S rRNA gene were
4 amplified with the primers 338F (5'-ACTCCTACGGGAGGCAGCAG-3') and 802R (5'-
5 TACNVGGGTATCTAATCC-3') using 25 amplification cycles with an annealing temperature
6 of 45°C . The PCR products were sequenced with the Illumina MiSeq at the GeT-PlaGe facility
7 (Toulouse, France).
8
9

10 11 12 **2.8. Oral microbiota analysis**

13
14 The FASTQ files from the GeT-PlaGe facility were processed with the QIIME2 software (v.
15 2018.4, <https://qiime2.org/>) following a pipeline adapted from the “Moving Pictures” tutorial
16 (<https://docs.qiime2.org/2018.4/tutorials/moving-pictures/>) (Caporaso et al. 2010). The files
17 were imported as “PairedEndFastqManifestPhred33” format. The pipeline DADA2 was used
18 to control the sequence quality and construct the feature table. The forward and reverse
19 sequences were truncated at 250 bases, with all other parameters set to default. Sequences count
20 per sample ranged between 4,041 and 17,201. Prior to the taxonomic assignment at the genus
21 level, reference reads were extracted from the “Ribosomal Database Project” based on matches
22 to the primers pair (338F/802R) and trained as a Naive Bayes classifier (RDP release 11,
23 training set No. 16, <http://rdp.cme.msu.edu/misc/re110info.jsp>). The reads that were classified
24 as Archaea or Unassigned were removed from the feature table. The core diversity analysis was
25 performed with a specific sampling depth (4,041 reads). The core diversity included *alpha* (S_{obs} ,
26 Shannon-Weaver) and *beta* (weighted UniFrac) diversity metrics.
27
28
29
30
31
32
33
34
35
36

37 38 **2.9. Statistics**

39
40 Data were analysed using the R (v. 3.5.0) and RStudio softwares (v. 1.1.383,
41 <https://www.rstudio.com/>). Non-parametric tests were used and considered significant for
42 $p < 0.05$. The results were expressed as mean \pm standard error of the mean. The Kruskal-Wallis
43 with Dunn’s multiple comparisons tests were used to compare means for quantitative data
44 related to weight, alveolar bone parameters, *alpha* diversity indices and taxa relative
45 abundances. The PERMANOVA and ANOSIM tests were performed on *beta* diversity metric
46 with the QIIME2 diversity plugin (Anderson 2001). A linear discriminant analysis of the taxa
47 relative abundance was computed with the LEfSe algorithm (parameters set to default) in
48 Galaxy (<https://huttenhower.sph.harvard.edu/galaxy/>). All plots were made with ‘ggplot2’ for
49 RStudio (Wickham et al. 2016), except for the LEfSe results and the 3D PCoA plot (EMPeror)
50 (Vázquez-Baeza et al. 2013).
51
52
53
54
55
56
57
58
59
60

3. Results

The body weight was not significantly different between the three groups ($n = 6$ mice/group) at any time of the experiments, and no adverse event has been observed (**Table 1**). The microCT analysis of the W83-treated mice showed a significant alveolar bone loss illustrated by the increase of the distance from the cemento-enamel junction to the alveolar bone crest, and the decrease of the percentage of remaining bone, in all sites that have been investigated. Conversely, in the TDC60-treated mice, we found a slight bone loss that did not reach the significance threshold (**Figure 1**).

During the *beta* diversity analysis of oral microbiota, the Principal Component Analysis (PCoA) revealed an apparent homogeneity in the samples from W83-treated mice (**Figure 2a**). Moreover, they appeared to be clustered together, on the side-lines of the two other groups, which were more distributed in the 3D exploration. The PERMANOVA and ANOSIM tests, performed on weighted UniFrac distances plotted in PCoA, showed significant differences between the samples from W83- and TDC60-treated mice (**Figure 2b**). Moreover, the *alpha* diversity metrics confirmed that W83-treated mice had a distinct oral microbiota, with significantly lower richness and evenness than both controls and TDC60-treated mice (**Figure 2c, d**).

The taxonomic analysis of the oral microbiota showed differentially abundant taxa when assessed with LEfSe algorithm (**Figure 3a**). In high taxonomic levels, the samples from controls were found to be enriched in Bacteroidetes and Erysipelotrichia, while samples from TDC60-treated mice had increased abundance of Clostridia and Delataproteobacteria. Samples from W83-treated mice had increased abundance of Alphaproteobacteria and Oceanospirillales. However, the lineages in the cladogram indicated that these variations were related with significant differences in taxa at the genus-level. These taxa were further filtered and assessed by Kruskal-Wallis and Dunn's multiple comparisons tests (**Figure 3b**). As in diversity analyses, significant variations were found between samples from W83-treated mice and the two other groups. Specifically, *Alistipes*, *Barnesiella*, *Clostridium_XIVa*, *Desulfovibrio*, *Oscillibacter*, *Turicibacter*, *Lachnospiraceae_Unclassified* and *Ruminococcaceae_Unclassified* were found significantly decreased in W83-treated mice; several of them were almost undetected. On the contrary, *Halomonas* and *Sphingomonas* were found significantly increased compared to controls and TDC60 groups.

4. Discussion

Despite the fact that some authors inoculated mice with other species from the Socransky's red complex (Sharma et al. 2005; Lee et al. 2009), most of the studies with periodontitis mouse model used *P. gingivalis*, which is reported as a keystone pathogen in periodontitis (Hajishengallis et al. 2012). *P. gingivalis* TDC60 is reported to have a higher pathogenicity than *P. gingivalis* W83 (Watanabe et al. 2011). However, to our knowledge, the impact of oral gavage using TDC60 has not been investigated yet in a mouse periodontitis model. Unexpectedly, in our experiments, TDC60 exhibited a lower virulence in causing alveolar bone loss, while the oral administration of W83 initiate periodontitis in both molar interproximal sites.

P. gingivalis has multiple virulence factors, such as gingipains, outer membrane vesicles, hemagglutinins and fimbriae (Darveau et al. 2012). Gingipains and fimbriae are suspected to take part in the dysregulation of the host's immune function (Klein et al. 2012). Very few *P. gingivalis* strains had their complete genome sequenced, which is the case for W83 and TDC60. Large *in silico* works have shown that both strains share similar nucleotide sequences for the catalytic domains of gingipains RgpA, RgpB and Kgp (Dashper et al. 2017). Conversely, they have two different genotypes for the major fimbriae FimA (type IV *fimA* in W83, type II *fimA* in TDC60), and for the fimbrial accessory proteins FimCDE (type I *fimCDE* in W83, type II *fimCDE* in TDC60). The fimbriae is involved in both bacterial adhesion and immune subversion (Enersen et al. 2013). Moreover, the different genotypes imply various protein structures that demonstrated differential antigenicity (Nagano et al. 2012). Hence, the genomic variations of *P. gingivalis* fimbriae are reported to be related to periodontitis initiation and progression. Such differences could therefore contribute for the different alveolar bone loss that we observed. Human and animal studies found that strains containing type II and type IV *fimA* are more commonly found in periodontitis patients, and are more cytotoxic and invasive than strains with other types of fimbriae (Missailidis et al. 2004; Nakano et al. 2004). It is worth noting that type II *fimA* genotype is frequently reported to be more prevalent than type IV *fimA* in periodontitis affected sites, while the latter was the most commonly genotype found among gingivitis patients (Missailidis et al. 2004; Enersen et al. 2008; Nagano et al. 2018); yet, another study found that the type II was the most widely distributed genotype, among both healthy and periodontitis sites (Moon et al. 2013). Unexpectedly, our results showed moderate virulence for TDC60. Interestingly, Baker *et al.* showed that a *P. gingivalis* W50 mutant for the fimbrial

1
2
3 protein (strain DPG3) could also induce bone loss (Baker et al. 2000), suggesting that other
4 virulence factors could be implicated and should be elucidated.
5
6

7 A previous study showed that *P. gingivalis* triggers changes in the composition of the oral
8 microbiota (Hajishengallis et al. 2011). Using aerobic/anaerobic cultures, the authors have
9 identified alterations in six different genera *spp.* Our results suggest that these alterations could
10 be a part of a major bacterial shift, detectable with high-throughput sequencing methods. This
11 shift, which could be linked to a dysbiosis, appeared to be strain-dependent in our diversity
12 analyses. Indeed, only W83-treated mice exhibited a poorly diversified oral microbiota, which
13 tended to be clustered away from the two other groups. It is noteworthy that the samples were
14 collected one month after the last oral inoculation; therefore, we cannot conclude about the
15 ability of *P. gingivalis* TDC60 to alter the microbiota during the experiments. However, strain
16 W83 appeared to be able to stably disrupt the host-microbiota balance in a persistent way, and
17 it was associated with a greater alveolar bone loss.
18
19

20
21 In an interesting way, the oral microbiota of W83-treated mice exhibited very low levels of
22 several unclassified sequences in the *Lachnospiraceae* and *Ruminococcaceae* families, both
23 belonging to Clostridiales order. Noteworthy, samples from TDC60-treated mice showed
24 increased, though not significant, proportions of these taxa. Although they may be less
25 numerous than previously thought, these not-yet-cultured bacteria still represent a substantial
26 part of the normal gut microbiota in mice, as well as *Clostridium* cluster XIVa, *Barnesiella*,
27 *Alistipes*, *Turicibacter* and *Oscillibacter* that were also depleted in W83-treated mice (Clavel
28 et al. 2016; Lagkouvardos et al. 2016). A recent study pointed out the protective role of the
29 Clostridia class, that is outcompeted by *Desulfovibrio* in a knocked-out mouse model
30 experiencing metabolic disease (Petersen et al. 2019). However, these taxa were significantly
31 decreased in W83-treated mice. In these mice, the taxa with significantly higher proportions
32 were *Halomonas* and *Sphingomonas*, two genera which are likely to be associated with
33 pathological conditions. *Halomonas* was detected in lung tissue from mice with lung fibrosis
34 (D'Alessandro-Gabazza et al. 2018), while *Sphingomonas spp.* are known to carry ligands for
35 NKT cells, an important member of the innate immune defence involved in autoimmunity
36 process (Vas et al. 2008).
37
38
39
40
41
42
43
44
45
46
47
48
49
50
51
52
53

54 In conclusion, this study showed strain-dependent alveolar bone loss associated to a major
55 alteration of the oral microbiota, in a mouse periodontitis model by oral gavage with
56 *P. gingivalis*. Although described as highly pathogenic, *P. gingivalis* TDC60 had weaker
57 consequences than W83. This could be due to their abilities to dysregulate the host's immune
58
59
60

1
2
3 responses. This study underlines the need for further clarifications about the various virulence
4 and pathogenicity among *P. gingivalis* strains. Moreover, the lasting nature of the host-
5 microbiota imbalance that we observed, should encourage us to: i) look for the occurrence of
6 long-term deleterious inflammatory effects in various body sites of the experienced animals
7 (gut microbiota, brain, joints, cardiovascular system, etc.), and ii) identify more precisely the
8 *P. gingivalis* strains emerging in severe periodontitis in humans.
9
10
11
12
13
14
15
16
17
18
19
20
21
22
23
24
25
26
27
28
29
30
31
32
33
34
35
36
37
38
39
40
41
42
43
44
45
46
47
48
49
50
51
52
53
54
55
56
57
58
59
60

For Peer Review

References

- Anderson MJ. 2001. A new method for non-parametric multivariate analysis of variance. *Austral Ecol.* 26(1):32–46. doi:10.1111/j.1442-9993.2001.01070.pp.x.
- Baker PJ, Dixon M, Evans RT, Roopenian DC. 2000. Heterogeneity of *Porphyromonas gingivalis* strains in the induction of alveolar bone loss in mice. *Oral Microbiol Immunol.* 15(1):27–32.
- Baker PJ, Evans RT, Roopenian DC. 1994. Oral infection with *Porphyromonas gingivalis* and induced alveolar bone loss in immunocompetent and severe combined immunodeficient mice. *Arch Oral Biol.* 39(12):1035–1040.
- Caporaso JG, Kuczynski J, Stombaugh J, Bittinger K, Bushman FD, Costello EK, Fierer N, Peña AG, Goodrich JK, Gordon JI, et al. 2010. QIIME allows analysis of high-throughput community sequencing data. *Nat Methods.* 7(5):335–336. doi:10.1038/nmeth.f.303.
- Chen T, Siddiqui H, Olsen I. 2017. In silico Comparison of 19 *Porphyromonas gingivalis* Strains in Genomics, Phylogenetics, Phylogenomics and Functional Genomics. *Front Cell Infect Microbiol.* 7. doi:10.3389/fcimb.2017.00028. [accessed 2018 Apr 23]. <http://journal.frontiersin.org/article/10.3389/fcimb.2017.00028/full>.
- Cho Y-J, Song HY, Ben Amara H, Choi B-K, Eunju R, Cho Y-A, Seol Y, Lee Y, Ku Y, Rhyu I-C, et al. 2016. In Vivo Inhibition of *Porphyromonas gingivalis* Growth and Prevention of Periodontitis With Quorum-Sensing Inhibitors. *J Periodontol.* 87(9):1075–1082. doi:10.1902/jop.2016.160070.
- Clavel T, Lagkouvardos I, Blaut M, Stecher B. 2016. The mouse gut microbiome revisited: From complex diversity to model ecosystems. *Int J Med Microbiol IJMM.* 306(5):316–327. doi:10.1016/j.ijmm.2016.03.002.
- D'Alessandro-Gabazza CN, Méndez-García C, Hataji O, Westergaard S, Watanabe F, Yasuma T, Toda M, Fujimoto H, Nishihama K, Fujiwara K, et al. 2018. Identification of Halophilic Microbes in Lung Fibrotic Tissue by Oligotyping. *Front Microbiol.* 9:1892. doi:10.3389/fmicb.2018.01892.
- Darveau RP, Hajishengallis G, Curtis MA. 2012. *Porphyromonas gingivalis* as a potential community activist for disease. *J Dent Res.* 91(9):816–820. doi:10.1177/0022034512453589.
- Dashper SG, Mitchell HL, Seers CA, Gladman SL, Seemann T, Bulach DM, Chandry PS, Cross KJ, Cleal SM, Reynolds EC. 2017. *Porphyromonas gingivalis* Uses Specific Domain Rearrangements and Allelic Exchange to Generate Diversity in Surface Virulence Factors. *Front Microbiol.* 8. doi:10.3389/fmicb.2017.00048. [accessed 2019 Oct 1]. <https://www.frontiersin.org/articles/10.3389/fmicb.2017.00048/full>.
- Enersen M, Nakano K, Amano A. 2013. *Porphyromonas gingivalis* fimbriae. *J Oral Microbiol.* 5. doi:10.3402/jom.v5i0.20265.
- Enersen M, Olsen I, Kvalheim Ø, Caugant DA. 2008. *fimA* Genotypes and Multilocus Sequence Types of *Porphyromonas gingivalis* from Patients with Periodontitis. *J Clin Microbiol.* 46(1):31–42. doi:10.1128/JCM.00986-07.

1
2
3 Hajishengallis G, Darveau RP, Curtis MA. 2012. The keystone-pathogen hypothesis. *Nat Rev*
4 *Microbiol.* 10(10):717–725. doi:10.1038/nrmicro2873.

5
6 Hajishengallis G, Lamont RJ. 2012. Beyond the red complex and into more complexity: the
7 polymicrobial synergy and dysbiosis (PSD) model of periodontal disease etiology. *Mol Oral*
8 *Microbiol.* 27(6):409–419. doi:10.1111/j.2041-1014.2012.00663.x.

9
10
11 Hajishengallis G, Liang S, Payne MA, Hashim A, Jotwani R, Eskan MA, McIntosh ML, Alsam
12 A, Kirkwood KL, Lambris JD, et al. 2011. Low-abundance biofilm species orchestrates
13 inflammatory periodontal disease through the commensal microbiota and complement. *Cell*
14 *Host Microbe.* 10(5):497–506. doi:10.1016/j.chom.2011.10.006.

15
16
17 Holt SC, Ebersole J, Felton J, Brunsvold M, Kornman KS. 1988. Implantation of *Bacteroides*
18 *gingivalis* in nonhuman primates initiates progression of periodontitis. *Science.* 239(4835):55–
19 57. doi:10.1126/science.3336774.

20
21 Klein BA, Tenorio EL, Lazinski DW, Camilli A, Duncan MJ, Hu LT. 2012. Identification of
22 essential genes of the periodontal pathogen *Porphyromonas gingivalis*. *BMC Genomics.*
23 13:578. doi:10.1186/1471-2164-13-578.

24
25
26 Lagkouvardos I, Pukall R, Abt B, Foessel BU, Meier-Kolthoff JP, Kumar N, Bresciani A,
27 Martínez I, Just S, Ziegler C, et al. 2016. The Mouse Intestinal Bacterial Collection (miBC)
28 provides host-specific insight into cultured diversity and functional potential of the gut
29 microbiota. *Nat Microbiol.* 1(10):16131. doi:10.1038/nmicrobiol.2016.131.

30
31 Lee SF, Andrian E, Rowland E, Marquez IC. 2009. Immune response and alveolar bone
32 resorption in a mouse model of *Treponema denticola* infection. *Infect Immun.* 77(2):694–698.
33 doi:10.1128/IAI.01004-08.

34
35
36 Missailidis CG, Umeda JE, Ota-Tsuzuki C, Anzai D, Mayer MPA. 2004. Distribution of *fimA*
37 genotypes of *Porphyromonas gingivalis* in subjects with various periodontal conditions. *Oral*
38 *Microbiol Immunol.* 19(4):224–229. doi:10.1111/j.1399-302X.2004.00140.x.

39
40
41 Moon J-H, Herr Y, Lee H-W, Shin S-I, Kim C, Amano A, Lee J-Y. 2013. Genotype analysis
42 of *Porphyromonas gingivalis fimA* in Korean adults using new primers. *J Med Microbiol.*
43 62(9):1290–1294. doi:10.1099/jmm.0.054247-0.

44
45
46 Nagano K, Hasegawa Y, Abiko Y, Yoshida Y, Murakami Y, Yoshimura F. 2012.
47 *Porphyromonas gingivalis* FimA fimbriae: fimbrial assembly by *fimA* alone in the fim gene
48 cluster and differential antigenicity among *fimA* genotypes. *PloS One.* 7(9):e43722.
49 doi:10.1371/journal.pone.0043722.

50
51
52 Nagano K, Hasegawa Y, Iijima Y, Kikuchi T, Mitani A. 2018. Distribution of *Porphyromonas*
53 *gingivalis fimA* and *mfal* fimbrial genotypes in subgingival plaques. *PeerJ.* 6:e5581.
54 doi:10.7717/peerj.5581.

55
56
57 Nakano K, Kuboniwa M, Nakagawa I, Yamamura T, Nomura R, Okahashi N, Ooshima T,
58 Amano A. 2004. Comparison of inflammatory changes caused by *Porphyromonas gingivalis*
59 with distinct *fimA* genotypes in a mouse abscess model. *Oral Microbiol Immunol.* 19(3):205–
60 209. doi:10.1111/j.0902-0055.2004.00133.x.

1
2
3 Park CH, Abramson ZR, Taba M, Jin Q, Chang J, Kreider JM, Goldstein SA, Giannobile WV.
4 2007. Three-Dimensional Micro-Computed Tomographic Imaging of Alveolar Bone in
5 Experimental Bone Loss or Repair. *J Periodontol.* 78(2):273–281.
6 doi:10.1902/jop.2007.060252.
7

8
9 Petersen C, Bell R, Klag KA, Lee S-H, Soto R, Ghazaryan A, Buhrke K, Ekiz HA, Ost KS,
10 Boudina S, et al. 2019. T cell-mediated regulation of the microbiota protects against obesity.
11 *Science.* 365(6451). doi:10.1126/science.aat9351.
12

13
14 Sharma A, Inagaki S, Honma K, Sfintescu C, Baker PJ, Evans RT. 2005. *Tannerella forsythia*-
15 induced alveolar bone loss in mice involves leucine-rich-repeat BspA protein. *J Dent Res.*
16 84(5):462–467.
17

18
19 Vas J, Mattner J, Richardson S, Ndonge R, Gaughan JP, Howell A, Monestier M. 2008.
20 Regulatory Roles for NKT Cell Ligands in Environmentally Induced Autoimmunity. *J*
21 *Immunol Baltim Md* 1950. 181(10):6779–6788.
22

23
24 Vázquez-Baeza Y, Pirrung M, Gonzalez A, Knight R. 2013. EMPeror: a tool for visualizing
25 high-throughput microbial community data. *GigaScience.* 2:16. doi:10.1186/2047-217X-2-16.
26

27
28 Watanabe T, Maruyama F, Nozawa T, Aoki A, Okano S, Shibata Y, Oshima K, Kurokawa K,
29 Hattori M, Nakagawa I, et al. 2011. Complete genome sequence of the bacterium
30 *Porphyromonas gingivalis* TDC60, which causes periodontal disease. *J Bacteriol.*
31 193(16):4259–4260. doi:10.1128/JB.05269-11.
32

33
34 Wickham H, Chang W, RStudio. 2016. ggplot2: Create Elegant Data Visualisations Using the
35 Grammar of Graphics. [accessed 2017 Jun 21]. [https://cran.r-](https://cran.r-project.org/web/packages/ggplot2/index.html)
36 [project.org/web/packages/ggplot2/index.html](https://cran.r-project.org/web/packages/ggplot2/index.html).
37
38
39
40
41
42
43
44
45
46
47
48
49
50
51
52
53
54
55
56
57
58
59
60

Time of experiment	Treatment			<i>p</i> -value
	Controls	<i>P. gingivalis</i> TDC60	<i>P. gingivalis</i> W83	
Baseline (g)	22.17 ± 0.36	23.34 ± 0.47	22.68 ± 0.60	0.29
Sacrifice (g)	26.95 ± 0.62	29.03 ± 0.91	28.23 ± 0.98	0.37

Table 1: Evolution of the animals' weight during the experiments. Data are presented as mean ± standard error ($n = 6$ mice/group). The *p*-value of the Kruskal-Wallis test is indicated.

For Peer Review

1
2
3 **Figure 1:** Alveolar bone loss in mice. Measurements of bone levels were made by comparing
4 the distance from the cemento-enamel junction (CEJ) to the alveolar bone crest (ABC) (**a, b**)
5 and the percentage of remaining bone (**c, d**) at two interdental sites: between the first and second
6 mandibular molars (M1M2) and between the second and the third mandibular molars (M2M3).
7 Root lengths (from the CEJ to the root apex) were also measured to assess the percentage of
8 remaining alveolar bone: Percent remaining bone (%) = $([\text{root length} - \text{CEJ-ABC}] / \text{root length})$
9 $\times 100$. Control and *P. gingivalis* infected mice were 16 weeks old ($n = 6$ mice/group). Dunn's
10 Kruskal-Wallis multiple comparisons, statistically significant at: $*p < 0.05$; $**p < 0.01$.
11
12
13
14
15
16
17
18
19
20
21
22
23
24
25
26
27
28
29
30
31
32
33
34
35
36
37
38
39
40
41
42
43
44
45
46
47
48
49
50
51
52
53
54
55
56
57
58
59
60

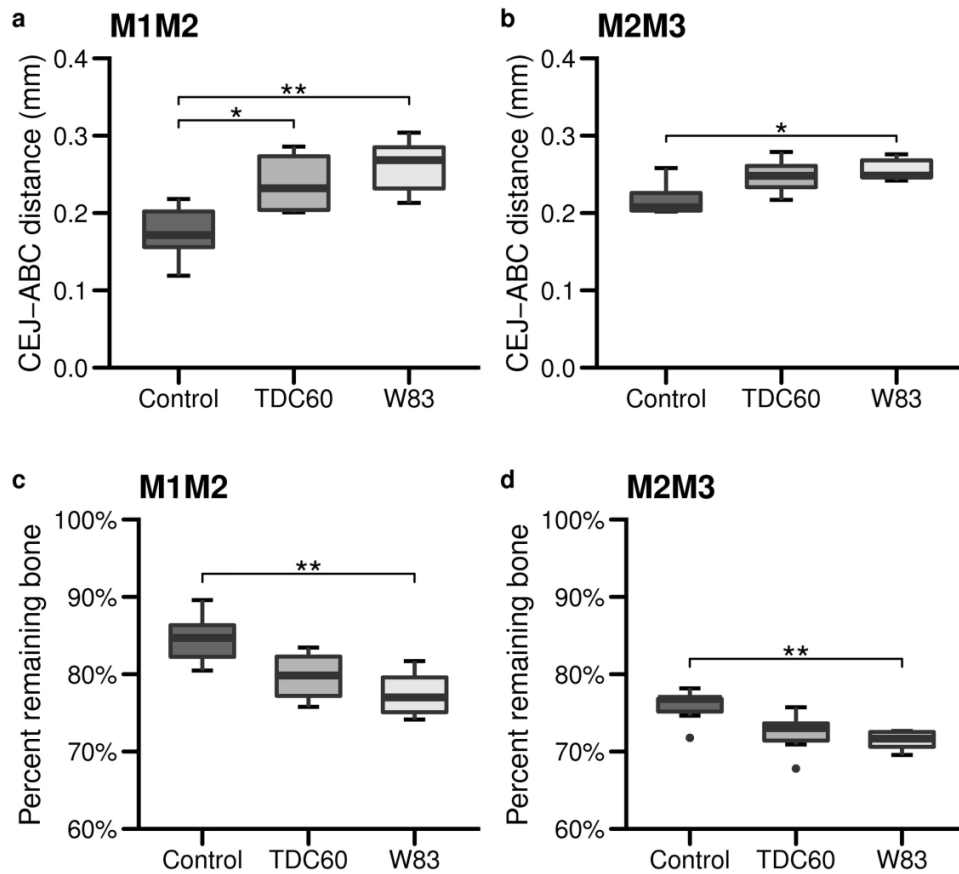
For Peer Review

1
2
3 **Figure 2:** *Alpha* and *beta* diversity of the oral microbiota of mice. Bioinformatics processing
4 of the microbiota samples from the oral cavity of control and *P. gingivalis* infected mice ($n = 6$
5 mice/group, 16 weeks old) allowed for Principal Coordinate Analysis (PCoA). The PCoA
6 calculated with weighted UniFrac metric revealed clustering of W83-treated mice (**a**). Analysis
7 of distances between samples showed significant differences between W83- and TDC60-treated
8 mice, with both PERMANOVA and ANOSIM tests (** $p < 0.01$, **b**). *Alpha* diversity analysis
9 showed significantly lower richness (S_{obs} , **c**) and lower evenness (Shannon-Weaver, **d**) in W83-
10 treated mice. Dunn's Kruskal-Wallis multiple comparisons, statistically significant at:
11
12
13
14
15
16
17
18
19
20
21
22
23
24
25
26
27
28
29
30
31
32
33
34
35
36
37
38
39
40
41
42
43
44
45
46
47
48
49
50
51
52
53
54
55
56
57
58
59
60

For Peer Review

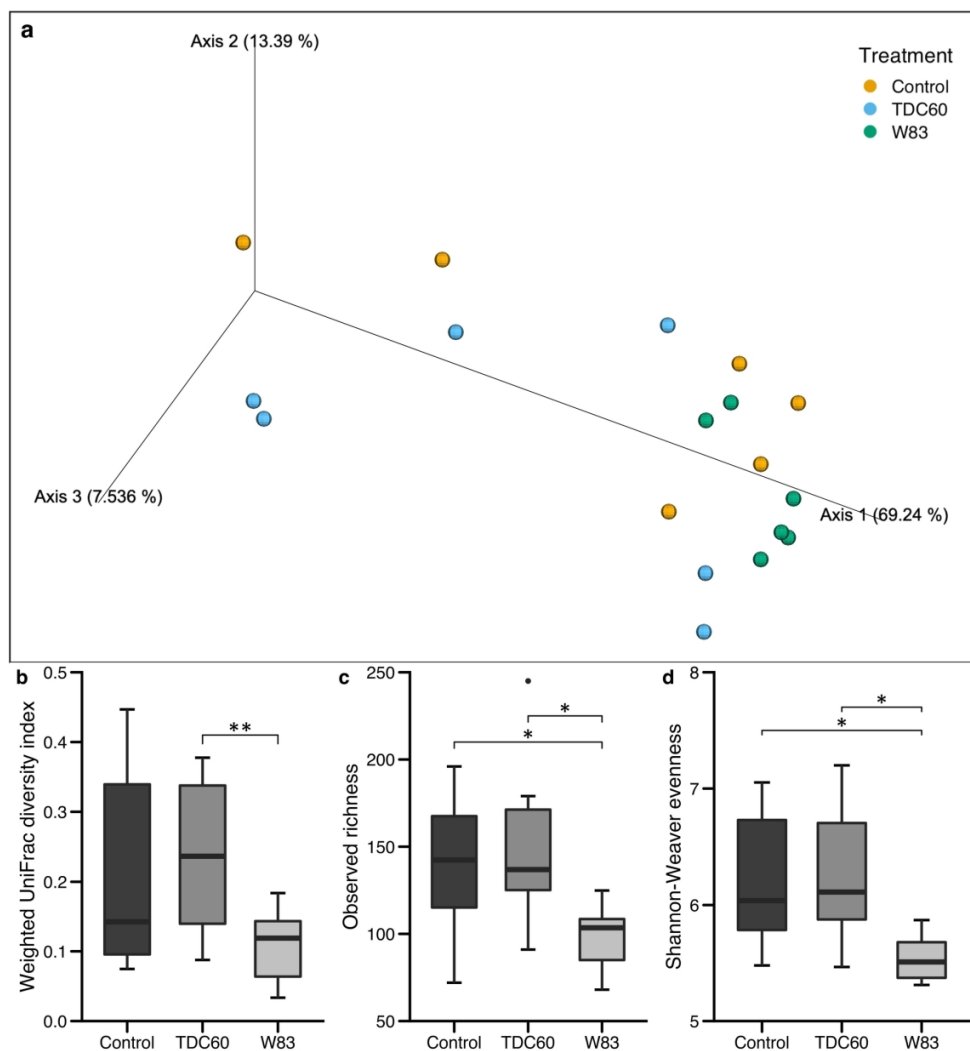
1
2
3 **Figure 3:** Analysis of taxa relative abundances in the oral cavity according to the treatment
4 of mice. The linear discriminant analysis with effect size (LEfSe) cladogram identified taxa that
5 were differentially abundant across the groups ($n = 6$ mice/group; $p < 0.05$) (a). Taxa at the
6 genus-level were then filtered (excluding those with a mean relative abundance $< 1\%$ in all
7 groups), and plotted when the Kruskal-Wallis test returned significant result ($p < 0.05$) (b).
8 Dunn's Kruskal-Wallis multiple comparisons, statistically significant at: $*p < 0.05$; $**p < 0.01$.
9
10
11
12
13
14
15
16
17
18
19
20
21
22
23
24
25
26
27
28
29
30
31
32
33
34
35
36
37
38
39
40
41
42
43
44
45
46
47
48
49
50
51
52
53
54
55
56
57
58
59
60

For Peer Review



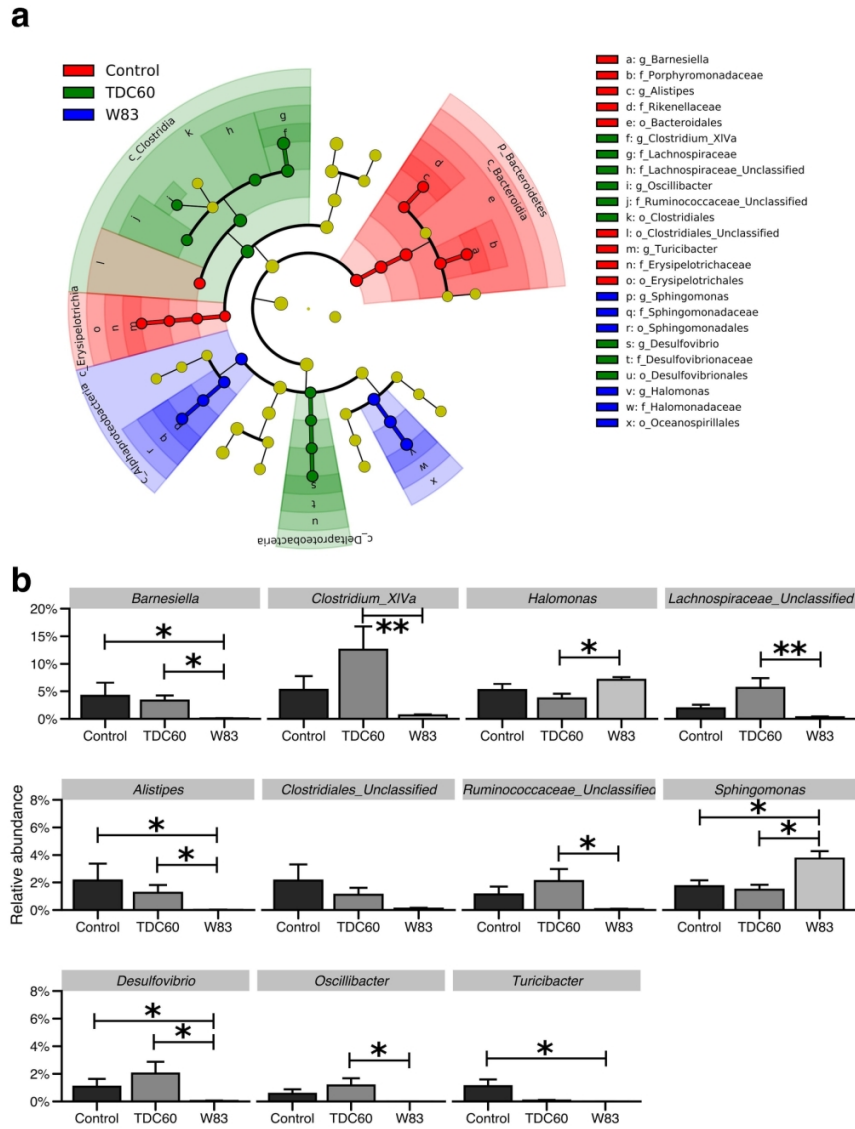
Alveolar bone loss in mice. Measurements of bone levels were made by comparing the distance from the cemento-enamel junction (CEJ) to the alveolar bone crest (ABC) (**a, b**) and the percentage of remaining bone (**c, d**) at two interdental sites: between the first and second mandibular molars (M1M2) and between the second and the third mandibular molars (M2M3). Root lengths (from the CEJ to the root apex) were also measured to assess the percentage of remaining alveolar bone: Percent remaining bone (%) = $([\text{root length} - \text{CEJ-ABC}] / \text{root length}) \times 100$. Control and *P. gingivalis* infected mice were 16 weeks old ($n = 6$ mice/group). Dunn's Kruskal-Wallis multiple comparisons, statistically significant at: * $p < 0.05$; ** $p < 0.01$.

191x181mm (300 x 300 DPI)



Alpha and *beta* diversity of the oral microbiota of mice. Bioinformatics processing of the microbiota samples from the oral cavity of control and *P. gingivalis* infected mice ($n = 6$ mice/group, 16 weeks old) allowed for Principal Coordinate Analysis (PCoA). The PCoA calculated with weighted UniFrac metric revealed clustering of W83-treated mice (**a**). Analysis of distances between samples showed significant differences between W83- and TDC60-treated mice, with both PERMANOVA and ANOSIM tests (** $p < 0.01$, **b**). *Alpha* diversity analysis showed significantly lower richness (S_{obs} , **c**) and lower evenness (Shannon-Weaver, **d**) in W83-treated mice. Dunn's Kruskal-Wallis multiple comparisons, statistically significant at: * $p < 0.05$.

174x193mm (300 x 300 DPI)



Analysis of taxa relative abundances in the oral cavity according to the treatment of mice. The linear discriminant analysis with effect size (LEfSe) cladogram identified taxa that were differentially abundant across the groups ($n = 6$ mice/group; $p < 0.05$) (a). Taxa at the genus-level were then filtered (excluding those with a mean relative abundance $< 1\%$ in all groups), and plotted when the Kruskal-Wallis test returned significant result ($p < 0.05$) (b). Dunn's Kruskal-Wallis multiple comparisons, statistically significant at: * $p < 0.05$; ** $p < 0.01$.

141x191mm (300 x 300 DPI)

3.3 Références

- [1] R. E. Fleming, Q. Feng, and R. S. Britton. Knockout Mouse Models of Iron Homeostasis. *Annu Rev Nutr*, 31(1) :117–137, 2011. doi : 10.1146/annurev-nutr-072610-145117.
- [2] P. J. Baker, R. T. Evans, and D. C. Roopenian. Oral infection with *Porphyromonas gingivalis* and induced alveolar bone loss in immunocompetent and severe combined immunodeficient mice. *Arch Oral Biol*, 39(12) :1035–1040, December 1994. ISSN 0003-9969.
- [3] A. Sharma, S. Inagaki, K. Honma, C. Sfintescu, P. J. Baker, and R. T. Evans. *Tannerella Forsythia*-induced alveolar bone loss in mice involves leucine-rich-repeat BspA protein. *J Dent Res*, 84(5) :462–467, May 2005. ISSN 0022-0345.
- [4] S. F. Lee, E. Andrian, E. Rowland, and I. C. Marquez. Immune response and alveolar bone resorption in a mouse model of *Treponema denticola* infection. *Infect Immun*, 77(2) :694–698, February 2009. ISSN 1098-5522. doi : 10.1128/IAI.01004-08.
- [5] X. Y. Zhou, S. Tomatsu, R. E. Fleming, S. Parkkila, A. Waheed, J. Jiang, Y. Fei, E. M. Brunt, D. A. Ruddy, C. E. Prass, R. C. Schatzman, R. O'Neill, R. S. Britton, B. R. Bacon, and W. S. Sly. *HFE* gene knockout produces mouse model of hereditary hemochromatosis. *Proc Natl Acad Sci U S A*, 95(5) :2492–2497, March 1998. ISSN 0027-8424. doi : 10.1073/pnas.95.5.2492.
- [6] P. Guggenbuhl, P. Brissot, and O. Loréal. Miscellaneous non-inflammatory musculoskeletal conditions. Haemochromatosis : The bone and the joint. *Best Pract Res Clin Rheumatol*, 25(5) :649–664, October 2011. ISSN 1532-1770. doi : 10.1016/j.berh.2011.10.014.
- [7] M. Doyard, D. Chappard, P. Leroyer, M.-P. Roth, O. Loréal, and P. Guggenbuhl. Decreased Bone Formation Explains Osteoporosis in a Genetic Mouse Model of Hemochromatosis. *PLoS One*, 11(2) :e0148292, 2016. ISSN 1932-6203. doi : 10.1371/journal.pone.0148292.
- [8] K. Buhnik-Rosenblau, S. Moshe-Belizowski, Y. Danin-Poleg, and E. G. Meyron-Holtz. Genetic modification of iron metabolism in mice affects the gut microbiota. *Biometals*, 25(5) :883–892, October 2012. ISSN 1572-8773. doi : 10.1007/s10534-012-9555-5.
- [9] N. Guañabens and A. Parés. Osteoporosis in chronic liver disease. *Liver Int*, 38(5) :776–785, 2018. ISSN 1478-3231. doi : 10.1111/liv.13730.
- [10] Y. Kawashima, A. Fujita, K. Buch, B. Li, M. M. Qureshi, M. N. Chapman, and O. Sakai. Using texture analysis of head CT images to differentiate osteoporosis from

- normal bone density. *Eur J Radiol*, 116 :212–218, July 2019. ISSN 0720-048X. doi : 10.1016/j.ejrad.2019.05.009.
- [11] P. Guggenbuhl, P. Fergelot, M. Doyard, H. Libouban, M.-P. Roth, Y. Gallois, G. Chalès, O. Loréal, and D. Chappard. Bone status in a mouse model of genetic hemochromatosis. *Osteoporos Int*, 22(8) :2313–2319, August 2011. ISSN 1433-2965. doi : 10.1007/s00198-010-1456-2.
- [12] D. T. Graves, D. Fine, Y.-T. A. Teng, T. E. Van Dyke, and G. Hajishengallis. The use of rodent models to investigate host-bacteria interactions related to periodontal diseases. *J Clin Periodontol*, 35(2) :89–105, February 2008. ISSN 1600-051X. doi : 10.1111/j.1600-051X.2007.01172.x.
- [13] T. Watanabe, F. Maruyama, T. Nozawa, A. Aoki, S. Okano, Y. Shibata, K. Oshima, K. Kurokawa, M. Hattori, I. Nakagawa, and Y. Abiko. Complete genome sequence of the bacterium *Porphyromonas gingivalis* TDC60, which causes periodontal disease. *J Bacteriol*, 193(16) :4259–4260, August 2011. ISSN 1098-5530. doi : 10.1128/JB.05269-11.
- [14] K. Nakano, M. Kuboniwa, I. Nakagawa, T. Yamamura, R. Nomura, N. Okahashi, T. Ooshima, and A. Amano. Comparison of inflammatory changes caused by *Porphyromonas gingivalis* with distinct *fimA* genotypes in a mouse abscess model. *Oral Microbiol. Immunol.*, 19(3) :205–209, June 2004. ISSN 0902-0055. doi : 10.1111/j.0902-0055.2004.00133.x.
- [15] C. G. Missailidis, J. E. Umeda, C. Ota-Tsuzuki, D. Anzai, and M. P. A. Mayer. Distribution of *fimA* genotypes of *Porphyromonas gingivalis* in subjects with various periodontal conditions. *Oral Microbiol. Immunol.*, 19(4) :224–229, August 2004. ISSN 0902-0055. doi : 10.1111/j.1399-302X.2004.00140.x.
- [16] J.-H. Moon, Y. Herr, H.-W. Lee, S.-I. Shin, C. Kim, A. Amano, and J.-Y. Lee. Genotype analysis of *Porphyromonas gingivalis fimA* in Korean adults using new primers. *J Med Microbiol*, 62(9) :1290–1294, 2013. ISSN 0022-2615. doi : 10.1099/jmm.0.054247-0.
- [17] K. Nagano, Y. Hasegawa, Y. Iijima, T. Kikuchi, and A. Mitani. Distribution of *Porphyromonas gingivalis fimA* and *mfa1* fimbrial genotypes in subgingival plaques. *PeerJ*, 6 :e5581, 2018. ISSN 2167-8359. doi : 10.7717/peerj.5581.
- [18] R. J. Lamont, H. Koo, and G. Hajishengallis. The oral microbiota : Dynamic communities and host interactions. *Nat Rev Microbiol*, 16(12) :745–759, December 2018. ISSN 1740-1534. doi : 10.1038/s41579-018-0089-x.

Chapitre 4

Perspectives

Sommaire

4.1 Croisement des modèles animaux	50
4.2 Lien entre microbiotes oral et digestif	52
4.3 Dysbioses induites par <i>Porphyromonas gingivalis</i> et altérations de l'état général	53
4.4 Études à long terme et prospectives	54
4.5 Références	56

4.1 Croisement des modèles animaux

Le but final de ce travail est de croiser les deux modèles animaux présentés précédemment. Les objectifs sont multiples : i) analyser les marqueurs de la réponse de l'hôte et du remodelage osseux, et ii) caractériser l'état du microbiote oral, pour iii) évaluer le degré d'implication de chacun dans l'association parodontite–hémochromatose. Au vu de nos précédents résultats et des données de la littérature, plusieurs hypothèses de mécanismes sont envisagées ; elles ne sont d'ailleurs pas incompatibles entre elles. Les observations chez l'Homme suggèrent une promotion des pathogènes parodontaux et d'une dysbiose par l'augmentation de fer circulant et l'apparition de fer non lié à la transferrine. La présence d'altérations de la micro-architecture trabéculaire chez le modèle animal, potentiellement en lien avec les atteintes ostéo-articulaires de l'hémochromatose, sous-tend une perturbation de l'homéostasie osseuse et une susceptibilité à l'ostéolyse. Enfin, un dérèglement de la réponse inflammatoire peut également être impliqué, car plusieurs auteurs ont rapporté des différences dans le phénotype des cellules immunitaires du modèle murin *Hfe*^(-/-). Ces variations restent encore à élucider, car, si certains résultats évoquent une atténuation de la réponse inflammatoire — diminution de la production de cytokines pro-inflammatoires dans les macrophages [1] et diminution du recrutement en polynucléaires neutrophiles [2] —, d'autres suggèrent une exacerbation de l'inflammation tissulaire, comme l'élévation de la voie Th17 dans un modèle d'infection pulmonaire [2].

Après une première phase de reproduction dans la colonie d'animaux *Hfe*^(-/-), qui a débuté en janvier 2018, la phase d'expérimentation proprement dite a démarré en octobre 2018. Quarante-huit individus ont été répartis en quatre groupes, selon leur génotype et leur traitement (voir Figure 4.1). Ce dernier a consisté en l'administration orale de *P. gingivalis* W83 ou d'une solution contrôle pendant cinq semaines, de la même façon que décrit dans le manuscrit précédent¹. Un mois après la fin des inoculations, les animaux ont été euthanasiés et échantillonnés. L'expérimentation s'est achevée en juillet 2019. Plusieurs types d'échantillons ont été collectés, en premier lieu pour analyser les paramètres cliniques du fer, de la perte osseuse et le microbiote oral.

Mandibules et maxillaires Une première hémi-mandibule sera d'abord utilisée pour réaliser des analyses du microbiote oral : l'extraction de l'ADN bactérien et l'amplification du gène de l'ARNr 16S seront réalisées au laboratoire, le séquençage par NGS à la plateforme Inra GeT-Plage de Toulouse. La seconde hémi-mandibule servira à l'analyse morphométrique par micro-tomographie : après fixation en formaldéhyde, l'acquisition radiographique sera réalisée en collaboration avec l'unité Inserm Bioscar de Paris.

Écouvillons buccaux Ils ont permis d'échantillonner le microbiote oral des animaux avant et pendant la période d'inoculation, et doivent nous servir à faire un suivi longitudinal de ce microbiote au cours de l'expérimentation.

1. Voir la section 3.2 Oral dysbiosis model with *Porphyromonas gingivalis* is strain-dependent, soumis dans *Journal of Dental Research* en page 45.

Foie, rate et plasma Ces éléments nous permettront de réaliser le statut fer des animaux : la concentration en fer stocké dans le foie et la rate, ainsi que les paramètres plasmatiques (coefficient de saturation de la transferrine, concentration en ferritine, taux de fer non lié à la transferrine).

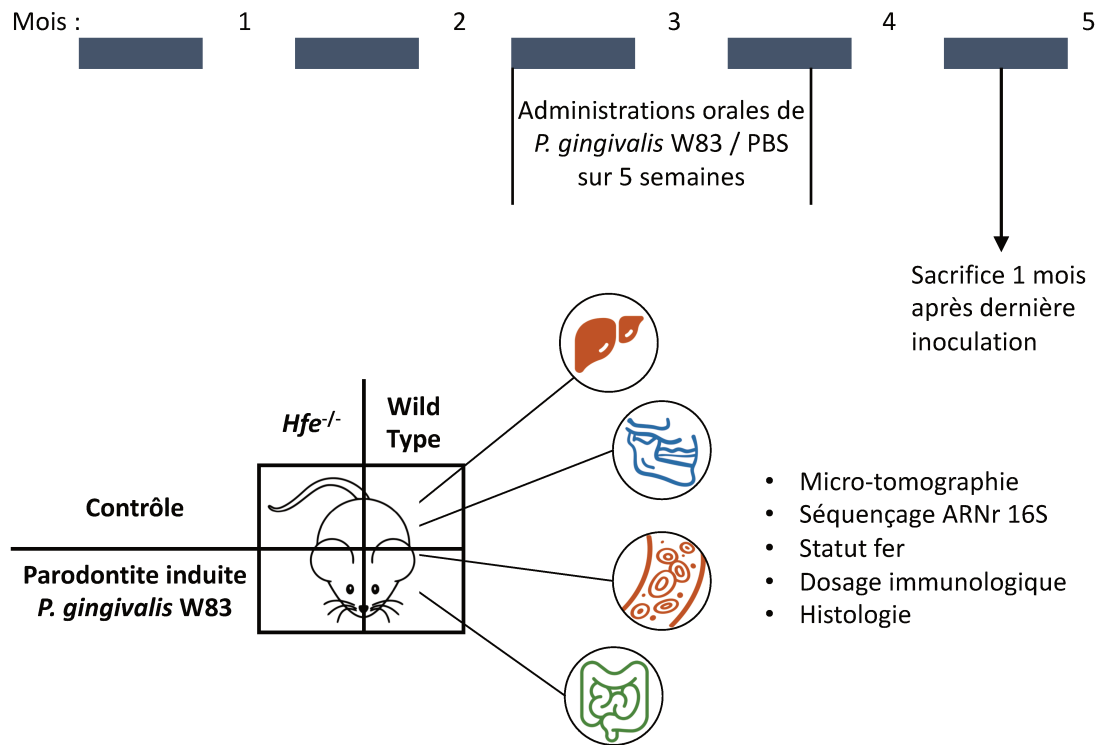


FIGURE 4.1 – Méthodologie de l'expérimentation de croisement des modèles *Hfe*^(-/-) et parodontite induite.

Les héli-mandibules destinées à l'analyse par micro-tomographie ont été exploitées. Elles ont toutes été acquises et les fichiers contenant les images radiographiques ont été réceptionnés. L'étape suivante, de reconstruction tridimensionnelle des échantillons, a été réalisée pour une partie d'entre eux avec le logiciel NRecon (Bruker® MicroCT). Cette étape sera ensuite suivie par les mesures de perte osseuse avec les logiciels DataViewer et CTan (Bruker® MicroCT).

Notre stratégie d'analyse immunologique se base sur les données de la littérature et prend également en compte les commentaires des relecteurs du manuscrit soumis au *Journal of Clinical Periodontology*². Elle peut encore évoluer et pourrait bénéficier d'une collaboration. Les tissus oraux restants exploitables après les analyses décrites

2. Voir l'annexe F en page 101.

ci-dessus comprennent, d'une part le maxillaire (os, gencive et dents) conservé à sec à -80°C , et d'autre part les héli-mandibules envoyées pour la micro-tomographie, qui nous ont été renvoyées après décalcification et inclusion en paraffine. Ces dernières peuvent donc être utilisées pour réaliser des analyses histologiques des tissus parodontaux et visualiser *in situ* l'état inflammatoire. Le maxillaire permettra à la fois de doser l'expression de cytokines dans le tissu gingival, et le ratio RANKL-OPG dans l'os sous-jacent.

4.2 Lien entre microbiotes oral et digestif

Le dogme d'une barrière gastrique infranchissable pour les bactéries résidentes de la cavité buccale a été battu en brèche avec les analyses par NGS. Pour le sujet sain, près de la moitié des individus du HMP possèdent des genres bactériens détectés à la fois dans la cavité buccale et dans les fèces [3]. Des quantités plus importantes de bactéries buccales ont été mesurées au niveau intestinal chez des patients souffrant de pathologies très variées : séropositivité, cirrhose hépatique, maladies inflammatoires chroniques de l'intestin ou cancer du colon [4–7].

De la même façon, il est très probable qu'un transfert, depuis la cavité buccale vers les étages inférieurs du tube digestif, ait lieu de façon plus importante en cas de parodontite chronique, étant donné le réservoir bactérien que constitue le biofilm sous-gingival. Au vu des concentrations salivaires de *P. gingivalis* chez les patients atteints de parodontite, il a été estimé que 10^8 à 10^{10} bactéries pouvaient être ingérées quotidiennement [8]. L'impact systémique d'un tel passage a d'ailleurs fait l'objet de plusieurs articles. Ils ont pu mettre en évidence, dans un modèle murin similaire à celui que nous avons mis en œuvre, des altérations de la composition du microbiote intestinal et de la barrière intestinale, mais également l'augmentation dans le plasma de marqueurs inflammatoires, de l'insuline et la détection d'endotoxines [9].

Dans le cadre de nos expérimentations, nous avons échantillonné une portion du duodénum et le contenu du cæcum. Il nous est donc également possible de pouvoir analyser le microbiote intestinal de nos animaux, à deux étages différents du tube digestif. En outre, nous bénéficierons du croisement avec le modèle *Hfe*^(-/-) de surcharge en fer. Celui-ci a déjà démontré avoir un effet sur la composition du microbiote dans le cæcum³. Il est donc intéressant d'étudier son impact conjugué à celui de l'inoculation bactérienne. Une portion du duodénum a également été fixée puis incluse en paraffine pour permettre des observations histologiques.

Dans le même ordre d'idée, il serait intéressant de pouvoir évaluer la capacité de différentes souches de *P. gingivalis* à induire une altération du microbiote intestinal. Compte tenu des résultats obtenus au niveau buccal lors de notre expérimentation de

3. Voir les résultats présentés dans le manuscrit de la section 3.1 [Alteration and loss of mandibular alveolar bone in *Hfe* knocked-out mice. A pilot study.](#) Soumis dans *Journal of Clinical Periodontology*, et le travail de Buhnik-Rosenblau et coll. [10].

parodontite induite par *P. gingivalis* W83 et TDC60, il est plausible qu'elles aient un impact variable au niveau digestif. Pour le savoir nous avons conçu une étude supplémentaire chez la souris pour évaluer l'état du microbiote digestif après l'induction d'une parodontite par l'administration orale de différentes souches de *P. gingivalis*. W83 et TDC60 ont été utilisées, ainsi que la souche H3. Cette dernière, d'origine colombienne, a été isolée depuis un échantillon sanguin [11]; elle provient donc d'une bactériémie, et possède, comme W83, un fimbriae de type IV. Des échantillons digestifs ont été collectés, et nous avons à notre disposition une portion de duodénum et le contenu du cæcum issus de ces quatre groupes (W83, TDC60, H3 et contrôle) que nous prévoyons d'exploiter. À notre connaissance, aucune étude comparant l'impact intestinal de différentes souches de *P. gingivalis* n'a encore été publiée.

En inoculant *P. gingivalis* W83, les événements précédemment décrits chez la souris seraient déjà observables après une seule administration de la bactérie [12]. Dans cette même étude, l'étude du microbiote fécal a montré l'absence de la bactérie, dès 3 heures après l'inoculation, ce qui suggère une clairance bactérienne rapide. On peut dès lors se demander si la dysbiose intestinale est causée par *P. gingivalis* lui-même ou par la dysbiose buccale qu'il a induit. De plus, il a été montré que des bactériémies sont observables après des inoculations de *P. gingivalis*, mais que ce n'est pas son ADN qui est retrouvé [9]. Il est ainsi probable que le déséquilibre hôte-microbiote au niveau intestinal soit un intermédiaire dans les connexions entre sphère orale et maladies systémiques.

4.3 Dysbioses induites par *Porphyromonas gingivalis* et altérations de l'état général

L'association santé buccale et santé générale fait actuellement l'objet de nombreux projets et études [13]. Les résultats obtenus chez l'Homme et dans les modèles animaux suggèrent l'implication d'un axe cavité buccale et intestin dysbiotique dans une large variété de pathologies systémiques. Certaines, comme les maladies cardiovasculaires ou la polyarthrite rhumatoïde, ont maintenant des liens établis avec la santé orale. Des pathogènes parodontaux ont été isolés dans des plaques d'athérome chez l'Homme [14], tandis que, dans les modèles animaux, l'athérosclérose est exacerbée par l'administration de *P. gingivalis* [15]. Pour la polyarthrite rhumatoïde, en parallèle d'une action directe de *P. gingivalis* au sein des articulations [16], la réponse inflammatoire Th17 générée dans l'intestin et initiée par l'exposition à la bactérie contribuerait à l'aggravation de l'arthrite [17].

D'autres pathologies font l'objet d'une attention plus récente. Chez des patients souffrant de cirrhose hépatique, par exemple, un changement majeur de microbiote intestinal est observé, causée par une invasion massive de bactéries issues de la cavité buccale, et ce, sans lien avec la consommation d'alcool [18, 19]. En cas de maladies hépatiques non liées à l'alcool (« *non-alcoholic fatty liver disease* », NAFLD), *P. gingiva-*

lis est plus fréquemment retrouvé au niveau intestinal, et l'exposition de souris atteintes de NAFLD par *P. gingivalis* accélère la progression de la maladie [20]. En cancérologie, des bactéries buccales ont été isolées sur des tissus de tumeurs colo-rectales [21]. Ces bactéries, actuellement soupçonnées de participer à la carcinogenèse de ces tumeurs [22], pourraient également être utilisées comme biomarqueurs [23]. En neurologie, enfin, l'implication de pathogènes parodontaux dans les maladies neurodégénératives est une nouvelle voie de recherche pour expliquer leur progression [24].

Cette liste, volontairement non exhaustive, montre bien l'étendue — à l'échelle de l'organisme entier — de l'impact d'un déséquilibre au niveau du microbiote du tube digestif. Cela nous a donc amené à collecter les échantillons supplémentaires suivants au moment de nos expérimentations animales : reins, cœur, pancréas et poumons. Initialement prélevés pour quantifier la surcharge en fer des animaux *Hfe*^(-/-), le foie et la rate s'ajoutent à cette liste. Chacun de ces échantillons est stocké, à la fois à sec à -80°C, et en paraffine après fixation. Ils pourront ainsi nous servir à détecter et évaluer la présence d'altérations à distance de la cavité buccale, en lien avec les dysbioses initiées par différentes souches de *P. gingivalis*, et l'effet d'une surcharge en fer sur ces altérations.

4.4 Études à long terme et prospectives

Les expérimentations décrites ci-dessus font néanmoins défaut sur le caractère chronique, élément caractéristique des pathologies précédemment citées. Qu'il s'agisse de la maladie parodontale, ou des maladies avec laquelle elle est associée, ces désordres se développent sur des décennies chez l'humain. Ce qui est probablement lié à des contraintes de temps et de coût nous amènent également à utiliser des animaux prédisposés pour les maladies que nous souhaitons étudier (*apoE*^(-/-) pour l'athérosclérose, « *high fat diet* » pour l'obésité et la NAFLD, lignée DBA/1J pour la polyarthrite, etc.) C'est pourquoi il serait intéressant de proposer des modèles expérimentaux avec des animaux sains, exposés régulièrement à des pathogènes parodontaux comme *P. gingivalis*, mais à bas bruit, et sur une longue période (6, 12, 18 mois), pour pouvoir observer les effets à long terme des déséquilibres hôte-microbiote. Un article, paru en 2016, a ainsi montré des perturbations métaboliques dans les tissus cardiaques, cérébraux et hépatiques, après 22 semaines d'expositions consécutives à *P. gingivalis* [25].

En parallèle, chez l'Homme, plusieurs voies sont à explorer. Concernant l'hémochromatose, l'inclusion d'un plus grand nombre de patients pourrait renforcer nos conclusions, de même que la constitution d'un groupe contrôle pour réaliser une étude cas-témoin. Initialement, une telle prévalence de parodontite parmi ces patients n'avait pas été envisagée, et nous pensions pouvoir inclure dans l'analyse des microbiotes sous-gingivaux de sujets avec hémochromatose mais au parodonte sain. Un suivi au cours de leur prise en charge, et la collecte de données relatives au statut fer dans le temps, permettrait également d'obtenir plus de preuves sur l'impact du niveau de fer sur les

bactéries ; d'autant plus si nous pouvons ajouter le dosage du fer non lié à la transferrine et la réalisation du statut fer dans le fluide gingival. Enfin, des groupes de patients souffrant de surcharge en fer d'origine génétique autre (acéruoplasminémie, mutation de l'hémojuvéline, etc.), et d'origine non génétique (certains syndromes métaboliques et hépatopathies) [26], constitueraient des contrôles intéressants à analyser, tant du point de vue clinique que microbiologique.

Devant l'accumulation des bases de données, il devient nécessaire d'utiliser des algorithmes pour nous aider à trier au mieux l'information qu'elles contiennent. Grâce aux progrès des intelligences artificielles, un outil comme le ratio de dysbiose devrait pouvoir être affiné, de façon à l'utiliser comme biomarqueur fiable. L'accroissement des données de séquençage disponibles permet de le tester sur un nombre croissant de sujets. Cependant, les métadonnées⁴ associées à ces données de séquençage sont encore assez rares et ne permettent qu'une comparaison entre sujets sains et malades. La constitution de banques d'échantillons, au sein des services hospitaliers prenant en charge des patients atteints de parodontite, permettrait à la fois d'obtenir un effectif large et une information détaillée pour chaque prélèvement. Ce serait également l'occasion d'évaluer sa valeur prédictive, pour identifier des sites à risque de développer une atteinte parodontale ou d'être réfractaire au traitement. Dans cette optique d'étude longitudinale, nous participons à l'étude de cohorte PÉLAGIE (<http://www.pelagie-inserm.fr/>) qui suit environ 3 500 mères-enfant depuis 2002, pour analyser l'impact de l'environnement chimique sur le développement de l'enfant. Après la collecte de salive et du statut dentaire de 500 enfants âgés de 12 ans, nous prévoyons ainsi de les revoir à l'âge de 18 ans pour un examen parodontal. Par la suite, nous envisageons de les suivre le plus longtemps possible, de façon à pouvoir reconstituer l'histoire, microbiologique et clinique, qui conduit aux problèmes bucco-dentaires de l'adulte. Conscients de leurs répercussions sur la santé générale et de leur statut d'enjeu majeur de santé publique, il nous apparaît donc essentiel de comprendre et prévenir leur apparition. C'est pourquoi nous participons également au WorkPackage 4 du consortium iVasc (<https://www.ivasc.eu>), qui vise à évaluer le rôle de la parodontite et de son traitement, dans l'initiation et la progression de l'athérombose.

4. Statut parodontal précis, âge et sexe de l'individu, etc.

4.5 Références

- [1] L. Wang, E. E. Johnson, H. N. Shi, W. A. Walker, M. Wessling-Resnick, and B. J. Cherayil. Attenuated Inflammatory Responses in Hemochromatosis Reveal a Role for Iron in the Regulation of Macrophage Cytokine Translation. *J Immunol*, 181(4) : 2723–2731, August 2008. ISSN 0022-1767, 1550-6606. doi : 10.4049/jimmunol.181.4.2723.
- [2] K. Benesova, M. V. Spasić, S. M. Schaefer, J. Stolte, T. Baehr-Ivacevic, K. Waldow, Z. Zhou, U. Klingmueller, V. Benes, M. A. Mall, and M. U. Muckenthaler. Hfe Deficiency Impairs Pulmonary Neutrophil Recruitment in Response to Inflammation. *PLOS ONE*, 7(6) :e39363, June 2012. ISSN 1932-6203. doi : 10.1371/journal.pone.0039363.
- [3] N. Segata, S. K. Haake, P. Mannon, K. P. Lemon, L. Waldron, D. Gevers, C. Huttenhower, and J. Izard. Composition of the adult digestive tract bacterial microbiome based on seven mouth surfaces, tonsils, throat and stool samples. *Genome Biology*, 13(6) :R42, June 2012. ISSN 1474-760X. doi : 10.1186/gb-2012-13-6-r42.
- [4] I. Vujkovic-Cvijin, R. M. Dunham, S. Iwai, M. C. Maher, R. G. Albright, M. J. Broadhurst, R. D. Hernandez, M. M. Lederman, Y. Huang, M. Somsouk, S. G. Deeks, P. W. Hunt, S. V. Lynch, and J. M. McCune. Dysbiosis of the Gut Microbiota Is Associated with HIV Disease Progression and Tryptophan Catabolism. *Sci Translat Med*, 5(193) :193ra91–193ra91, July 2013. ISSN 1946-6234, 1946-6242. doi : 10.1126/scitranslmed.3006438.
- [5] Y. Chen, F. Ji, J. Guo, D. Shi, D. Fang, and L. Li. Dysbiosis of small intestinal microbiota in liver cirrhosis and its association with etiology. *Sci Rep*, 6(1) :1–9, September 2016. ISSN 2045-2322. doi : 10.1038/srep34055.
- [6] D. Gevers, S. Kugathasan, L. A. Denson, Y. Vázquez-Baeza, W. Van Treuren, B. Ren, E. Schwager, D. Knights, S. J. Song, M. Yassour, X. C. Morgan, A. D. Kostic, C. Luo, A. González, D. McDonald, Y. Haberman, T. Walters, S. Baker, J. Rosh, M. Stephens, M. Heyman, J. Markowitz, R. Baldassano, A. Griffiths, F. Sylvester, D. Mack, S. Kim, W. Crandall, J. Hyams, C. Huttenhower, R. Knight, and R. J. Xavier. The Treatment-Naive Microbiome in New-Onset Crohn’s Disease. *Cell Host & Microbe*, 15(3) :382–392, March 2014. ISSN 1931-3128. doi : 10.1016/j.chom.2014.02.005.
- [7] C. L. Sears and W. S. Garrett. Microbes, Microbiota, and Colon Cancer. *Cell Host & Microbe*, 15(3) :317–328, March 2014. ISSN 1931-3128. doi : 10.1016/j.chom.2014.02.007.
- [8] I. Olsen and K. Yamazaki. Can oral bacteria affect the microbiome of the gut? *J Oral Microbiol*, 11(1) :1586422, January 2019. ISSN null. doi : 10.1080/20002297.2019.1586422.

- [9] K. Arimatsu, H. Yamada, H. Miyazawa, T. Minagawa, M. Nakajima, M. I. Ryder, K. Gotoh, D. Motooka, S. Nakamura, T. Iida, and K. Yamazaki. Oral pathobiont induces systemic inflammation and metabolic changes associated with alteration of gut microbiota. *Sci Rep*, 4 :4828, 2014. ISSN 2045-2322. doi : 10.1038/srep04828.
- [10] K. Buhnik-Rosenblau, S. Moshe-Belizowski, Y. Danin-Poleg, and E. G. Meyron-Holtz. Genetic modification of iron metabolism in mice affects the gut microbiota. *Biometals*, 25(5) :883–892, October 2012. ISSN 1572-8773. doi : 10.1007/s10534-012-9555-5.
- [11] P. J. Pérez-Chaparro, G. I. Lafaurie, P. Gracieux, V. Meuric, Z. Tamanai-Shacoori, J. E. Castellanos, and M. Bonnaure-Mallet. Distribution of *Porphyromonas gingivalis* fimA genotypes in isolates from subgingival plaque and blood sample during bacteremia. *Biomedica*, 29(2) :298–306, June 2009. ISSN 0120-4157.
- [12] M. Nakajima, K. Arimatsu, T. Kato, Y. Matsuda, T. Minagawa, N. Takahashi, H. Ohno, and K. Yamazaki. Oral Administration of *P. gingivalis* Induces Dysbiosis of Gut Microbiota and Impaired Barrier Function Leading to Dissemination of Enterobacteria to the Liver. *PLoS ONE*, 10(7) :e0134234, 2015. ISSN 1932-6203. doi : 10.1371/journal.pone.0134234.
- [13] P. Monsarrat, A. Blaizot, P. Kémoun, P. Ravaut, C. Nabet, M. Sixou, and J.-N. Vergnes. Clinical research activity in periodontal medicine : A systematic mapping of trial registers. *J Clin Periodontol*, 43(5) :390–400, May 2016. ISSN 1600-051X. doi : 10.1111/jcpe.12534.
- [14] V. I. Haraszthy, J. J. Zambon, M. Trevisan, M. Zeid, and R. J. Genco. Identification of periodontal pathogens in atheromatous plaques. *J Periodontol*, 71(10) :1554–1560, October 2000. ISSN 0022-3492. doi : 10.1902/jop.2000.71.10.1554.
- [15] F. C. Gibson, C. Hong, H.-H. Chou, H. Yumoto, J. Chen, E. Lien, J. Wong, and C. A. Genco. Innate immune recognition of invasive bacteria accelerates atherosclerosis in apolipoprotein E-deficient mice. *Circulation*, 109(22) :2801–2806, June 2004. ISSN 1524-4539. doi : 10.1161/01.CIR.0000129769.17895.F0.
- [16] K. J. Maresz, A. Hellvard, A. Sroka, K. Adamowicz, E. Bielecka, J. Koziel, K. Gawron, D. Mizgalska, K. A. Marcinska, M. Benedyk, K. Pyrc, A.-M. Quirke, R. Jonsson, S. Alzabin, P. J. Venables, K.-A. Nguyen, P. Mydel, and J. Potempa. *Porphyromonas Gingivalis* facilitates the development and progression of destructive arthritis through its unique bacterial peptidylarginine deiminase (PAD). *PLoS Pathog*, 9(9) :e1003627, September 2013. ISSN 1553-7374. doi : 10.1371/journal.ppat.1003627.
- [17] K. Sato, N. Takahashi, T. Kato, Y. Matsuda, M. Yokoji, M. Yamada, T. Nakajima, N. Kondo, N. Endo, R. Yamamoto, Y. Noiri, H. Ohno, and K. Yamazaki. Aggravation of collagen-induced arthritis by orally administered *Porphyromonas gingivalis*

- through modulation of the gut microbiota and gut immune system. *Sci Rep*, 7(1) : 6955, July 2017. ISSN 2045-2322. doi : 10.1038/s41598-017-07196-7.
- [18] N. Qin, F. Yang, A. Li, E. Prifti, Y. Chen, L. Shao, J. Guo, E. Le Chatelier, J. Yao, L. Wu, J. Zhou, S. Ni, L. Liu, N. Pons, J. M. Batto, S. P. Kennedy, P. Leonard, C. Yuan, W. Ding, Y. Chen, X. Hu, B. Zheng, G. Qian, W. Xu, S. D. Ehrlich, S. Zheng, and L. Li. Alterations of the human gut microbiome in liver cirrhosis. *Nature*, 513(7516) : 59–64, September 2014. ISSN 1476-4687. doi : 10.1038/nature13568.
- [19] V. B. Dubinkina, A. V. Tyakht, V. Y. Odintsova, K. S. Yarygin, B. A. Kovarsky, A. V. Pavlenko, D. S. Ischenko, A. S. Popenko, D. G. Alexeev, A. Y. Taraskina, R. F. Nasyrova, E. M. Krupitsky, N. V. Shalikiani, I. G. Bakulin, P. L. Shcherbakov, L. O. Skorodumova, A. K. Larin, E. S. Kostyukova, R. A. Abdulkhakov, S. R. Abdulkhakov, S. Y. Malanin, R. K. Ismagilova, T. V. Grigoryeva, E. N. Ilina, and V. M. Govorun. Links of gut microbiota composition with alcohol dependence syndrome and alcoholic liver disease. *Microbiome*, 5(1) :141, October 2017. ISSN 2049-2618. doi : 10.1186/s40168-017-0359-2.
- [20] M. Yoneda, S. Naka, K. Nakano, K. Wada, H. Endo, H. Mawatari, K. Imajo, R. Nomura, K. Hokamura, M. Ono, S. Murata, I. Tohnai, Y. Sumida, T. Shima, M. Kuboniwa, K. Umemura, Y. Kamisaki, A. Amano, T. Okanou, T. Ooshima, and A. Nakajima. Involvement of a periodontal pathogen, *Porphyromonas gingivalis* on the pathogenesis of non-alcoholic fatty liver disease. *BMC Gastroenterol*, 12 :16, February 2012. ISSN 1471-230X. doi : 10.1186/1471-230X-12-16.
- [21] T. Tahara, E. Yamamoto, H. Suzuki, R. Maruyama, W. Chung, J. Garriga, J. Jelinek, H.-o. Yamano, T. Sugai, B. An, I. Shureiqi, M. Toyota, Y. Kondo, M. R. H. Estécio, and J.-P. J. Issa. Fusobacterium in Colonic Flora and Molecular Features of Colorectal Carcinoma. *Cancer Res*, 74(5) :1311–1318, March 2014. ISSN 0008-5472, 1538-7445. doi : 10.1158/0008-5472.CAN-13-1865.
- [22] M. R. Rubinstein, X. Wang, W. Liu, Y. Hao, G. Cai, and Y. W. Han. *Fusobacterium Nucleatum* promotes colorectal carcinogenesis by modulating E-cadherin/ β -catenin signaling via its FadA adhesin. *Cell Host Microbe*, 14(2) :195–206, August 2013. ISSN 1934-6069. doi : 10.1016/j.chom.2013.07.012.
- [23] B. Flemer, R. D. Warren, M. P. Barrett, K. Cisek, A. Das, I. B. Jeffery, E. Hurley, M. O’Riordain, F. Shanahan, and P. W. O’Toole. The oral microbiota in colorectal cancer is distinctive and predictive. *Gut*, 67(8) :1454–1463, August 2018. ISSN 0017-5749, 1468-3288. doi : 10.1136/gutjnl-2017-314814.
- [24] S. S. Dominy, C. Lynch, F. Ermini, M. Benedyk, A. Marczyk, A. Konradi, M. Nguyen, U. Haditsch, D. Raha, C. Griffin, L. J. Holsinger, S. Arastu-Kapur, S. Kaba, A. Lee, M. I. Ryder, B. Potempa, P. Mydel, A. Hellvard, K. Adamowicz, H. Hasturk, G. D. Walker, E. C. Reynolds, R. L. M. Faull, M. A. Curtis, M. Dragunow, and J. Potempa. *Porphyromonas Gingivalis* in Alzheimer’s disease brains : Evidence for disease

- causation and treatment with small-molecule inhibitors. *Sci Adv*, 5(1) :eaau3333, January 2019. ISSN 2375-2548. doi : 10.1126/sciadv.aau3333.
- [25] V. Ilievski, J. M. Kinchen, R. Prabhu, F. Rim, L. Leoni, T. G. Unterman, and K. Watanabe. Experimental Periodontitis Results in Prediabetes and Metabolic Alterations in Brain, Liver and Heart : Global Untargeted Metabolomic Analyses. *J Oral Biol (Northborough)*, 3(1), 2016. ISSN 2377-987X. doi : 10.13188/2377-987X.1000020.
- [26] Y. Deugnier, F. Lainé, C. Le Lan, E. Bardou-Jacquet, A.-M. Jouanolle, and P. Brissot. Hémochromatoses et autres surcharges hépatiques en fer. *EMC - Traité d'Hépatologie*, 7-007-B-22 :1–12, January 2011. ISSN 11551976. doi : 10.1016/S1155-1976(11)40364-8.

Conclusion

L'amélioration des outils d'analyse et l'essor technologique qui a permis l'étude du microbiote humain mettent en évidence le dialogue permanent entre l'organisme hôte et les micro-organismes qui l'habitent. La reconnaissance de l'être humain et de son microbiote comme un ensemble, un holobionte, est un nouveau paradigme. Il ouvre de nombreuses perspectives de recherche pour décrypter les mécanismes sous-jacents aux associations entre maladies bucco-dentaires et pathologies systémiques, qui sont longtemps restées cloisonnées. Aujourd'hui, les liens entre santé générale et santé bucco-dentaire sont nombreux et reconnus comme pouvant être bi-directionnels.

Notre travail a permis de mettre en évidence une susceptibilité à la maladie parodontale chez les patients atteints d'hémochromatose héréditaire : une susceptibilité qui n'était jusque là qu'une observation empirique, partagée par quelques praticiens. Les travaux que nous avons publiés sont des études transversales, clinique et microbiologique, menées chez l'Homme, et qui mettent l'accent sur le coefficient de saturation de la transferrine — et implicitement, sur le fer non lié à la transferrine — comme facteur de risque potentiel pour la parodontite. Cependant, compte tenu des données de la littérature et des premières observations obtenus sur le modèle animal de l'hémochromatose héréditaire, la façon précise dont la surcharge en fer influe sur l'équilibre hôte-microbiote reste encore à déterminer. Elle pourrait agir à la fois sur les bactéries, en changeant leur environnement physico-chimique, et sur les réponses de l'hôte, en altérant les fonctions immunitaire et de remodelage osseux. Les expérimentations animales que nous avons menées devraient nous permettre d'explorer ces différentes pistes.

En premier lieu, nous avons voulu insister, dans les conclusions de nos articles, sur la nécessité pour les professionnels de santé de reconnaître l'hémochromatose héréditaire comme un facteur de risque, afin de guider le patient vers sa prise en charge bucco-dentaire et d'adapter cette dernière. Deuxièmement, en plus d'un bénéfice pour les patients, nous pensons que ce champ d'investigation — le métabolisme du fer, et des métaux en général — présente également un intérêt pour notre discipline du point de vue fondamental. En effet, étudier la façon dont ces dérèglements, d'apparence mineurs, peuvent influencer l'écosystème sous-gingival pourrait nous aider à mieux comprendre la pathophysiologie de la maladie parodontale, qui est encore théorique à ce jour.

Appendices

Annexe A

Communication affichée au *Oral Health Research Congress* de Vienne

Periodontal microbiota in patients with hemochromatosis, an iron overload disease

Boyer E^{1,2}, Le Gall-David S², Deugnier Y^{3,4}, Bonnaure-Mallet M^{1,2}, Meuric V^{1,2}

¹CHU Rennes, Service d'Odontologie et de Chirurgie Buccale, Rennes, France
²NuméCan, CIMAD (Control of Iron Metabolism and Iron-Associated Diseases), Université Rennes 1, UMR 1241, Rennes, France
³INSERM, CIC 1414, Rennes, France
⁴CHU Rennes, Service des maladies du Foie, Rennes, France



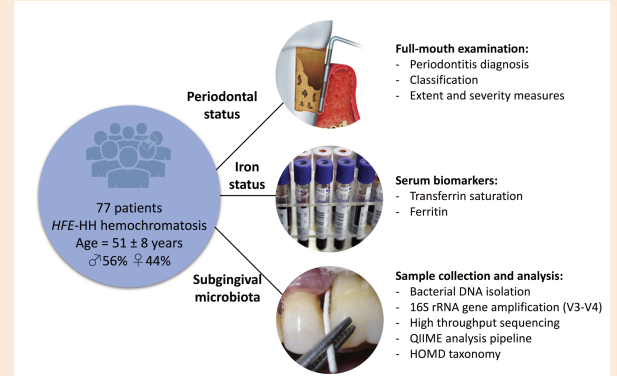
Introduction

HFE-related hereditary hemochromatosis (*HFE*-HH) is the most common form of inherited iron overload disease in European populations [1]. This condition is characterized by a hepcidin-deficiency state leading to increased transferrin saturation (TSAT) and serum ferritin rate. Classically, *HFE*-HH is responsible for hepatic cirrhosis, diabetes and skin pigmentation [2]. Lately, other symptoms have been increasingly associated to *HFE*-HH: chronic asthenia, arthropathy [3] and osteoporosis [4]. Standard treatment is therapeutic venesection, and international guidelines recommend to keep serum ferritin under 50 µg/L during maintenance [5-8].

In a previous study, we observed significant association between periodontitis severity and elevated TSAT in patients with *HFE*-HH [9]. Iron is an essential growth factor for bacteria, and also acts as a virulence regulator for *Porphyromonas gingivalis* and *Prevotella intermedia*, two common periodontal pathogens [10]. Non-transferrin bound iron (NTBI) can be identified in the plasma of patients with TSAT > 45% and is suspected to drive *HFE*-HH symptoms [11]. Besides, these toxic iron species could modulate bacterial growth and virulence [12]. We have hypothesized that *HFE* mutation and iron overload in hemochromatosis patients could alter and modulate their subgingival microbiota toward dysbiosis and explain the severity of their periodontitis.

The aim of this study was to investigate potential association between subgingival microbiota and serum biomarker levels in *HFE*-HH patients that have previously shown a significant relationship between their iron burden and their periodontal status.

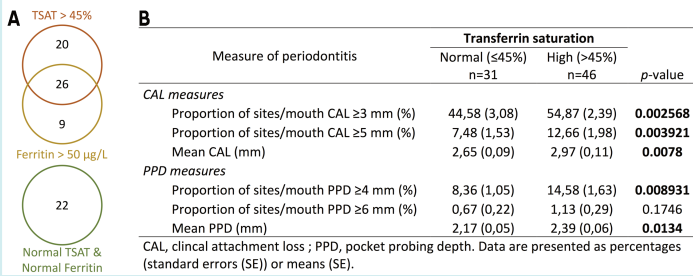
Materials & Methods



Patients with *HFE*-HH were recruited in the unit of Hepatology, University Hospital of Rennes. As described in Meuric et al., 2017, they underwent a periodontal examination and serum markers of iron metabolism were collected from medical records. Bacterial DNA from subgingival biofilm of 77 patients was extracted. *In silico*, alpha and beta diversity analysis was performed with QIIME (Figure 2). Statistical analysis of clinical and microbiological data was performed using R with clinical cut-offs (TSAT = 45%; Ferritin = 50 µg/L) (Figure 1, 3). *P* values < 0.05 were considered to indicate statistical significance.

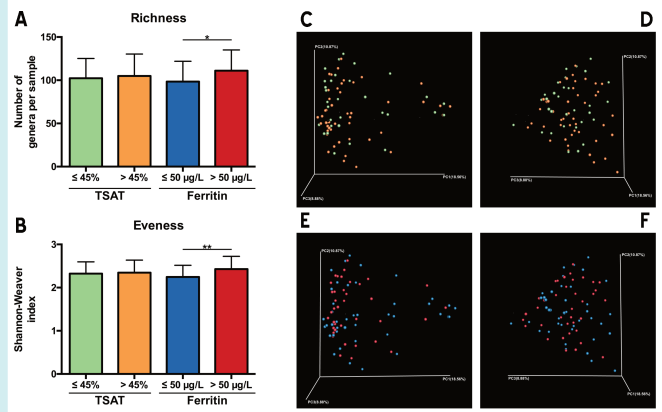
Results & Discussion

Figure 1



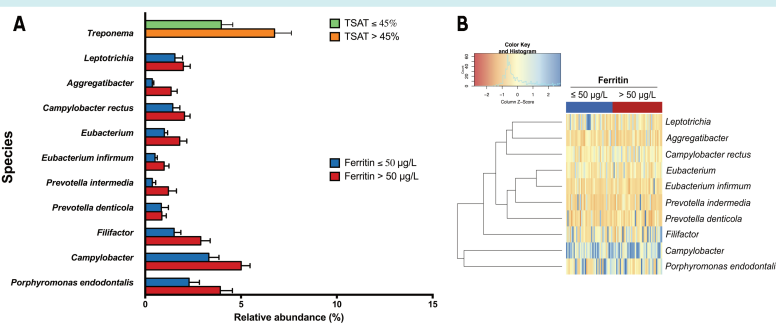
The serum iron markers cut-offs allowed us to classify patients in 4 categories (A). Our previous study reported a risk 5-fold higher for severe periodontitis in patients with TSAT over 45%. To confirm this result, we compared periodontitis measures and found that patients with a high TSAT had CAL and PPD measures significantly increased (B). Conversely, there was no difference when comparing patients with normal and high ferritin (data not shown).

Figure 2



Surprisingly, alpha-diversity analysis showed significant difference only between patients with normal and high ferritin (AB). There was an increased microbial richness and diversity in subgingival microbiota of patients with ferritin over 50 µg/L. As revealed by the 3D principal coordinates analysis (PCoA) with Bray-Curtis metrics, beta-diversity analysis showed no clustering according to the TSAT (CD) or ferritin (EF) level. PCoA with UniFrac distances did not show any cluster either (data not shown).

Figure 3



To further investigate the potential impact of iron burden on the subgingival microbiota, taxonomic comparison at the genus and species levels were made. Only *Treponema* relative abundance was found significantly increased in patients with high TSAT (A). In contrast, five genera (*Campylobacter*, *Filifactor*, *Aggregatibacter*, *Eubacterium* and *Leptotrichia*) and five species (*Campylobacter rectus*, *Prevotella denticola*, *Porphyromonas endodontalis*, *Eubacterium infirmum* and *Prevotella intermedia*) were found significantly increased in patients with high ferritin (AB).

Potential association between iron burden and bacterial taxa that showed different proportions in TSAT or ferritin groups was assessed by correlation. Four taxa were found significantly correlated to ferritin rate. The genus *Campylobacter* showed the highest correlation with coefficient rho=0.40 (p<0.001)(C), followed by *Filifactor* (rho=0.28), *Campylobacter rectus* (rho=0.26) and *Porphyromonas endodontalis* (rho=0.24).

Conclusions

The present study shows a clear association between iron and periodontal status. Transferrin saturation appears to be a relevant biomarker in this association, as a TSAT > 45% implied an increase of almost all periodontitis measures. Conversely, ferritin level had no effect on periodontal status.

Except for a doubled relative abundance of the periopathogen *Treponema* in iron-overloaded patients, there was only minor microbiological difference regarding to the TSAT level. There was a stronger effect of ferritin rate. Patients with ferritin > 50 µg/L had a more diverse and richer microbiota, though they did not present a distinct microbial signature. Surprisingly, several genera and species implicated in periodontitis (*Aggregatibacter*, *Filifactor*, *Porphyromonas endodontalis*, *Campylobacter rectus* and *Prevotella intermedia*) were more abundant in those patients, although they did not present a more severe periodontitis.

Some studies have already shown an iron influence on microbiota [13,14], and *in vitro* on *Porphyromonas gingivalis* [15]. Our results tend to show an impact on periodontitis, a polymicrobial infectious and chronic inflammatory disease. Still, the underlying mechanisms remain unknown, as iron overload may also have an impact on the host's immune response [16,17]. Further studies are necessary to complete our analysis of iron influence on microbiota. They could also provide a better understanding of the host-microbiota dynamics and periodontitis pathogenesis.

The authors wish to acknowledge and thank the French Institute for Odontologic Research (IFRO) for its support in developing this document.

References

- Powell LW et al. Lancet 2016. PMID: 27004087.
- O'Neil J, Powell L. Semin Liver Dis 2005. PMID: 16315132.
- Guggenbuhl P et al. Best Pract Res Clin Rheumatol 2011. PMID: 22142745.
- Guggenbuhl P et al. Osteoporos Int 2005. PMID: 15928800.
- European Association for the Study of the Liver. J Hepatol 2010. PMID: 20471131
- Bismuth M, Peynaud-Debayle E. Haute Autorité de Santé 2005. Available on: <http://cpc.cx/k5o>.
- Swinkels DW et al. Neth J Med 2007. PMID: 18079569.
- Bacon BR et al. Hepatology 2011. PMID: 21452290.
- Meuric et al. J Clin Periodontol 2017. PMID: 28586532.
- Byrne DP et al. Mol Oral Microbiol 2013. PMID: 23336115.
- Brisson P et al. Biochim Biophys Acta 2012. PMID: 21855608.
- Jolivet-Gougeon et al. Am J Gastroenterol 2008. PMID: 18684194.
- Buhnik-Rosenblau et al. Biometals 2012. PMID: 22580926.
- Alexeev EE et al. PLoS One 2017. PMID: 28662197.
- Lewis JP. Periodontol 2000 2010. PMID: 20017798.
- Benesova K et al. PLoS One 2012. PMID: 22745741.
- Maia ML et al. J Clin Immunol 2015. PMID: 25479931

Annexe B

Communication orale à la 97^e session générale de l'*IADR* à Vancouver



97TH GENERAL SESSION & EXHIBITION OF THE IADR
48TH ANNUAL MEETING OF THE AADR
43RD ANNUAL MEETING OF THE CADR

Vancouver Convention Centre West
Vancouver, BC, Canada

www.iadr.org/2019iags

PROGRAM BOOK

#IADR2019



IAGS 2019 Meeting App
www.iadr.org/2019iagsapp



2929 8:15 a.m. Outcomes for Painful TMD Patients in the National Dental PBRN. E. SCHIFFMAN*, J. LOOK, M. LITAKER, G. ANDERSON, K. JOHNSON, J. RILEY, D. RINDAL, A. VELLY, V. BENAVENT, J. COHEN, V. GORDAN, W. HARRELL, H. MINYE, J. WAHLEN-POORMAN, NATIONAL DENTAL PBRN COLLABORATIVE GROUP (School of Dentistry, University of Minnesota, Minneapolis, Minnesota, USA)

2930 8:30 a.m. Headache Co-morbidity with TMD: Characteristics of Primary vs Secondary Headaches. R. OHRBACH*, C. SESSON, S. SHARMA (University at Buffalo, Buffalo, New York, USA)

2931 8:45 a.m. Are the DC/TMD Suitable for Diagnosis of TMDs in Schoolchildren? N. GIANNAKOPOULOS*, S. SCHWIEGERT, G. ORHAN, M. SCHMITTER, C. LUX, E. KATSIKOGLIANI (Department of Prosthodontics, University Clinic Würzburg, Würzburg, Germany)

2932 9 a.m. Identifying Criteria for Diagnosis of Persistent Dentoalveolar Pain Disorder and Similar Conditions: A Systematic Review. S. SHUEB*, A. CERVANTES CHAVARRIA, J. DURHAM, D. NIXDORF (Oral Biology, University of Minnesota, Minneapolis, Minnesota, USA)

2933 9:15 a.m. Sleep Bruxism and Sleep-related Breathing Disorders – a Polysomnographic Study. J. SMARDZ*, H. MARTYNOWICZ, A. WOJAKOWSKA, M. MICHALEK-ZRABKOWSKA, G. MAZUR, M. WIECKIEWICZ (Department of Experimental Dentistry, Wrocław Medical University, Wrocław, Poland)

Seq#: 334 Saturday, 22 June 2019, 8 a.m. – 9:30 a.m.
Oral Session, Room 224

Microbiology/Immunology – Oral Microbes and Systemic Disease I

Chairperson: E. Boyer

C2934 8 a.m. Pregnant Women's Oral Microbiome and Low-birth Weight Infant. P. LIU*, Y. CHAN, X. GAO, E. LO, R. WATTI, M. WONG (Dental Public Health, Faculty of Dentistry, The University of Hong Kong, Hong Kong, Hong Kong)

SC2935 8:15 a.m. Systemic Condition, Local Disorder: A Periodontitis-haemochromatosis Relationship Through Iron Homeostasis. E. BOYER*, S. LE GALL-DAVID, O. LORÉAL, Y. DEUGNIER, M. BONNAURE-MALLET, V. MEURIC (Univ Rennes, INSERM, INRA, CHU Rennes, Institut NUMECAN (Nutrition, Metabolism and Cancer), Rennes, France)

S2936 8:30 a.m. Metabolomic Profiling of Antibody Response to Periodontal Pathogens. J. LESKÉLA*, A. SALMINEN, T. PALVAINEN, M. PIETÄINEN, A.-M. MÄÄTTÄ, S. PAJU, J. SINISALO, V. SALOMAA, J. KAPRIO, P. PUSSINEN (Department of Oral and Maxillofacial Diseases, University of Helsinki, Helsinki, Finland)

8:45 a.m. Discussion.

Seq#: 335 Saturday, 22 June 2019, 8 a.m. – 9:30 a.m.
Oral Session, Room 306

Mineralized Tissue – Mineralized Tissue IV Bone: From Pathology to Regeneration

Chairperson: G. Garlet

SC2937 8 a.m. Sclerostin Impact on Craniofacial Bone Regeneration in a Murine Model. S. MAILLARD*, J. LESIEUR, B. BAROUKH, J. SADOINE, A. POLIARD, L. SLIMANI, C. CHAUSSAIN (EA 2496 Orofacial pathologies, Imaging and Biotherapies, Dental School University, Paris Descartes, Paris, Ile de France, France)

SE2938 8:15 a.m. BMP6-laden Calcium Phosphate Scaffolds for Bone Regeneration. W. Ji*, G. KERCKHOFS, C. GEEROMS, M. MARECHAL, L. GERIS, F. LUYTEN (Promethues, Division of Skeletal Tissue Engineering, KU Leuven, Leuven, Belgium, KU Leuven, Leuven, Belgium)

2939 8:30 a.m. Alveolar Bone Healing in Mice Genetically Selected for Maximum/Minimum Inflammatory Reaction. P. COLAVITE, A. VIEIRA, C. REPEKE, R. LINHARI, A. BORREGO, M. DEFRANCO, A. TROMBONE, G. GARLET* (Department of Biological Sciences, Universidade de São Paulo, Bauru, Sao Paulo, Brazil)

S2940 8:45 a.m. BOT-64 Enhances Alveolar Bone Regeneration in a Periodontitis Mouse Model. M. FRANCIS, A. SALAFATAS, T. DIEKWISCH, X. LIJIAN* (Dept. of Periodontics, TAMU College of Dentistry, Dallas, Texas, USA)

S2941 9 a.m. Role of NF-κB in MSC Expansion during Diabetic Fracture Healing. R. KRALIK*, K. KO, D. GRAVES (University of Pennsylvania, Philadelphia, Pennsylvania, USA)

2942 9:15 a.m. Myeloid Cell-Specific *IrB* Deletion Provides Novel Insights into Osteoclast Differentiation. A. DAS, X. WANG, A. COULTER, J. KANG, M. BACHLI, B. FOSTER, S. BROOKS, K. MANSKY, K. OZATO, M. SOMERMAN, V. THUMBIGERE MATH* (Periodontics, University of Maryland School of Dentistry, Baltimore, Maryland, USA)

Seq#: 336 Saturday, 22 June 2019, 8 a.m. – 9:30 a.m.
Oral Session, Room 211

Oral & Maxillofacial Surgery Research – Oral & Maxillofacial Research IV: Orthognathic Surgery and Reconstruction

Chairpersons: X. Wang and W. Fang

SC2943 8 a.m. Virtual Surgical Planning in the Management of Benign Maxillofacial Pathology. V. VINH*, J. MELVILLE, J. SHUM (University of Texas Health Science Center at Houston School of Dentistry, Houston, Texas, USA)

C2944 8:15 a.m. Long-term Results of Mandibular Reconstruction of Continuity Defects with Fibula Free Flap and Implant-borne Dental Rehabilitation. W. FANG* (Department of Dental Implant, School of Stomatology, Xian, Shaanxi, China)

C2945 8:30 a.m. Clinical Accuracy of a CAD/CAM Surgical Template for Mandibular Distraction. X. WANG*, B. LI (Department of Oral and Craniomaxillofacial Surgery, Ninth People's Hospital, Shanghai JiaoTong University School of Medicine, Shanghai, Shanghai, China)

SC2946 8:45 a.m. A Three-Dimensional Analysis for Nasolabial Changes Following Bimaxillary Orthognathic Surgery. Y. XU*, X. WANG (Department of Oral and Craniomaxillofacial Surgery, Shanghai Ninth People's Hospital, Shanghai, China)

Annexe C

Communication affichée à la Journée Scientifique des Hôpitaux Universitaires du Grand Ouest

Subgingival microbiota and iron overload in patients with hemochromatosis

Boyer E^{1,2}, Le Gall-David S², Deugnier Y^{3,4}, Bonnaure-Mallet M^{1,2}, Meuric V^{1,2}

¹CHU Rennes, Service d'Odontologie et de Chirurgie Buccale, Rennes, France
²Numecan, CIMAD (Control of Iron Metabolism and Iron-Associated Diseases), Université Rennes 1, UMR 1241, Rennes, France
³INSERM, CIC 1414, Rennes, France
⁴CHU Rennes, Service des maladies du Foie, Rennes, France

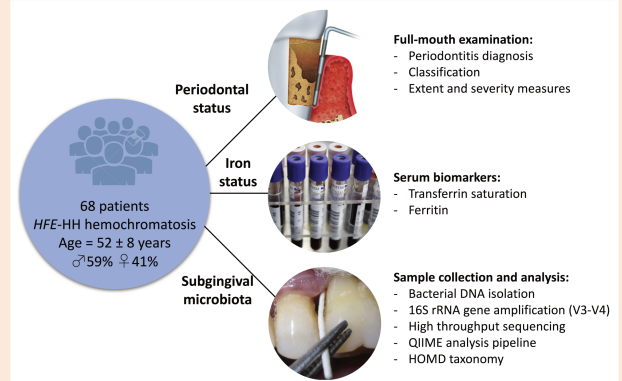
Introduction

HFE-related hereditary hemochromatosis (*HFE*-HH) is the most common form of inherited iron overload disease in European populations [1]. This condition is characterized by a hepcidin-deficiency state leading to increased transferrin saturation (TSAT) and serum ferritin rate. Classically, *HFE*-HH is responsible for hepatic cirrhosis, diabetes and skin pigmentation [2]. Lately, other symptoms have been increasingly associated to *HFE*-HH: chronic asthenia, arthropathy [3] and osteoporosis [4]. Standard treatment is therapeutic venesection, and international guidelines recommend to keep serum ferritin under 50 µg/L during maintenance [5-8].

In a previous study, we observed significant association between periodontitis severity and elevated TSAT in patients with *HFE*-HH [9]. Iron is an essential growth factor for bacteria, and also acts as a virulence regulator for *Porphyromonas gingivalis* and *Prevotella intermedia*, two common periodontal pathogens [10]. Non-transferrin bound iron (NTBI) can be identified in the plasma of patients with TSAT > 45% and is suspected to drive *HFE*-HH symptoms [11]. Besides, these toxic iron species could modulate bacterial growth and virulence [12]. We have hypothesized that *HFE* mutation and iron overload in hemochromatosis patients could alter and modulate their subgingival microbiota toward dysbiosis and explain the severity of their periodontitis.

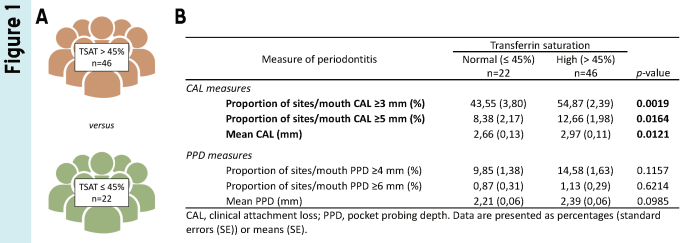
The aim of this study was to investigate potential association between subgingival microbiota and serum biomarker levels in *HFE*-HH patients that have previously shown a significant relationship between their iron burden and their periodontal status.

Materials & Methods

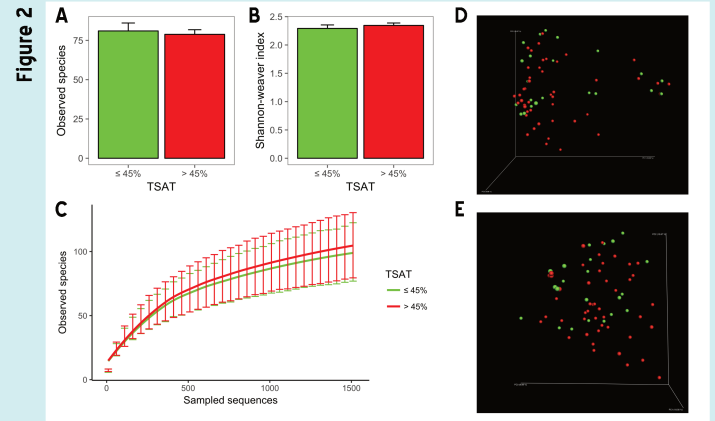


Patients with *HFE*-HH were recruited in the unit of Hepatology, University Hospital of Rennes. As described in Meuric et al., 2017, they underwent a periodontal examination and serum markers of iron metabolism were collected from medical records. Bacterial DNA from subgingival biofilm of 68 patients was extracted. *In silico*, alpha and beta diversity analysis was performed with QIIME (Figure 2). Statistical analysis of clinical and microbiological data was performed using R with clinical cut-offs (TSAT = 45%; Ferritin = 50 µg/L) (Figure 1). Co-occurrence network analysis was performed with the CoNet app for Cytoscape (Figure 3). *P* values < 0.05 were considered to indicate statistical significance.

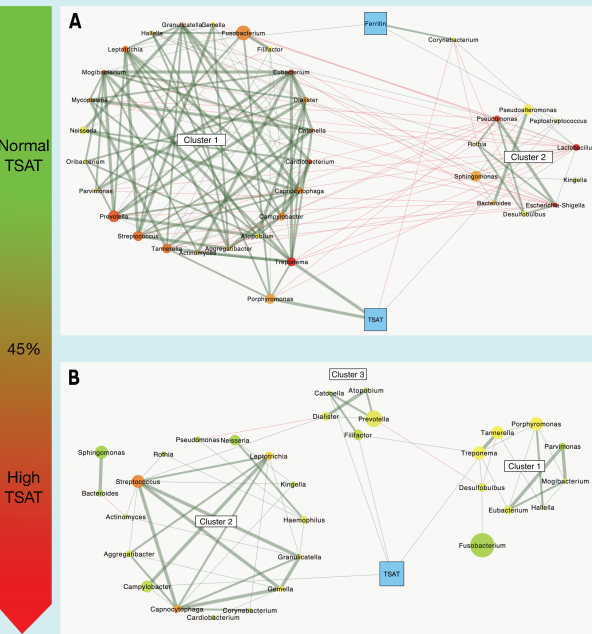
Results & Discussion



The TSAT cut-off allowed us to classify patients in 2 categories (A). Our previous study reported a risk 5-fold higher for severe periodontitis in patients with TSAT over 45%. To confirm this result, we compared periodontitis measures and found that patients with a high TSAT had clinical attachment loss measures significantly increased (B). Furthermore, 31.8% of patients with normal TSAT presented severe periodontitis versus 70.0% in patients with high TSAT (p=0.007). Conversely, there was no difference when comparing patients with normal and high ferritin (data not shown). The following analyzes were performed on the normal and high TSAT groups.



Surprisingly, alpha diversity analysis showed no significant difference in richness or evenness between patients with normal and high TSAT (AB). The rarefaction curves stabilized around 100 genus-level taxa with 1500 sampled sequences (C). As revealed by the 3D principal coordinates analysis (PCoA) with Bray-Curtis metrics, beta diversity analysis showed no clustering according to the TSAT level (DE). PCoA with UniFrac metrics did not show any cluster either (data not shown).



Genera that were present in at least 70% of the subjects with normal TSAT (A) and in 70% of the subjects with high TSAT (B) showed distinct co-occurrence patterns. The two groups shared 31 genera, and only 5 were unique to the normal TSAT patients.

In the normal TSAT group, the network showed two distinct bacterial clusters. While classic periopathogens were in cluster 1 (73.9% of total microbiota on average), frequently health-associated genera were in the cluster 2 (15.6% of total microbiota on average). In each cluster, genera were positively and strongly associated with each other. Conversely, there was a clear opposition between the two clusters. Moreover, TSAT presented a positive association with *Porphyromonas* and *Treponema* (Spearman coefficient $r=0.43$ $p<0.05$ for both), and a negative association with *Corynebacterium* (Spearman coefficient $r=-0.55$ $p<0.01$).

On the contrary, the high TSAT network appeared simpler, with less connections (58 edges versus 149 in the normal TSAT group) and very few negative associations. Genera still gathered in clusters, however no opposition was found. On average, clusters 1 and 3 accounted for 65.9% of total microbiota and contained the genera usually described in periodontitis while cluster 2 only accounted for 16.4%. The TSAT was positively associated with *Campylobacter*, *Catonella*, *Fillifactor* and *Treponema*, but with a lower strength, since only Bray-Curtis dissimilarity returned significant co-occurrences.

References

- Powell LW et al. Lancet 2016. PMID: 27004087.
- O'Neil J, Powell L. Semin Liver Dis 2005. PMID: 16315132.
- Guggenbuhl P et al. Best Pract Res Clin Rheumatol 2011. PMID: 22142745.
- Guggenbuhl P et al. Osteoporos Int 2005. PMID: 15928800.
- European Association for the Study of the Liver. J Hepatol 2010. PMID: 20471131
- Bismuth M, Peynaud-Debayle E. Haute Autorité de Santé 2005. Available on: <http://cpc.cx/k5o>.
- Swinkels DW et al. Neth J Med 2007. PMID: 18079569.
- Bacon BR et al. Hepatology 2011. PMID: 21452290.
- Meuric V et al. J Clin Periodontol 2017. PMID: 28586532.
- Byrne DP et al. Mol Oral Microbiol 2013. PMID: 23336115.
- Brissot P et al. Biochim Biophys Acta 2012. PMID: 21855608.
- Jolivet-Gougeon et al. Am J Gastroenterol 2008. PMID: 18684194.
- Goulet V et al. Infect Immun 2004. PMID: 15271890.
- Benesova K et al. PLoS One 2012. PMID: 22745741.
- Maia ML et al. J Clin Immunol 2015. PMID: 25479931

The authors wish to acknowledge and thank the French Institute for Odontologic Research (IFRO) for its support in developing this document.

Conclusions

The present study shows a clear association between iron and periodontal status. Transferrin saturation above 45% implied an increase of periodontitis measures and severity. Conversely, ferritin level had no effect on periodontal status.

The major finding of this study is the radical change of microbial pattern according to the iron burden. In patients with normal TSAT level, two bacterial communities appeared to compete. As TSAT was correlated with *Porphyromonas* and *Treponema*, the elevation of circulating iron could be in favor of periopathogenic bacteria and potentially facilitate dysbiosis. *Porphyromonas gingivalis* is able to use iron-binding proteins such as transferrin as an iron source [13]. Conversely, the bacterial network of high TSAT patients was characterized by a lack of competition between clusters and TSAT showed no significant correlation with any bacteria. The NTBI occurring when TSAT is above 45% may promote the growth of all genera and not only those with advanced iron capture mechanisms.

Our results tend to show an impact of the iron burden on periodontitis. However, iron overload may also have an impact on the host's immune response [14,15]. Further studies are necessary to complete our analysis of iron influence on microbiota. They could also provide a better understanding of the host-microbiota dynamics and periodontitis pathogenesis.

Annexe D

Communication affichée au Forum des Jeunes Chercheurs en Odontologie

Emile Boyer, François Robin, Sandrine Le Gall-David, Pascal Guggenbuhl, Olivier Loréal, Shao Bing Fong, Martine Bonnaure-Mallet, Vincent Meuric
INSERM, INRA, Univ Rennes 1, Univ Bretagne Loire, CHU de Rennes, Nutrition Metabolisms and Cancer, Rennes, France

OBJECTIVES

To complete the description of the *Hfe*^(-/-) animal model phenotype by assessing the mandibular and teeth-surrounding alveolar bone, and by characterizing their oral and gut microbiota.

INTRODUCTION

Haemochromatosis related to HFE gene (HH-HFE) is the most common inherited iron overload disease¹. Recently, HH-HFE patients have shown an increased risk of periodontitis associated with high transferrin saturation rates². An increased transferrin saturation is also associated with a dysbiosis of the subgingival microbiota³. The *Hfe*^(-/-) mouse is the murine model of the HH-HFE disease⁴, and have been widely used to better understand the metabolism of iron. However, the periodontal status of *Hfe*^(-/-) mice has not been characterized yet, as well as their oral and gut microbiota.

CONCLUSION

We demonstrated alterations of the mandibular bone in *Hfe*^(-/-) mice at 6 months, with periodontal bone loss, reduced alveolar bone and trabecular impairment. These results support the periodontal susceptibility observed in haemochromatosis patients, however, the periodontal defects in mice were not associated with a specific oral microbiota. Variations in gut microbiota composition could imply long-term effects and potential complications for older animals.

RESULTS

Parameters	WT	<i>Hfe</i> ^(-/-)	p-value
Body weight (g)	32.32 (1.10)	30.96 (1.08)	0.310
Hepatic iron concentration (µmol iron/liver g)	4.63 (0.39)	17.32 (2.54)	0.007**
Plasma iron concentration (µmol iron/L)	18.6 (0.67)	33.32 (2.06)	0.007**
Transferrin saturation (%)	37.88 (0.01)	82.72 (0.05)	0.007**

Table 1: General and iron parameters in *Hfe*^(-/-) and Wild-Type (WT) mice. Data are presented as mean (standard error) (n = 5 mice/group). Mann-Whitney, statistically significant at: **p < 0.01.

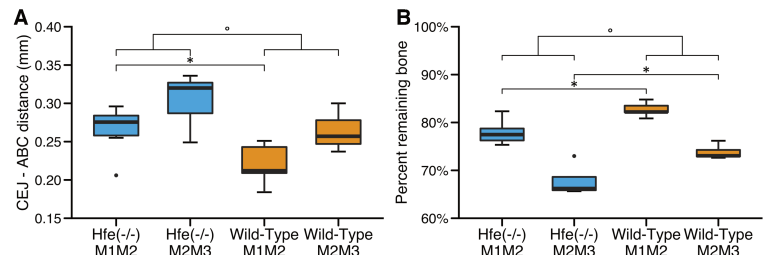


Figure 1: Alveolar bone loss in mice. **A:** distance from cementoamel junction (CEJ) to the alveolar bone crest (ABC). **B:** percent remaining bone (%) = [(root length - CEJ-ABC) / root length] x 100. Two interdental sites: between the first and second mandibular molars (M1M2) and between the second and the third mandibular molars (M2M3). Mann-Whitney, statistically significant at: *p < 0.05; Wilcoxon matched-pairs, statistically significant at: °p < 0.05.

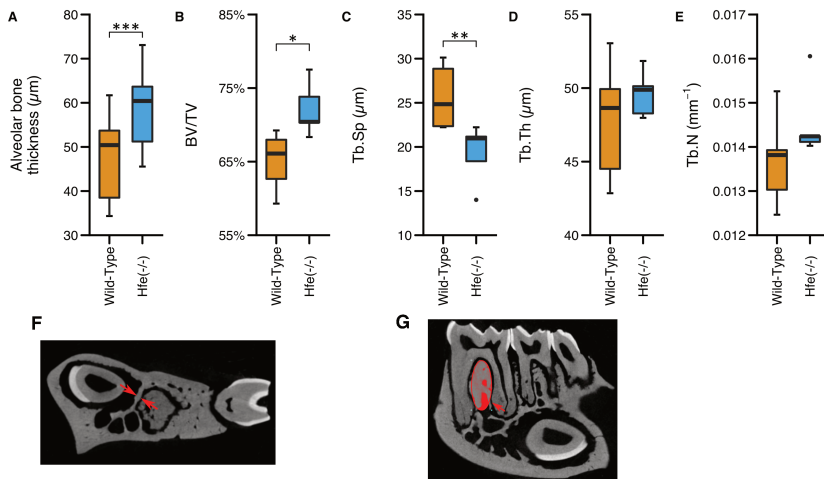


Figure 2: Characterization of alveolar bone structure. **A:** thickness of alveolar bone between the incisor and molar roots (red arrows in F). **B:** bone volume fraction (Bone Volume/Tissue Volume); **C:** trabecular thickness; **D:** trabecular separation; **E:** trabecular number, in the alveolar process between the roots of the first molar (red ellipse in G). Mann-Whitney, statistically significant at: *p < 0.05, **p < 0.01, ***p < 0.001.

MATERIAL & METHODS

Wild-type and *Hfe*^(-/-) mice (n = 5 mice/group) were anaesthetised and sacrificed at 6 months-old.

Blood samples, liver, cecum content and mandibles were collected, and analyzed for:

- Plasma iron parameters by biochemistry
- Trace elements detection by ICP-MS
- Assessment of mandibular alveolar bone by microCT (SkyScan 1172®, CTan, DataViewer)
- Oral and gut microbiota characterization (16S V3V4, Illumina MiSeq®, QIIME2)
- Statistics (RStudio)

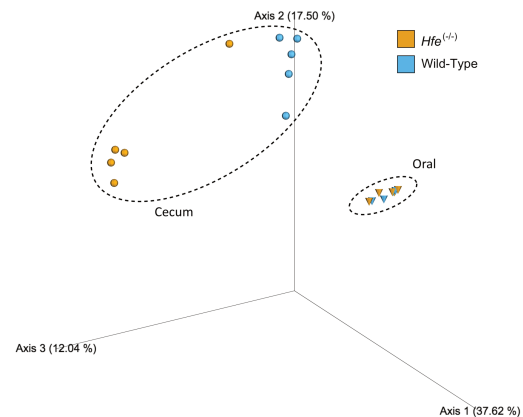


Figure 3: Beta diversity of the oral and gut microbiota of mice. Bioinformatics processing of the microbiota samples from the oral cavity and the cecum of *Hfe*^(-/-) and Wild-Type (WT) mice allowed for Principal Coordinate Analysis (PCoA) calculated with Bray-Curtis metric. Significant differences were found between *Hfe*^(-/-) and WT mice for cecum samples (PERMANOVA and ANOSIM: p < 0.05).

REFERENCES

1. PMID: 26975792
2. PMID: 28586532
3. PMID: 30341355
4. PMID: 21548776

Download the



PDF version!

Annexe E

**Première version du manuscrit
adressé au *Journal of Clinical
Periodontology***

Alteration and loss of mandibular alveolar bone in *Hfe* knocked-out mice

Journal:	<i>Journal of Clinical Periodontology</i>
Manuscript ID	Draft
Manuscript Type:	Original Article Clinical Periodontology
Date Submitted by the Author:	n/a
Complete List of Authors:	Boyer, Emile; Université de Rennes 1 - INSERM NuMeCan, EA1254/CIMIAD UMR1241 Robin, François; Université de Rennes 1 - INSERM NuMeCan, EA1254/CIMIAD UMR1241 Le gall-David, Sandrine; Université de Rennes 1 - INSERM NuMeCan, EA1254/CIMIAD UMR1241 Guggenbuhl, Pascal; Université de Rennes 1 - INSERM NuMeCan, EA1254/CIMIAD UMR1241 Loréal, Olivier; Université de Rennes 1 - INSERM NuMeCan, EA1254/CIMIAD UMR1241 Fong, Shao Bing; Université de Rennes 1 BONNAURE-MALLET, Martine; Université de Rennes 1, Equipe de Microbiologie UPRES-EA 1254 Meuric, Vincent; Université de Rennes 1 - INSERM NuMeCan, EA1254/CIMIAD UMR1241
Topic:	Aetiology
Main Methodology:	Animal Model
Keywords:	Alveolar Bone Loss, Microbiota, Haemochromatosis, Iron Overload, Mice

SCHOLARONE™
Manuscripts

1
2
3
4 Title: Alteration and loss of mandibular alveolar bone in *Hfe*
5
6
7 knocked-out mice
8
9

10
11 Running title: Alveolar bone loss in *Hfe*^(-/-) mice
12
13
14

15
16
17 **Emile Boyer^{1*}, François Robin^{1†}, Sandrine Le Gall-David^{1†}, Pascal Guggenbuhl¹, Olivier**
18 **Loréal¹, Shao Bing Fong¹, Martine Bonnaure-Mallet¹, Vincent Meuric¹**
19

20
21
22
23 ¹ INSERM, INRA, Univ Rennes 1, Univ Bretagne Loire, CHU de Rennes, Nutrition Metabolisms
24 and Cancer, Rennes, France
25

26
27 † These authors contributed equally to this work
28

29 *** Corresponding author**
30

31 Emile Boyer, <https://orcid.org/0000-0002-0208-2084>.

32 Phone: +33 (0)2 23 23 49 19
33

34 Email: emile.boyer@univ-rennes1.fr
35
36
37
38
39

40 **Acknowledgments**
41

42 The authors would like to thank Patricia Leroyer for her valuable technical assistance, as
43 well as the teams of Prof. Daniel Chappard (GEROM research unit, Angers, France) for the
44 micro computed tomography, and the AEM2 facility (Rennes, France) for the elemental
45 analysis and metal metabolism. We thank the GeT-PlaGe facility and the NED team (Toulouse,
46 France) for sequencing the samples. This study was funded by the *Institut Français pour la*
47 *Recherche en Odontologie* (IFRO).
48
49
50
51

52
53
54
55 **Abstract (200 words)**
56

57 **Aim:** *Hfe*^(-/-) mouse is the murine model of the *HFE*-related haemochromatosis, which is the
58 most common inherited iron overload disease in northern European descents. The aim of this
59
60

1
2
3 study was to characterize the *Hfe*^(-/-) phenotype for the mandibular bone microarchitecture, the
4 periodontal status, and the oral and gut microbiota.
5
6

7 **Materials and methods:** C57BL/6 mice knocked-out for the *Hfe* gene were analysed at 6
8 months-old regarding iron phenotype, alveolar bone loss and microarchitecture (by
9 morphometric analysis from micro-computed tomography), and taxonomic composition of the
10 oral and gut microbiota (by high-throughput sequencing of the 16S rRNA gene).
11
12
13

14 **Results:** Alike humans, the *Hfe*^(-/-) mice demonstrated an iron overload phenotype with higher
15 transferrin saturation, plasma and hepatic iron concentration than wild-type littermates. The
16 *Hfe*^(-/-) mice also exhibited alterations of the alveolar bone with reduced bone volume, increased
17 trabecular separation and alveolar bone loss. While no difference was found in the taxonomic
18 composition of the oral microbiota, the analysis revealed a significant clustering of the gut
19 microbiota according to the genotype of the mice, which could be due to variations of not-yet-
20 cultured bacteria.
21
22
23
24
25
26

27 **Conclusions:** The *Hfe*^(-/-) mice showed bone microarchitectural impairments, susceptibility to
28 periodontal damage and a specific gut microbiota.
29
30
31
32

33 **Keywords**

34 Alveolar Bone Loss; Microbiota; Haemochromatosis; Iron Overload; Mice
35
36
37
38
39

40 **Clinical Relevance (100 words)**

41 **Scientific rationale for study:** Haemochromatosis patients have shown an increased risk of
42 periodontitis and severe periodontitis is predominant in the patients with high transferrin
43 saturation rates.
44
45
46
47

48 **Principal findings:** Alterations in the alveolar bone of *Hfe*^(-/-) mice have been observed, with
49 periodontal bone loss, reduced alveolar bone and trabecular impairment. While no specific oral
50 microbiota was found in this model, complementary hypotheses should also be considered to
51 explain the periodontal susceptibility in case of iron overload.
52
53
54

55 **Practical implications:** These results support both the periodontal vulnerability observed in
56 haemochromatosis patients, and the need for dental examination for such patients.
57
58
59
60

1. Introduction

Haemochromatosis is the most common inherited iron overload disease (Powell, Seckington, & Deugnier, 2016). The main mutation leading to the clinical syndrome involved the *HFE* gene, which participates in the production of hepcidin, a regulatory protein engaged in the iron homeostasis. The substitution p.Cys282Tyr (C282Y) is the major *HFE* mutation that leads to a hepcidin-deficient state, which is responsible for excessive expression of ferroportin at the cell surfaces and the subsequent iron egress in the bloodstream. Iron deposition in the tissues and especially the occurrence of highly reactive forms of iron are considered the main causes of the symptoms of this disease (Brissot, Ropert, Le Lan, & Loréal, 2012).

Nowadays, most of the patients with hereditary haemochromatosis caused by the *HFE* gene (HH-HFE) are asymptomatic or present with chronic fatigue, and musculoskeletal conditions. One in three patients has osteoporosis, that is not explained by cirrhosis (Guañabens & Parés, 2018). Previous studies have shown that such bone lesions can be found in *Hfe* knockout mice (*Hfe*^{-/-}) morphometric and histological analysis of tibia revealed bone loss with an altered microarchitecture and an unbalanced bone homeostasis (Doyard et al., 2016; Guggenbuhl et al., 2011).

Recently, HH-HFE patients have also shown an increased risk of periodontitis in a case-series study (Meuric et al., 2017). This chronic inflammatory disease is characterized by the loss of the alveolar bone surrounding the teeth. Like osteoporosis, it seems that iron overload is the driver for this increased risk. Indeed, severe periodontitis is predominant in the patients with high transferrin saturation rates (Meuric et al., 2017). Nonetheless, a bacterial interplay has also been mentioned because increased transferrin saturation is associated with a dysbiosis of the subgingival microbiota, which is a leading cause of periodontitis (Boyer et al., 2018).

Animal models of hereditary haemochromatosis have been widely used to better understand the metabolism of iron, as well as the various iron overload related lesions and the pathogenesis of the disease. The *Hfe*^{-/-} mouse is the murine model of the HH-HFE disease (Fleming, Feng, & Britton, 2011). Alike humans, the *Hfe*^{-/-} mice demonstrate elevated transferrin saturation, increased iron concentration in blood and liver, as well as hepatic dysfunction and cardiac damage (Sukumaran et al., 2017).

However, the periodontal status of *Hfe*^{-/-} mice has not been characterized yet, as well as their oral and gut microbiota. The aim of this study was therefore to assess the mandibular and teeth-surrounding alveolar bone, and to characterize the oral and gut microbiota of 6 months-

1
2
3 old *Hfe*^(-/-) mice compared to wild-type animals, in order to complete the description of the
4 *Hfe*^(-/-) animal model phenotype.
5
6

7 **2. Materials and Methods**

8 **2.1. Animal model**

9
10
11 The study was approved by the ethical committee of Rennes for animal experimentation. All
12 experimented mice were male of a C57BL/6J background. *Hfe*^(-/-) (knock-out) mice were
13 produced in the animal facilities of UMS Biosit in Rennes (Arche). Controls consisted of Wild-
14 Type (WT) littermates. Animals were maintained under standard conditions of temperature,
15 atmosphere and light, and experimental procedures were performed in agreement with
16 European law and regulations. Mice were given free access to tap water and food (Teklad 19 %
17 Protein Rodent Diet). Mice were anaesthetised and sacrificed at 6 months for *Hfe*^(-/-) and
18 controls ($n = 5$ mice/group). Blood was obtained from a trans-diaphragmatic intracardiac
19 puncture and sampled in sodium heparin tubes suitable for trace element analysis. Livers,
20 digestive tract and mandibles were dissected. Samples from liver, cecum content and one hemi-
21 mandible were quickly frozen in liquid nitrogen and stored at -80°C to perform the
22 measurement of trace elements concentrations and microbiota analyses. The other hemi-
23 mandible was fixed in 70 % ethanol 10 % formaldehyde for 24h at 4°C, and then stored in
24 absolute acetone at 4°C until micro-computed tomography (micro-CT).
25
26
27
28
29
30
31
32
33
34
35

36 **2.2. Plasma iron parameters**

37
38 The concentration of iron in the plasma and the unsaturated iron-binding capacity were
39 measured in the Biochemistry Laboratory of the University Rennes Hospital on Cobas 8000
40 analyzer (Roche). Plasma transferrin saturation was then calculated as (Iron plasma) / (Iron
41 plasma + UIBC) × 100.
42
43
44
45

46 **2.3. Trace elements**

47
48 Liver samples were desiccated for 15 hours at 120°C. Then, dried samples were weighed
49 and mineralized by nitric acid solution (Fischer Chemical – Optima Grade) in special
50 polypropylene tubes for 2 hours at 110°C in a heating block. Specimens were then preserved at
51 4°C until quantification of iron. Iron was measured by Inductively Coupled Plasma Mass
52 Spectrometry (ICP-MS), on a X-Series II from Thermo Scientific equipped with collision cell
53 technology (AEM2 facility, University of Rennes 1 and Biochemistry Laboratory of the
54 University Rennes Hospital) as previously described (Cavey et al., 2015).
55
56
57
58
59
60

2.4. Micro-computed tomography

Micro-CT was performed on the hemi-mandible in the GEROM research unit (Angers, France) with a Skyscan 1272 (Bruker). The samples were placed in microtubes, filled with water to prevent desiccation. The tubes were fixed on brass stubs with plasticine and scanned with the following parameters: 9 μm resolution, Xray energy of 70 kV and 142 μA for 1.9 s exposure, 0.2° rotation step, 5.000097 μm image pixel size. The data were reconstructed with NRecon (v. 1.7.0.4, Bruker-MicroCT)

2.5. Quantification of alveolar bone loss

The DataViewer software (v. 1.5.6, Bruker-MicroCT) was used to visualise bone and produce the sagittal slices. All images were reoriented such that the cemento-enamel junction (CEJ) and the root apex (RA) appeared (Cho et al., 2016). Among the sagittal images, the image which showed the most recession of alveolar bone was selected for measurement. The distance from the alveolar bone crest (ABC) to the CEJ was measured in μm with the CTAn software (v. 1.18.8, Bruker-MicroCT) at two interdental sites: between the first and the second mandibular molars (M1M2) or between the second and the third mandibular molar (M2M3). As described elsewhere, the CEJ-ABC distance was the shortest distance from ABC to the line connecting the adjacent CEJs (Cho et al., 2016). Measurements of root lengths from the CEJ to the RA were also taken to assess the percentage of remaining alveolar bone using an equation previously described: Percent remaining bone (%) = $([\text{root length} - \text{CEJ-ABC}] / \text{root length}) \times 100$ (Park et al., 2007).

2.6. Characterization of alveolar bone microarchitecture

The bone microarchitecture of the hemi-mandible was characterized with the CTAnalyzer software (v. 1.18.8.0, Bruker-MicroCT), as described elsewhere (Bouvard, Gallois, Legrand, Audran, & Chappard, 2013). Briefly, each hemi-mandibular alveolar bone was measured on two types of 2D sections: five frontal sections through the middle of the pulp chamber of M1 were used to evaluate the thickness of alveolar bone (between the incisor and the M1 roots, five measurements per mouse) (see **Figure 1f**); eleven sagittal sections through the pulp chamber of M1, M2 and M3 were used to measure the trabecular characteristics of the bone. The volume of interest was an ellipse (1080 μm x 440 μm) centred in the alveolar process between the M1 roots (see **Figure 1g**). The following parameters were measured by 2D morphometric analysis: the trabecular bone volume (BV/TV, in %), the trabecular thickness (Tb.Th, in μm), the trabecular separation (Tb.Sp, in μm) and the trabecular number (Tb.N, in mm^{-1}).

2.7. Extraction and amplification of bacterial DNA

Total DNA was extracted from frozen cecum content and hemi-mandible using the QIAamp DNA Mini Kit (Qiagen, France) according to the manufacturer's recommendations. The DNA was then kept frozen at -80°C prior to amplification. The V3-V4 regions of the 16S rRNA gene were amplified with the primers 338F (5'-ACTCCTACGGGAGGCAGCAG-3') and 802R (5'-TACNVGGGTATCTAATCC-3') using 25 amplification cycles with an annealing temperature of 45°C. The PCR products were sequenced with the Illumina MiSeq at the GeT-PlaGe facility (Toulouse, France).

2.8. Oral and gut microbiota analysis

The FASTQ files from the GeT-PlaGe facility were processed with the QIIME2 software (v. 2018.4, <https://qiime2.org/>) following a pipeline adapted from the "Moving Pictures" tutorial (<https://docs.qiime2.org/2018.4/tutorials/moving-pictures/>) (Caporaso et al., 2010). The files were imported as "PairedEndFastqManifestPhred33" format. The pipeline DADA2 was used to control the sequence quality and construct the feature table. The forward and reverse sequences were truncated at 250 bases, with all other parameters set to default. After summarizing the sequence count, one oral sample was excluded from further analyses due to low sequence count (< 1 500 sequences). Prior to the taxonomic assignment at the genus level, reference reads were extracted from the "Ribosomal Database Project" based on matches to the primers pair (338F/802R) and trained as a Naive Bayes classifier (RDP release 11, training set No. 16, <http://rdp.cme.msu.edu/misc/rel10info.jsp>). The reads that were classified as Archaea or Unassigned were removed from the feature table. The table was then divided according to the sample localization (oral and cecum) and the core diversity analysis was performed on each table with a specific sampling depth (2 386 and 4 986, respectively). The core diversity included *alpha* (Sobs, Shannon-Weaver) and *beta* (Bray-Curtis, weighted UniFrac) diversity metrics.

2.9. Statistics

Data were analysed using the R (v. 3.5.0) and RStudio softwares (v. 1.1.383, <https://www.rstudio.com/>). Non-parametric tests were used and considered significant for $p < 0.05$. The results were expressed as mean \pm standard error of the mean. The Mann-Whitney and Wilcoxon matched-pairs signed rank tests were used to compare means for quantitative data related to iron, alveolar bone parameters and *alpha* diversity indices. The PERMANOVA and ANOSIM tests were performed on *beta* diversity metric with the QIIME2 diversity plugin (Anderson, 2001). A linear discriminant analysis on the taxa relative abundance between *Hfe*^(-/-)

1
2
3 and WT mice was computed on each sample type (oral and cecum) with the LefSe algorithm
4 (parameters set to default) in Galaxy (<https://huttenhower.sph.harvard.edu/galaxy/>). All plots
5 were made with 'ggplot2' for RStudio (Wickham, Chang, & RStudio, 2016), except for the
6 LefSe results and the 3D PCoA plot (EMPeror) (Vázquez-Baeza, Pirrung, Gonzalez, & Knight,
7 2013).

11 3. Results

14 3.1. Iron phenotype

16 General and iron parameters are summarized in **Table 1**. The *Hfe*^(-/-) mice were found to
17 have an iron overload phenotype with significantly higher transferrin saturation, plasma and
18 hepatic iron concentration than WT littermate mice ($p < 0.01$). No difference was found in the
19 body weight of mice between groups.

24 3.2. Alveolar bone microarchitecture

26 When looking at the bone parameters of the mandible, significant differences were found
27 between *Hfe*^(-/-) and WT (**Figure 1**). The thin bony slab between the incisor and the first molar
28 roots appeared to be significantly reduced in *Hfe*^(-/-) mice *versus* WT ($48.3 \pm 1.7 \mu\text{m}$ *versus* 58.3
29 $\pm 1.6 \mu\text{m}$, respectively; $p < 0.001$) (**Figure 1a**). There was a decreased in BV/TV in *Hfe*^(-/-) mice
30 *versus* WT ($65.1 \pm 1.6 \%$ *versus* $72.1 \pm 1.6 \%$, respectively; $p < 0.05$) (**Figure 1b**). An increased
31 in Tb.Sp occurred in *Hfe*^(-/-) mice *versus* WT ($25.6 \pm 1.5 \mu\text{m}$ *versus* $19.3 \pm 1.5 \mu\text{m}$, respectively;
32 $p < 0.01$) (**Figure 1c**). While no significant difference was found in Tb.Th, we observed a trend
33 towards a decrease Tb.N in *Hfe*^(-/-) *versus* WT (0.0137 ± 0.0004 *versus* $0.0145 \pm 0.0004 \text{ mm}^{-1}$,
34 respectively; $p < 0.10$) (**Figure 1d, e**).

42 3.3. Alveolar bone loss

44 We observed a generalized alveolar bone loss in *Hfe*^(-/-) mice. The average CEJ-ABC
45 distance was increased in *Hfe*^(-/-) mice *versus* WT mice ($282.8 \pm 11.4 \mu\text{m}$ *versus* 241.8 ± 10.7
46 μm , respectively; $p < 0.05$). This variation was higher in M1M2 region ($265.3 \pm 13.3 \mu\text{m}$ in
47 *Hfe*^(-/-) mice *versus* $219.8 \pm 12.2 \mu\text{m}$ in WT mice, $p < 0.05$) than in M2M3 region (303.8 ± 16.0
48 μm in *Hfe*^(-/-) mice *versus* $263.8 \pm 11.3 \mu\text{m}$ in WT mice, $p < 0.10$) (**Figure 2a**).

50 When the CEJ-ABC distances were related to the molar roots length, we obtained the
51 percentage of remaining bone and significant differences were also found (**Figure 2b**). *Hfe*^(-/-)
52 mice had a decrease in remaining bone compared to WT mice, in both M1M2 ($77.9 \pm 1.0 \%$
53 *versus* $82.7 \pm 0.7 \%$, respectively; $p < 0.05$) and M2M3 regions ($67.9 \pm 1.4 \%$ *versus* $73.8 \pm$
54 1.4% , respectively; $p < 0.05$).

1
2
3 0.7 %, respectively; $p < 0.05$). No significant difference was found in the molar roots length
4 between *Hfe*^(-/-) and WT mice (data not shown; $p > 0.05$).
5
6
7
8

9 **3.4. Oral and gut microbiota analysis**

10
11 The microbiota of the mice was sampled in two sites: oral cavity and cecum. The entire
12 taxonomic composition gathered by genotype and sample site is available in **Supplementary**
13 **Figure 1**. The overall observed richness of microbiota was increased in *Hfe*^(-/-), but the
14 differences were not found to be significant (**Table 2**). The cecum of *Hfe*^(-/-) harboured a
15 microbiota with significantly greater evenness compared to WT mice ($p < 0.01$). The evenness
16 of the oral samples of *Hfe*^(-/-) mice and controls were similar.
17
18
19
20
21

22 As expected, the two sampling sites harboured distinct microbiota (**Figure 3a**). For the oral
23 samples, no difference was found between *Hfe*^(-/-) and WT mice using the Bray-Curtis (**Figure**
24 **3b, c**) and Weighted UniFrac metrics. The principal coordinate analysis using the Bray-Curtis
25 metric showed a significant clustering of the samples from the cecum, according to the genetic
26 background of the mice (ANOSIM and PERMANOVA; $p < 0.05$) (**Figure 3d**). Although not
27 significant, a trend towards clustering of these samples was also observed using the Weighted
28 UniFrac metric (ANOSIM and PERMANOVA; $p < 0.10$) (**Supplementary Figure 2**).
29
30
31
32
33
34

35 The differential abundance testing with the LEfSe algorithm showed no significant
36 difference in oral samples according to the genotype of the mice, while the cecum samples
37 returned significant results (**Figure 4**). Noteworthy, several differentially abundant taxa
38 belonged to the Clostridiales order; the proportion of *Lachnospiraceae* Unclassified was found
39 decreased in *Hfe*^(-/-) (42.43 % versus 58.45% in controls; $p < 0.05$), while the proportions of
40 *Clostridium* cluster *XIVa*, *Ruminococcaceae*, *Ruminococcaceae* Unclassified *Clostridium*
41 cluster *IV* and *Oscillibacter* were found increased (17.13%, 13.62%, 9.55%, 1.82% and 1.94%
42 versus 6.94%, 7.45%, 4.93%, 1.44% and 0.98% in controls; $p < 0.05$). The Unclassified
43 variants in the *Lachnospiraceae* family were the most abundant taxa in the cecum samples
44 (**Supplementary Figure 1**).
45
46
47
48
49
50
51
52
53
54

55 **4. Discussion**

56
57 Iron overload related to genetic haemochromatosis has deleterious effects on multiple organs
58 and sites. Bone disorders are now a subject of greater attention, because of the scarcity of the
59
60

1
2
3 classic signs of the disease (cirrhosis, diabetes and skin pigmentation). Available clinical data
4 show that HH-HFE patients are more likely to have osteoporosis, (Guañabens & Parés, 2018).
5
6 The same phenotype has been observed in *Hfe*^(-/-) mice, the mouse model of HH-HFE. Recently,
7
8 a case-series study has reported a greater risk of severe periodontitis in these patients (Meuric
9
10 et al., 2017). This chronic inflammatory disease is characterized by the loss of the alveolar bone
11
12 surrounding the teeth. In this study, we investigated the periodontal and alveolar bone status in
13
14 the mandibles of *Hfe*^(-/-) mice.

15
16 As previously described, the *Hfe*^(-/-) mice demonstrated an increased body iron level with
17
18 elevated transferrin saturation, hepatic and blood iron concentrations (Fleming et al., 2011).
19
20 Precedent studies have found significant osteoporosis in the tibias of 12 months-old *Hfe*^(-/-)
21
22 mice, although minor changes in bone microarchitecture was observed at 6 months (Doyard et
23
24 al., 2016; Guggenbuhl et al., 2011). Specifically, the minor changes in the tibias at 6 months
25
26 included a slight decrease in the BV/TV and, inconstantly, an enhanced Tb.Sp. In our study,
27
28 the *Hfe*^(-/-) mice exhibited a significant reduction in mandibular BV/TV. This microarchitectural
29
30 impairment was confirmed by a significantly increased Tb.Sp as well. Taken together with a
31
32 decreased Tb.N, it could explain the reduced BV/TV and be interpreted as early signs of
33
34 osteoporosis in the model. The mandibular bone could therefore be used as a marker for early
35
36 detection of osteoporosis in HH-HFE patients, as it has already been proposed for routine
37
38 screening of at-risk women (Kavitha et al., 2015; Kawashima et al., 2019). Moreover, we
39
40 assessed the thickness of the mandibular alveolar bone as shown in Bouvard *et al.* (Bouvard et
41
42 al., 2013). In their study, the authors analysed the effects of glucocorticoids on trabecular bone
43
44 in mice. Although they used another line of mice (Swiss-Webster), we found similar reduction
45
46 in the thickness of the mandibular alveolar bone, thus confirming an alteration in the mandibular
47
48 bone of *Hfe*^(-/-) mice.

49
50 In order to test the presence of periodontal defects, we also performed measurements of the
51
52 alveolar bone surrounding the mandibular molars. The CEJ-ABC distance measured in WT
53
54 mice were consistent with a previous study on mice at the same age (Damanaki et al., 2018).
55
56 Interestingly, this CEJ-ABC distance was significantly increased in *Hfe*^(-/-) mice. In addition,
57
58 the remaining alveolar bone surrounding teeth was significantly decreased in *Hfe*^(-/-). These
59
60 results indicated an alveolar bone loss in *Hfe*^(-/-) mice, although the C57BL/6 strain is not
considered susceptible to periodontitis (Baker, Dixon, & Roopenian, 2000).

Furthermore, these results support the relationship that was recently uncovered between iron
overload in haemochromatosis patients and periodontitis (Boyer et al., 2018; Meuric et al.,

1
2
3 2017). In the latter study, it has been proposed that an increased transferrin saturation may drive
4 a dysbiosis of the oral microbiota by promoting genera strongly associated with periodontitis
5 (*Porphyromonas* and *Treponema*) (Boyer et al., 2018). However, no significant difference was
6 found between the oral bacterial community of *Hfe*^(-/-) model and control mice. The sample size
7 did not allow for relevant correlation tests and the taxonomic analysis did not detect known or
8 potential pathogens implicated in periodontitis. Therefore, complementary hypotheses may be
9 considered to explain this periodontal susceptibility in the *Hfe* knock-out line, which could
10 involve bone imbalance. On one hand, as mentioned earlier, *Hfe*^(-/-) mice have been shown to
11 develop an osteoporosis phenotype with a decrease in bone mass and a disorganization of the
12 trabecular microarchitecture, probably due to an impaired bone remodelling (Guggenbuhl et
13 al., 2011). On the other hand, a 2012 study has reported an impaired immune response in a
14 *Hfe*^(-/-) model of pulmonary inflammation (Benesova et al., 2012). The authors found an
15 attenuated recruitment of neutrophils, as well as differences in mRNA levels of several
16 cytokines and chemokines. Although the vulnerability to infection was probably not the cause
17 of alveolar bone loss in the *Hfe*^(-/-) mice, minor microbiota modification as discussed below and
18 dysregulated inflammatory response may have a negative impact on bone homeostasis through
19 the RANKL/OPG ratio with an increased bone resorption (Darveau, 2010).
20
21
22
23
24
25
26
27
28
29
30
31
32

33 The *Hfe*^(-/-) mice harboured an oral and gut microbiota with greater *alpha* diversity measures,
34 though only the evenness of the gut microbiota was found significantly increased. The cecum
35 was also the only site where the microbiota profile significantly clustered according to the
36 genotype of the mice. This result supports the findings of Buhnik-Rosenblau *et al.* that the gut
37 microbiota of mice is affected by a genetic deletion that disrupts the systemic and intestinal iron
38 homeostasis and metabolism (Buhnik-Rosenblau, Moshe-Belizowski, Danin-Poleg, &
39 Meyron-Holtz, 2012). In their study, the faeces of *Hfe*^(-/-), *Irp2*^(-/-) and WT mice were sampled
40 to analyse their bacterial profile. The authors reported wide differences between the faecal
41 bacterial profiles of the two knock-out lines. In contrast with our results, the profile of their WT
42 mice was found similar to those of each of their mutant lines. However, their principal
43 component analysis was based on bacterial profiles that were grown on agar plates. This could
44 have underestimated the variation of the profiles by a lack of detection of not-yet-cultured
45 bacteria. Although they may be less numerous than previously thought, these bacteria still
46 represent a substantial part of the healthy gut microbiota and need to be explored by Next
47 Generation Sequencing (Clavel, Lagkouvardos, Blaut, & Stecher, 2016; Lagkouvardos et al.,
48
49
50
51
52
53
54
55
56
57
58
59
60

1
2
3 2016). These taxa were, indeed, the most abundant in our samples from the cecum content and
4 allowed for clustering according to the genotype of the mice.
5
6

7 In conclusion, we demonstrated alterations of the mandibular bone in *Hfe*^(-/-) mice at 6
8 months, with periodontal bone loss, reduced alveolar bone and trabecular impairment. These
9 results support the periodontal susceptibility observed in haemochromatosis patients, however,
10 the periodontal defects in mice were not associated with a specific oral microbiota. Variations
11 in gut microbiota composition could imply long-term effects and potential complications for
12 older animals.
13
14
15
16
17
18
19
20
21
22
23
24
25
26
27
28
29
30
31
32
33
34
35
36
37
38
39
40
41
42
43
44
45
46
47
48
49
50
51
52
53
54
55
56
57
58
59
60

- 1
2
3 Anderson, M. J. (2001). A new method for non-parametric multivariate analysis of variance.
4
5 *Austral Ecology*, 26(1), 32–46. doi: 10.1111/j.1442-9993.2001.01070.pp.x
6
7
8 Baker, P. J., Dixon, M., & Roopenian, D. C. (2000). Genetic control of susceptibility to
9
10 Porphyromonas gingivalis-induced alveolar bone loss in mice. *Infection and Immunity*,
11
12 68(10), 5864–5868.
13
14
15 Benesova, K., Spasić, M. V., Schaefer, S. M., Stolte, J., Baehr-Ivacevic, T., Waldow, K., ...
16
17 Muckenthaler, M. U. (2012). Hfe Deficiency Impairs Pulmonary Neutrophil
18
19 Recruitment in Response to Inflammation. *PLOS ONE*, 7(6), e39363. doi:
20
21 10.1371/journal.pone.0039363
22
23
24
25 Bouvard, B., Gallois, Y., Legrand, E., Audran, M., & Chappard, D. (2013). Glucocorticoids
26
27 reduce alveolar and trabecular bone in mice. *Joint, Bone, Spine: Revue Du Rhumatisme*,
28
29 80(1), 77–81. doi: 10.1016/j.jbspin.2012.01.009
30
31
32
33 Boyer, E., Le Gall-David, S., Martin, B., Fong, S. B., Loréal, O., Deugnier, Y., ... Meuric, V.
34
35 (2018). Increased transferrin saturation is associated with subgingival microbiota
36
37 dysbiosis and severe periodontitis in genetic haemochromatosis. *Scientific Reports*,
38
39 8(1), 15532. doi: 10.1038/s41598-018-33813-0
40
41
42
43 Brissot, P., Ropert, M., Le Lan, C., & Loréal, O. (2012). Non-transferrin bound iron: A key role
44
45 in iron overload and iron toxicity. *Biochimica Et Biophysica Acta*, 1820(3), 403–410.
46
47 doi: 10.1016/j.bbagen.2011.07.014
48
49
50 Buhnik-Rosenblau, K., Moshe-Belizowski, S., Danin-Poleg, Y., & Meyron-Holtz, E. G. (2012).
51
52 Genetic modification of iron metabolism in mice affects the gut microbiota. *BioMetals*,
53
54 25(5), 883–892. doi: 10.1007/s10534-012-9555-5
55
56
57
58
59
60

- 1
2
3 Caporaso, J. G., Kuczynski, J., Stombaugh, J., Bittinger, K., Bushman, F. D., Costello, E. K.,
4
5 ... Knight, R. (2010). QIIME allows analysis of high-throughput community
6
7 sequencing data. *Nature Methods*, 7(5), 335–336. doi: 10.1038/nmeth.f.303
8
9
10 Cavey, T., Ropert, M., de Tayrac, M., Bardou-Jacquet, E., Island, M.-L., Leroyer, P., ... Loréal,
11
12 O. (2015). Mouse genetic background impacts both on iron and non-iron metals
13
14 parameters and on their relationships. *Biometals: An International Journal on the Role*
15
16 *of Metal Ions in Biology, Biochemistry, and Medicine*, 28(4), 733–743. doi:
17
18 10.1007/s10534-015-9862-8
19
20
21
22 Cho, Y.-J., Song, H. Y., Ben Amara, H., Choi, B.-K., Eunju, R., Cho, Y.-A., ... Koo, K.-T.
23
24 (2016). In Vivo Inhibition of Porphyromonas gingivalis Growth and Prevention of
25
26 Periodontitis With Quorum-Sensing Inhibitors. *Journal of Periodontology*, 87(9),
27
28 1075–1082. doi: 10.1902/jop.2016.160070
29
30
31
32 Clavel, T., Lagkouvardos, I., Blaut, M., & Stecher, B. (2016). The mouse gut microbiome
33
34 revisited: From complex diversity to model ecosystems. *International Journal of*
35
36 *Medical Microbiology: IJMM*, 306(5), 316–327. doi: 10.1016/j.ijmm.2016.03.002
37
38
39
40 Damanaki, A., Memmert, S., Nokhbeh-saim, M., Sanyal, A., Gnad, T., Pfeifer, A., & Deschner,
41
42 J. (2018). Impact of obesity and aging on crestal alveolar bone height in mice. *Annals*
43
44 *of Anatomy - Anatomischer Anzeiger*, 218, 227–235. doi: 10.1016/j.aanat.2018.04.005
45
46
47 Darveau, R. P. (2010). Periodontitis: A polymicrobial disruption of host homeostasis. *Nature*
48
49 *Reviews Microbiology*, 8(7), 481–490. doi: 10.1038/nrmicro2337
50
51
52 Doyard, M., Chappard, D., Leroyer, P., Roth, M.-P., Loréal, O., & Guggenbuhl, P. (2016).
53
54 Decreased Bone Formation Explains Osteoporosis in a Genetic Mouse Model of
55
56 Hemochromatosis. *PloS One*, 11(2), e0148292. doi: 10.1371/journal.pone.0148292
57
58
59
60

- 1
2
3 Fleming, R. E., Feng, Q., & Britton, R. S. (2011). Knockout Mouse Models of Iron
4 Homeostasis. *Annual Review of Nutrition*, *31*(1), 117–137. doi: 10.1146/annurev-nutr-
5 072610-145117
6
7
8
9
10 Guañabens, N., & Parés, A. (2018). Osteoporosis in chronic liver disease. *Liver International*,
11 *38*(5), 776–785. doi: 10.1111/liv.13730
12
13
14
15 Guggenbuhl, P., Fergelot, P., Doyard, M., Libouban, H., Roth, M.-P., Gallois, Y., ... Chappard,
16 D. (2011). Bone status in a mouse model of genetic hemochromatosis. *Osteoporosis*
17 *International: A Journal Established as Result of Cooperation between the European*
18 *Foundation for Osteoporosis and the National Osteoporosis Foundation of the USA*,
19 *22*(8), 2313–2319. doi: 10.1007/s00198-010-1456-2
20
21
22
23
24
25
26
27
28 Kavitha, M. S., An, S.-Y., An, C.-H., Huh, K.-H., Yi, W.-J., Heo, M.-S., ... Choi, S.-C. (2015).
29 Texture analysis of mandibular cortical bone on digital dental panoramic radiographs
30 for the diagnosis of osteoporosis in Korean women. *Oral Surgery, Oral Medicine, Oral*
31 *Pathology and Oral Radiology*, *119*(3), 346–356. doi: 10.1016/j.oooo.2014.11.009
32
33
34
35
36
37
38 Kawashima, Y., Fujita, A., Buch, K., Li, B., Qureshi, M. M., Chapman, M. N., & Sakai, O.
39 (2019). Using texture analysis of head CT images to differentiate osteoporosis from
40 normal bone density. *European Journal of Radiology*, *116*, 212–218. doi:
41 10.1016/j.ejrad.2019.05.009
42
43
44
45
46
47
48 Lagkouvardos, I., Pukall, R., Abt, B., Foessel, B. U., Meier-Kolthoff, J. P., Kumar, N., ... Clavel,
49 T. (2016). The Mouse Intestinal Bacterial Collection (miBC) provides host-specific
50 insight into cultured diversity and functional potential of the gut microbiota. *Nature*
51 *Microbiology*, *1*(10), 16131. doi: 10.1038/nmicrobiol.2016.131
52
53
54
55
56
57
58
59
60 Meuric, V., Lainé, F., Boyer, E., Le Gall-David, S., Oger, E., Bourgeois, D., ... Deugnier, Y.
(2017). Periodontal status and serum biomarker levels in *HFE* hemochromatosis

1
2
3 patients. A case series study. *Journal of Clinical Periodontology*, 44(9), 892–897. doi:
4
5 10.1111/jcpe.12760
6

7
8 Park, C. H., Abramson, Z. R., Taba, M., Jin, Q., Chang, J., Kreider, J. M., ... Giannobile, W.
9
10 V. (2007). Three-Dimensional Micro-Computed Tomographic Imaging of Alveolar
11
12 Bone in Experimental Bone Loss or Repair. *Journal of Periodontology*, 78(2), 273–281.
13
14 doi: 10.1902/jop.2007.060252
15
16

17
18 Powell, L. W., Seckington, R. C., & Deugnier, Y. (2016). Haemochromatosis. *Lancet (London,*
19
20 *England)*, 388(10045), 706–716. doi: 10.1016/S0140-6736(15)01315-X
21

22
23 Sukumaran, A., Chang, J., Han, M., Mintri, S., Khaw, B.-A., & Kim, J. (2017). Iron overload
24
25 exacerbates age-associated cardiac hypertrophy in a mouse model of hemochromatosis.
26
27 *Scientific Reports*, 7(1), 5756. doi: 10.1038/s41598-017-05810-2
28
29

30
31 Vázquez-Baeza, Y., Pirrung, M., Gonzalez, A., & Knight, R. (2013). EMPeror: A tool for
32
33 visualizing high-throughput microbial community data. *GigaScience*, 2, 16. doi:
34
35 10.1186/2047-217X-2-16
36

37
38 Wickham, H., Chang, W., & RStudio. (2016). ggplot2: Create Elegant Data Visualisations
39
40 Using the Grammar of Graphics (Version 2.2.1). Retrieved from [https://cran.r-](https://cran.r-project.org/web/packages/ggplot2/index.html)
41
42 [project.org/web/packages/ggplot2/index.html](https://cran.r-project.org/web/packages/ggplot2/index.html)
43
44
45
46
47
48
49
50
51
52
53
54
55
56
57
58
59
60

Parameters	WT	<i>Hfe</i> ^(-/-)	<i>p</i> -value
Body weight (g)	32.32 (1.10)	30.96 (1.08)	0.310
Hepatic iron concentration (μmol iron/liver g)	4.63 (0.39)	17.32 (2.54)	0.007**
Plasma iron concentration (μmol iron/L)	18.6 (0.67)	33.32 (2.06)	0.007**
Transferrin saturation (%)	37.88 (0.01)	82.72 (0.05)	0.007**

Table 1: General and iron parameters in *Hfe*^(-/-) and Wild-Type (WT) mice. Data are presented as mean (standard error) (*n* = 5 mice/group). Mann-Whitney, statistically significant at: ***p* < 0.01.

For Peer Review

Alpha diversity metric	Sample Type	WT	<i>Hfe</i> ^(-/-)
Observed richness	Oral	54.5 (5.7)	74.4 (6.1)
	Cecum	106.0 (10.7)	124.8 (6.0)
Shannon-Weaver evenness	Oral	4.4 (0.1)	4.4 (0.1)
	Cecum	5.1 (0.1)	6.0 (0.2)**

Table 2: *Alpha* diversity of the oral and gut microbiota of *Hfe*^(-/-) and Wild-Type (WT) mice. Data are presented as mean (standard error) ($n = 4$ or 5 mice/group). Mann-Whitney, statistically significant at: ** $p < 0.01$.

For Peer Review

1
2
3
4
5
6
7
8
9
10
11
12
13
14
15
16
17
18
19
20
21
22
23
24
25
26
27
28
29
30
31
32
33
34
35
36
37
38
39
40
41
42
43
44
45
46
47
48
49
50
51
52
53
54
55
56
57
58
59
60

Figure 1: Characterization of alveolar bone structure. Following the microCT analysis of the hemi-mandibles of *Hfe*^(-/-) and Wild-Type mice ($n = 5$ mice/group, 6 months old), five frontal sections were used to evaluate the thickness of alveolar bone (**a**) between the incisor and molar roots (red arrows in **f**). Eleven sagittal sections of the alveolar process between the first molar roots were used to measure the bone volume fraction (Bone Volume/Tissue Volume) (**b**), the trabecular thickness (**c**), the trabecular separation (**d**) and the trabecular number (**e**) in the alveolar process between the roots of the first molar (red ellipse in **g**). Mann-Whitney, statistically significant at: * $p < 0.05$, ** $p < 0.01$, *** $p < 0.001$.

1
2
3
4
5
6
7
8
9
10
11
12
13
14
15
16
17
18
19
20
21
22
23
24
25
26
27
28
29
30
31
32
33
34
35
36
37
38
39
40
41
42
43
44
45
46
47
48
49
50
51
52
53
54
55
56
57
58
59
60

Figure 2: Alveolar bone loss in mice. Measurements of bone levels were made by comparing the distance from the cementoenamel junction (CEJ) to the alveolar bone crest (ABC) (**a**) and the percentage of remaining bone (**b**) at two interdental sites: between the first and second mandibular molars (M1M2) and between the second and the third mandibular molars (M2M3). Root lengths (from the CEJ to the root apex) were also measured to assess the percentage of remaining alveolar bone: Percent remaining bone (%) = $([\text{root length} - \text{CEJ-ABC}] / \text{root length}) \times 100$. *Hfe*^(-/-) and Wild-Type mice were 6 months old (*n* = 5 mice/group). Mann-Whitney, statistically significant at: **p* < 0.05; Wilcoxon matched-pairs, statistically significant at: #*p* < 0.05.

1
2
3
4
5
6
7
8
9
10
11
12
13
14
15
16
17
18
19
20
21
22
23
24
25
26
27
28
29
30
31
32
33
34
35
36
37
38
39
40
41
42
43
44
45
46
47
48
49
50
51
52
53
54
55
56
57
58
59
60

Figure 3: *Beta* diversity of the oral and gut microbiota of mice. Bioinformatics processing of the microbiota samples from the oral cavity and the cecum of *Hfe*^(-/-) and Wild-Type (WT) mice ($n = 4$ to 5 mice/group, 6 months old) allowed for Principal Coordinate Analysis (PCoA) calculated with Bray-Curtis metric. The PCoA have been performed with all samples (**a**) and within each sample type (**b**, **c**). Significant differences were found between *Hfe*^(-/-) and WT mice for cecum samples (**c**) (PERMANOVA and ANOSIM: $p < 0.05$).

1
2
3
4
5
6
7
8
9
10
11
12
13
14
15
16
17
18
19
20
21
22
23
24
25
26
27
28
29
30
31
32
33
34
35
36
37
38
39
40
41
42
43
44
45
46
47
48
49
50
51
52
53
54
55
56
57
58
59
60

Figure 4: Analysis of taxa relative abundances in the cecum according to the genotype of mice. The represented taxa showed significant differences with the LEfSe analysis in their relative abundance between *Hfe*^(-/-) and Wild-Type mice ($n = 5$ mice/group; $p < 0.05$). The percentages are the average relative abundance of the corresponding taxa in mice of the related genotype.

For Peer Review

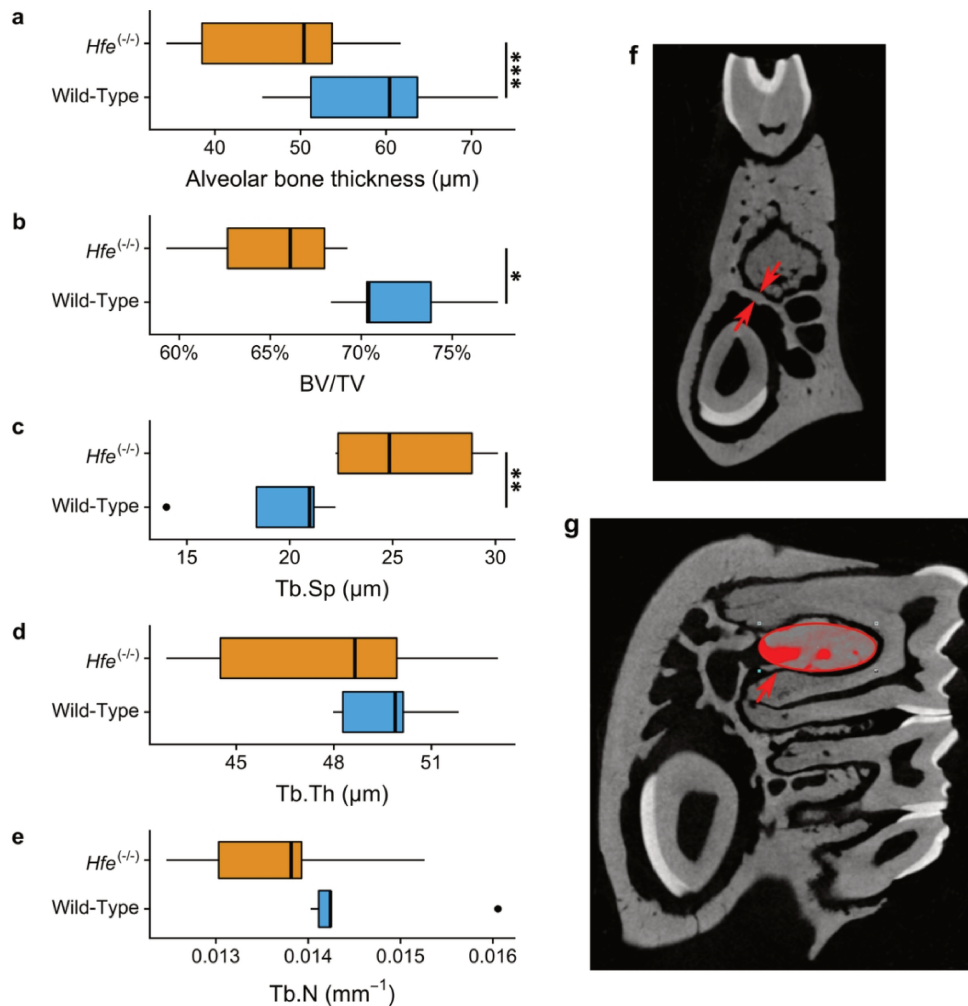
1
2
3
4
5
6
7
8
9
10
11
12
13
14
15
16
17
18
19
20
21
22
23
24
25
26
27
28
29
30
31
32
33
34
35
36
37
38
39
40
41
42
43
44
45
46
47
48
49
50
51
52
53
54
55
56
57
58
59
60

Supplementary Figure 1: Taxonomic composition of the oral and gut microbiota in mice. The QIIME2 pipeline allowed for taxonomic assignment with the “Ribosomal Database Project” (RDP, release 11, training set No. 16). The taxonomic table was divided according to the sampling site (oral and cecum) and the genotype (*Hfe*^{-/-} and Wild-Type (WT)) (*n* = 4 or 5 mice/group). The bar plots show the average relative abundance of taxa that were identified in each group at different taxonomic level: phylum (a), family (b) and genus (c).

1
2
3
4
5
6
7
8
9
10
11
12
13
14
15
16
17
18
19
20
21
22
23
24
25
26
27
28
29
30
31
32
33
34
35
36
37
38
39
40
41
42
43
44
45
46
47
48
49
50
51
52
53
54
55
56
57
58
59
60

Supplementary Figure 2: *Beta* diversity of the microbiota in the cecum of mice. The Principal Coordinate Analysis (PCoA) was calculated with the Weighted UniFrac metric. The samples are showed according to their genotype *Hfe*^(-/-) and Wild-Type (WT) (*n* = 5 mice/group, 6 months old). PERMANOVA and ANOSIM: *p* < 0.10.

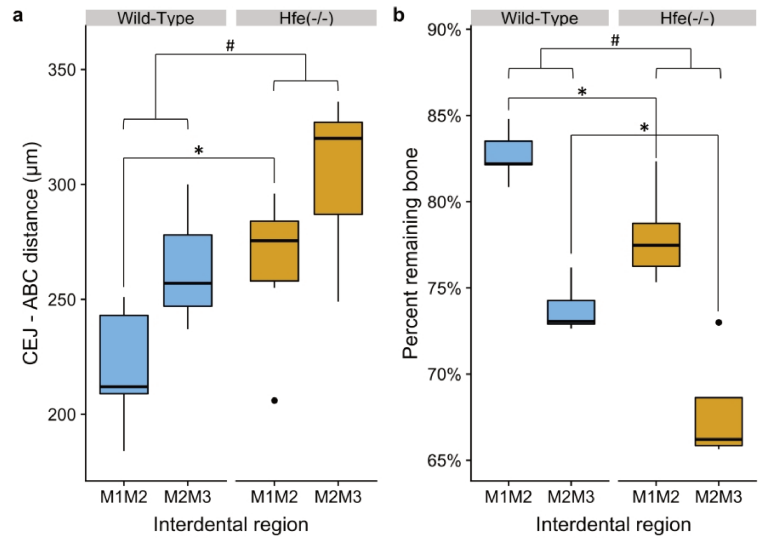
For Peer Review



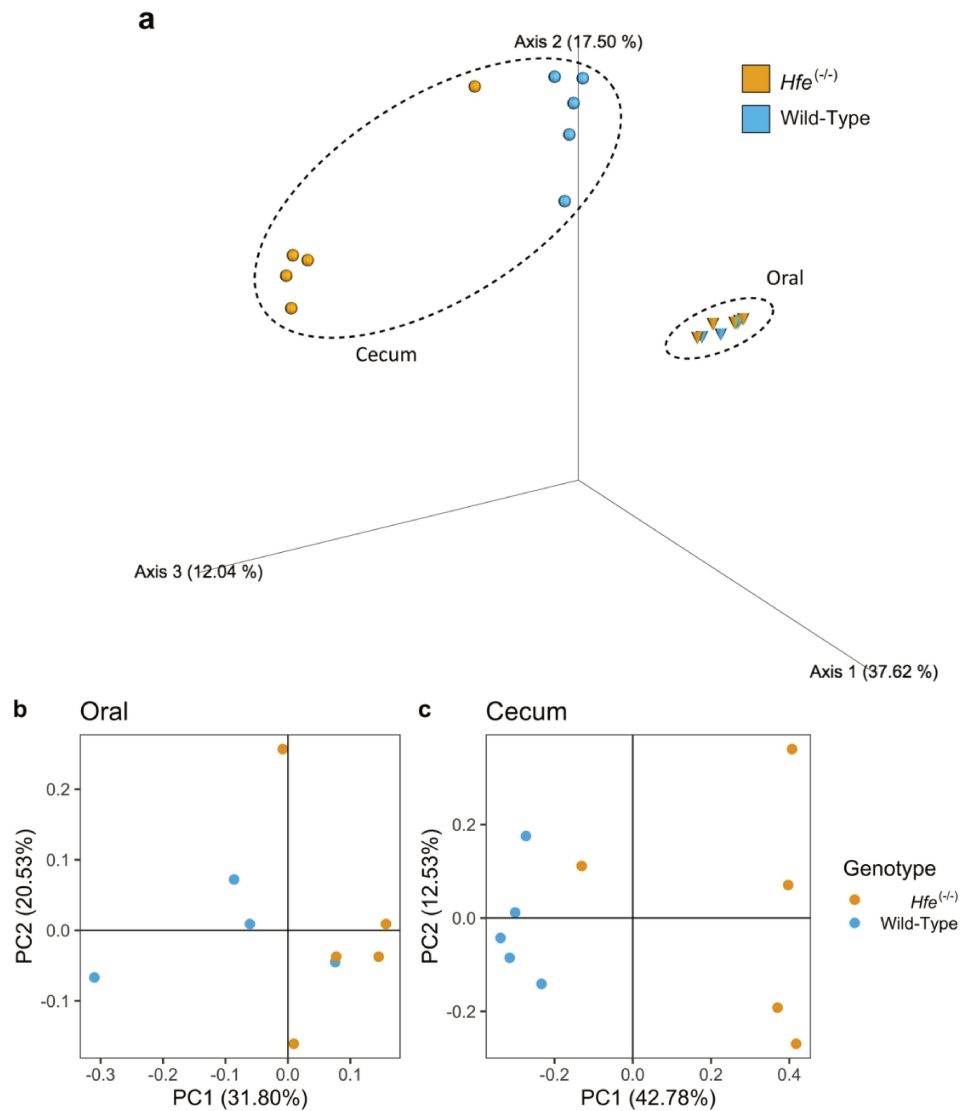
Characterization of alveolar bone structure. Following the microCT analysis of the hemi-mandibles of *Hfe*^(-/-) and Wild-Type mice ($n = 5$ mice/group, 6 months old), five frontal sections were used to evaluate the thickness of alveolar bone (**a**) between the incisor and molar roots (red arrows in **f**). Eleven sagittal sections of the alveolar process between the first molar roots were used to measure the bone volume fraction (Bone Volume/Tissue Volume) (**b**), the trabecular thickness (**c**), the trabecular separation (**d**) and the trabecular number (**e**) in the alveolar process between the roots of the first molar (red ellipse in **g**). Mann-Whitney, statistically significant at: $*p < 0.05$, $**p < 0.01$, $***p < 0.001$.

104x109mm (300 x 300 DPI)

1
2
3
4
5
6
7
8
9
10
11
12
13
14
15
16
17
18
19
20
21
22
23
24
25
26
27
28
29
30
31
32
33
34
35
36
37
38
39
40
41
42
43
44
45
46
47
48
49
50
51
52
53
54
55
56
57
58
59
60



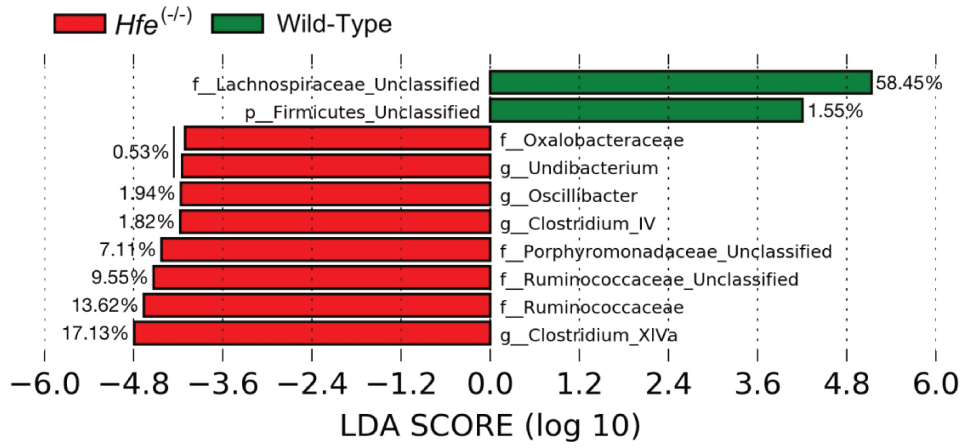
Alveolar bone loss in mice. Measurements of bone levels were made by comparing the distance from the cemento-enamel junction (CEJ) to the alveolar bone crest (ABC) (**a**) and the percentage of remaining bone (**b**) at two interdenal sites: between the first and second mandibular molars (M1M2) and between the second and the third mandibular molars (M2M3). Root lengths (from the CEJ to the root apex) were also measured to assess the percentage of remaining alveolar bone: Percent remaining bone (%) = $([\text{root length} - \text{CEJ-ABC}] / \text{root length}) \times 100$. *Hfe*^(-/-) and Wild-Type mice were 6 months old (*n* = 5 mice/group). Mann-Whitney, statistically significant at: **p* < 0.05; Wilcoxon matched-pairs, statistically significant at: #*p* < 0.05.



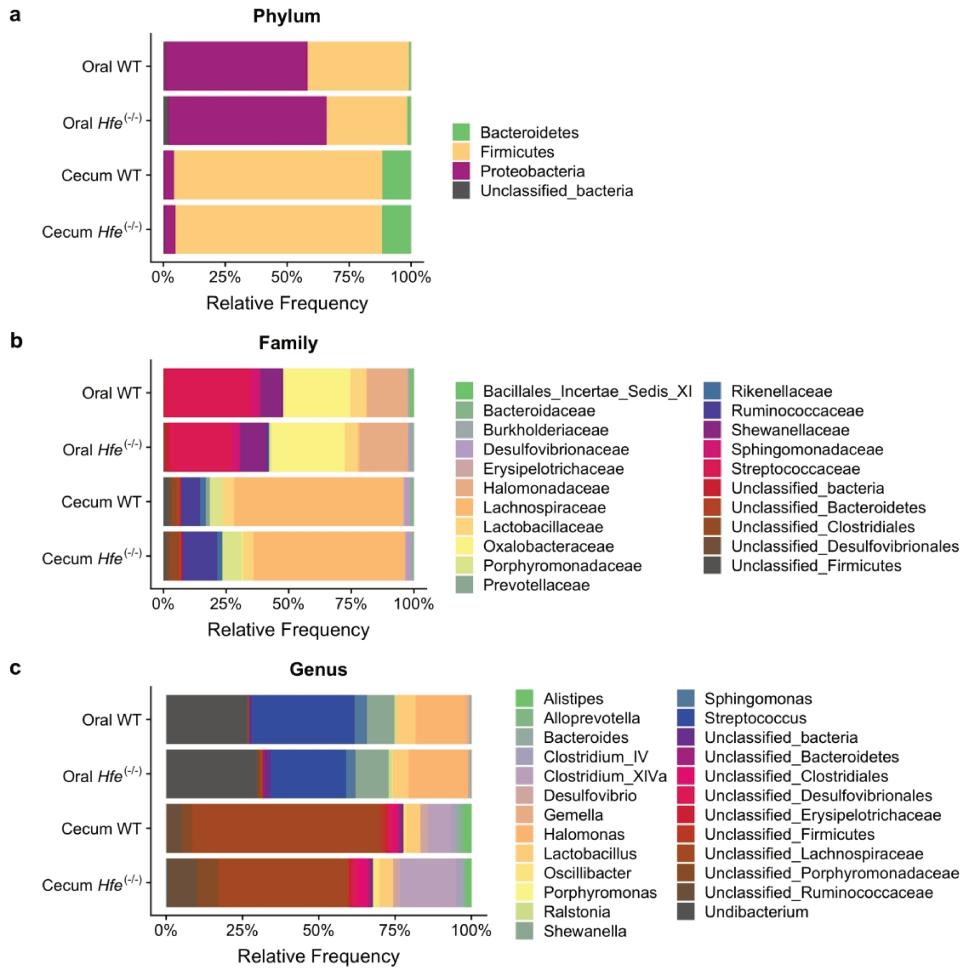
43 *Beta* diversity of the oral and gut microbiota of mice. Bioinformatics processing of the microbiota samples from the oral cavity and the cecum of $Hfe^{(-/-)}$ and Wild-Type (WT) mice ($n = 4$ to 5 mice/group, 6 months old) allowed for Principal Coordinate Analysis (PCoA) calculated with Bray-Curtis metric. The PCoA have been performed with all samples (**a**) and within each sample type (**b**, **c**). Significant differences were found between $Hfe^{(-/-)}$ and WT mice for cecum samples (**c**) (PERMANOVA and ANOSIM: $p < 0.05$).

48 131x150mm (300 x 300 DPI)

1
2
3
4
5
6
7
8
9
10
11
12
13
14
15
16
17
18
19
20
21
22
23
24
25
26
27
28
29
30
31
32
33
34
35
36
37
38
39
40
41
42
43
44
45
46
47
48
49
50
51
52
53
54
55
56
57
58
59
60

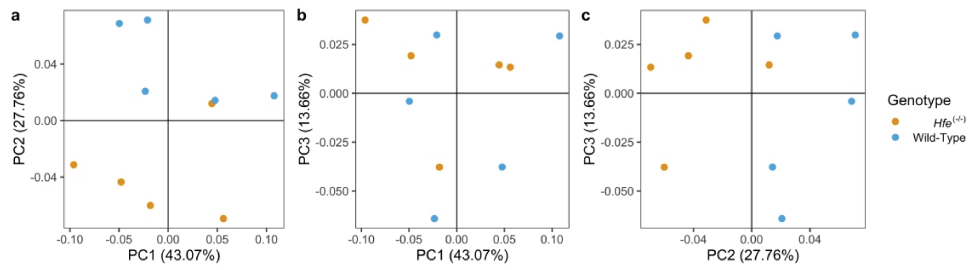


Analysis of taxa relative abundances in the cecum according to the genotype of mice. The represented taxa showed significant differences with the LEfSe analysis in their relative abundance between *Hfe*^(-/-) and Wild-Type mice (*n* = 5 mice/group; *p* < 0.05). The percentages are the average relative abundance of the corresponding taxa in mice of the related genotype.



1063x1070mm (72 x 72 DPI)

1
2
3
4
5
6
7
8
9
10
11
12
13
14
15
16
17
18
19
20
21
22
23
24
25
26
27
28
29
30
31
32
33
34
35
36
37
38
39
40
41
42
43
44
45
46
47
48
49
50
51
52
53
54
55
56
57
58
59
60



3117x857mm (72 x 72 DPI)

Annexe F

Commentaires des relecteurs du *Journal of Clinical Periodontology*

De: Jannani Perumal onbehalfof@manuscriptcentral.com
Objet: Journal of Clinical Periodontology - Decision on Manuscript ID CPE-07-19-8446
Date: 12 août 2019 à 16:26
À: emile.boyer@univ-rennes1.fr



12-Aug-2019

Dear Dr. Boyer:

Manuscript ID CPE-07-19-8446 entitled "Alteration and loss of mandibular alveolar bone in *Hfe* knocked-out mice" which you submitted to the Journal of Clinical Periodontology, has been reviewed. The comments from reviewer(s) are included at the bottom of this letter.

In view of the criticisms of the reviewer(s), I must decline the manuscript for publication in the Journal of Clinical Periodontology at this time. However, a new manuscript may be submitted which takes into consideration these comments.

Please note that resubmitting your manuscript does not guarantee eventual acceptance, and that your resubmission will be subject to re-review by the reviewer(s) before a decision is rendered.

You will be unable to make your revisions on the originally submitted version of your manuscript. Instead, revise your manuscript using a word processing program and save it on your computer.

When resubmitting, please provide your response to the comments made by the reviewer(s) in a separate document and upload it under the file designation 'Response to reviewers'. In order to expedite the processing of the resubmitted manuscript, please be as specific as possible in your response to the reviewer(s).

Once you have revised your manuscript, go to <https://mc.manuscriptcentral.com/jcpe> and login to your Author Center. Click on "Manuscripts with Decisions," and then click on "Create a Resubmission" located next to the manuscript number. Then, follow the steps for resubmitting your manuscript.

If you feel that your paper could benefit from English language polishing, you may wish to consider having your paper professionally edited for English language by a service such as Wiley's at <http://wileyeditingservices.com>. Please note that while this service will greatly improve the readability of your paper, it does not guarantee acceptance of your paper by the journal.

Because we are trying to facilitate timely publication of manuscripts submitted to the Journal of Clinical Periodontology, your revised manuscript should be uploaded as soon as possible. If it is not possible for you to submit your revision within a reasonable amount of time, we will consider your paper as a new submission.

I look forward to a resubmission.

Sincerely,
Maurizio Tonetti
Editor in Chief, Journal of Clinical Periodontology

Associate Editor's Comments to Author:

Associate Editor
Comments to the Author:

Low sample size does not allow strong conclusions at present. Moreover, the study is descriptive and lacks mechanisms. Specifically, the study simply confirms that the phenotype of *Hfe* deficient mice is consistent with that of patients with hereditary haemochromatosis caused by the *Hfe* gene. A major reason for using animal models is to provide mechanistic insights into the human disease.

Reviewer #1

The manuscript by Boyer et al. presents an analysis of the mandibular and alveolar bone and oral and gut microbiome in *Hfe*(-/-) mice and littermate controls. *Hfe*(-/-) mice are a model for human hereditary haemochromatosis, displaying elevated transferrin saturation and increased iron concentration in blood and liver. Humans with HFE hereditary haemochromatosis have been shown to have increased prevalence of periodontitis. The manuscript is for the most part well written (although correction of some grammar mistakes is needed) and the study is important and relevant. The authors show that *Hfe*(-/-) mice have reduced bone volume and alveolar bone loss. While differences in the composition of the gut microbiome were found, no differences in the composition of the oral microbiome were seen. Although the microbiome analysis applied was adequate, the lack of significant differences in oral samples could have been due to a very low sample size. With an n of 5 (in fact n=4 as one oral sample was not included due to low read counts), it is likely that lack of differences in oral microbiome communities was due to low power. Figure 3 indeed suggests a trend for oral communities from the two groups to cluster apart from each other. As it is, the findings are important, but the conclusion that the oral microbiome of *Hfe*(-/-) mice and controls is similar seems premature. The study would benefit from inclusion of more oral microbiome samples. Larger sample size could also allow correlational analysis to relate host markers of iron overload to microbial features.

Specific comment:

Abstract: The authors state that "the analysis revealed a significant clustering of the gut microbiota according to the genotype of the mice, which could be due to variations of not-yet cultured bacteria." It is not clear what they mean with that statement as the 16S rRNA gene analysis captures uncultivated microorganisms.

Reviewer #2

The authors showed alterations of the mandibular bone that are signs of osteoporosis in six-month-old Hfe deficient mice. The phenotype of the Hfe deficient mice in periodontal bone loss is consistent with that of patients with hereditary haemochromatosis caused by the Hfe gene (HH-HFE). The authors also analyzed oral and cecal microbiota in the Hfe deficient mice. Major and minor concerns are listed below.

Major concern

1) Although the authors showed the consistent phenotype of periodontal bone loss in the Hfe deficient mice with HH-HFE patients, the investigation is quite descriptive. In other words, the authors have not provided a mechanism. Why did the lack of the Hfe gene result in the severer bone loss in mandible? Since there was no statistical difference in the oral microbiota, there should be biological difference derived from host response. At least one possible mechanism should be proved experimentally.

Minor concerns

1) The authors should clarify how the Hfe deficient mice and their wild-type (WT) littermate controls were housed. Were they in the same cage or separated? If they were in the same cage, the duration of co-housing should be specified. This information is important when the microbiota analysis is performed.

2) Can the authors analyze mRNA expression of inflammatory cytokines, Rankl and Opg in periodontium of Hfe deficient mice and their WT controls in order to get a global idea to clarify the possible mechanism?

3) Histological or flow cytometry analysis characterizing immune cells may help to reveal the mechanism.

Reviewer(s)' Comments to Author:

Referee: 1

Comments to the Author
see attached comments

Referee: 2

Comments to the Author

The authors showed alterations of the mandibular bone that are signs of osteoporosis in six-month-old Hfe deficient mice. The phenotype of the Hfe deficient mice in periodontal bone loss is consistent with that of patients with hereditary haemochromatosis caused by the Hfe gene (HH-HFE). The authors also analyzed oral and cecal microbiota in the Hfe deficient mice. Major and minor concerns are listed below.

Major concern

1) Although the authors showed the consistent phenotype of periodontal bone loss in the Hfe deficient mice with HH-HFE patients, the investigation is quite descriptive. In other words, the authors have not provided a mechanism. Why did the lack of the Hfe gene result in the severer bone loss in mandible? Since there was no statistical difference in the oral microbiota, there should be biological difference derived from host response. At least one possible mechanism should be proved experimentally.

Minor concerns

1) The authors should clarify how the Hfe deficient mice and their wild-type (WT) littermate controls were housed. Were they in the same cage or separated? If they were in the same cage, the duration of co-housing should be specified. This information is important when the microbiota analysis is performed.

2) Can the authors analyze mRNA expression of inflammatory cytokines, Rankl and Opg in periodontium of Hfe deficient mice and their WT controls in order to get a global idea to clarify the possible mechanism?

3) Histological or flow cytometry analysis characterizing immune cells may help to reveal the mechanism.

Annexe G

**Accusé de réception du manuscrit
révisé soumis à *Journal of Clinical
Periodontology***

De: Jannani Perumal onbehalfof@manuscriptcentral.com
Objet: Manuscript ID CPE-11-19-8687 - Journal of Clinical Periodontology
Date: 14 novembre 2019 à 13:37
À: emile.boyer@univ-rennes1.fr



14-Nov-2019

Dear Dr. Emile Boyer,

Your manuscript entitled "Alteration and loss of mandibular alveolar bone in *Hfe* knocked-out mice. A pilot study." has been successfully submitted online. Within the next few days your manuscript will be checked for its compliance with the journal's requirements. If any required part is found missing, you will be notified by email that your manuscript has been unsubmitted and returned to your Author Centre. The email will include detailed explanation of the changes to be made before your manuscript can be resubmitted for review in Journal of Clinical Periodontology.

Your manuscript ID is CPE-11-19-8687.

Please mention the above manuscript ID in all future correspondence or when contacting the editorial office for questions. If there are any changes in your street address or e-mail address, please log in to ScholarOne Manuscripts (formerly known as Manuscript Central) at <https://mc.manuscriptcentral.com/jcpe> and edit your user information as appropriate.

You can also view the status of your manuscript at any time by checking your Author Centre after logging in to <https://mc.manuscriptcentral.com/jcpe>.

Please note that authors receive a 25% discount on all Wiley books.

Thank you for submitting your manuscript to the Journal of Clinical Periodontology.

Yours sincerely,
James Cook
Journal of Clinical Periodontology Editorial Office

Annexe H

**Accusé de réception du manuscrit
soumis à *Journal of Dental
Research***

De: Journal of Dental Research onbehalfof@manuscriptcentral.com

Objet: Journal of Dental Research JDR-19-1065

Date: 17 octobre 2019 à 16:03

À: emile.boyer@univ-rennes1.fr, lmalherbe@unistra.fr, patricia.leroy@univ-rennes1.fr, shaobing.fong@gmail.com, olivier.loreal@univ-rennes1.fr, martine.bonnaure@univ-rennes1.fr, vincent.meuric@univ-rennes1.fr



17-Oct-2019

Dear Dr. Boyer:

Your manuscript entitled "Oral dysbiosis model with *Porphyromonas gingivalis* is strain-dependent" has been successfully submitted online and is presently being given full consideration for publication in Journal of Dental Research.

Your manuscript ID is JDR-19-1065.

You have listed the following individuals as authors of this manuscript:

Boyer, Emile; Malherbe, Ludivine; Leroy, Patricia; Fong, Shao Bing; Loréal, Olivier; Bonnaure, Martine; Meuric, Vincent

Please mention the above manuscript ID in all future correspondence or when calling the office for questions. If there are any changes in your street address or e-mail address, please log in to ScholarOne Manuscripts at <https://mc.manuscriptcentral.com/jdr> and edit your user information as appropriate.

You can also view the status of your manuscript at any time by checking your Author Center after logging in to <https://mc.manuscriptcentral.com/jdr>.

As part of our commitment to ensuring an ethical, transparent and fair peer review process SAGE is a supporting member of ORCID, the Open Researcher and Contributor ID (<https://orcid.org/>). We encourage all authors and co-authors to use ORCID iDs during the peer review process. If you have not already logged in to your account on this journal's ScholarOne Manuscripts submission site in order to update your account information and provide your ORCID identifier, we recommend that you do so at this time by logging in and editing your account information. In the event that your manuscript is accepted, only ORCID iDs validated within your account prior to acceptance will be considered for publication alongside your name in the published paper as we cannot add ORCID iDs during the Production steps. If you do not already have an ORCID iD you may login to your ScholarOne account to create your unique identifier and automatically add it to your profile.

Thank you for submitting your manuscript to Journal of Dental Research.

Sincerely,
JDR Editorial Office
Journal of Dental Research
jdr@iadr.org

Titre : Maladie parodontale, microbiote et fer

Mots clés : parodontite ; microbiote ; hémochromatose ; *Porphyromonas gingivalis* ; transferrine ; modèles animaux

Résumé : Dans la cavité buccale, la santé parodontale repose sur un équilibre entre la communauté bactérienne sous-gingivale et la fonction immunitaire de l'hôte, toutes deux compatibles avec un état sain. Le modèle pathophysiologique actuel de la parodontite chronique montre un cercle vicieux entre un microbiote dysbiotique et une dérégulation de la réponse inflammatoire. Alors qu'un nombre croissant d'associations entre maladie parodontale et pathologie systémique sont rapportées, ce travail décrit comment une maladie génétique de surcharge en fer — l'hémochromatose héréditaire liée au gène *HFE* — est susceptible d'influencer l'équilibre hôte-microbiote au sein du sillon sous-gingival. Les études transversales, clinique et

microbiologique, que nous avons menées, ont ainsi montré un impact du coefficient de saturation de la transferrine sur la sévérité de la parodontite, probablement en lien avec la sélection d'espèces pathogènes pour le parodonte. Cependant, l'analyse morphométrique du modèle murin de l'hémochromatose héréditaire *Hfe*^(-/-) a révélé des altérations de la micro-architecture de l'os alvéolaire mandibulaire, suggérant un dérèglement du remodelage osseux. Un croisement entre deux modèles animaux, parodontite induite par *Porphyromonas gingivalis* et *Hfe*^(-/-), a donc été mis en œuvre, afin d'explorer les mécanismes de cette association entre excès de fer, dysbiose bactérienne et parodontite.

Title : Periodontal disease, microbiota and iron

Keywords : periodontitis; microbiota; haemochromatosis; *Porphyromonas gingivalis*; transferrin; animal models

Abstract : In the oral cavity, periodontal health relies on a balance between the subgingival bacterial community and the host's immune function. The current pathophysiological model of chronic periodontitis shows a negative feedback loop that implies a dysbiotic microbiota and a dysregulation of the inflammatory response. As an increasing number of associations between the periodontal disease and systemic conditions are reported, this work describes how a genetic iron overload disease — *HFE*-related hereditary haemochromatosis — is likely to influence the host-microbiota interactions within the subgingival sulcus. We conducted clinical and microbiological cross-

sectional studies, that showed transferrin saturation coefficient having an impact on the severity of periodontitis, probably related to the promotion of periodontal pathogenic species. However, morphometric analysis of the murine model for hereditary haemochromatosis *Hfe*^(-/-) revealed alterations in the mandibular alveolar bone micro-architecture, suggesting a disruption of bone remodeling. A mixed animal model, with *Porphyromonas gingivalis*-induced periodontitis and *Hfe*^(-/-) mice, was therefore performed, in order to explore the underlying mechanisms of the relationships between iron excess, bacterial dysbiosis, and periodontitis.